Dissertation zur Erlangung des Doktorgrades

der Fakultät für Chemie und Pharmazie

der Ludwig-Maximilians-Universität München

Tetraspanin 5 (TSPAN5) controls the effects of loss of the tumor suppressor Deleted in Liver Cancer 1 (DLC1) on hepatocellular carcinoma (HCC) growth

Laura Dagmar Schreyer

aus

Weilheim i.OB, Deutschland

2021

Erklärung

Diese Dissertation wurde im Sinne von § 7 der Promotionsordnung vom 28. November 2011 von Herrn PD Dr. Dietmar Martin betreut.

Eidesstattliche Versicherung

Diese Dissertation wurde eigenständig und ohne unerlaubte Hilfe erarbeitet.

München, den 10.02.2022

……

Laura Schreyer

Dissertation eingereicht am 09.12.2021

1.Gutachter: PD Dr. Dietmar Martin

2.Gutachter: Prof. Dr. Bernhard Liebl

Mündliche Prüfung am 02.02.2022

Table of Content

1 Summary 10

2 Introduction 12

2.1 Hepatocellular carcinoma (HCC) 12

2.2 The Rho GTPase Deleted in Liver Cancer 1 (DLC1) as tumor suppressor 13

2.2.1 Proto-oncogenes and tumor suppressor genes 13

2.2.2 Rho GTPases 15

2.3 SRF-/MKL1 signaling pathway 25

2.3.1 The transcription factor serum response factor (SRF) 25

2.3.2 Signaling pathways of SRF activation 26

2.3.3 The coactivators Megakaryoblastic Leukemia 1 and 2 (MKL1/MKL2) 29

2.4 Tetraspanins (TSPANs) 34

2.4.1 Structure of the tetraspanin proteins 34

2.4.2 Biological function of tetraspanin proteins 35

2.4.3 Tetraspanins and their role in viral infections 37

2.4.4 Tetraspanins and cancers 38

2.5 Senescence in aging and cancer 40

2.5.1 Cellular senescence 40

2.5.2 Oncogene-induced senescence 42

2.5.3 Signaling pathways inducing senescence 43

3 Aim of the thesis 46

4 Materials 47

4.1 Cell culture 47

4.1.1 Cell lines 47

4.1.2 Cell culture media 48

4.1.3 Transfection reagents 48
4.2 Nucleic acids 48
4.2.1 Plasmid constructs 48
4.2.2 Primers 49
4.2.3 siRNAs 51
4.3 Antibodies 52
4.3.1 Primary antibodies for immunoblotting 52
4.3.2 Secondary antibodies for immunoblotting 53
4.3.3 Antibodies for RhoA assay 54
4.3.4 Antibodies for chromatin immunoprecipitation (ChIP) 54
4.3.5 Primary antibodies used for immunofluorescence and proximity ligation assay (Duolink®) 54
4.3.6 Secondary antibodies used for immunofluorescence 55
4.3.7 Antibodies used for immunohistochemistry of CAM-Assay 55
4.4 Antibiotics 56
4.5 Enzymes 56
4.6 Stimulants and inhibitors 57
4.7 Ladders 57
4.8 Kits 58
4.9 Buffers and solutions 58
4.9.1 Agarose gel electrophoresis 58
4.9.2 Bacteria cultivation 59
4.9.3 cDNA synthesis and qRT-PCR 59
4.9.4 Chromatin immunoprecipitation (ChIP) assay 60
4.9.5 Duolink® in situ solutions and wash buffers 61
4.9.6 Buffers for RhoA activation assay 62

4.9.7 Buffer for determination of the F-actin to the G-actin ratio 63
4.9.8 Immunoblotting and detection 63
4.9.9 Immunofluorescence 64
4.9.10 Invasion assay 65
4.9.11 Protein isolation 65
4.9.12 Sodium dodecyl sulfate polyacrylamide gel electrophoresis (SDS-PAGE) 66
4.9.13 Universal solutions for washing and dissolving 66
4.10 SDS-Gels 67
4.11 Bacterial strains 69
4.12 Chemicals 69
4.13 Consumable supplies 72
4.14 Technical devices and other equipment 73
5 Methods 76
5.1 Cell culture methods 76
5.1.1 Cultivation of mammalian cell lines 76
5.1.2 Thawing cells 76
5.1.3 Freezing cells 76
5.1.4 Serum starvation 77
5.1.5 Serum stimulation 77
5.1.6 Drug treatment 77
5.1.7 Transient transfection with siRNA by Lipofectamine RNAiMax 77
5.1.8 Transient transfection of DNA plasmids by Lipofectamine 2000 78
5.1.9 Transient transfection of DNA plasmids by GenJet transfection reagent 79
5.1.10 Cell proliferation assay 79
5.1.11 Scratch-wound assay 80

5.1.12 Cell invasion assay 80
5.1.13 Spheroid assay 80
5.1.14 Senescence associated ß-galactosidase staining 81
5.2 Methods of nucleic acids analyses 81
5.2.1 RNA isolation 81
5.2.2 cDNA synthesis 82
5.2.3 Quantitative real-time polymerase chain reaction (qRT-PCR) 83
5.2.4 Microarray analysis 84
5.2.5 Transformation of DNA into competent E. coli DH5alpha bacteria 84
5.2.6 Midi scale plasmid preparation 85
5.3 Methods of protein analyses 85
5.3.1 Protein isolation 85
5.3.2 Measurement of total protein concentration 85
5.3.3 Sodium dodecyl sulfate polyacrylamide gel electrophoresis (SDS-PAGE) 86
5.3.4 Immunoblotting 86
5.3.5 Agarose gel electrophoresis 87
5.3.6 Chromatin immunoprecipitation (ChIP) 87
5.3.7 RhoA activation assay 88
5.3.8 Immunofluorescence 89
5.3.9 Proximity ligation assay by Duolink® 89
5.3.10 Determination of the F-actin to G-actin ratio 90
5.4 Chorio-allantoic-membrane assay (CAM assay) 91
5.4.1 General implementation of CAM assay 91
5.4.2 RNA, DNA and protein isolation of CAM tumors 91
5.4.3 Immunohistochemistry (IHC) of CAM tumors 92

5.4.4 Scanning of IHC sections 92
5.5 Subcutaneous tumor xenograft 93
5.6 Statistical analysis 93
5.7 Software and databases 93
6 Results 95
6.1 Novel target genes induced by DLC1 loss in HCC 95
6.1.1 Gene expression profiling identifies genes induced by DLC1 loss 95
6.1.2 Validation of gene expression profiling via transient knockdown of DLC1 95
6.2 MKL1, FLNA and SRF dependence of novel gene targets 98
6.2.1 MKL1 and FLNA dependence of the newly identified gene targets 98
6.2.2 MKL1 dependence in DLC1 deficient cell line 100
6.2.3 SRF dependence of newly identified target genes in HCC cells 101
6.3 Regulation of the target gene TSPAN5 upon inhibitor or stimulant treatment 102
6.3.1 Inhibition of TSPAN5 expression upon Latrunculin B und Y-27632 treatment 102
6.3.2 Stimulation of TSPAN5 protein level upon LPA treatment 103
6.4 Effects of novel target genes on HCC growth and tumorigenesis 104
6.4.1 TSPAN5 is required for proliferation in HCC cells 104
6.4.2 TSPAN5 depletion leads to decreased migration 109
6.4.3 TSPAN5 depletion results in decreased invasion 111
6.4.4 TSPAN5 depletion provokes spheroid formation 112
6.5 Tumorigenic characteristics of TSPAN5 114
6.5.1 TSPAN5 depletion induces senescence 114
6.5.2 TSPAN5 depletion induces oncogene-induced senescence 116
6.5.3 TSPAN5 depletion inhibits epithelial-mesenchymal transition 121
6.6 Effects of TSPAN5 depletion on MKL1/SRF signal pathway 123

6.6.1 Depletion of TSPAN5 reduces RhoA activity 123
6.6.2 Downregulation of F-actin upon TSPAN5 depletion 123
6.6.3 Reduced actin stress fibers upon TSPAN5 depletion 124
6.6.4 Abrogation of MKL1-FLNA interaction upon TSPAN5 knockdown 125
6.6.5 Decreased expression of MKL1/SRF target genes upon TSPAN5 depletion 126
6.6.6 Reconstitution of TSPAN5 induces re-expression of MKl1 target genes 128
6.7 CAM model shows decreased tumorigenicity upon TSPAN5 depletion 130
6.7.1 Decreased tumor proliferation after TSPAN5 loss in CAM model 130
6.7.2 Reduced MKL1 target gene expression upon TSPAN5 depletion in CAM assay 134
6.7.3 Senescence induction in CAM assay after TSPAN5 knockdown 136
6.8 TSPAN5 overexpression in human HCC 137
6.9 Anti-tumor effects of TSPAN5 depletion in HCC Xenograft 139
6.9.1 Reduced tumor growth after TSPAN5 depletion *in vivo* 139
6.9.2 Decreased MKL1 target gene expression after TSPAN5 loss *in vivo* 140
6.9.3 Senescence induction upon TSPAN5 depletion *in vivo* 141
7 Discussion 143
7.1 DLC1 loss-dependent expression of novel gene targets in HCC 143
7.2 MKL1- and Filamin A dependency of newly identified DLC1 dependent genes 148
7.3 Effects of TSPAN5 on the tumorigenicity of HCC cells 150
7.3.1 Functional effects of TSPAN5 on HCC cells 150
7.3.2 Induction of oncogene-induced senescence due to TSPAN5 depletion 153
7.4 Depletion of TSPAN5 affects the actin cytoskeleton, epithelial transition and MKL1 signaling pathway 157
7.4.1 Depletion of TSPAN5 affects the actin cytoskeleton 157
7.4.2 Depletion of TSPAN5 affects the epithelial-mesenchymal transition (EMT) ... 159

7.4.3 Depletion of TSPAN5 affects the MKL1/SRF target gene expression 161

7.5 *In vivo* anti-tumor effects of TSPAN5 depletion 161

7.5.1 Anti-tumor effects of TSPAN5 silencing in CAM assay 161

7.5.2 Evaluation on TSPAN5 as a novel anti-tumor target in HCC-xenograft 164

7.5.3 Comparison of *in vivo* models used: chicken CAM assay versus mouse xenograft model 166

7.5.4 Summary model of tumorigenic effects of TSPAN5 and anti-tumorigenic effects of TSPAN5 depletion 167

7.6 TSPAN5 overexpression in human HCC and possible therapeutical approaches ... 169

7.6.1 TSPAN5 overexpression in human HCC tissue samples 169

7.6.2 Potential therapeutical approaches to target TSPAN5 overexpression in HCC 169

7.6.3 TSPAN5 as a diagnostic marker for HCC 174

7.6.4 Long-term HCC therapy using a combination of senescence induction by TSPAN5 depletion and senolytic therapy. 174

8 Abbreviation index 177

9 Index of tables 188

10 Index of figures 190

11 References 193

12 Publications 236

13 Acknowledgements 238

1 Summary

Human hepatocellular carcinoma (HCC) is one of the most common and lethal cancers in the human population and there is an urgent need to develop innovative therapeutic approaches as well as new molecular targets. Deleted in Liver Cancer 1 (DLC1) was originally identified as a tumor suppressor gene in HCC whose allele is lost in 50 % of liver, lung, breast and 70 % of colon cancers. DLC1 encodes a Rho-GTPase-activating protein (RhoGAP) which accelerates the return of RhoGTPases to the inactive state. Upon loss of DLC1, the RhoA/actin signaling cascade promotes the activation of Megakaryoblastic Leukemia 1 (MKL1), a coactivator of the transcription factor serum response factor (SRF). Activation of MKL1 is mediated by binding to Filamin A (FLNA), which ultimately supports translocation of MKL1 into the nucleus. The nuclear MKL1 subsequently facilitates the expression of MKL1/SRF-dependent target genes, which promote cell proliferation, cell migration, cell adhesion and differentiation and thus enhance HCC growth. Microarray analysis of DLC1 depleted HepG2 cells versus control HepG2 cells revealed several novel target genes induced by DLC1 loss that are potential mediators of the tumorigenic effects on HCC development and progression. In this context, we identified the transmembrane protein Tetraspanin 5 (TSPAN5), which is strongly upregulated after DLC1 loss in both HCC cells and human HCCs. We provided evidence that knockdown of TSPAN5 results in reduced cell proliferation, migration invasion and spheroid formation ability *in vitro*, as well as reduced tumor growth *in vivo*. Further studies demonstrated that oncogene-induced senescence (OIS) is the underlying mechanism of growth arrest upon TSPAN5 knockdown. Data such as elevated $p16^{INK4a}$ protein level, hypophosphorylation of retinoblastoma (Rb), or enhanced phosphorylation of ERK1/2 due to TSPAN5 loss suggest that senescence induction is mediated via activation of oncogenic Ras. Moreover, the results obtained *in vitro* on OIS-induced arrest of tumor progression upon TSPAN5 depletion were confirmed in further *in vivo* studies using chicken chorioallantoic membrane assay (CAM) and HCC mouse xenograft model. Besides, the xenograft model, in which siRNAs targeting TSPAN5 complexed in polyethylenimine (PEI) nanoparticles were able to inhibit tumor growth in the xenograft mice after systemic administration, opens the first potential therapeutic approach that targets TSPAN5 for the treatment of DLC1 deficient HCC. In summary, we pointed out in this thesis that knockdown of upregulated TSPAN5 strongly inhibits the tumorigenic

properties of a DLC1 deficient HCC by OIS induction. By this way, TSPAN5 represents a novel promising and innovative target in the personalized therapy of DLC1 deficient HCCs.

2 Introduction

2.1 Hepatocellular carcinoma (HCC)

Cancer remains one of the major and insufficiently solved problems of our time. The number of cancer patients continues to rise due to an increasingly large and aging population, as well as partly unhealthy behavior. According to the Global Cancer Observatory (GLOBACON), 19 million new cases were reported in 2020 alone, and 10 million cancer deaths were estimated worldwide in 2020 (Sung et al. 2021). This makes cancer the second leading cause of death, but it is estimated that by 2060 deaths caused by cancer will overtake deaths caused by heart disease (Bray et al. 2021; Sleeman et al. 2019). The overall risk of developing cancer by up to the age of 74 is 20.4% (22.6% in men and 18.6% in women) (WHO 2021). The highest death rates show pancreatic cancer with 94%, followed by liver and intrahepatic bile ducts with 93% each (Sung et al. 2021). Overall, liver cancer is predicted to be the sixth most common cancer, although women are slightly less affected, with a men/women ratio of 2.44 (Bray et al. 2018). With one of the worst 5-year survival of less than 20 %, liver cancer is one of the most malignant cancers (ACS 2021). Among primary liver cancers, hepatocellular carcinoma (HCC) is the most represented histologic subgroup, accounting for 70% - 85% of total liver cancers (Perz et al. 2006). The highest HCC levels are found in parts of Asia, especially China, and in Middle and Western Africa. Lower values are found in South-Central and Western Asia, and especially in Northern and Eastern Europe (Sung et al. 2021). The high rates of HCC in parts of Asia and Africa are mainly due to a high prevalence of chronic hepatitis B (HBV) and chronic hepatitis C (HCV) infections, as well as increased exposure to aflatoxin B1 (AFB) (Farazi and DePinho 2006; Ming et al. 2002; Perz et al. 2006). The HCC disease in developed regions such as Europe or the USA is often due to an unhealthy lifestyle. Thus, heavy alcohol consumption can lead to alcoholic and type II diabetes, obesity or the metabolic syndrome to non-alcoholic fatty liver disease (NAFLD) (El-Serag 2007; Reeves et al. 2016). These two disorders, in turn, can further develop into hepatic cirrhosis and finally degenerate into HCC. Staging is used to estimate the extent of malignant tumor carcinogenesis. In addition to the size and localization of the primary tumor (T), findings regarding lymph node involvement (N) and distant metastases (M) are also included in the staging evaluation. The ultimate purpose of tumor staging is to evaluate the disease situation, assess the chances of recovery, and design the

appropriate therapy (Tellapuri et al. 2018). Despite the high incidence rate and mortality of HCC, the numerous reasons and mechanisms that ultimately lead to malignant proliferation of liver cells are poorly understood. The reason why elucidating the underlying mechanisms is so difficult is that the development of HCC is a very complex, multistep process that is gradual over years. This process is due to an accumulation of genetic and epigenetic alterations, eventually followed by changes in key regulatory genes and disruption of multiple signaling pathways. For example, it is already known that HBV, HCV and aflatoxin B1 exposure can lead to inactivation or mutation of the tumor suppressor protein p53, inflammatory responses and oxidative stress, which provide a fundamental way to HCC development (Farazi and DePinho 2006). Furthermore, HBV and HCV lead to mitogen-activated protein kinase (MAPK) pathway activation, which probably also contributes to pathogenesis. In addition to molecular alterations, HBV is also suspected to integrate into the host genome and thereby causing alterations in relevant genes. All the different HCC inducing aetiologies ultimately lead to a continuous cycle of liver cell damage and regeneration, resulting in chronic liver disease (Farazi and DePinho 2006). Dysplastic nodules gradually develop, altering the structure of the liver and finally resulting in HCC, which may also have the potential to invade surrounding fibrotic tissue and metastasize (Okuda 2000). Whereas the genetic changes just mentioned are irreversible, some epigenetic changes such as DNA methylation or histone modification are reversible with the help of epigenetic drugs (Ghoshal et al. 2005; Ma et al. 2014; Yoo and Jones 2006). The prerequisite for this is, of course, that hepatocellular changes are detected as early as possible and before the development of HCC. However, the more precise interactions and processes still need to be explored in order to better understand the pathogenesis and thus find new targets for drugs in HCC or even minimize its likelihood of development given certain existing risk factors.

2.2 The Rho GTPase Deleted in Liver Cancer 1 (DLC1) as tumor suppressor

2.2.1 Proto-oncogenes and tumor suppressor genes

As described above, alterations in DNA sequences and epigenetic regulations underlie the development of many cancers (Martincorena and Campbell 2015). More specifically, so-called proto-oncogenes and tumor suppressor genes are known to play a critical role in

tumorigenesis by influencing cell proliferation (Kugoh et al. 2015). When proto-oncogenes, which often effect processes of cell proliferation or differentiation, are dysregulated or abnormally overexpressed by mutations, for example, it gives us insight into why cancer cells misbehave (Sherr 2004; Stehelin et al. 1976). On the other hand, there are also genes that have the opposite effect and thus prevent tumor development (Harris et al. 1969; Stanbridge 1976). In the course of time, many tumor suppressor genes have been identified.

The first tumor suppressor ever discovered was the retinoblastoma (Rb) gene (Friend et al. 1987). Rb proteins interact with transcription factors such as E2F1 and can repress their gene expression by recruiting histone acetylases and chromatin remodeling factors to these loci (Chellappan et al. 1991; Harbour and Dean 2000; Nevins 2001). Thus, Rb acts in the G1 phase of the cell cycle through a suppressive role on growth, metabolism and replication. Another very important tumor suppressor gene is p53 (Lane and Crawford 1979; Linzer and Levine 1979). In 1989, Finlay and colleagues published that p53 acts as a suppressor for transformation (Finlay et al. 1989). It was shown that p53 mutations are also common in human cancer (more than 50 %) and that p53 is induced after DNA damage to initiate a G1 phase arrest as a cell cycle “checkpoint function” (Finlay et al. 1989; Hollstein et al. 1991; Kastan et al. 1991; Sherr 2001; Sherr 2004). Also revealed to be a very important tumor suppressor gene is $p16^{INK4a}$-ARF, which in turn regulates the expression of the two aforementioned tumor suppressors p53 and Rb. $p16^{INK4}$ belongs to the INK4 family of cyclin-dependent kinases (CDK) inhibitors. By binding to CDK4, $p16^{INK4a}$ can inhibit the catalytic activity of the CDK4/cyclin D enzyme, which promotes cell cycle progression by phosphorylating critical proteins such as Rb protein (Serrano et al. 1993). Inactivation of $p16^{INK4}$ has been demonstrated in many cancers (Kamb et al. 1994). In addition to $p16^{INK4}$, the protein “alternative reading frame” (ARF) can be encoded from the INK-ARF gene by other splicing and an alternative reading frame, which ultimately activates p53 (Quelle et al. 1995; Sharpless and DePinho 1999; Sherr 2001). It should be emphasized that mostly the presence of a single functional gene is sufficient to suppress the development of cancer. The reason for this is that they are recessive and both alleles must be switched off so that no protein is encoded (Knudson 1971, 1973).

2.2.2 Rho GTPases

The small GTPases of the Rho family are highly conserved molecular switches that belong to the Ras superfamily. The members of the Ras family have in common that they all possess a GTPase domain. This superfamily of small GTPases is nearly found in all eukaryotes and there are more than 60 different types in mammals, whereas they can be classified into 5 main groups Ras, Rho, Rab, Arf and Ran (Etienne-Manneville and Hall 2002; Haga and Ridley 2016). In turn, the three best characterized members of the Rho family are Rho, Rac, and Cdc42. Rho GTPases have been described to use a simple biochemical strategy to control complex biological processes such as actin and microtubule cytoskeleton organization, cell proliferation, cell migration, vesicle transport, cell polarity, as well as gene expression and activation of enzymatic reactions (Etienne-Manneville and Hall 2002).

The switch function of GTPases is that they alternate between two conformational states (Figure 1). If GTP is bound to GTPases, they are in the active state, which changes to the inactive state, where only GDP is bound, by hydrolysis of GTP to GDP. The whole cycle is strictly regulated by three classes of proteins. Guanine nucleotide exchange factors (GEFs) catalyze the exchange of GDP to GTP, thereby converting the Rho protein to the active state (Rossman et al. 2005). GTPase-activating proteins (GAPs) then stimulate the hydrolysis of GTP to GDP, thus inactivating the Rho protein (Bos et al. 2007). Further guanine nucleotide dissociation inhibitors (GDIs) finally remove the inactive GTPase from the membrane (Cho et al. 2019; Dransart et al. 2005).

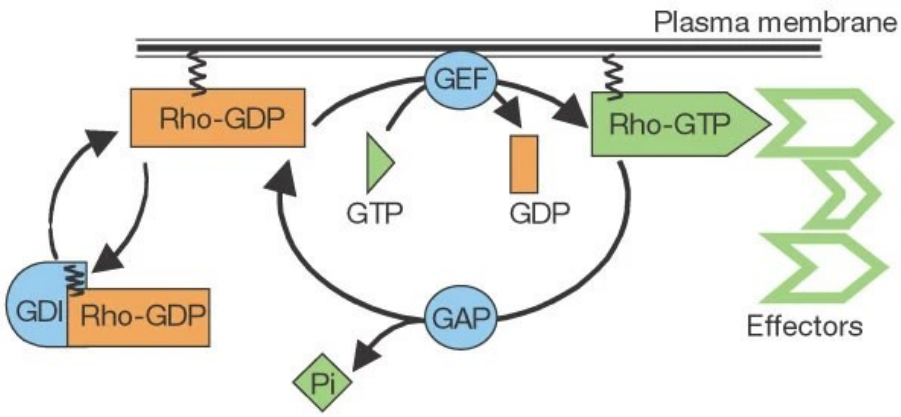

Figure 1: Rho GTPases and their function as complexly regulated molecular switches. RhoGTPases are molecular switches with an active, GTP-bound and an inactive, GDP-bound state. The exchange of GDP to GTP is promoted by GEFs. GAPs promote the hydrolysis of GTP to GDP, causing the active RhoGTPase to switch to the inactive state. Finally, GDIs remove the inactive GDP-bound RhoGTPases from the membrane to the cytoplasm. This picture is taken from (Etienne-Manneville and Hall 2002).

Due to their temporary anchorage in the membrane, Rho proteins are able to be stimulated by extracellular factors via membranous integrins, G-protein coupled proteins or tyrosine kinase receptors, in order to subsequently modulate specific intracellular effectors. Thus, changes in the extracellular environment can simply affect intracellular signaling pathways (Etienne-Manneville and Hall 2002).

2.2.2.1 The role of Rho GTPases in cancer

Rho GTPases take an important role in signal transduction for cell proliferation and migration, for gene expression and thus for cell survival. In case of dysregulation, they can promote tumorigenesis, tumor growth and metastasis by inducing cell proliferation, evasion from apoptosis, tissue invasion, altered morphological characteristics, and supporting neovascularization (Sahai and Marshall 2002; Vega and Ridley 2008).

For example, if the role of Rho proteins in the regulation of cell motility is considered in more detail, it is very likely that they are involved in tumor cell invasion when they are dysregulated (Figure 2). The Rho proteins RhoA, Rac1, Cdc42, and Par6 are required for cell polarity and for the organization of cell-cell junctions of a normal epithelial layer (Figure 2A). Increased levels of Rnd3/RhoE will reverse the effect of RhoA which can lead to a loss of cell polarity and cell monolayer (Guasch et al. 1998; Hansen et al. 2000; Nobes et al. 1998). Benign tumors are the result (Figure 2B). Loss of tissue barriers, increased cell motility and remodeling of the extracellular matrix (ECM) can locally increase the invasiveness of a tumor. Here, modulations of Rac1 and Rho/Rock activity play a role in polarity loss and loss of cell-cell junctions on the one hand, and increased RhoA, Rock, Rac, and Cdc42 activity are involved in increasing cell motility on the other (O'Brien et al. 2001). Furthermore, disruption of the regulation of RhoA and Rac1 of metalloproteinases (MMPs) expression can degrade or remodel the ECM (Matsumoto et al. 2001; Zhuge and Xu 2001) (Figure 2C). In order to eventually form metastases, it is necessary for tumor cells to enter blood or lymphatic vessels. Here, RhoA and Rock are required, not only in the migrating but also in the endothelial cells, to cross the vascular endothelium (Adamson et al. 1999; Worthylake et al. 2001) (Figure 2D). Furthermore, overexpressed RhoC may accelerate tumor vascularization by inducing the expression of angiogenic factors (van Golen et al. 2000; Sahai and Marshall 2002).

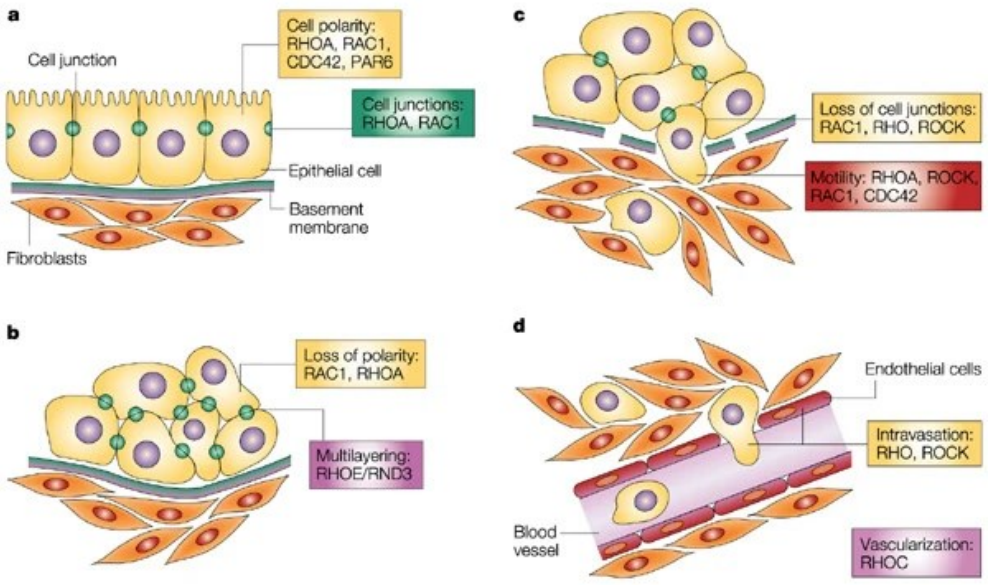

Figure 2: Dysregulation of RhoA leads to tumor development and progression. **A)** Cell polarity is given by RhoA, Rac1 and Cdc42. In addition, RhoA and Rac1 are important for the formation of cell junctions. **B)** Formation of benign tumors by a loss of cell polarity and multilayering of epithelial cells. **C)** Loss of tissue boundaries and increased cell mobility give rise to invasive tumors. **D)** Rho and Rock promote intravasation and vascularization, allowing metastasis to distant sites. This picture is taken from (Sahai and Marshall 2002).

Due to their numerous members and their frequent occurrence in all eukaryotic cells, RhoGTPases are of high importance as oncogenes. Besides mutations in the RhoGTPase genes, the Rho proteins are in most tumor cases upregulated or their activity has been increased by changes in the expression of GAPs, GEFs or GDIs. Furthermore, RhoGTPases may also be deregulated by post translational modifications such as ubiquitination or alternative splicing (Haga and Ridley 2016; Porter et al. 2016; Visvikis et al. 2010). Using the example of HCC, Xue and colleagues have shown that in the gene region of the RhoGAP "Deleted in Liver Cancer 1" (DLC1), one allele is deleted in more than 50% of cases, thus significantly increasing the probability of tumor development (Xue et al. 2008). This finding makes DLC1 a very important gene for tumorigenesis, which must be further investigated in order to improve HCC therapies.

2.2.2.2 The "Deleted in Liver Cancer" (DLC) genes

The human genome encodes estimated 70 different types of RhoGAPs, all with a conserved GAP domain whose function is to regulate the Rho signaling cascade by switching them off (Tcherkezian and Lamarche-Vane 2007). A subgroup of RhoGAPs are the "Deleted in Liver Cancer" (DLC) proteins, which are encoded by three different genes of the human genome. The first member DLC1, also referred to as STARD12 or ARHGAP7, was discovered in 1998 by Yuan and colleagues by representational difference analysis (RDA), a PCR based subtractive hybridization technique, as a gene frequently (approximately 50 %) deleted in primary HCCs and in a majority of HCC cell lines. In some cell lines, such as WRl and 7703, the DLC1 gene is not expressed at all. The DLC1 gene has 86 % homology with the rat p122 RhoGAP gene and was localized to chromosome 8 p21.3-22 via fluorescence in situ hybridization (Yuan et al. 1998). It is precisely in this region of chromosome 8 those recurrent deletions frequently occur, which have been detected not only in HCCs but also in other solid tumors in the prostate, lung and breast (Brothman 1997; Isola et al. 1995; Marchio et al. 1997; Petersen et al. 1997; Yuan et al. 1998). From these results, it can be considered that the DLC1 gene plays an important role as a tumor suppressor gene. Meanwhile, DLC1 expression was detected in a wide variety of normal tissues such as brain, heart, kidney, liver, lung, skin, spleen and testis (Durkin et al. 2002). That DLC1 is indeed a major tumor suppressor is shown by the fact that its expression is lost or downregulated in further different tumors such as brain, stomach, colon, bone marrow or nasopharyngeal in addition to the already mentioned and early discovered tumors in breast, lung and liver (Kim et al. 2003; Liao and Lo 2008; Seng et al. 2007; Song et al. 2006; Yuan et al. 2003a). Under-expression of DLC1 occurs in addition to frequent heterozygous or homozygous deletion of the DLC1 gene, particularly due to hypermethylation of the GC-rich and with typical CpG islands provided promoter region of DLC1, leading to transcriptional silencing (Wong et al. 2005; Yuan et al. 2003a). As another alternative epigenetic mechanism for gene silencing, histone deacetylation was demonstrated on the example of prostate cancer (Guan et al. 2006). At the cellular level, experiments with inhibitors of hypermethylation (e.g.: 5-aza-deoxycytidine) and histone deacetylation (e.g.: Trichostatin A) have partially reversed epigenetic changes in the DLC1 gene (Guan et al. 2006; Wong et al. 2003). Somatic mutations, on the other hand, have tended to be dismissed as rare, although in 2008 Liao and colleagues reported that they occur in prostate and colon cancers (Liao et al.

2008). There are two other members of the DLC family. One is DLC2, which is also called STARD13 and is located on chromosome 13q12. The other one is DLC3, which is also named KIAA0189 or STARD8 and is located on q13 of the X chromosome (Ching et al. 2003; Durkin et al. 2007a). Similar to DLC1, homologous DLC2 was also ubiquitously expressed in normal tissues, whereas it is frequently under expressed in HCC. Also, deletion of DLC2 often underlies a loss of heterozygosity (LOH) on the long arm of chromosome 13 in HCCs (Ching et al. 2003; Guan et al. 2000; Laurent-Puig et al. 2001). Durkin and colleagues further found that DLC3 expression is downregulated in a high proportion of kidney, lung, uterine, ovarian and breast cancer tissues compared to healthy tissue (Durkin et al. 2007a).

2.2.2.3 Structure of the DLC1 proteins

Each of the DLC proteins has three distinct domains with specific functions (Figure 3). The sterile a motif (SAM) is located at the N-terminus, the conserved RhoGAP domain in the middle region and the steroidogenic acute regulatory-related lipid transfer (START) domain at the C-terminus (Ching et al. 2003; Durkin et al. 2007a; Durkin et al. 2007b).

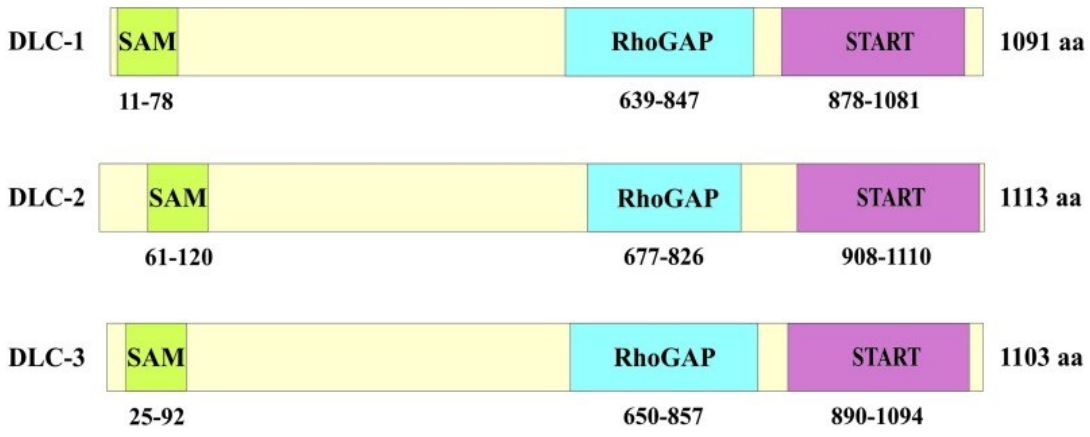

Figure 3: The modular structure of DLC protein family. The three typical functional domains SAM, RhoGAP and START of DLC proteins. This picture is taken from (Lukasik et al. 2011).

The best characterized domain is the approximately 150-200 amino acids (aa) long RhoGAP domain, which is responsible for the biological activity of DLC1s. This domain catalyzes the hydrolysis of active GTP-bound Rho proteins to inactive GDP-bound ones as described above.

More specifically, "arginine fingers" are responsible for catalytic activity, with DLC1 and DLC3 having conserved "arginine fingers" in position 677 and 688 (Durkin et al. 2007a; Durkin et al. 2007b). For DLC1 itself, as well as the isolated RhoGAP domain, high activity was shown on RhoA, RhoB, and RhoC, but only low activity on Cdc42 and none at all on Rac1 (Sekimata et al. 1999; Wong et al. 2003). Similarly, DLC2 and DLC3 exert RhoGAP activity on RhoA and Cdc42, whereas these also exhibit almost no GAP activity for Rac1 (Ching et al. 2003; Kawai et al. 2007). SAM domains, which are approximately 77 amino acids long, are also found primarily in signaling and nuclear proteins, where they play a role in protein interactions. Here they modulate with other SAM domains the formation of homo- or hetero-oligomers or even the direct interaction with RNA or DNA (Chi et al. 1999; Qiao and Bowie 2005; Stapleton et al. 1999). In contrast, much less is known about the function of the SAM domain in DLC proteins. For the SAM domain of DLC1 but not DLC2, a new interaction partner, eukaryotic elongation factor 1A1 (EF1A1), was recently identified by protein precipitation and “Matrix Assisted Laser Desorption lonization - Time of Flight” (MALDI-TOF) mass spectrometry analyses by Zhong and colleagues (Zhong et al. 2009). EF1A1 participates in protein synthesis and transport of ß-actin mRNA and is also involved in regulation of the actin cytoskeleton through G-actin binding and F-actin bundling (Gross and Kinzy 2005; Liu et al. 2002; Murray et al. 1996; Thornton et al. 2003). Moreover, EF1A1 expression is increased in melanoma and pancreatic, breast, lung, prostate and colon tumors (Thornton et al. 2003). These data suggest that EF1A1 have a significant role in the regulation of cell growth and migration. Zhong and colleagues demonstrated further that EF1A1 is translocated by interaction with SAM to the membrane periphery and facilitates the formation of membrane ruffles, which can suppress cell migration independent of RhoGAP function (Zhong et al. 2009). For DLC2, on the other hand, it has been shown by structural studies, for example, that it can interact with fats such as sodium dodecyl sulfate (SDS) in micelles. Further, Li and colleagues showed that the SAM domain is not responsible for dimerization of DLC2 but reasoned that the SAM domain of DLC2 might have something to do with membrane binding (Li et al. 2007). At the C-terminus is the well-conserved START domain, which is approximately 210 amino acids long and is known primarily to bind lipids, including sterols. In mammals, 15 START domain-containing proteins are known, among which steroidogenic acute regulatory protein (StAR) is one of the best-characterized and plays a role in lipid transport to mitochondria. In general, these proteins

with a start domain are involved in physiological processes such as lipid transfer between intracellular compartments, lipid metabolism and regulation of cell signaling (Alpy et al. 2009; Lukasik et al. 2011). For DLC2, it was shown by Ng and colleagues that the protein is localized to mitochondria due to its START domain (Ng et al. 2006). Furthermore, a functional interaction partner at the START domain of DLC1 was recently identified. This identified protein is caveolin 1 (CAV-1), which has been reported to interfere with tumor progression including metastasis and angiogenesis, may sometimes also be involved in tumorigenesis (Du et al. 2012; Goetz et al. 2008). Here, authors Du and colleagues propose a RhoGAP-independent mechanism of tumor suppression through complex formation of DLC1 and CAV-1 by the START domain (Du et al. 2012). The extent to which the START domain of the DLC proteins plays a role in mitochondrial lipid transport, their overall physiological function or their interaction partners remains to be investigated. Between the SAM and RhoGAP domains a long unstructured region called the "focal adhesion targeting" (FAT) domain exists (Kawai et al. 2004). It has been shown that DLC1, DLC2 and DLC3 interact via their FAT region with SRC Homology 2 (SH2) domain of tensin proteins and are thus localized at the focal adhesions (Kawai et al. 2009; Liao et al. 2007; Qian et al. 2007). It is suggested that the localization of the DLC proteins at the focal adhesions has something to do with their tumor suppressive properties, but nevertheless, this also needs to be further explored.

2.2.2.4 Biological functions of DLC proteins and their prominent contribution to carcinogenesis

DLC1 proteins play an important role in the regulation of signal transduction, mainly as RhoGAPs, but also through the fact that they interact with focal adhesions via the FAT domain. Thus, they have important influence on cell proliferation, cell morphology and cell migration (Kim et al. 2009; Liao and Lo 2008). Using a DLC1 knockout mouse model, Durkin and colleagues found that DLC1 is mandatory for embryogenesis (Durkin et al. 2005). Histological analysis showed that homozygous mutant embryos were absent or necrotic at 12.5-day postcoital. The embryos showed severe abnormalities in brain, heart, placenta and neural tube development and in the formation of blood vessels. Furthermore, by extracting DLC1 deficient fibroblasts from the knockout mice embryos, they found that the cytoskeletal organization was altered. The cells formed fewer long stress fibers and less focal adhesion-like

structures (Durkin et al. 2005; Petit and Thiery 2000). Since DLC1 affects phosphoinositide and RhoGTPase signaling pathways, which in turn regulate stress fiber assembly and focal adhesion, respectively, it can be concluded that DLC1 affects cell adhesion and migration. Furthermore, the study also indicates that the loss of DLC1 cannot be compensated by DLC2 and/or DLC3. Several studies have shown that the re-expression of DLC1 inhibits not only the growth of liver, lung and breast cancer cells *in vitro*, but also *in vivo*, confirming the importance of DLC1 as a tumor suppressor (Goodison et al. 2005; Wong et al. 2005; Yuan et al. 2003b; Yuan et al. 2004). In a report by Goodison, DLC1 was found to have metastasis suppressing properties in addition to tumor suppressing properties. In breast cancer cells, re-expression of DLC1 was observed to inhibit migration and invasion, as well as a significantly reduce metastasis in nude mouse experiments (Goodison et al. 2005). Further studies confirmed the inhibition of invasion and cell motility upon DLC1 reconstitution also in liver, ovarian and lung cell lines (Qian et al. 2007; Syed et al. 2005; Wong et al. 2005; Yuan et al. 2004). In general, it is assumed that the suppressive functions of DLC1 are based on several already known regulatory roles of DLC1, such as regulation of the actin cytoskeleton, assembly of focal adhesions, or cell shape (Sekimata et al. 1999). Also, induction of apoptosis was observed after restoration of DLC1 gene expression in HCC cells, which may further inhibit cell proliferation and prevent tumorigenesis (Zhou et al. 2004). Recently, Tripathi and colleagues found that expression of DLC1 in metastatic prostate carcinoma increases the expression of E-cadherin. E-cadherin acts as a cell-cell adhesion molecule to oppose cancer cell invasion and is decreased expressed in many human cancers (Tripathi et al. 2014). By combining a novel "mosaic" mouse model and RNA interference, Xue and colleagues were able to validate DLC1 as a potent tumor suppressor gene in HCC *in vivo* (Xue et al. 2008; Zender et al. 2005). Furthermore, they were able to observe the tumorigenic effects of DLC1 loss *in vivo*. Besides, Xie and colleagues focused on genetic variants in the DLC1 gene and the extent to which these may be associated with the development of HCC (Xie et al. 2015). By exon sequencing of the DLC1 gene in human HCC tissue samples, they identified, among others, a novel missense mutation and several single nucleotide polymorphisms (SNPs), which they correlated with HCC susceptibility and clinical prognosis. While they found no significant association of the DLC1 SNPs with patient prognosis, their results suggest that genetic variations in the DLC1 gene may mediate an increased risk for HCC development (Xie et al. 2015). Due to the fact that in many

tumors Myc oncogenes are overexpressed and p53 tumor suppressors are lacking, but this combination alone had only a weak oncogenic effect, DLC1 was additionally knocked out in the mouse model using shRNA (Staib et al. 2003; Xue et al. 2008; Zender et al. 2006). In this context, formation of aggressive liver tumors was observed only in the case of additional DLC1 loss. Moreover, their data suggest that this occurs in dependence of the RhoA signaling pathway, opening novel therapeutic targets (Xue et al. 2008). The therapeutic effects of stable Myc knockdown with shRNA and re-expression of DLC1 via adenovirus transduction were further investigated by Yang and colleagues (Yang et al. 2016). They found that a combination of the two therapeutic approaches inhibited RhoA levels, cell proliferation, soft agar colony forming, and cell invasion significantly more strongly and excessively than either Myc knockdown or DLC1 re-expression alone. Using a subcutaneous mouse xenograft, they also demonstrated that additional targeted liver cell delivery of DLC1 to Myc knockdown had cooperative effects on xenograft tumor growth *in vivo* (Yang et al. 2016). Another therapeutic approach for use in humans, instead of DLC1 re-expression via adenovirus transduction, would be the administration of compounds that increase DLC1 expression itself or inhibit its degradation. Here, Chung and colleagues first postulated promising results with the compound ursodeoxycholic acid (UDCA). They demonstrated that UDCA may suppress HCC growth by inhibiting DLC1 degradation and increasing DLC1 expression (Chung et al. 2011).

Studies have shown that in addition to RhoGAP activity and the START domain of DLC1, its interaction with tensin itself is very important for tumor suppressive activity (Liao et al. 2008). Mutations such as missense or nonsense mutations in the DLC1 gene can prevent interaction to tensin and thus to focal adhesions leading to a loss of suppressor properties (Liao et al. 2008). In fact, there is also evidence that DLC1 without GAP function can inhibit cell growth. For example, a GAP deficient DLC1 mutant hindered colony forming of small lung cancer cells or reduced the migratory ability of NIH3T3 fibroblasts (Healy et al. 2008; Zhong et al. 2009). It is conceivable that DLC1 functions as a tumor suppressor via GAP-dependent as well as GAP-independent mechanisms. Recent studies by Wu and colleagues demonstrated that downregulation of DLC1, which occurs very often in HCC tissue samples, is associated with alpha-fetoprotein (AFP) levels, vascular invasion, low-level differentiation, and poor prognosis for patients (Wu et al. 2018). Furthermore, functional assays revealed that DLC1 loss not only promotes tumor growth, migration and invasion, but also autophagy of HCC cells via an

increase in Rho-associated kinase 1 (Rock1) activity as well as an increased T-cell factor 4 (TCF4) expression affecting the WNT/ß-Catenin pathway (Wu et al. 2018). Using bioinformatic analysis, Wu and colleagues further confirmed that autophagic activity, which promotes HCC progression, is enhanced, among other factors, by an altered DLC1 expression (Wu et al. 2020). Overall, it can be said that all three DLCs are downregulated in a wide range of malignancies and that their loss promotes tumorigenesis. The Cancer Genome Atlas (TCGA) database also confirms that DLC1 expression is downregulated not only in HCC, but also in lung squamous cell carcinoma (LSC), lung adenocarcinoma (LAD) and breast cancer (Wang et al. 2016a). In particular, a reduced number of DLC1 copies in HCC samples compared to cancer-free samples is associated with a worse prognosis than if only DLC2 or DLC3 levels were low. The worst prognosis is for patients with both low DLC1 and DLC2 levels (Wang et al. 2016a). When, where and why which form of the DLC1 gene predominates and which exact processes are affected by changes in DLC1 expression and how these promote HCC progression remains to be determined.

2.3 SRF-/MKL1 signaling pathway

2.3.1 The transcription factor serum response factor (SRF)

The transcription of DNA segments into mRNA is an essential process for the function of a cell, which must be extremely controlled and coordinated. This occurs in response to extracellular and intracellular signals by transcription factors alone or in combination with co-regulators, like coactivators and corepressors. Transcription factors are proteins that are able to bind to DNA and thus have a positive or negative regulatory effect on the transcription of one or more genes. The human serum response factor (SRF) is a ubiquitous and nuclear transcription factor that belongs to the MADS-box family of proteins. The MADS-box motif is a conserved 56 amino acids long region located in the DNA binding domain of numerous transcription factors. The name of the MADS box can be attributed to its first found members MCM1, Agamous, Deficiens and SRF (Pellegrini et al. 1995; Schwarz-Sommer et al. 1990; Shore and Sharrocks 1995). SRF forms homodimers via its C-terminus, which can then bind specifically to the serum response element (SRE) via the N-terminus. The SRE is located upstream of all SRF-regulated genes and contains a 10-base pair long consensus sequence $CC(AT)_6GG$, also called CArG box (Minty and Kedes 1986; Treisman 1986). By Sun and colleagues, more than 100 SRF-dependent target genes were identified, remarkably many of which encode cytoskeletal, contractile or adhesion proteins, suggesting that SRF is a master regulator of the actin cytoskeleton (Miano et al. 2007; Sun et al. 2006). In addition, a majority of SRF target genes are also so-called immediate early genes (IEG), which is due to the extremely rapid (within a few minutes) transcriptional activation of the genes after stimulation of the cell e.g., by serum or growth factors (Nurrish and Treisman 1995; Winkles 1998). Thus, SRF regulates essential cellular processes such as cell proliferation, migration, differentiation, myogenesis and actin cytoskeleton organization via expression of its target genes (Johansen and Prywes 1995; Knöll and Nordheim 2009; Schratt et al. 2002; Treisman 1986; Treisman 1992). The fact, that SRF is essential for embryogenesis was shown in SRF deficient mouse embryos, as they were unable to form mesoderm and therefore died from gastrulation defects (Arsenian et al. 1998). Furthermore, Parlakin and colleagues investigated the role of SRF in cardiac functions in embryos and postnatal. They were able to show that cardiac-specific silencing of SRF leads to cardiac defects that are lethal for the embryos between the embryonic day 10.5 and 13.5 (Parlakian et al. 2004). Similar studies with knockout mice have also highlighted the

importance of SRF for the central nervous system, liver or skin development, and skeletal muscle (Alberti et al. 2005; Li et al. 2005; Sun et al. 2009; Verdoni et al. 2010). Some of the first discovered and already well characterized SRF target genes are *c-fos*, *egr-1* or the *srf* gene itself, who are all members of the immediate early genes and whose encoded proteins can act as transcription factors again (Shaw et al. 1989; Treisman and Ammerer 1992). Other target genes that have also been characterized in more detail include transgelin (TAGLN or SM22), intergrin alpha-5 (Itga5) and connective tissue growth factor (CTGF) (Leitner et al. 2011; Mack et al. 2001; Muehlich et al. 2007).

2.3.2 Signaling pathways of SRF activation

SRF can be activated in parallel by two independent signal pathways, on the one hand the Ras/MPK/TCF cascade and on the other hand the Rho/actin signal pathway. Of these two, the first is ternary complex factor (TCF) dependent and the second is TCF independent (Figure 4).

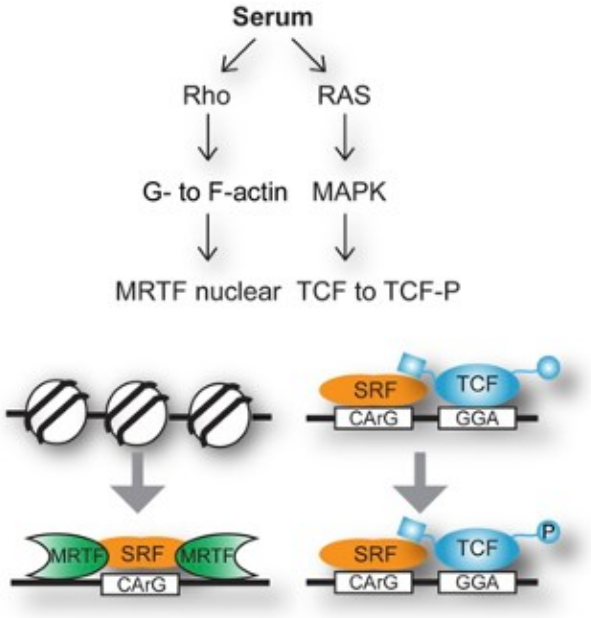

Figure 4: Model of the two different signaling pathways leading to SRF activation. SRF is activated after serum stimulation on the one hand via the Rho/actin/MRTF signaling pathway and on the other hand via the RAS/MAPK/TCF cascade. This picture is taken from (Clark & Graves, 2014)

The TCF-dependent activation of SRF is initiated by extracellular stimuli such as serum, growth factors, or lysophosphatidic acid (LPA). Stimulation of the cell leads to immediate activation of small GTPase Ras, which in turn activates mitogen activated protein kinase (MAPK) by phosphorylation. In the following, the three TCFs Elk-1, SAP-1 and SAP-2/NET are also phosphorylated by the three MAPK subfamilies "Extracellular signal regulated kinase" (ERK), "c-Jun N-terminal kinase" (JNK) and p38 (Sharrocks 2001; Whitmarsh et al. 1997). The phosphorylated TCFs, belonging to the subgroup of the Ets (erythroblast transformation specific) family and acting as co-transcription factor, finally bind to the "Ets Binding Site" (EBS) with the core sequence GGA(A/T), which is located in close proximity to the CARG box (Janknecht and Nordheim 1993; Treisman 1994, 1995). In this way, the TCFs, SRF and the SRE region form a ternary complex that finally induces target gene expression. An overview of the TCF dependent activation of SRF is presented in Figure 5.

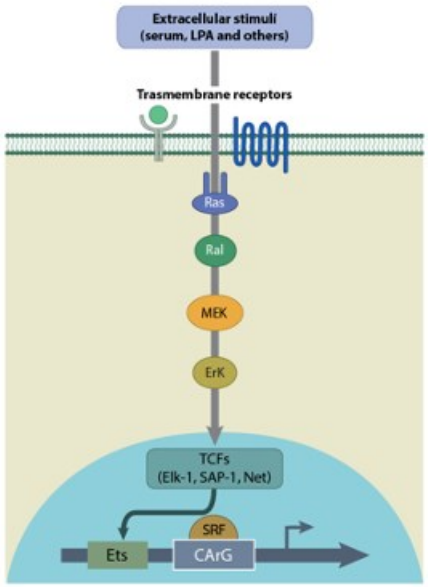

Figure 5: Model of the TCF-dependent SRF activation. Via extracellular stimuli such as serum stimulation, the TCFs Elk-1, SAP-1, and Net are phosphorylated via the Ras/Raf/Mek/Erk, thereby activating SRF and its target gene expression. This picture is taken from (Mechanobiology Institute 2021).

Initial evidence for a TCF-independent activation pathway was provided by the finding that even after mutation of the TCF-binding site, serum-induced activation of SRF and thus transcription of e.g., *c-fos* was not completely abolished (Hill et al. 1994). The TCF independent pathway was corroborated by the fact that Rho inhibition also hinders SRF activation and microinjection of active RhoA activates SRF (Hill et al. 1995; Hill and Treisman 1995). It was

finally revealed by Sotiropoulos and colleagues that actin dynamics of the cytoskeleton plays an important part in the process of SRF activation (Posern et al. 2004; Sotiropoulos et al. 1999). The second, TCF-independent signaling pathway for SRF stimulation can therefore be described as follows (Figure 6): This signaling pathway is also triggered by extracellular stimuli such as serum, LPA or growth factors, which in turn activate RhoA, a member of the Rho family of small GTPases. It was elucidated that RhoA signaling leads by filament stabilization as well as by de novo polymerization to an accumulation of filamentous actin (F-actin) and simultaneously to a reduction of globular actin (G-actin) (Sotiropoulos et al. 1999). The decrease in cytosolic G-actin caused by polymerization of monomeric G-actin to polymeric F-actin, leads to a release of the bound and thus deactivated transcriptional coactivator Megakaryoplastic Leukemia 1 (MKL1, also called Myocardin-Related Transcription Factor A (MRTF-A)). Thus, the unbound MKL1 can translocate to the nucleus, bind to SRF, and activate SRF-related target gene expression through its coactivator abilities (Miralles et al. 2003; Muehlich et al. 2008). The phosphorylation status of MKL1 in the nucleus regulates further SRF activity and associated gene expression. If MKL1 is phosphorylated by ERK1/2, it binds again to G-actin and is thus shuttled out of the nucleus into the cytoplasm, whereby SRF is again deactivated and gene expression is interrupted (Muehlich et al. 2008).

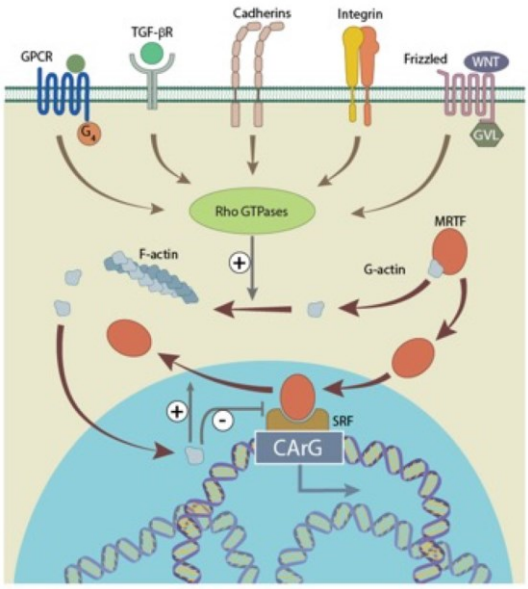

Figure 6: Model of MRTF (MKL) regulation and consequent SRF activation. Extracellular stimuli lead to activation of RhoGTPases, resulting in increased polymerization of monomeric G-actin to filamentous F-actin. MRTF (MKL), previously bound to monomeric G-actin, is thus released, can shuttle into the nucleus and activates SRF target gene expression by binding to SRF. Phosphorylation of MRTF (MKL1) consequently exports it from the nucleus to the cytoplasm, thereby inhibiting target gene expression. This picture is taken from (Mechanobiology Institute 2021).

2.3.3 The coactivators Megakaryoblastic Leukemia 1 and 2 (MKL1/MKL2)

2.3.3.1 Structure of the MKL proteins

MKL1 and 2 are coactivators of the transcription factor SRF. Originally, myocardin was first discovered as a highly potent transcriptional coactivator for SRF in cardiac and smooth muscle cells by Wang and colleagues, using bioinformatics-based screens to identify unknown cardiac-specific genes (Wang et al. 2001). Since SRF regulates many genes inducible by growth factors, which are also expressed in cells lacking myocardin, Wang and colleagues subsequently investigated whether myocardin-related proteins can activate SRF outside the cardiovascular system. They finally identified the two myocardin-related transcription factors (MRTFs) A and B, also called Megakaryoblastic Leukemia 1 and 2 (MKL1/2), which are ubiquitously expressed in embryonic and adult tissues (Guettler et al. 2008; Wang et al. 2002). The proteins of the myocardin family show a certain similarity in their sequence, thus they all contain the following functional domains, which are outlined using MKL1 (MRTF-A) as an example (Figure 7):

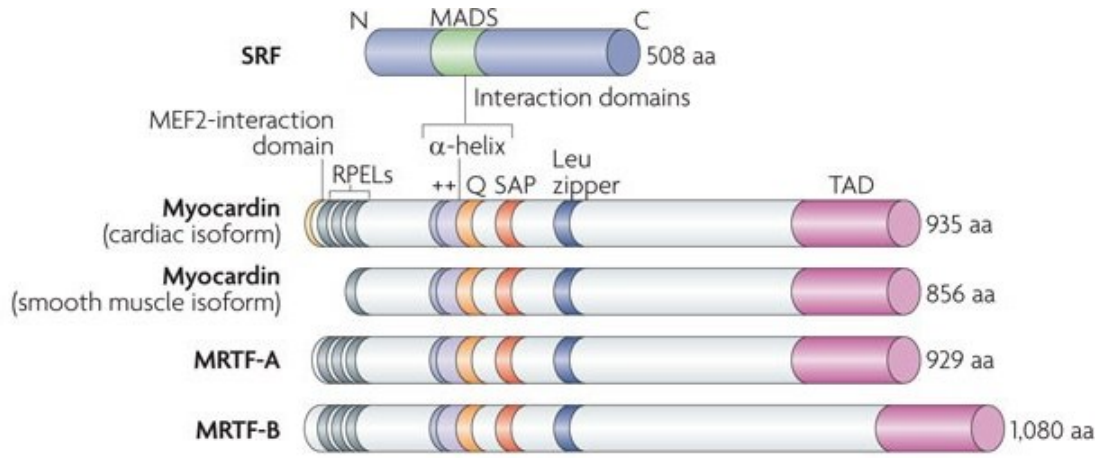

Figure 7: Structure of myocardin family members. The functional domains RPELs, ++, Q, SAP, Leuzipper as well as the TAD domain are shown. In addition, the amino acid length of each myocardin family member and the interaction domain of SRF are shown. This picture is taken from (Olson and Nordheim 2010).

Each member of the myocardin family has three Arg-Pro-X-X-Glu-Leu (RPEL) motifs at the N-terminus called the RPEL domains. The RPEL domain can form a stable complex with three G-actin molecules that keeps MKL1 in cytoplasm and thus inactive it in an unstimulated cell

(Guettler et al. 2008). Stimulation with, for example, serum activates the RhoA signaling pathway leading to polymerization of monomeric G-actin to F-actin (Sotiropoulos et al. 1999). The (three) G-actins bound to RPEL release, thereby allowing translocation of MKL1 into the nucleus (Miralles et al. 2003; Posern et al. 2004; Vartiainen et al. 2007). If MKL1 is located in the nucleus, it interacts with the transcription factor SRF via its basic region (++) and the adjacent glutamine-rich region (Q) and can thus activate it (Wang et al. 2001; Wang et al. 2002). Another important region is the so-called SAP domain, named after SAF-A/B, Acinus, and PIAS, which is also present as a conserved motif in many other nuclear proteins. For example, the SAP structure forms two amphipathic helices that are responsible for some DNA binding activity. Furthermore, the SAP motif in nuclear proteins is probably also associated with their function in transcription with splicing and regulation of apoptosis by chromatin degradation (Aravind and Koonin 2000; Göhring et al. 1997). Nevertheless, the SAP domain of MKL1 does not appear to be required for SRF activation, as deletions of the motif in MKL1 did not affect SRF activation (Cen et al. 2003). The highly conserved leucine zipper structure mediates homo- and heterodimerization of myocardin family proteins (Wang et al. 2001). At the C-terminus of myocardin and myocardin-related proteins is the transcription activation domain (TAD), the depletion of which causes MKL1 to extinguish its abilities as a coactivator for SRF (Cen et al. 2003). In addition, MKL1 is known to be phosphorylated at amino acids 449, 450 and 454 by extracellular-signal regulated kinase 1/2 (ERK1/2), which promotes nuclear export and thus inactivation of MKL1 (Muehlich et al. 2008). Recently, a new interaction domain of MKL1 was identified that is able to interfere with the actin-binding protein filamin A (FLNA), which turns out to be essential for the activity of MKL1 as a coactivator for the transcription factor SRF (Kircher et al. 2015).

2.3.3.2 Biological activity and function of MKL1 and MKL2

As described above, MKL1 and MKL2 act as coactivators of the transcription factor SRF and thus influence essential biological processes such as cell proliferation, migration, differentiation and organization of the cytoskeleton (Pipes et al. 2006). Especially in the field of skeletal muscle differentiation and muscle growth, MKL1/2 play an important role (Selvaraj and Prywes 2003). To learn more about the influence of MKL1 and 2 in embryogenesis and

embryo development, some MKL1 and/or MKL2 knockout studies were performed in mice. Despite the fact that MKL1 is involved in numerous physiological cellular processes through SRF activation, most MKL1 knockout mice are viable and fertile. However, some MKL1 knockout embryos died from cardiac defects and due to myoepithelial cell differentiation defects of the mammary gland, female mice were unable to lactate their offspring with milk (Li et al. 2006; Sun et al. 2006). Furthermore, MKL1/2 also play a prominent role in the physiological maturation of megakaryocytes. Thus, in both MKL1 and MKL2 knockout mice, as well as in MKL1 knockouts alone, a reduced number of platelets as well as a diminished number of mature and differentiated megakaryocytes could be found (Cheng et al. 2009; Smith et al. 2012). A study by Rahman and colleagues further outlined that knockout of either MKL1 or SRF decreases megakaryocyte maturation, resulting in thrombocytopenia as well as that MKL1 overexpression results in increased megakaryopoiesis (Rahman et al. 2018). In addition to the SRF/TCF signaling axis, they suggested the MKL1/SRF signaling pathway as the underlying mechanism in which MKl1 increases both genomic association and SRF activity, which upregulates human megakaryopoiesis (Rahman et al. 2018). Besides, MKL1/2 and SRF in macrophages are essential for cytoskeletal gene expression and promote their proinflammatory specificity (Sullivan et al. 2011). Recent studies suggest that the requirement of MKL1 for proinflammatory transcription in macrophages occurs because MKL1 is co-responsible for the recruitment of members of the H3K4 methylation complex to the inflammatory promoters (Xu et al. 2019). Unlike global MKL1 knockout mice, global MKL2 knockout mouse embryos are unable to develop and die during mid-gestation. The reasons for this are a wide range of cardiovascular defects and also differentiation defects in the smooth muscle, which show that MKL2 is essential for development of the mice embryos (Oh et al. 2005). MKL1 is also implicated in Hutchinson-Gilford progeria syndrome (HGPS), a disease characterized by premature and accelerated cardiovascular dysfunction with extensive fibrosis (Osmanagic-Myers et al. 2019). Thus, the disease is caused by a mutation that leads to increased expression of prelamin A (progerin). At the molecular level, the increased progerin levels lead to increased F-actin/G-actin ratios and increased MKL1 expression in addition to mechanoresponsive changes in the nuclear envelope. The increased MKL1 levels in turn lead to increased endothelial nitric oxide synthase (eNOS) expression in fibroblasts, which ultimately triggers the profibrotic changes (Osmanagic-Myers et al. 2019).

The RhoA/actin/MKL1 signaling cascade also plays a critical role in cellular differentiation of adipocytes (Nobusue et al. 2014). Thus, Nobusue and colleagues showed that during adipocyte differentiation, the RhoA/actin signaling pathway is inhibited, preventing nuclear translocation of MKL1, which in turn leads to expression of the transcription factor peroxisome proliferator-activated receptor γ (PPARγ), which enables adipocyte differentiation. Moreover, they found that MKL1 and PPARγ even act reciprocally antagonistically in the adipocyte differentiation program (Nobusue et al. 2014). Interestingly, McDonald and colleagues uncovered a new regulatory pathway that attenuates the anti-adipogenic activity of MKL1/SRF (McDonald et al. 2015). They showed that loss of MKL1 in MKL1-/- mice leads to increased formation of so-called beige adipocytes. These beige adipocytes develop in response to physiological stimuli in white adipose tissue and, analogous to brown adipose tissue, release their energy thermogenically as heat through expression of the mitochondrial uncoupling protein UCP1. Due to the beige adipocytes, the MKL1 KO mice show an improved metabolic profile, protection against diet-induced adiposity and insulin resistance. This finding could be used to develop new therapeutics to combat obesity and associated comorbidities (McDonald et al. 2015).

In recently published studies, Bian and colleagues identified that MKL1 acts as the effector of RhoA to regulate the skeletal homeostasis by controlling the balance between adipogenic and osteogenic differentiation in bone marrow stem cells (Bian et al. 2016; McDonald et al. 2015; Nobusue et al. 2014). Using MKL1 KO mice, they demonstrated that MKL1 loss leads to lower total body weight, shorter femoral and tibial lengths, as well as significantly decreased bone mass in their femurs and the development of osteopenia with age (Bian et al. 2016). At the molecular level, they hypothesize that, among other factors, the decrease in expression of the MKL1/SRF target gene smooth muscle actin (SMA) plays an important role in the decreased osteogenic differentiation of bone marrow mesenchymal stem cells (BMSCs) (Bian et al. 2016).

Due to the fact that MKL1/2 are translocated into the nucleus via an active RhoA (a potential proto-oncogenic) signaling pathway as described above and thus lead to an increased target gene expression of SRF, they may also be involved in tumorigenesis. Thus, MKL1 was first described in megakaryoblastic leukemia as a fusion protein of MKL1 and RBM15 (RNA binding motif protein 15), which is generated by translocation of chromosomes 1 and 22 (Mercher et al. 2009). Due to the RBM15 moiety, MKL1 is deregulated, is permanently present in the

nucleus, and thus ensures a constant expression of SRF-dependent target genes promoting tumor progression (Cen et al. 2003; Descot et al. 2008). Mouse models were performed to further investigate the RBM15-MKL1 fusion protein (Mercher et al. 2009). Homozygotes were found to be embryonically lethal; heterozygotes were viable but showed an accumulation of megakaryoblasts in the fetal liver and 5% of these transgenic mice developed leukemia (Lee and Skalnik 2012; Mercher et al. 2009). RBM15-MKL1 causes the oncogenic effects in addition to dysregulation of the Notch signaling pathway through altered SRF target gene expression as the fusion protein is constitutively nuclear (Descot et al. 2008; Ma et al. 2007b; Mercher et al. 2009). Experiments by Medjkane and colleagues, for example, showed that MKL1/2 knockdown via RNA interference in human breast cancer cell lines, as well as mouse melanoma cells, diminished cell adhesion, spreading, motility and invasion. This suggests that the presence of MKL1 and MKL2 are required for tumor invasion and metastasis (Medjkane et al. 2009). Moreover, Hampl and colleagues demonstrated in an *in vivo* xenograft that tumor growth could be completely abolished after systemic treatment with MKL1/2 siRNA complexed in polyethyleneimine (PEI) (Hampl et al. 2013). In a recent study, Dong and colleagues established a link between Rictor, a signaling molecule of the mTOR pathway, and MKL1 localization (Dong et al. 2020). They postulate that overexpression of Rictor found in HCC tissue samples leads to phosphorylation of actin-binding LIM protein 1 (ABLIM1), which promotes actin polymerization and thus nuclear localization of MKL1. This results in increased transcription of MKL1/SRF-dependent target genes such as c-fos, which promote HCC migratory ability (Dong et al. 2020). Another current study reveals that the long non-coding RNA PVT1 (plasma cell tumor heterotopic gene 1), which is aberrantly expressed in various cancers, is associated with overexpressed MKL1 levels and thus promotes the migration of HCC cells (Liu et al. 2021). Using bioinformatic analysis, the scientists found that this occurs via the miRNA miR-3619-5p and that this miRNA itself can inhibit MKL1 expression by degradation. However, if the miRNA is increasingly bound to the same protein by elevated PVT1 levels, the degradation of MKL1 does not occur and its protein levels in the nucleus increase (Liu et al. 2021).

2.4 Tetraspanins (TSPANs)

2.4.1 Structure of the tetraspanin proteins

Tetraspanins (TSPANs) are a family of membrane proteins characterized by 4 transmembrane (TM) helices. There are 34 different TSPANs known, 33 of which are found in humans. TSPANs are abundant expressed in the plasma membrane, but also in membranes of intracellular organelles and granules in almost all cells and tissue types (Charrin et al. 2009; Hemler 2005).

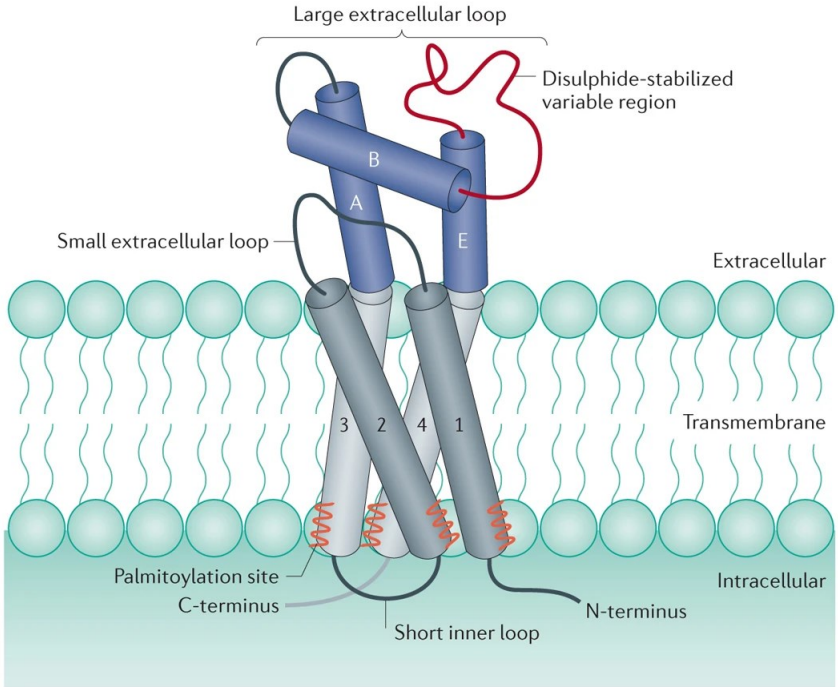

Figure 8: The structure of tetraspanin proteins. Tetraspanin proteins are folded into 4 transmembrane (TM) helices, a large and small extracellular and a small intracellular loop. This picture is taken from (Hemler 2014).

The intact protein is folded into a structure containing 4 TM helices (1-4) (Figure 8). A large extracellular loop connects TM domains 3 and 4 and in turn contains a conserved region with 3 additional helices (A, B, E), as well as a variable region that plays an important role in interaction with other proteins (Kitadokoro et al. 2001; Rajesh et al. 2012; Seigneuret 2006). Typically, this variable region contains two to four disulfide bridges to stabilize the loop structure. A second, smaller extracellular loop of approximately 13-30 amino acids connects TM domains 1 and 2. The third loop of only about 4 amino acids, connecting helices 2 and 3, is located in the cytoplasm. N- and C-termini also terminate in the cytoplasm as short 6-19

amino acid long tails and may represent specific functional links to the cytoskeleton or signaling proteins (Stipp et al. 2003). It is suggested that TSPANs are often present as homodimers in the membrane; furthermore, palmitoylation of membrane-bound cysteines is predicted to further facilitate the association of TSPANs with other proteins (Kovalenko et al. 2004; Stipp et al. 2003). The transmembrane regions themselves are also partly responsible for the biosynthesis and assembly of the so-called "tetraspanin web", a network of tetraspanin-linked membrane proteins, through intra- and intermolecular interactions (Stipp et al. 2003).

2.4.2 Biological function of tetraspanin proteins

Unlike most other cell surface proteins, TSPANs have no obvious function as receptor molecules. Sporadic reports assume that TSPANs can interact directly with cellular or soluble ligands. For example, Waterhouse and colleagues have published that pregnancy-specific glycoprotein 17, a protein secreted in the placenta of mice, binds to TSPAN29 (also known as CD9) from macrophages, which then secrete anti-inflammatory cytokines (Waterhouse et al. 2002). Another group around Bandyopadhyay identified “duffy antigen receptor for chemokines” (DRAK), an endothelial cell surface protein as an interaction partner of TSPAN27 (also called CD82), which is hypothesized to be essential for the function of CD82 as a suppressor for metastases (Bandyopadhyay et al. 2006). However, it is very typical for TSPANs to organize with other membrane proteins into so-called tetraspanin-enriched microdomains (TEMs). These TEMs are in turn assembled into a larger network of secondary interactions, also called "tetraspanin web" (Charrin et al. 2009; Hemler 2005). Due to the component of TEMs, TSPANs have a strong influence on cell adhesion, migration, invasion, signaling, cell-cell fusion and also virus infections, all of which are important in cancer development (Hemler 2005, 2014; Peñas et al. 2000; Yáñez-Mó et al. 2009). For example, some of the TSPANs such as CD151 interact with different integrins and thus modulate cell adhesion to different lamins of epithelial or endothelial cells influencing in turn cell morphology, migration and signaling (Berditchevski 2001; Yauch et al. 1998). Physiologically important lamin-binding complexes are formed by TSPAN CD151 with the integrins α3ß1 and α6ß1 in the kidney and with α3ß1 and α6ß4 in the skin. Furthermore, CD151 was discovered by Karamatic Crew and colleagues

to be part of the MER2 antigen on erythrocytes. In rare cases, mutations of CD151 have been detected in which the TSPAN protein is truncated and its integrin-binding domain is missing. Patients with this mutation suffer from end-stage hereditary nephritis and a type of skin-blistering disease known as pretibial epidermolysis bullosa. These findings suggest that TSPAN CD151 is essential for the correct assembly of the glomerular and tubular basement membrane in the kidney and is also of importance for the skin (Karamatic Crew et al. 2004).

Other studies show the importance of TSPAN28 (CD81) in T-cell development. Interaction between immature thymocytes and stromal cells expressing CD81 is necessary for their development. Thus, a specific CD81 mouse antibody suppressed T-cell development in fetal organ cultures (Boismenu et al. 1996). Furthermore, TSPAN26 (referred to as CD37) plays a critical role in the interaction of T-cells and B-cells in the humoral immune response. Thus, in CD37 knockout mice, only strongly reduced IgG1 levels and alterations in the immune response to T-cell dependent antigens could be observed (Knobeloch et al. 2000). One of the first discovered interactions of TSPANs and integrins was the interaction of CD9 with αIIbß3 integrin at the glycoprotein Hb-IIIa complex, which stimulates thrombocyte activation (Slupsky, JR et al. 1989). Moreover, the importance of CD9 for successful fertilization was demonstrated in a mouse model. Here, CD9 knockout mice showed reduced fertility because sperm did not fuse with ovulated oocytes. CD9 seems to be essential for sperm-egg fusion, in which CD9 associated integrin α6ß1 is involved (Le Naour et al. 2000). Another TSPAN22 (also called peripherin-2 or tetraspanin RDS) is essential for the visual process. More than 70 different mutations are known in this protein, which leads to retinal dystrophies by disturbing the parallel layer structure of the outer segments of the photoreceptor cells (Hemler 2005; Kohl et al. 1998). Studies by Berditchevsky and Odintsova show that TSPANs are colocalized with "myristolated alanine-rich C kinase substrates" (MARCKS), which are prominent substrates for various members of the protein kinase C (PKC) family and probably influence cell migration by regulating the dynamics of the cortical cytoskeleton (Berditchevski and Odintsova 1999; Wiederkehr et al. 1997). In addition, certain TSPANs themselves such as CD9, CD81, CD82, or CD151 can also associate with PKC, making it probable that the TSPANs are involved in actin organization through their interaction with PKCs and MARCKs (Zhang et al. 2001). Several of the TSPANs interact with and regulate the ADAM metalloproteases (a disintegrin and metalloproteinase). For example, TSPAN5 has a regulatory effect on the exit

of ADAM10 from the endoplasmic reticulum and its transport to the plasma membrane, where ADAM10 interacts with TSPAN15. ADAM10 is responsible for the cleavage of various substrates such as cadherins, growth factors or chemokines and activation of signaling pathways through its proteolytic capabilities. Dysregulation of this interplay can be linked to disorders that lead to cancer, Alzheimer's disease or inflammation (Koo et al. 2020; Saint-Pol et al. 2017).

2.4.3 Tetraspanins and their role in viral infections

It is also known that TSPANs as a component of TEMs, located in the plasma membrane, assist some viruses such as HPV16, coronaviruses, influenza viruses or hepatitis viruses in virus-cell fusion and thus virus entry (Earnest et al. 2015; Harris et al. 2010; Mikuličić et al. 2020). Several proteases are bundled in the TEMs, which, for example, cleave the viral glycoproteins from coronavirus or influenza A virus, which is essential for virus-cell fusion. Thus, TEMs are particularly suitable virus entry portals (Earnest et al. 2015). In the case of human papillomavirus (HPV16), which also acts as an agent for various cancers such as cervical cancer, it has been determined that endocytosis of the virus in keratinocytes occurs through interaction with TEMs. More specifically, CD9, also known as TSPAN29, interacts with ADAM17 and capsid proteins of the virus, triggers an ADAM17-dependent ERK1/2 signal transduction and sets up the entry platform for the viral particles. Interestingly, both increased and decreased CD9 levels seem to inhibit virus uptake and thus infection rates. This suggests that a specific CD9 optimum promotes ADAM and ERK-1/2 activity and associated viral infection (Mikuličić et al. 2020). In the case of hepatitis C virus (HCV), which can lead to progressive liver disease and hepatocellular carcinoma, Harris and colleagues found that CD81 (TSPAN28), the scavanger receptor class B member I (SR-B1), the tight junction proteins Claudin-1 (CLDN1) and Occludin play a significant role (Figure 9). After circulating HCV particles come into contact with the cell's low density lipoprotein receptor (LDLR) and glycosaminoglycans (GAG) via their low and very low density lipoprotein (LP), virus entry can begin. Here, CD81 and the SR-BI are suggested to mediate viral attachment to the host cell through interaction with HCV-encoded glycoproteins (Moradpour et al. 2007). Furthermore, the complex of CD81 and CLDN1 is essential for viral infection, since after mutations in CLDN1 there is no interaction between

the two proteins and no viral entry (Harris et al. 2010). Moreover, HCV infection could be inhibited by the application of anti-CD81 antibodies even after viral internalization, leading to the assumption that intracellular CD81 also contributes to HCV infection (Farquhar et al. 2012).

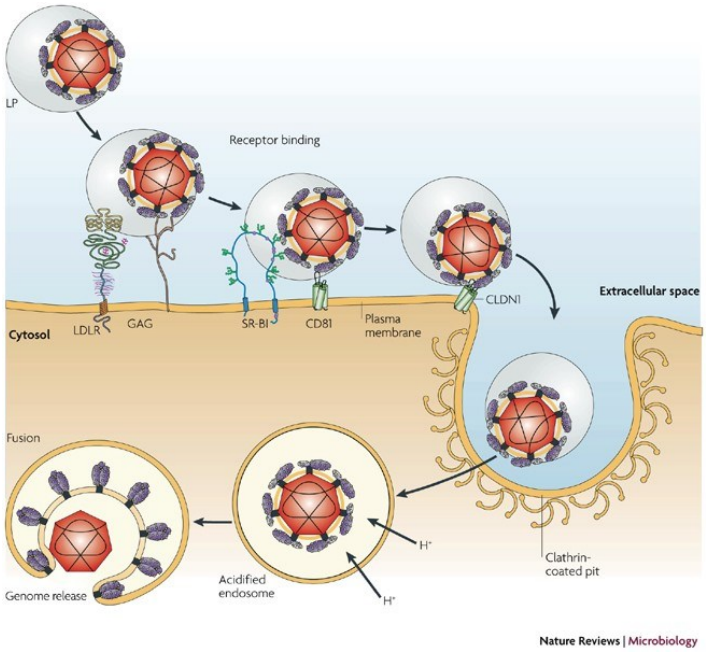

Figure 9: The involvement of TSPAN CD81 in hepatitis C virus particle uptake. Circulating HCV particles presumably associate with the cell's low density lipoprotein receptor (LDLR) and glycosaminoglycans (GAG) via their low and very low-density lipoprotein (LP), which can initiate virus uptake. The surface proteins CD81 (TSPANs 28), SR-BI, as well as claudin 1 (CLDN1) are assumed to promote further viral attachment. Internalization of the virus occurs via clathrin-mediated endocytosis. This picture is taken from (Moradpour et al. 2007).

2.4.4 Tetraspanins and cancers

Through various studies, some TSPANs are known to promote tumorigenesis, development and metastasis, as well as TSPANs, which counteract it and prevent tumor progression. For example, the TSPANs CD9 and CD81, just described above, contribute to possible developing tumor disease by their involvement in the uptake of HPV16 and HCV particles (Harris et al. 2010; Mikuličić et al. 2020). For TSPAN CD37, which is expressed on mature B-cells and to a lesser extent on T-cells, high levels of CD37 expression have been identified in non-Hodgkin lymphoma (NHL) or chronic lymphocytic leukemia (CLL) (Krause et al. 2012). Since then, there have been some attempts to use CD37 as a therapeutic target, for example with specific anti-

CD37 antibodies or with CD37 specific “small modular immunopharmaceuticals” (CD37-SMIP) (Krause et al. 2012; Zhao et al. 2007). In the presence of a crosslinker CD37-SMIP molecules induce potent apoptosis and antibody-dependent cellular cytotoxicity against corresponding NHL and CLL cell models. Moreover, significant therapeutic efficacy has been demonstrated in a severe combined immunodeficiency (SCID) mouse xenograft leukemia/lymphoma model (Zhao et al. 2007). High CD151 expression is also associated with increased tumor progression, larger tumor size, and poorer survival in various cancer types (Kwon et al. 2012; Zöller 2009). For example, in liver cancer, the expression of CD151 is elevated compared to healthy cells and could be correlated with an increased metastatic tendency in the HCC cell model and thus a poor prognosis (Ke et al. 2009). TSPAN CD9 (TSPAN29) is considered a surface marker of acute lymphoblastic leukemia, expressed in 90 % of cases, as well as in acute myeloid leukemias and acute promyelocytic leukemia (Boucheix et al. 1985). Analogous to CD151, CD9 is associated with tumor cell migration and metastasis, whereas CD9 expression is associated with less aggressive potential compared to CD151 expression. In fact, it appears that CD9 effects may be progressive or suppressive, depending on the type of cancer. Thus, in lung or fibrosarcoma cell lines as well as in colon carcinoma cells, CD9 has an inhibitory role on motility and proliferation, whereas low CD9 expression promotes ovarian carcinoma progression (Chen et al. 2011; Furuya et al. 2005; Ikeyama et al. 1993; Ovalle et al. 2007). Both siRNA and CD9 antibodies have been used to target CD9 in tumors. Experiments here even showed that anti-CD9 antibodies stimulated the invasion of endometrial cancer cell lines, indicating an inhibitory effect of CD9 on invasion (Park et al. 2000). In contrast, increased levels of CD9 are expressed in end-stage head and neck squamous cancer and in gastric cancer (Erovic et al. 2003; Nakamoto et al. 2009). Here, anti-CD9 antibody treatment of gastric cancer cell xenografts showed antitumor effects (Nakamoto et al. 2009). Also, TSPAN8 (also Co-029) is known to be increasingly expressed in tumor tissues of gastric, colon, rectal, pancreatic or hepatocellular carcinoma (Zöller 2009). Since it is also present in metastases from melanoma, liver or colon cancer, it is thought to contribute to tumor progression and metastasis (Berthier-Vergnes et al. 2011; Greco et al. 2010; Kanetaka et al. 2003). TSPAN CD82 (also TSPAN27 or KAI1) is usually found widespread in human tissues, but its expression in invasive or metastatic tumor tissues is significantly reduced or even lost. This in turn leads to the assumption that

CD82 plays a metastatic suppressor role in many different tissues and its absence correlates with a poor clinical outcome (Tonoli and Barrett 2005; Zöller 2009).

In summary, the TSPAN family is a very large and widespread protein family in human tissues that has a significant impact on the biological activity of a cell but also on its pathogenesis through interaction with a wide variety of proteins in the context of TEMs. Because of this enormous importance and the fact that TSPANs have often been neglected in research, it is an important task to find out more about their function and how they interact with other proteins.

2.5 Senescence in aging and cancer

2.5.1 Cellular senescence

The term cellular senescence originates from Hayflick and Moorhead, who discovered that normal human fibroblasts no longer replicate after a certain number of cell doublings in culture and enter a kind of irreversible growth arrest (Hayflick and Moorhead 1961). In contrast, cancer cells do not enter a state of growth arrest but continue to proliferate indefinitely (Hayflick and Moorhead 1961). The Hayflick limit, named after its discoverer, states that normal mitotic cells can replicate about 50 times before they eventually become senescent and undergo permanent growth arrest. They also showed that the senescent cells no longer proliferate, but nevertheless remain viable and metabolically active (Hayflick and Moorhead 1961; Sherwood et al. 1988). Furthermore, senescent cells also undergo structural and morphological changes, such as having an enlarged, circular and flat shape and a vacuole-rich cytoplasm (Sikora et al. 2016). Also very characteristic is an increased lysosomal activity of senescence associated ß-galactosidase, a cytoplasmic enzyme which, due to its pH optimum of 4, can only be active in senescent cells with a pH of 6 and not in normal cells (Dimri et al. 1995; Morreau et al. 1989). With initially colorless substrates such as 5-bromo-4-chloro-3-indolyl-ß-D-galactopyranoside (X-Gal) cleaved by ß-galactosidase into colored products, the ß-galactosidase senescence assay became the gold standard for histochemical detection of senescence *in vitro* or *in vivo* (Dimri et al. 1995; Lee et al. 2006). In 1990, Harley and colleagues confirmed that the cellular senescence model was due to a loss of telomeric DNA. Telomeres, which are a repetitive sequence of TTAGGG, are located at the ends of the chromosomes and

are shortened by each cell cycle until they exceed a certain threshold that forces the cells into senescence (Harley 1991). This natural type of senescence is therefore also called replicative senescence. The reason for the progressive shortening of the telomeres is that the DNA synthesis by DNA polymerase always takes place only from the 5' to the 3' end. Thus, the end of the lagging strand from the 3' to the 5' end cannot be duplicated and is therefore shortened by one section after each cell division (Harley et al. 1990; Olovnikov 1971). The process of telomere shortening can be stopped efficiently by the reverse transcriptase activity of the enzyme telomerase (Greider and Blackburn 1985, 1987). However, telomerase activity is absent or very low in most normal somatic cells, whereas it is significantly abundant in germline tissues, stem cells or in cancer cells (Shay and Bacchetti 1997; Wright et al. 1996). Harley and colleagues already correctly observed that the older the tissue donor, the shorter the telomere length, and thus the cells are more likely to convert to senescent cells (Harley et al. 1990). For example, senescent cells have been found to be more abundant in aging skin as well as in liver tissue or the retina, thus establishing a link between senescent cells and the process of aging (Dimri et al. 1995; Mishima et al. 1999; Paradis et al. 2001). Furthermore, senescence can contribute to the aging process not only by accumulation of senescent cells in tissues, but also by limiting stem cell function (Collado et al. 2007). In addition to the progressive shortening of telomeres, other independent senescence-triggering factors have been identified in recent years (Figure 10). These different stress stimuli for cells can be, for example, oxidative stress, DNA damage, telomeric dysfunction or several chemotherapeutic agents such as cisplatin or doxorubicin (Collado and Serrano 2006).

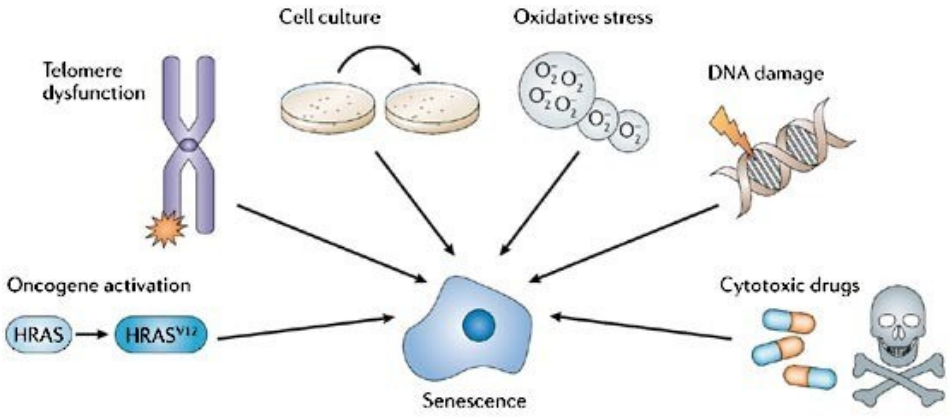

Figure 10: Various factors leading to senescence. Due to various stresses such as oxidative stress, telomere dysfunction, DNA damage or several chemotherapy drugs, cells go into irreversible proliferation arrest of senescence. This picture is taken from (Collado and Serrano 2006).

2.5.2 Oncogene-induced senescence

In addition to the previously known replicative senescence, a new form of senescence, the so-called oncogene-induced senescence (OIS), was described by Serrano and colleagues in 1997 (Serrano et al. 1997). As just described, various stress stimuli can induce senescence. Since cancer cells are exposed to many types of stress, here senescence induction could counteract tumor progression. Thus, Serrano and colleagues were able to show for the first time that the expression of the oncogene H-Ras (*H-Ras*^{GV12}) leads to a permanent G1 arrest accompanied by upregulation of p53 and p16^{INK4a} and p21$^{CIP/WAF1}$, which is indistinguishable from the state of cellular senescence (Serrano et al. 1997). Their findings suggest that senescence not only occurs after an accumulation of natural cell divisions, but can be activated prematurely in the early stages of tumorigenesis in response to oncogenes (Serrano et al. 1997). Studies based on this finding showed that, in addition to overexpression of the oncogenic H-Ras, the individual oncogenic variants of the Ras signal cascade, such as Raf, Mek, or Braf, also trigger an OIS response (Lin et al. 1998; Michaloglou et al. 2005; Zhu et al. 1998). Meanwhile, many oncogenes are known to induce OIS, such as the mentioned oncogene Braf, EGFR, HER2 or PI3K (Angelini et al. 2013; Garbers et al. 2013). Braf for example, a protein kinase and effector of Ras, which is often expressed as an oncogene Braf^{V600E} in human naevi, induces a senescence-induced arrest of the cell cycle in human melanocytes and can thus often prevent the development of a malignant tumor (melanoma) *in vivo* (Gorgoulis and Halazonetis 2010;

Michaloglou et al. 2005). As OIS emerged as an effective tumor suppressor mechanism, it has become an important area of tumor research where much remains to be explored due to the multifaceted processes and multiple effector mechanisms.

2.5.3 Signaling pathways inducing senescence

Investigations revealed that two signaling pathways in particular, firstly the $p16^{INK4a}$/Rb and secondly the ARF/p53 signaling pathway, play a significant role in the execution of the proliferation arrest characteristic of senescence (Campisi 2005). Since these two signaling pathways are thought to be responsible for tumor suppression through OIS and they frequently mutate in formed tumors, they are of great importance in the field of research and alterations in the individual proteins are often detected as senescence markers (Hollstein et al. 1991; Sharpless and DePinho 1999). As shown in Figure 11, the two most important signaling cascades for OIS development are described here:

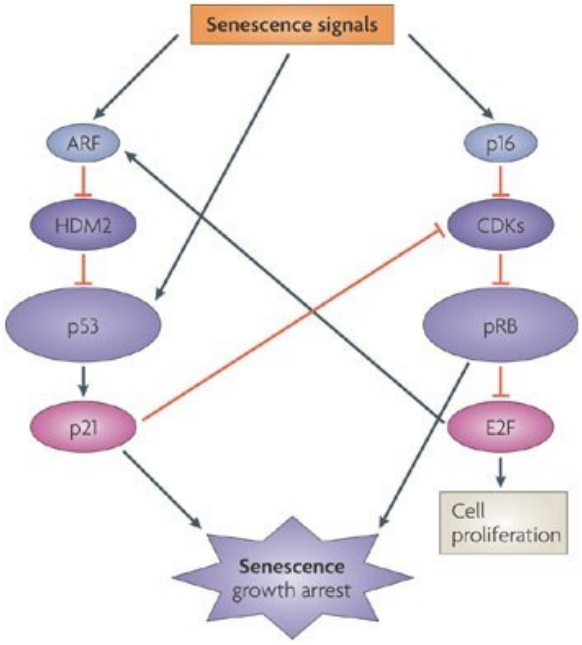

Figure 11: Senescence induction by the ARF/p53 and $p16^{INK4a}$/pRb signaling pathways. Left panel: Senescence-inducing signals activate ARF, which consequently activates p53 via inactivation of HDM2. Active p53 induces the expression of the cyclin-dependent inhibitor p21, which ultimately executes the senescence response. Right panel: senescence triggers induce expression of CDK inhibitor $p16^{INK4a}$, which disrupts phosphorylation of Rb by inhibiting CDK4/6. Inactivation of Rb stops transcription factor E2F and thus transcription of genes essential for cell proliferation and induces senescence with growth arrest. This picture is taken from (Campisi and Di d'Adda Fagagna 2007).

First, the most important signaling pathway for senescence induction, $p16^{INK4a}$/Rb, which was already described by Serrano and colleagues in 1997 and is also known as the Raf/Mek/ERK pathway (Lin et al. 1998; Serrano et al. 1997; Zhu et al. 1998). $p16^{INK4a}$ is downstream of the small RhoGTPase Ras and, as a CDK inhibitor protein, $p16^{INK4a}$ inhibits CDK4/6 by binding (Zhu et al. 1998). By inhibiting the kinase activity of CDK4/6, $p16^{INK4a}$ prevents the phosphorylation of Rb and the active hypophosphorylated Rb associates with the transcription factor E2F (Chicas et al. 2010; Futreal and Barrett 1991; Hara et al. 1996; Serrano et al. 1997). This complex formation between hypophosphorylated Rb and the transcription factor E2F in turn inhibits the transcription of the target genes cyclin A and cyclin E, which are ultimately essential for the transition of G1 phase to S phase (Riley et al. 1994; Serrano et al. 1997; Weinberg 1995). In summary, $p16^{INK4a}$ regulates the transition from G1 to S phase by inhibiting the CDK4/6 kinases. Indeed, increased $p16^{INK4a}$ protein and mRNA levels can be detected, for example, in senescent fibroblasts compared to normal control cells (Hara et al. 1996; Serrano et al. 1997). Second, the Arf/p53/p21 signaling pathway (ARF stands for alternate reading frame) plays a significant role in the senescence response. Again, Serrano and colleagues published in 1997 that the activity of the tumor suppressor p53 is increased upon accumulation of cell doublings and cells exposed to stress stimuli (Serrano et al. 1997). The expression of the tumor suppressor p53 is regulated by ARF by binding to and thus inactivating the E3 ubiquitin protein ligase Mdm2/Hdm2. Thereby ARF refrains the ubiquitination of p53 and thus forcing p53 activity (Kim and Sharpless 2006). Subsequently, p53 itself leads to transcription and translation of p21, a CDK inhibitor protein, which induces a senescence response by accumulating in the cells (Brown et al. 1997). In addition to p21-induced senescence induction and accumulation of p21 in senile cells, it has been shown that loss of p21 leads to increased longevity (Brown et al. 1997; Tahara et al. 1995). Furthermore, the ARF/p53 and the $p16^{INK4a}$ /Rb signaling pathways are interconnected via p21. Thus, p21 was found to additionally inhibit the cyclin/CDK2 complex, so that p21 also ultimately inhibits the phosphorylation of Rb in addition to $p16^{INK4a}$ (Serrano et al. 1997). In murine tissues, as well as in human premalignant neoplastic lesions, increased expression levels of $p16^{INK4a}$, ARF, and p53 were found as markers that the cells were undergoing oncogene-induced senescence (Braig et al. 2005; Chen et al. 2005; Collado et al. 2005; Lazzerini Denchi et al. 2005;

Michaloglou et al. 2005). This demonstrates that the p53, $p16^{INK4a}$, and ARF proteins play crucial roles in the activation of senescence *in vitro* as well as *in vivo*.

In summary, both pathways, either alone or in combination, can control and interrupt cell cycle steps, leading to senescence induction and preventing tumorigenesis. This suggests that senescence induction is also a promising strategy in the field of tumor therapy.

3 Aim of the thesis

Previous studies by our group have revealed that loss of the tumor suppressor Deleted in Liver Cancer 1 (DLC1) promotes a persistently active RhoA signaling cascade. This results in MKL1, a coactivator of the transcription factor serum response factor (SRF), being permanently translocated into the nucleus, leading to increased expression of MKL1/SRF target genes that exhibit tumor-promoting effects. Further, our group recently described that restoration of DLC1 expression can prevent tumorigenic effects by senescence induction. However, since this principle is not amenable to therapeutic application, gene expression profiling was performed in HepG2 cells depleted of DLC1 to identify druggable gene targets mediating the effects of DLC1 on senescence induction. Above the threshold of 3.0-fold increased expression in the DLC1 knockdown cells compared to the control cells, five novel DLC1 dependent genes were identified: Versican (VCAN), Tetraspanin 5 (TSPAN5), Meprin 1A (MEP1A), Histon cluster 1 H2B family member K (HIST1H2BK) and N-Cadherin (CDH2).

Given the existing preliminary data, the following three main issues will be addressed within this thesis:

I. Validation of upregulation of newly identified gene targets after DLC1 loss
II. Investigation of the newly found DLC1 dependent genes target for MKL1 and FLNA dependency
III. Determination of the functional effects of the newly identified DLC1 dependent gene targets on HCC development and progression
IV. Uncovering the molecular mechanism underlying the HCC growth arrest upon TSPAN5 depletion
V. Revealing the effects of TSPAN5 depletion on the MKL1/SRF signaling pathway and its target gene expression
VI. Confirming the *in vitro* results revealing TSPAN5 as a potential therapeutic target in HCC by different *in vivo* models

4 Materials

4.1 Cell culture

4.1.1 Cell lines

Table 1: Cell lines and their culture medium

Cell line	Origin and cell type	Culture medium	Provider
3T3	murine fibroblast cell line	DMEM	ATCC, Manassas, VA, USA
A7	human melanoma cell line	MEM	ATCC, Manassas, VA, USA
Hep3B	human hepatocellular carcinoma cell line	DMEM	Prof. Claus Hellerbrand, FAU Erlangen, Germany
HepG2	human hepatocellular carcinoma cell line	RPMI	Prof. Dr. Stephan Singer, University of Tübingen, Tübingen, Germany
HepG2 DLC1 CRISP Cas9 KO	human hepatocellular carcinoma cell line	RPMI	Synthego Corporation, Menlo Park, CA, USA
HepG2 MLC	human hepatocellular carcinoma cell line with empty vector	RPMI	Dr. Scott Lowe, Cold Spring Harbor, New York, NY, USA
HepG2 shRNA DLC	human hepatocellular carcinoma cell line with stable DLC1 knockdown	RPMI	Dr. Scott Lowe, Cold Spring Harbor, New York, NY, USA
HLF	human hepatocellular carcinoma cell line	RPMI	Prof. Dr. Stephan Singer, Ernst-Moritz-Arndt-Universität Greifswald, Greifswald, Germany
HuH6	human hepatocellular carcinoma cell line	DMEM	Prof. Dr. Stephan Singer, University of Tübingen, Tübingen, Germany
HuH7	human hepatocellular carcinoma cell line	RPMI	ATCC, Manassas, VA, USA
M2	human FLNA-deficient melanoma cell line	MEM	ATCC, Manassas, VA, USA

4.1.2 Cell culture media

Table 2: Cell culture media and their supplements

Medium or supplement	Manufacturer
DMEM (Dulbecco's Modified Eagle Medium)	Merck KGaA, Darmstadt, Germany
Opti-MEM	Merck KGaA, Darmstadt, Germany
RPMI (RPMI 1640 medium)	Merck KGaA, Darmstadt, Germany
Gibco® Fetal Bovine Serum (FBS)	Thermo Fisher Scientific, Waltham, MA, USA
Penicillin-Streptomycin (5000 U/mL)	Thermo Fisher Scientific, Waltham, MA, USA

4.1.3 Transfection reagents

Table 3: Transfection reagents

Reagent	Manufacturer
GenJet™ DNA In Vitro Transfection Reagent	SignaGen Laboratories, Rockville, MD, USA
Lipofectamine® 2000 Reagent	Thermo Fisher Scientific, Waltham, MA, USA
Lipofectamine®RNAiMAX™ Reagent	Thermo Fisher Scientific, Waltham, MA, USA

4.2 Nucleic acids

4.2.1 Plasmid constructs

Table 4: Plasmid constructs used for transient plasmid transfection

Plasmid construct	Vector	Manufacturer
p3xFlag-MKL1-N100 (MKL1N100)	pCin4	Kind gift of Prof. Ron Prywes, Columbia University, NY, USA

p3xFlag 7.1 (empty vector)	pCin4	Merck KGaA, Darmstadt, Germany
pCMV-AC-GFP-TSPAN5 (GFP-TSPAN5)	pCMV6-AC-GFP	OriGene Technologies, Inc., Rockville, MD, USA
pEGFP-N1 (empty vector)	pCMV6-AC-GFP	Merck KGaA, Darmstadt, Germany

4.2.2 Primers

Target gene specific primers were custom-synthesized and delivered as lyophilisates (Merck KGaA, Darmstadt, Germany). Before use, they were dissolved with nuclease free H_2O to a final concentration of 50 nM.

Table 5: Human primers for qRT-PCR and their sequences

Primer	Sequence
18S Fw **18S Rv**	5'-TCG AGG CCC TGT AAT TGG AAT-3' 5'-CCC TCC AAT GGA TCC TCG TTA-3'
Catenin Fw **Catenin Rv**	5'-CACAAGCAGAGTGCTGAAGGTG-3' 5'- GATTCCTGAGAGTCCAAAGACAG-3'
CDH2 Fw **CDH2 Rv**	5'-CTCCATGTGCCGGATAGC-3' 5'-CGATTTCACCAGAAGCCTCTAC-3'
CNN1 Fw **CNN1 Rv**	5'-GCT GTC AGC CGA GGT TAA GA-3' 5'-CCC TCG ATC CAC TCT CTC AG-3'
CTGF Fw **CTGF Rv**	5'-TTG GCA GGC TGA TTT CTA GG-3' 5'-GGT GCA AAC ATG TAA CTT TTG G-3'
CXCL10 Fw **CXCL10 Rv**	5'-CCC CAC GTT TTC TGA GAC AT-3' 5'-TGG CAG TTT GAT TCA TGG TG-3'
DLC1 Fw **DLC1 Rv**	5'-GAGCAGTGTCATGCCTTGG-3' 5'-GCGAATGAGTTCTGTCATTTCA-3'
FLNA Fw **FLNA Rv**	5'-TCG CTC TCA GGA ACA GCA-3' 5'-TTA ATT AAA GTC GCA GGC ACC TA-3'

GLIPR1 Fw	5’-TCT TTC CAA TGG AGC ACA TTT-3’
GLIPR1 Rv	5’-TCT TAT ATG GCC AAG TTG GGT AA-3’
HIST1H2KB Fw	5´-ACC TCC AGG GAG ATC CAG AC -3´
HIST1H2KB Rv	5´- TCC AGA GAA AGT CCC TCC TGG -3´
Ki67 Fw	5´- TCA AGG ACC TGA TTC AGG AGA AG -3´
Ki67 Rv	5´- GTG CAC TGA AGA ACA CAT TCC -3´
MEP1A Fw	5’-CTTGTTGGGACAATGCACAG-3’
MEP1A Rv	5’-GGGTAAAGAATCCGAGACTCC-3’
MKL1 Fw	5’-CCC AAT TTG CCT CCA CTT AG-3’
MKL1 Rv	5’-CCT TGG CTC ACC AGT TCT TC-3’
SM22 Fw	5’-GGC CAA GGC TCT ACT GTC TG-3’
SM22 Rv	5’-CCC TTG TTG GCC ATG TCT-3’
SRF Fw	5’-AGC ACA GAC CTC ACG CAG A-3’
SRF Rv	5’-GTT GTG GGC ACG GAT GAC-3’
TGFβ1 Fw	5’-ACT ACT ACG CCA AGG AGG TCA C-3’
TGFβ1 Rv	5’-TGC TTG AAC TTG TCA TAG ATT TCG-3’
TNFSF 10 Fw	5’-TTC ACA GTG CTC CTG CAG TC-3’
TNFSF 10 Rv	5’-GCC ACT TTT GGA GTA CTT GTC C-3’
TSPAN5 Fw	5’-ATGCAAGTCGAGAGCGATGT-3’
TSPAN5 Rv	5’-GGCATCATAGCCACACTGAG-3’
VCAN Fw	5’-GCACCTGTGTGCCAGGATA-3’
VCAN Rv	5’-CAGGGATTAGAGTGACATTCATCA-3’
Random Hexamers	5’-NNN NNN-Wobbles-3’

Table 6: Human primers for ChIP qRT-PCR and their sequences

Primer	Sequence
CDH2 Fw	5´-ACCCAGAGATCAAGGAGGTG-3’
CDH2 Rv	5´-CTCCACTTCCACCTCCACAT-3’
TSPAN5 Fw	5´-GCTCATCAATCCCGGTCA-3’
TSPAN5 Rv	5´-GGCGAGAGGGAGAAGGAA-3’

VCAN Fw	5´-ACCTCTTGGCGTTTCTTCCT-3’
VCAN Rv	5´-CTCCTTTCCCCTAACCCAGA-3’

4.2.3 siRNAs

All siRNA oligonucleotides were custom-synthesized (Merck KGaA, Darmstadt, Germany). The lyophilized siRNAs were dissolved in nuclease free H_2O to a final concentration of 50 µM.

Table 7: Human siRNAs and their sequences

siRNA	Sequence of sense and antisense
sictrl	5’-CGUACGCGGAAUACUUCGA[dT][dT]-3’ 5’-UCGAAGUAUUCCGCGUACG[dT][dT]-3’
siCDH2	5’-AAAGTGGCAAGTGGCAGTAAA[dT][dT]-3’ 5’-UUUACUGCCACUUGCCACUUU[dT][dT]-3’
siDLC1	5’-UUAAGAACCUGGAGGACUA[dT][dT]-3’ 5’-UAGUCCUCCAGGUUCUUAA[dT][dT]-3’
siFLNA	5’-GCACAUGUUCCGUGUCCUA[dT][dT]-3’ 5’-UAGGACACGGAACAUGUGC[dT][dT]-3’
siMKL1/2	5’-AUGGAGCUGGUGGAGAAGAA[dT][dT]-3’ 5’-UUCUUCUCCACCAGCUCCAU[dT][dT]-3’
siSRF	5’-GUGAGACAGGCCAUGUGUA[dT][dT]-3’ 5’-UACACAUGGCCUGUCUCAC[dT][dT]-3’
siTSPAN5 V1	5´-GAGCAUAUCGGGAUGACAU[dT][dT]-3’ 5´-AUGUCAUCCCGAUAUGCUC[dT][dT]-3’
siTSPAN5 V2	5´-GACCAGCUGUAUUUCUUUA[dT][dT]-3’ 5’-UAAAGAAAUACAGCUGGUC[dT][dT]-3’
siVCAN	5´-GAGGCUGGAACUGUUAUUA[dT][dT]-3’ 5´-UAAUAACAGUUCCAGCCUC[dT][dT]-3’

4.3 Antibodies

4.3.1 Primary antibodies for immunoblotting

Primary antibodies used for immunoblotting were diluted in 10 ml Tris-buffered saline with Tween 20 supplemented with a spatula tip bovine serum albumin (BSA) and 100 µl of a 2 % sodium azide solution to get a final concentration of 0.02 % for conservation.

Table 8: Primary antibodies and their indicated dilution for immunoblotting

Antibody (host)	Dilution	Manufacturer
anti-Actin (rabbit)	1:1000	Merck KGaA, Darmstadt, Germany
anti-DLC1 (mouse)	1:1000	BD Bioscience, San Jose, CA, USA
anti-E-Cadherin (rabbit)	1:1000	Cell Signaling Technology, Danvers, MA, USA
anti-Erk1/2 (p44/42 MAPK) (rabbit)	1:10000	Cell Signaling Technology, Danvers, MA, USA
anti-GLIPR1 (rabbit)	1:500	Thermo Fisher Scientific, Waltham, MA, USA
anti-H3K9me3 (rabbit)	1:500	Actif Motif, Carlsbad, USA
anti-HSP90 (mouse)	1:1000	Santa Cruz Biotechnology, Inc., Dallas, TX, USA
anti-Myoferlin (mouse)	1:250	Santa Cruz Biotechnology, Inc., Dallas, TX, USA
anti-N-Cadherin (rabbit)	1:500	Cell Signaling Technology, Danvers, MA, USA
anti-p16^{INK4a} (goat)	1:250	R&D Systems, Inc., Minneapolis, MN, USA
anti-phospho-p44/42 MAPK (Erk1/2) (Thr202/Tyr204) (rabbit)	1:1000	Cell Signaling Technology, Danvers, MA, USA
anti-pRb (mouse)	1:500	BD Bioscience, San Jose, CA, USA
anti-SLUG (rabbit)	1:1000	Cell Signaling Technology, Danvers, MA, USA

anti-SMA (rabbit)	1:500	Abcam, Cambridge, UK
anti-SRF (rabbit)	1:500	Santa Cruz Biotechnology, Inc., Dallas, TX, USA
anti-Transgelin (SM22) (mouse)	1:1000	Merck KGaA, Darmstadt, Germany
anti-TSPAN5 (rabbit)	1:500	Merck KGaA, Darmstadt, Germany
anti-Versican (mouse)	1:500	Santa Cruz Biotechnology, Inc., Dallas, TX, USA
anti-Vimentin (rabbit)	1:1000	Cell Signaling Technology, Danvers, MA, USA
anti-Vincullin (mouse)	1:1000	Merck KGaA, Darmstadt, Germany
anti-ZO-1 (rabbit)	1:1000	Cell Signaling Technology, Danvers, MA, USA

4.3.2 Secondary antibodies for immunoblotting

Secondary antibodies were diluted as indicated in TBS-T immediately prior to use.

Table 9: Secondary antibodies and their indicated dilution for immunoblotting

Antibody	Dilution	Manufacturer
anti-goat IgG, HRP-linked antibody	1:50000	Santa Cruz Biotechnology, Inc., Dallas, TX, USA
anti-mouse IgG, HRP-linked antibody	1:10000	Cell Signaling Technology, Danvers, MA, USA
anti-rabbit IgG, HRP-linked antibody	1:10000	Cell Signaling Technology, Danvers, MA, USA

4.3.3 Antibodies for RhoA assay

Table 10: Antibodies used for RhoA assay

Antibody	Manufacturer
anti-active RhoA (mouse)	NewEast Bioscience, Malvern, USA
anti-RhoA (rabbit)	NewEast Bioscience, Malvern, USA

4.3.4 Antibodies for chromatin immunoprecipitation (ChIP)

Table 11: Antibodies used for pulldown

Antibody	Volume	Manufacturer
anti-IgG Normal (rabbit)	5 µl	Cell Signaling Technology, Danvers, MA, USA
anti-MKL1 (mouse)	75 µl	Santa Cruz Biotechnology, Inc., Dallas, TX, USA

4.3.5 Primary antibodies used for immunofluorescence and proximity ligation assay (Duolink®)

Table 12: Primary antibodies and their dilution for immunofluorescence or proximity ligation assay

Antibody	Dilution	Manufacturer
anti-DLC1 (mouse)	1:100	BD Bioscience, San Jose, CA, USA
anti-Filamin A (mouse)	1:100	Merck KGaA, Darmstadt, Germany
anti-Filamin A (rabbit)	1:100	Santa Cruz Biotechnology, Inc., Dallas, TX, USA
anti-MKL1 (goat)	1:100	Santa Cruz Biotechnology, Inc., Dallas, TX, USA
anti-MKL1 (rabbit)	1:100	Santa Cruz Biotechnology, Inc., Dallas, TX, USA
anti-PML (mouse)	1:100	Santa Cruz Biotechnology, Inc., Dallas, TX, USA

4.3.6 Secondary antibodies used for immunofluorescence

Table 13: Secondary antibodies and their dilution for immunofluorescence

Antibody	Dilution	Manufacturer
donkey anti-mouse, ALEXA 488	1:500	Thermo Fisher Scientific, Waltham, MA, USA
donkey anti-mouse, ALEXA 555	1:500	Thermo Fisher Scientific, Waltham, MA, USA
donkey anti-rabbit, ALEXA 488	1:500	Thermo Fisher Scientific, Waltham, MA, USA
donkey anti-rabbit, ALEXA 555	1:500	Thermo Fisher Scientific, Waltham, MA, USA

4.3.7 Antibodies used for immunohistochemistry of CAM-Assay

Table 14: Primary and secondary antibodies and their dilution used for immunohistochemistry

Antibody	Dilution	Manufacturer
anti-E-Cadherin, polyclonal (mouse)	1:2000	BD Bioscience, San Jose, CA, USA
anti-H3K9me3, polyclonal (rabbit)	1:200	Merck, Darmstadt, Germany
anti-Ki-67, monoclonal (mouse)	1:100	Dako/Agilent, Santa Clara, CA, USA
anti-MKL1, polyclonal (rabbit)	1:200	Merck, Darmstadt, Germany
anti-p16, monoclonal (mouse)	1:20	BD Bioscience, San Jose, CA, USA
anti-rabbit, biotinylated (goat)	1:100	Vector-Laboratories, Burlingame, CA, USA
anti-TSPAN5, polyclonal (rabbit)	1:200	OriGene Technologies, Rockville, MD, USA

4.4 Antibiotics

For each batch of plasmid preparation, 50 µl of the specified antibiotics were used in a stock solution of 50 mg/ml.

Table 15: Antibiotics

Antibiotic	Manufacturer
Gibco® Ampicillin	Thermo Fisher Scientific, Waltham, MA, USA
Gibco® Kanamycin	Thermo Fisher Scientific, Waltham, MA, USA

4.5 Enzymes

Table 16: Enzymes

Enzyme	Manufacturer
Duolink® Ligase	Merck KGaA, Darmstadt, Germany
Duolink® Polymerase	Merck KGaA, Darmstadt, Germany
Proteinase K	Merck KGaA, Darmstadt, Germany
RNase A	Thermo Fisher Scientific, Waltham, MA, USA
SuperScript® II Reverse Transcriptase	Thermo Fisher Scientific, Waltham, MA, USA
Trypsin-EDTA solution 0.05 %	Merck KGaA, Darmstadt, Germany

4.6 Stimulants and inhibitors

Stimulants and inhibitors were used as sterile solutions in cell culture with following final working concentrations:

Table 17: Stimulants and inhibitors with final working concentration

Reagent	Final concentration	Manufacturer
Fetale bovine serum (FBS)	20 %	Thermo Fisher Scientific, Waltham, MA, USA
Human recombinant epidermal growth factor (EGF)	10 µM	Merck KGaA, Darmstadt, Germany
Latrunculin B (LatB)	0.3 µM	Merck KGaA, Darmstadt, Germany
Lysophosphatidic acid (LPA)	10 µM	Merck KGaA, Darmstadt, Germany
NS8593	30 µM	Alomone Labs, Jerusalem, Israel
Y27632	10 µM	Merck KGaA, Darmstadt, Germany

4.7 Ladders

12 µl of protein ladder was used for SDS-PAGE and 1 µl DNA ladder was used for agarose gel electrophoresis.

Table 18: DNA and protein ladders

Ladder	Manufacturer
100 bp DNA ladder	Thermo Fisher Scientific, Waltham, MA, USA
Spectra™ Multicolor Broad Range Protein Ladder	Thermo Fisher Scientific, Waltham, MA, USA
Spectra™ Multicolor High Range Protein Ladder	Thermo Fisher Scientific, Waltham, MA, USA

4.8 Kits

Kits were used according to the manufacturer´s instruction.

Table 19: Kits

Kit	Manufacturer
AllPrep DNA/RNA/Protein Mini Kit	Qiagen GmbH, Hilden, Germany
Duolink® In Situ Red Starter Kit	Merck KGaA, Darmstadt, Germany
Epithelial-Mesenchymal Transition (EMT) Antibody Sampler Kit	Cell Signaling Technology, Danvers, MA, USA
GenElute™ HP Plasmid Midiprep Kit	Merck KGaA, Darmstadt, Germany
MinElute PCR Purification Kit	Qiagen GmbH, Hilden, Germany
QIAquick PCR Purification Kit	Qiagen GmbH, Hilden, Germany
Senescence β-Galactosidase Staining Kit	Cell Signaling Technology, Danvers, MA, USA

4.9 Buffers and solutions

4.9.1 Agarose gel electrophoresis

Table 20: Buffers used for agarose gel electrophoresis

50x TAE buffer	
242.0 g	Tris
57.1 ml	Acetic acid (100 %)
100.0 ml	0.5 M EDTA, pH 8.0
ad 1 l	H_2O, ultrapure
50x TAE buffer	
100 ml	50 x TAE buffer
ad 5 l	H_2O, ultrapure

4.9.2 Bacteria cultivation

After compounding lysogeny broth (LB) agar and LB medium, the preparations were autoclaved at 121°C and 2 bar for 20 min. Optionally LB agar was supplemented with 100 µl antibiotic for bacteria selection.

Table 21: Quantities of corresponding components for the preparation of LB agar and LB medium

LB agar	
10 g	Tryptone
5 g	Yeast extract
10 g	NaCl
15 g	Agar
ad 1 l	H_2O, ultrapure, pH 7.5
LB medium	
10 g	Tryptone
5 g	Yeast extract
10 g	NaCl
ad 1 l	H_2O, ultrapure, pH 7.5

4.9.3 cDNA synthesis and qRT-PCR

Table 22: Reagents used for cDNA synthesis and qRT-PCR

Reagent	**Manufacturer**
5x First-Strand Buffer	Thermo Fisher Scientific, Waltham, MA, USA
Deoxynucleoside triphosphates (dNTPs) (10 mM)	Thermo Fisher Scientific, Waltham, MA, USA
LightCycler® 480 SYBR Green I Master	Roche, Basel, Switzerland

4.9.4 Chromatin immunoprecipitation (ChIP) assay

Table 23: Buffers and their composition used for ChIP assay

Farnham Lysis buffer	
0.76 g (5 mM)	PIPES, pH 8.0
3.17 g (85 mM)	KCl
2.50 ml (0.5 %)	NP-40
ad 500 ml	H_2O, ultrapure
Lysis buffer 0.1%	
5.00 ml (10 mM)	1M Tris, pH 7.5
1.00 ml (1 mM)	0.5 M EDTA
5.00 ml (0.1 %)	10 % SDS
ad 500 ml	H_2O, ultrapure
LiCl Wash buffer	
50.0 ml (100 mM)	1 M Tris, pH 7.5
10.60 g (500 mM)	LiCl
5.00 ml (1 %)	NP-40
5.00 g (1 %)	Sodium deoxycholate
ad 500 ml	H_2O, ultrapure
IP buffer	
6.70 g (56.25 mM)	HEPES
4.60 g (157.5 mM)	NaCl
1.00 ml (1 mM)	0.5 M EDTA
5.625 ml (1.125 %)	Triton X-100
0.5625 g (0.1125 %)	Sodium deoxycholate
ad 500 ml	H_2O, ultrapure

IP Elution buffer	
50.00 ml (1 %)	10 % SDS
4.20 g (100 mM)	$NaHCO_3$
ad 500 ml	H_2O, ultrapure
TE buffer	
5.00 ml (10 mM)	1 M Tris, pH 7.5
1.00 ml (1 mM)	0.5 M EDTA
ad 500 ml	H_2O, ultrapure
Sonication buffer	
5.00 ml (10 mM)	1 M Tris, pH 7.5
1.00 ml (1 mM)	0.5 M EDTA
20.00 ml (0.4 %)	10 % SDS
ad 500 ml	H_2O, ultrapure

4.9.5 Duolink® in situ solutions and wash buffers

Table 24: Solutions and buffers used for Duolink®

Duolink® in situ amplification solution	
8.0 µl	5x Duolink® in situ amplification buffer
31.5 µl	H_2O, ultrapure
0.5 µl	Duolink® in situ polymerase
Duolink® in situ ligation solution	
8.0 µl	5x Duolink® in situ ligation buffer
31.0 µl	H_2O, ultrapure
1.0 µl	Duolink® in situ ligase

Duolink® in situ wash buffer A	
8.8 g	NaCl
1.2 g	Tris base
0.5 ml	Tween 20
ad 1000 ml	H_2O, ultrapure, pH 7.4 adjusted with HCl
Duolink® in situ wash buffer B	
5.84 g	NaCl
4.24 g	Tris base
26.0 ml	Tris HCl
ad 1000 ml	H_2O, ultrapure, pH 7.5 adjusted with HCl

Duolink® in situ wash buffers were sterilized by filtration and stored at 4°C.

4.9.6 Buffers for RhoA activation assay

Table 25: Buffers used for RhoA activation assay

IP lysis buffer	
5 ml	1 M Tris, pH 8.0
0.876 g	NaCl
1 ml	Triton X-100
10 ml	Glycerol
ad 100 ml	H_2O, ultrapure
IP washing buffer	
25 ml	1 M Tris-HCl, pH 8.0
15 ml	5 M NaCl
5 ml	1 M $MgCl_2$
1 ml	0.5 M EDTA

5 ml	Triton X-100
ad 500 ml	H_2O, ultrapure

4.9.7 Buffer for determination of the F-actin to the G-actin ratio

Table 26: Buffer used for lysis of cells during actin fractionation

F-actin/G-actin lysis buffer	
10 ml	0.5 M MES, pH 6.8
5 ml	1 M KCl
0.4 ml	0.25 EGTA
0.1 ml	1 M $MgCl_2$
0.5 ml	Triton X-100
ad 100 ml	H_2O, ultrapure

To the F-actin / G-actin lysis buffer, 10 µl PI per 1000 µl lysis buffer was added immediately before use.

4.9.8 Immunoblotting and detection

Table 27: Buffers used for immunoblotting

10x Transfer buffer	
7.25 g	Tris base
3.65 g	Glycine
0.47 g	SDS
200 ml	Methanol
ad 1000 ml	H_2O, ultrapure
10x TBS	
60.55 g	Tris base

85.20 g	NaCl
ad 1000 ml	H_2O, ultrapure, pH 7.6 with HCl
1x TBS-T	
500 ml	10 x TBS
5 ml	Tween 20
ad 5000 ml	H_2O, ultrapure

Table 28: Reagents used for detecting blots

Reagent	Manufacturer
Clarity ECL Western Substrate	Bio-Rad Laboratories, Inc., Hercules, CA, USA
Clarity Max ECL Western Blotting	Bio-Rad Laboratories, Inc., Hercules, CA, USA
SuperSignal™ West Femto Maximum Sensitivity Substrate	Thermo Fisher Scientific, Waltham, MA, USA

4.9.9 Immunofluorescence

Table 29: Fixing solution used for immunofluorescence

4 % Paraformaldehyde (PFA)	
250 ml	H_2O, ultrapure, 60°C
20 g	PFA
50 µl	10 M NaOH
50 ml	10 x PBS
ad 500 ml	H_2O, ultrapure

4.9.10 Invasion assay

Table 30: Solutions used for invasion assay

Staining solution	
16 ml	1 x PBS
4 ml (20 %)	Methanol
0.02 g (0.1 %)	Crystal violet
Destaining solution	
16 ml	1 x PBS
4 ml	Methanol

4.9.11 Protein isolation

Table 31: Solution and buffer used for protein isolation

0.25 M Phenylmethanesulfonyl fluoride (PMSF)	
435.5 mg	PMSF
10 ml	Isopropanol
Kralewski lysis buffer	
5 ml	1 M HEPES, pH 7.4
3 ml	5 M NaCl
1 ml	Triton X-100
0.2 ml	0.5 M EDTA, pH 8.0
10 ml	Glycerine
ad 100 ml	H_2O, ultrapure

Before starting protein isolation, 2 µl 0.25 M PMSF, 4 µl 0.25 DTT and 10 µl Protease Inhibitor Cocktail were added freshly to 1 ml Kralewski lysis buffer.

4.9.12 Sodium dodecyl sulfate polyacrylamide gel electrophoresis (SDS-PAGE)

Table 32: Buffers and their composition used for SDS-PAGE

10x SDS-PAGE running buffer	
10.26 g	Tris
10.00 g	SDS
143.20 g	Glycine
ad 1000 ml	H_2O, ultrapure
4x SDS loading sample buffer (stock solution)	
8 ml	1 M Tris, pH 8.8
16 ml	20 % SDS
16 ml	Glycerine
320 µl	0.5 M EDTA
4 mg	Bromphenol blue

For ready-to-use 4x SDS loading sample buffer (Laemmli buffer), 960 µl of the stock solution were mixed with 40 µl ß-mercaptoethanol and shaken vigorously.

4.9.13 Universal solutions for washing and dissolving

Table 33: PBS solutions

10x Phosphate-buffered saline (PBS)	
2 g	KCl
2 g	KH_2PO_4
80 g	NaCl
21.6 g	Na_2HPO_4 x 7 H_2O
ad 1000 ml	H_2O, ultrapure, pH 7.4

1x PBS	
100 ml	10 x PBS
ad 1000 ml	H_2O, ultrapure

1 x PBS solutions were autoclaved at 121°C and 2 bar for 20 min prior to use.

Table 34: Composition of DEPC H_2O

Diethyl pyrocarbonate H_2O (DEPC H_2O)	
0.5 g	DEPC
500 ml	H_2O, ultrapure

After mixing ultrapure H_2O with the required amount of DEPC, mixture was heated at 37°C for 1 h to completely dissolve and finally autoclaved at 121°C and 2 bar for 20 min.

4.10 SDS-Gels

The gels were each cast with the corresponding Biorad apparatus according to the manufacturer´s instruction. First the specified running gel was produced and polymerized for 20 min, then the 5 % stacking gel was added and polymerized again for 20 min.

Table 35: Compound of running and stacking gels used for SDS-PAGE

5 % running gel	
8.50 ml	H_2O, ultrapure
2.50 ml	30 % acrylamide
3.75 ml	1.5 M Tris, pH 8.8
0.150 ml	10 % SDS
0.200 ml	10 % APS
0.012 ml	TEMED

10 % running gel	
3.97 ml	H_2O, ultrapure
3.33 ml	30 % acrylamide
2.50 ml	1.5 M Tris, pH 8.8
0.100 ml	10 % SDS
0.100 ml	10 % APS
0.004 ml	TEMED
12 % running gel	
4.8 ml	H_2O, ultrapure
6.00 ml	30 % acrylamide
3.90 ml	1.5 M Tris, pH 8.8
0.150 ml	10 % SDS
0.150 ml	10 % APS
0.006 ml	TEMED
15 % running gel	
3.30 ml	H_2O, ultrapure
7.50 ml	30 % acrylamide
3.90 ml	1.5 M Tris, pH 8.8
0.150 ml	10 % SDS
0.150 ml	10 % APS
0.006 ml	TEMED
5 % stacking gel	
5.40 ml	H_2O, ultrapure
1.34 ml	30 % acrylamide
2.00 ml	1.5 M Tris, pH 6.8

0.080 ml	10 % SDS
0.080 ml	10 % APS
0.008 ml	TEMED

Table 36: Tris buffers used for SDS-gels

1.5 M Tris pH 6.8	
121.1 g	Tris base
ad 1000 ml	H_2O, ultrapure, pH 6.8 adjusted with HCl
1.5 M Tris pH 8.8	
121.1 g	Tris base
ad 1000 ml	H_2O, ultrapure, pH 8.8 adjusted with HCl

4.11 Bacterial strains

Table 37: Bacterial strains

Bacterial strains	Manufacturer
***E. coli* DH5α**	Takara Bio, Kyoto, Japan
NEB® 5-alpha competent *E. coli*	New England Biolabs GmbH, Frankfurt am Main, Germany

4.12 Chemicals

Table 38: Chemicals

Chemical	Manufacturer
16 % Formaldehyde (w/v), methanol-free	Thermo Fisher Scientific, Waltham, MA, USA
6x DNA loading dye	Thermo Fisher Scientific, Waltham, MA, USA
β-Mercaptoethanol	Merck KGaA, Darmstadt, Germany

Agar	Carl Roth GmbH, Karlsruhe, Germany
Ammonium peroxodisulfate (APS)	Carl Roth GmbH, Karlsruhe, Germany
Bovine Serum Albumin (BSA)	Carl Roth GmbH, Karlsruhe, Germany
Chloroform	Merck KGaA, Darmstadt, Germany
Crystal violet	Merck KGaA, Darmstadt, Germany
Diethyl dicarbonate (DEPC)	Carl Roth GmbH, Karlsruhe, Germany
Dimethyl sulfoxide (DMSO)	Carl Roth GmbH, Karlsruhe, Germany
Dithiothreitol (DTT)	Thermo Fisher Scientific, Waltham, MA, USA
Dynabeads® Protein G	Thermo Fisher Scientific, Waltham, MA, USA
Matrigel® Basement Membrane Matrix	Corning Incorporated, Corning, NY, USA
Ethanol	Merck KGaA, Darmstadt, Germany
Ethylenediaminetetraacetic acid (EDTA)	Carl Roth GmbH, Karlsruhe, Germany
FBS (Fetal Bovine Serum)	Thermo Fisher Scientific, Waltham, MA, USA
Fluoromount	Merck KGaA, Darmstadt, Germany
Glycerol	Carl Roth GmbH, Karlsruhe, Germany
Glycine	Carl Roth GmbH, Karlsruhe, Germany
4-(2-hydroxyethyl)-1-piperazineethanesulfonic acid (HEPES)	Carl Roth GmbH, Karlsruhe, Germany
Hydrochloric acid (HCl)	Merck KGaA, Darmstadt, Germany
Immersion oil Immersol 518 F	Carl Zeiss AG, Oberkochen, Germany
Isopropyl alcohol	Carl Roth GmbH, Karlsruhe, Germany
Lithium chloride (LiCl)	Merck KGaA, Darmstadt, Germany
Low fat milk powder	Heirler, Radolfzell, Germany
Methanol	Carl Roth GmbH, Karlsruhe, Germany
N,N-Dimethylformamide (DMF)	Merck KGaA, Darmstadt, Germany

N,N,N',N'-Tetramethylethylenediamine (TEMED)	Carl Roth GmbH, Karlsruhe, Germany
Nonidet P-40 (NP-40)	Merck KGaA, Darmstadt, Germany
Nuclease free H_2O	Thermo Fisher Scientific, Waltham, MA, USA
Paraformaldehyde (PFA)	Carl Roth GmbH, Karlsruhe, Germany
peqGold universal agarose	VWR International GmbH, Darmstadt, Germany
Phenylmethylsulfonyl fluoride (PMSF)	Merck KGaA, Darmstadt, Germany
Piperazine-N,N'-bis(2-ethanesulfonic acid) (PIPES)	Carl Roth GmbH, Karlsruhe, Germany
Potassium chloride (KCl)	Carl Roth GmbH, Karlsruhe, Germany
Potassium dehydrogen phosphatase (KH_2PO_4)	Carl Roth GmbH, Karlsruhe, Germany
Protease Inhibitor Cocktail Set III, Animal-Free	Merck KGaA, Darmstadt, Germany
Roti®-Quant	Carl Roth GmbH, Karlsruhe, Germany
Roti®-Safe GelStain	Carl Roth GmbH, Karlsruhe, Germany
Rotiphorese®Gel 30 (37.5:1) (30 % acrylamide)	Carl Roth GmbH, Karlsruhe, Germany
Sodium azide (NaN_3)	Carl Roth GmbH, Karlsruhe, Germany
Sodium chloride (NaCl)	Carl Roth GmbH, Karlsruhe, Germany
Sodium deoxycholate	Carl Roth GmbH, Karlsruhe, Germany
Sodium dodecyl sulfate (SDS)	Carl Roth GmbH, Karlsruhe, Germany
Sodium hydrogen carbonate ($NaHCO_3$)	Carl Roth GmbH, Karlsruhe, Germany
Sodium hydrogen phosphate (Na_2HPO_4)	Carl Roth GmbH, Karlsruhe, Germany
Sodium hydroxide (NaOH)	Carl Roth GmbH, Karlsruhe, Germany
Tris base	Carl Roth GmbH, Karlsruhe, Germany
Tris hydrochloride	Carl Roth GmbH, Karlsruhe, Germany

Triton X-100	Carl Roth GmbH, Karlsruhe, Germany
TRIzol® Reagent	Thermo Fisher Scientific, Waltham, MA, USA
Tryptone	Carl Roth GmbH, Karlsruhe, Germany
Tween® 20	Carl Roth GmbH, Karlsruhe, Germany
Urea	Carl Roth GmbH, Karlsruhe, Germany
Yeast extract	Carl Roth GmbH, Karlsruhe, Germany

4.13 Consumable supplies

Table 39: Consumables

Consumable	Manufacturer
Cell culture 6 well and 12 well plate	Sarstedt AG, Nürnbrecht, Germany
Cell culture dishes, 6 cm and 10 cm	Sarstedt AG, Nürnbrecht, Germany
Cell culture TC-flasks, 125 ml	Sarstedt AG, Nürnbrecht, Germany
Cell scraper	Sarstedt AG, Nürnbrecht, Germany
Cover slips 20x20 mm	Carl Roth GmbH, Karlsruhe, Germany
Cryovials CryoPure 1.6 mL	Sarstedt AG, Nürnbrecht, Germany
Eppendorf tubes 0.5 ml, 1.5 ml, 2 ml and 5 ml	Eppendorf AG, Hamburg, Germany
Eppendorf low binding tube 1.5 ml and 2 ml	Eppendorf AG, Hamburg, Germany
Falcon tubes, 15 mL and 50 ml	Sarstedt AG, Nürnbrecht, Germany
LightCycler® 480 Multiwell Plate 96	Roche, Basel, Switzerland
LightCycler® 480 Sealing Foil	Roche, Basel, Switzerland
Microscope slides 76x26 mm	Carl Roth GmbH, Karlsruhe, Germany
Pasteur pipettes, 230 mm	Carl Roth GmbH, Karlsruhe, Germany
Pipette tips 10 µl, 200 µl and 1000 µl	Sarstedt AG, Nürnbrecht, Germany

PVDF membrane	Merck KGaA, Darmstadt, Germany
Serological pipettes, 2 ml, 5 ml, 10 ml and 25 ml and 50 ml	Sarstedt AG, Nürnbrecht, Germany
Tube with ventilation cap, 13 ml	Sarstedt AG, Nürnbrecht, Germany
UV-transparent cuvettes	Sarstedt AG, Nürnbrecht, Germany
Whatman Blotting Papers®	Merck KGaA, Darmstadt, Germany

4.14 Technical devices and other equipment

Table 40: Technical devices

Apparatus	Manufacturer
Biological Safety Cabinet, PHCBI MHE-N400A2	PHC Europe B.V., Etten-Leur, Netherlands
BioPhotometer plus	Eppendorf AG, Hamburg, Germany
Blotting equipment Mini Protean® Tetra Cell	Bio-Rad Laboratories, Inc., Hercules, CA, USA
Centrifuge 5424	Eppendorf AG, Hamburg, Germany
Centrifuge 5424R	Eppendorf AG, Hamburg, Germany
Centrifuge 5810R	Eppendorf AG, Hamburg, Germany
Chemi-Smart™ 5100 (chemiluminescent imager)	VWR International GmbH, Darmstadt, Germany
ChemiDoc Imaging System	Bio-Rad Laboratories, Inc., Hercules, CA, USA
Confocal microscope LSM 980	Carl Zeiss AG, Oberkochen, Germany
Confocal microscope Leica SP5 II	Leica Microsystems GmbH, Wetzlar, Germany
Duomax 1030	Heidolph Instruments GmbH & Co. KG, Schwabach, Germany
DynaMag™-2 magnet	Thermo Fisher Scientific, Waltham, MA, USA
FlexCycler²	Analytik Jena AG, Jena, Germany

Freezer, -20°C	Liebherr GmbH, Ochsenhausen, Germany
Freeze, -80°C, HS1286-A	Hettich AG, Bäch, Switzerland
Fridge 4°C	Liebherr GmbH, Ochsenhausen, Germany
HERAcell® 240 incubator	Thermo Fisher Scientific, Waltham, MA, USA
Heraeus™ Biofuge™ Stratos	Thermo Fisher Scientific, Waltham, MA, USA
Heraeus™Labofuge™400	Thermo Fisher Scientific, Waltham, MA, USA
Incubator MaxQ 6000	Thermo Fisher Scientific, Waltham, MA, USA
Incu-Shaker 10l	Benchmark Scientific, Sayreville, NJ, USA
Inversion microscope AE2000	MoticEurope, Barcelona, Spain
Laminar flow HERASafe KS18	Thermo Fisher Scientific, Waltham, MA, USA
Loopster basic	IKA-Werke GmbH & Co. KG, Staufen, Germany
LightCycler® 480 II	Roche, Basel, Switzerland
LightCycler® 96	Roche, Basel, Switzerland
Microscope Axiovert135M/ Microscope Axiovert 40 CFL	Carl Zeiss AG, Oberkochen, Germany
Mini Star	VWR International GmbH, Darmstadt, Germany
Neubauer cell counting chamber (0.1 mm)	Paul Marienfeld GmbH, Lauda Königshofen, Germany
pH-meter Lab 555	Schott AG, Mainz, Germany
Pipetus	Hirschmann, Eberstadt, Germany
Power Supply PowerPac HC	Bio-Rad Laboratories, Inc., Hercules, CA,USA
Precision balance, ABS-220 4N	Kern & Sohn GmbH, Balingen-Frommern, Germany
Rotiphorese® Chamber PROfessional IV	Carl Roth GmbH, Karlsruhe, Germany
SDS-PAGE equipment	Bio-Rad Laboratories, Inc., Hercules, CA,USA

Sonopuls GM mini 20	Bandelin electronic GmbH & Co. KG, Berlin, Germany
Thermomixer compact	Eppendorf AG, Hamburg, Germany
Thermostatic Cabinet, Lovibond	Tintometer GmbH, Dortmund, Germany
TissueRuptur II	Thermo Fisher Scientific, Waltham, MA, USA
Vortex-Genie™	Bender & Hobein AG, Zürich, Switzerland
Water bath WNB14	Memmert GmbH & Co. KG, Schwabach, Germany
Weighing scales	Kern & Sohn GmbH, Balingen-Frommern, Germany

5 Methods

5.1 Cell culture methods

5.1.1 Cultivation of mammalian cell lines

Sterile work with cells was carried out in a biosafety level S1 laboratory using a laminar flow cabinet and 70 % Ethanol for sterilisation. All cell lines were cultured in appropriate medium (listed in Table 1) containing 10 % (v/v) heat inactivated fetal bovine serum (FBS) and 1 % (v/v) penicillin/streptomycin. Cells were maintained as a monolayer in 10 cm cell culture dishes in a humidified atmosphere containing 5 % CO_2 at 37°C until they reached a confluence about 90 %. For passaging they were splitted twice a week by aspirating the old medium, washing once with 5 ml sterile phosphate buffered saline (PBS) and detaching with 2 ml room tempered Trypsin-EDTA. After an incubation for 4 minutes at 37°C, cells were carefully resuspended with 8 ml 37°C warm medium. A suitable volume of the cell suspension was transferred to a new 10 cm cell culture dish containing fresh medium with FBS and penicillin/streptomycin. The cell dilution was typically in the range from 1:5 to 1:10 and a confluence of about 90 % was aspired for experiments.

5.1.2 Thawing cells

For thawing long-term stored cells, frozen in cryovials in -196°C liquid nitrogen, were gently shaked in 37°C warm water bath. Cell suspension was transferred to 5 ml of prewarmed medium in a 15 ml falcon tube and centrifuged for 5 min at 1000 rpm at room temperature. After aspirating the old medium, cell pellets were resuspended in 1 ml of new medium and transferred to 6 cm dishes with appropriated medium containing FBS and penicillin/streptomycin.

5.1.3 Freezing cells

For long term storage, the cells were frozen in liquid nitrogen at a temperature of - 196°C in cryovials. For this purpose, confluent cell dishes were aspirated from old medium, washed with 5 ml sterile PBS and trypsinized with 2 ml Trypsin-EDTA for 4 min in an incubator at 37°C.

After adding 3 ml new medium and resuspending the cells, the cell suspension was transferred to a 15 ml falcon tube and centrifuged for 5 min at 1000 rpm at room temperature. The pelleted cells were resuspended in 900 µl of ice cold FBS and 100 µl of Dimethylsulfoxamid (DMSO). Cell suspension was aliquoted in 3 cryogenic vials, which were placed into a cryofreezing container filled with isopropanol for a slow cooling rate to -80°C. After 30 days the cryovials were relocated in liquid nitrogen with -156°C.

5.1.4 Serum starvation

For serum starvation cells were washed two times with sterile PBS and cultured in appropriate medium containing only 0.2 % FBS for 16 hours (h) in incubator with 37°C and 5 % CO_2 atmosphere.

5.1.5 Serum stimulation

Before serum stimulation, serum starvation with 0.2 % FBS (see chapter 5.1.4) is carried out. After 16 h the serum-starved medium was aspirated, the cells were washed twice with sterile PBS and medium with 20 % FBS was added for experimental indicated time intervals.

5.1.6 Drug treatment

Cells were washed twice with sterile PBS and new suitable medium with the diluted stimulants or inhibitors in the required working concentration was added. Cells were cultured common at 37°C and 5 % CO_2 atmosphere for attended time.

5.1.7 Transient transfection with siRNA by Lipofectamine RNAiMax

Transient knockdown of target genes expression was carried out by RNA interference with small-interfering RNA (siRNA), (listed in Table 7). Reverse transfection of the cells was performed with Lipofectamine RNAiMax according to the manufacturer's script. 1 ml OptiMEM was placed in a 6 cm cell culture dish and successively 50 nM scrambled siRNA for

control or 50 nM gene specific siRNA and 10 µl Lipofectamine RNAiMax added, carefully mixed by slow pipetting and incubated for 20 min at room temperature. Simultaneously the cells to be transfected were washed with sterile PBS, trypsinized with 2 ml for 4 min at 37°C and resuspended with 8 ml prewarmed medium. The cell suspension was then transferred into falcon tubes and centrifuged for 5 min at 1000 rpm and room temperature. After aspirating the supernatant, the pelleted cells were resuspended in 10 ml OptiMEM and counted with a Neubauer counting chamber. The desired number of cells was diluted in 3 ml OptiMEM and finally dropwise added to the cell culture dish with the provided siRNA/Lipofectamine RNAiMax mix. These dishes were cultured for 16 h in an incubator with 37°C and 5 % CO_2 atmosphere. Afterwards the transfected cells were washed once with sterile PBS to remove transfection medium and subsequently cultured in suitable medium with 10 % FBS and 1 % penicillin/streptomycin. Knockdown efficiency of the target gene was proved after 48 h after transfection by quantitative real-time PCR (qPCR) or Western Blot.

5.1.8 Transient transfection of DNA plasmids by Lipofectamine 2000

For all cell lines except HepG2, Lipofectamine 2000 was used for transient overexpression of plasmids. Transfection was carried out according to the manufacturer´s instructions. Confluent cell dishes were washed once with sterile PBS, cells were detached with 2 ml Trypsin-EDTA for 4 min at 37°C, resuspended with 8 ml convenient medium and then counted in a Neubauer counting chamber. The required quantity of cells was set to new 6 cm cell culture dish with medium containing 10 % FBS and 1 % penicillin/streptomycin. The next morning, after washing twice with sterile PBS, the medium was changed to medium without any additives. For the actual transfection, two 1.5 ml Eppendorf tubes were prepared with 500 µl OptiMEM each and then 10 µl Lipofectamine 2000 pipetted into one tube and 4 µg of indicated DNA plasmids into the other, mixed gently and incubated for 5 min at room temperature. Afterwards the Lipofectamine 2000/OptiMEM mix was transferred to the DNA plasmid/OptiMEM mix, flicked carefully and incubated for a further 20 min at room temperature. Finally, the whole mix was distributed in droplets on the seeding cells. After 4 h-6 h, the transfection medium was aspirated, the cells were washed with sterile PBS and fresh

medium with growth factors and antibiotics was added. Transfection efficiency was proved after 48 h after transfection by Western Blot or quantitative real-time PCR (qPCR).

5.1.9 Transient transfection of DNA plasmids by GenJet transfection reagent

For transient overexpression of DNA plasmids in HepG2, the transfection reagent GenJet was used according to the manufacturer´s instructions. 24 h before transfection, confluent cell dishes were washed once with sterile PBS, trypsinized, resuspended with prewarmed medium and counted in a Neubauer counting chamber. Finally, the required amount of HepG2 was transferred to new 6 cm dishes that already contained medium. The medium was replaced with new medium without antibiotics one hour before transfection. 4 µg DNA plasmid and 12 µl GenJet reagent were each diluted in one Eppendorf tube containing 200 µl medium without any additions. Subsequently the GenJet solution was transferred into the DNA plasmid solution, mixed gently and incubated for 20 min at room temperature. The transfection cocktail was next pipetted drop by drop onto the seeded cells and incubated at 37°C and 5 % CO_2 atmosphere. Finally, the medium was replaced again by fresh medium containing growth factors and penicillin/streptomycin after 16 h. Transfection efficiency was proved after 48 h after transfection by quantitative real-time PCR (qPCR).

5.1.10 Cell proliferation assay

For cell proliferation assays 80 % to 90 % confluent cell dishes were aspirated from old medium, washed with sterile PBS, trypsinized for 4 min at 37°C and resuspended with 8 ml of appropriated medium. After counting the cells in the Neubauer counting chamber, the required amount of cell suspension to get 1.2 x 10^5 cells per well was transferred in each well of a 6 well plate where already an indicated volume of medium was placed. For 5 days at 24 h intervals the cell count of one well was determined by Neubauer counting chamber after detaching cells with 500 µl Trypsin-EDTA and resuspending with 500 µl medium.

5.1.11 Scratch-wound assay

A necessary amount of cells was seeded and transfected to obtain a confluent monolayer after an incubation for 24 h at 37°C and 5 % CO_2. Next, a uniform wound was scratched with the tip of a pipette. The migrated cells were counted at regular intervals and the width of the wound was measured until that of the control sample was closed. Images were taken with a Zeiss optical microscope.

5.1.12 Cell invasion assay

To perform a cell invasion assay, the Corning BioCoat Matrigel invasion chambers were used and the manufacturer´s instructions were followed. After rehydration of the Matrigel inserts of the provided 24 well plate, the required volume of transfected cells suspension containing only 5 % FBS was transferred in the inserts. The wells were filled with 2 ml medium with 20 % FBS as chemoattractant. The invasion chambers were incubated for 22 h at 37°C and 5 % CO_2 atmosphere. Cells were allowed to invade trough the three-dimensional Matrigel that revetted the surface of the insert due to the concentration gradient of growth factors. To remove the non-invading cells after incubation time and carefully aspirate the medium, the upper surface of the membrane at the bottom of the inserts was gently scrubbed with a cotton swab. The cells on the lower surface of the membrane were fixed with 100 % methanol for 2 min and subsequently stained with 0.1 % crystal violet solution (Table 30) for 5 min. This was followed by an incubation with destaining solution (Table 30) for further 5 min. Excess of staining and destaining solution were removed by washing twice with distilled water. After drying of the inserts, the immigrated cells were counted under the light microscope and images were acquired.

5.1.13 Spheroid assay

Spheroid assays were performed by using Kugelmeiers Sphericalplate 5D® according to the manufacturer's instructions. In order to pre-wet the functionalized wells of Sphericalplate 5D®, they were each rinsed with 1 ml of medium. Afterwards the functionalized wells were prepared with 500 µl of fresh medium with 10 % FBS and antibiotics. The desired

number of cells was added as a single cell suspension in volume of 500 µl into the wells already containing 500 µl of medium. Cells were sunk by gravity into the microwells at the conical bottom of the wells. Sphericalplate 5D® was incubated for 11 days at 37°C and CO_2 atmosphere. Each day, the spheroid formation and growth were monitored and images were captured using an optical microscope with an integrated camera.

5.1.14 Senescence associated ß-galactosidase staining

The senescence ß-galactosidase staining kit was used to determine cellular senescence according to the manufacturer´s instructions. After washing with sterile PBS, trypsinizing, resuspending with appropriate medium and counting the cells, the indicated volume of cell suspension was transferred in 6 well plate wells. Cells were incubated at 37°C and 5 % CO_2 atmosphere for 5 days. Ensuing the growth medium was aspirated, cells were washed with sterile PBS and then fixed with fixative solution for 15 min. After rinsing the plate twice with sterile PBS, the ß-galactosidase staining solution was added and the 6 well plate was incubated in a dry incubator without $C0_2$ at 37°C overnight. While the ß-galactosidase staining solution was still on the plate, it was investigated whether the development of a blue coloration could be detected. The blue colored cells were counted under magnification by a light microscope and proportioned to the total number of cells. For long-term storage, the staining solution was aspirated, 70 % glycerol overlaid and stored at 4°C.

5.2 Methods of nucleic acids analyses

5.2.1 RNA isolation

For RNA isolation first of all, cells grown in a monolayer were washed twice with PBS and 500 µl TRIzol reagent per 6 cm dish was directly added to lyse the cells. Then cells were scraped off the plate with a cell scraper and the cell suspension was transferred to an Eppendorf tube after first homogenization by pipetting up and down. After an incubation for 5 min at room temperature, 200 µl of chloroform was added, the tube was shaken vigorously for 15 secs and incubated again for 3 min at room temperature. Thereafter the sample was centrifuged at 13000 rpm for 15 min at 4°C, the clear RNA containing phase was translocated

into a new Eppendorf tube and 250 µl isopropanol 70 % was added to precipitate RNA. The gently mixed suspension was incubated for 15 min at room temperature and centrifuged at 13000 rpm for 15 min at 4°C. Afterwards the supernatant was removed and the pellet was washed with 1 ml ethanol 75 % by centrifugation at 12000 rpm for 5 min at 4°C. The supernatant was again discarded completely and the RNA pellet was air dried for 10 min at room temperature. To solubilize the RNA pellet, it was resuspended in 20 µl DEPC-H_2O by pipetting up and down and afterwards heated to 55°C for 10 min. Concentration and purity of isolated RNA were determined using a photometer, measuring the absorbance at 260 nm and 280 nm. RNA was stored at -80°C.

5.2.2 cDNA synthesis

For cDNA synthesis, RNA was transcribed to cDNA by using the enzyme SuperScript II Reverse Transcriptase. Therefor 1 µg RNA was mixed with 1 µl Random Hexamer (50 µM) and filled up to 5 µl with nuclease free H_2O. This mixture was heated to 70°C for 5 min in a thermocycler to denature the template and subsequently incubated on ice for 5 min. Afterwards the reverse transcriptase mix (Table 41) was added to the RNA solution and cDNA synthesis was started in the thermocycler at 25°C for 5 min and operated at 42°C for 60 min. Finally, reverse transcriptase was inactivated by heating to 70°C for 15 min and the reaction was stopped by cooling down to 4°C. The cDNA was stored at -20°C.

Table 41: Mixture with reverse transcriptase for cDNA synthesis

Reverse transcriptase mix	
4 µl	5x First Strand Buffer
2 µl	DTT (0.1 M)
1 µl	dNTPs (10 mM)
1 µl	SuperScript II Reverse Transcriptase
ad 15 µl	Nuclease free H_2O

5.2.3 Quantitative real-time polymerase chain reaction (qRT-PCR)

Amplification and quantification of nucleic acids was performed by quantitative real-time polymerase chain reaction (qRT-PCR). For this purpose, 14 µl of the qRT-PCR mix (Table 42) containing the target gene primers to be examined (Table 5) were placed in each required well of a 96 well plate. 6 µl cDNA in a dilution of 1:10 for respective target genes and 6 µl cDNA in a dilution of 1:100 for the endogenous housekeeping control gene 18S were added to the qRT-PCR mix in the multiwell plate.

Table 42: Primer mix for qRT-PCR

qRT-PCR mix	
10 µl	LightCycler® 480 SYBR Green I Master
1 µl	Primer forward (10 µM)
1 µl	Primer reverse (10 µM)
ad 14 µl	Nuclease free H_2O

The qRT-PCR was performed with the LightCycler® 480 II according to the temperature program listed below (Table 43).

Table 43: Temperature program used for qRT-PCR

Step	Temperature	Time	Cycles
Preincubation	42°C	300 sec	1
Denaturation	95°C	10 sec	
Amplification	55°C	10 sec	50
Elongation	72°C	10 sec	
Melting curve analysis	95°C	30 sec	
	60°C	60 sec	1
	95°C	10 sec	
Cooling	4°C	30 sec	1

Measurements were analyzed by the LightCycler® 480 II Software. Gene expression was normalized to the endogenous housekeeping gene 18S, which is not significantly changed under different experimental conditions. The relative expression of the genes was calculated by the $\Delta\Delta C_T$ method.

5.2.4 Microarray analysis

DNA GeneChip Array analysis was performed by isolating total cellular RNA from stable shRNA and shDLC1 expressing HepG2. Therefore, the RNaesy Mini Kit was used according to the manufacturer´s instruction. Next, for synthesizing sense-strand cDNA from total RNA the Ambion WT Expression Kit was used, which allows specific priming of non-ribosomal RNA. After fragmenting the sense-strand cDNA, it was biotin-labelled by Affymetrix GeneChip® WT Terminal Labelling Kit according to the manufacturer's instruction. Hybridization was performed by incubation of the fragmented cRNA on the Human Gene 1.0 ST array at 45°C for 17 h. On a microfluidic workstation the array was washed and stained by streptavidin-phycoerythrin solution and finally scanned by a laser scanner (Affymetrix). Analysis of gene expression profiling was done using Partek Microarray Analysis software.

5.2.5 Transformation of DNA into competent E. coli DH5alpha bacteria

Transformation of DNA was performed via heat shock method. Therefore, an aliquot of competent bacteria stored at -80°C was thawed on ice for 15 min. Next, 50 µl of the bacteria suspension was pipetted into a cooled Eppendorf tube and 1 µl of DNA plasmid was added. This mixture was incubated for 30 min on ice while snapping the tube every 5 min. Afterwards, to initiate the DNA uptake, the heat shock was carried out by slewing the tube in a 42°C water bath for exactly 90 secs and then immediately cooling down on ice for 2 min. 900 µl prewarmed LB medium was added to the suspension, everything was transferred into a tube with ventilation cap and incubated at 150 rpm and 37°C for 1 h. Thereafter 150 µl of this bacteria suspension was distributed on agar plates containing the appropriate antibiotic for selection. Finally, to allow the colonies to grow, the plates were incubated at 37°C overnight. Until use, the plates could be stored at 4°C for a week, sealed with parafilm.

5.2.6 Midi scale plasmid preparation

For plasmid preparation 50 ml LB medium, containing 50 µl of the respective selection antibiotic, was prepared in a sterile Erlenmeyer flask. A single bacterial colony grown on an agar plate was picked up with a sterile pipette tip, transferred into the Erlenmeyer flask and incubated at 37°C overnight with gentle agitation. Next day the plasmid DNA isolation was performed by using the GenElute™ HP Plasmid Midiprep Kit according to the manufacturer´s instructions. Therefore, the bacterial suspension was centrifuged at 3500 rpm for 10 min at 4°C, the supernatant was discarded and the pellet was resuspended, lysed and neutralized with respective solutions relating to the kit. In the following the suspension was put on the prewashed binding column, washed and then eluted with 800 µl elution solution. Finally, the plasmid DNA was relocated into a new Eppendorf tube on ice and stored at -20°C.

5.3 Methods of protein analyses

5.3.1 Protein isolation

Adherent cells, grown in a monolayer on a 6 cm plate, were aspirated of old medium and washed twice with 2 ml ice cold PBS. For harvesting the cells, the cell density appropriate volume of Kralewski lysis buffer, supplemented with protease inhibitor cocktail (PI) 1:100, dithiothreitol (DTT) 1:250 and phenylmethylsulfonyl fluoride (PMSF) 1:500, was added. Subsequently the cells were scraped with a cell scraper, transferred to an Eppendorf tube and incubated on ice for 15 min to lyse. Afterwards the lysed cells were pelleted by centrifugation at 12.700 rpm and 4°C for 15 min and finally the clear supernatant containing the proteins was transferred to a new Eppendorf tube. Isolated proteins were stored at -20°C.

5.3.2 Measurement of total protein concentration

Measurement of protein concentration was determined by Bradford protein assay. Therefore 2 µl of the relevant cell lysates or Kralewski buffer as control were diluted in 1000 µl of 1x Roti®-Quant Bradford reagent, which was used according to the manufacturer´s instruction. The solutions were mixed thoroughly and incubated for 10 min at room temperature. Finally, for analyzing the protein concentration, the mixtures were transferred

into UV-transparent cuvettes and the absorbance was measured at 595 nm by BioPhotometer. Usually an amount of 10-40 µg of protein was calculated and applied for immunoblot analysis.

5.3.3 Sodium dodecyl sulfate polyacrylamide gel electrophoresis (SDS-PAGE)

Proteins were separated according to their molecular weight and electrophoretic mobility in an electric field by SDS-PAGE. Firstly, the indicated amount of cell lysates was mixed with ¼ of the volume of 4x Laemmli SDS sample buffer and boiled at 95°C for 10 min to denature the proteins. After centrifugation at 12.000 rpm for 1 min, the samples and a molecular weight marker were loaded onto a polyacrylamide gel with respective separation capacity regulated by the polyacrylamide content used (Table 18, Table 35). Previously, the polymerized gel was placed in the appropriated electrophoresis apparatus that was filled up with running buffer. Following, the protein separation was done by electrophoresis run at a constant voltage of 100 V for around 1:50 h until the dye front almost reached the end of the running gel.

5.3.4 Immunoblotting

After separating the proteins by gel electrophoresis, the proteins were transferred from SDS gel to a polyvinylidene fluoride (PVDF) membrane. First of all, the PVDF membrane was activated in 100 % methanol and equilibrated for 5 min with gentle shaking in transfer buffer. Immunoblot was performed by using the wet blotting method. For this purpose, the blotting chamber was filled up with blotting buffer and cooled with ice, while a constant current of 350 mA for 1:15 h ensured that proteins were completely blotted onto the membrane. Afterwards the PVDF membrane was blocked in 5 % milk powder in tris-buffered saline with Tween 20 (TBS-T, Table 27) for 1 h at room temperature and gently shaken to prevent unspecific bindings. The primary antibody (Table 8), appropriately diluted in 10 ml TBS-T containing 5 % bovine serum albumin (BSA) and 0.1 % sodium azide, was added to the membrane after it was washed three times with TBS-T for 5 min. Then the membrane was incubated with the specific antibody overnight at 4°C with gentle agitation. The next day, the membrane was washed three times with TBS-T for 15 min, thereafter incubated with the

secondary antibody (Table 9) for 1 h at room temperature and washed again three times with TBS-T for 5 min. Subsequently the TBS-T was removed and the membrane was swivelled in TBS for 5 min. To detect the protein bands, the membrane was incubated with 1.5 ml of each Biorad detection reagent for 3 min. Finally, to visualize the protein bands, the chemiluminescence was performed at the luminescent imager ChemiDoc.

5.3.5 Agarose gel electrophoresis

Agarose gel electrophoresis was used to separate DNA fragments by size in an electric field. To produce an agarose gel, 1.5 g agarose was dissolved in 150 ml 1x tris-acetate-EDTA buffer (1x TAE-buffer, Table 20) in an Erlenmeyer flask. Gel-solution was boiled in a microwave until all streaks had disappeared, then transferred into the electrophoresis chamber, 7.5 µl Roti®-Safe GelStain was added and the curing of the gel was awaited. Thereafter the apparatus was filled with 1x TAE buffer and both 1 µg of DNA and appropriate ladder were mixed with an adequate amount of 6x DNA loading dye and pipetted into the slots. The gel run was performed at a constant voltage of 100 V for 1 h. For imaging the DNA bands, the agarose gel was photographed with the Infinity gel documentation imager.

5.3.6 Chromatin immunoprecipitation (ChIP)

Chromatin immunoprecipitation (ChIP) assays were used to evaluate protein-DNA interactions in nucleus. 30 X 10^6 cells per ChIP were seeded in cell culture flasks and incubated at 37°C and 5 % CO_2 atmosphere. For cross-linking of protein and associated chromatin, 16 % methanol-free formaldehyde was added directly to growth medium on the cells to a final concentration of 1 % for 7.5 min. Afterwards sterile glycine in a total concentration of 0.125 M was used for quenching for 5 min at room temperature. Cells were detached and transferred to 50 ml falcon tubes, pelleted by centrifugation at 1000 g and 4°C for 5 min and washed twice with cold PBS. Lysis of the cells was carried out by incubation with Farnham lysis buffer (Table 23) on ice for 10 min. After washings with PBS and lysis buffer (Table 23), lysates were sonicated six times for respectively 1 min to generate DNA fragments of 200-2000 bp, which were controlled via agarose gel electrophoresis. Following, 100 µg of the sheared chromatin

was immunoprecipitated with 15 µg anti-MKL1 or anti-IgG as control overnight at 4°C with continuous slow rotation. Prior each antibody was coupled to 50 µl Dynabeads Protein G per IP by rotating for 30 min at room temperature. Additionally, 1 % of the used, sonicated chromatin was set aside without antibody as input. Next day the immune complexes were washed with lithium chloride buffer (LiCl buffer, Table 23) and Tris-EDTA buffer (TE-buffer, Table 23) and DNA was eluted in input and ChIP samples by shaking vigorously with elution buffer (Table 23) and heating to 70°C for 10 min. DNA was purified using the MinElute PCR Purification Kit according to the manufacturer´s instruction. QRT-PCR was performed with specific primers for target gene promoters (Table 6) and the evaluation was made according to the % input method.

5.3.7 RhoA activation assay

Immunoprecipitation (IP) of the GTP-bound form of RhoA was used to determine active, GTP-bound RhoA levels. Therefore, cells were plated out in a 10 cm plate, incubated at 37°C and 5 % CO_2 atmosphere and should have reached a confluence of 80-90 % by harvest time. Cells were serum-starved for 16 h and stimulated with 10 µm lysophosphatidic acid (LPA) for exactly 2 min to activate RhoA. Immediately, cells were washed twice with 5 ml ice cold PBS and lysed in 500 µl lysis buffer (Table 25) on ice for 45 min, after being scraped from dishes and transferred to Eppendorf tubes. Lysates were pelleted by centrifugation at 12.000 rpm at 4°C for 15 min, supernatant was removed to a new Eppendorf tube on ice and the total protein content was calculated by measuring absorbance at 595 nm. For determination of total cellular RhoA levels, 20 µg protein amount was used and mixed with ¼ of the volume of 4x Laemmli SDS sample buffer. To perform the IP, 500 µg protein was incubated with 1 µl anti active RhoA mouse antibody by rotating head-over-end at 4°C overnight. To generate a negative beads-only control, another equally volume of the sample was treated in parallel, but no antibody was added. The next day, 50 µl ProteinG-Sepharose beads were mixed with 50 µl IP washing buffer (Table 25), washed three times with ice cold IP washing buffer, added to the lysates and incubated by slowly rotating head-over-end at 4°C for 3 h. Afterwards the supernatant was discarded and to dissolve the proteins from the Sepharose beads, 15 µl 4x Laemmli was added, shaken vigorously and boiled at 95°C for 3 min. After spinning down by

centrifugation at 12.700 rpm for 30 secs, the supernatant as well as the lysates for total cellular RhoA levels were loaded onto a 12 % polyacrylamide gel and SDS-PAGE followed by immunoblotting was performed. Analysis of immunoblot was done by using the anti-RhoA polyclonal antibody and detection of the protein bands via ChemiDoc.

5.3.8 Immunofluorescence

Cells were seeded and grown on glass coverslips placed in 6 well plates. For immunostaining, cells were first washed three times with 2 ml PBS, fixed in 4 % paraformaldehyde (PFA) for 10 min at room temperature, washed again three times with PBS and permeabilized with 0.1 % TritonX-100 in PBS for 7 min (in case of HepG2 for 10 min). In a next step coverslips were washed again three times with PBS, 2 ml of 1 % BSA in PBS was added and incubated at 37°C for 1 h to block nonspecific binding sites. Further cells were incubated with the primary antibody (usually 1:100 dilutions in PBS) at room temperature for 1 h, washed three times with PBS and then incubated with fluorescently labelled ALEXA conjugated secondary antibody (1:500 dilutions in PBS) at room temperature for 1 h in the dark. F-actin staining was performed by using Phallotoxin A555 diluted 1:250 in PBS at room temperature for 20 min in the dark. For nuclei staining, the cells on coverslips were incubated with 4'6-diamidion-2-phenylindole (DAPI) diluted 1:1000 in PBS at room temperature for 30 min also in the dark. After last staining step, the cell-coated coverslips were washed three times with PBS, embedded with mounting medium Fluoromount® and placed on slides. After drying, coverslips were sealed with nail polish and stored at 4°C in the dark until images were taken at the confocal microscope.

5.3.9 Proximity ligation assay by Duolink®

Proximity ligation assay was performed using the Duolink® kit according to the manufacturer´s instructions to investigate whether two proteins interact with each other. For this purpose, cells were seeded and grown in a 1 cm^2 ring drawn with a grease pencil on glass coverslip in 6 well plates to delimit the reaction area. Before starting the Duolink® kit, cells were washed three times with PBS, fixed in 4 % paraformaldehyde (PFA) for 10 min at room temperature,

washed again three times with PBS, and permeabilized with 0.1 % TritonX-100 in PBS for 7 min (in case of HepG2 for 10 min). For blocking, one drop of Blocking Solution included in the kit was added to the reaction area of the glass coverslip and the 6 well plate was incubated in a humidity chamber for 30 min at 37°C. After removing the Blocking Solution, the coverslips were incubated with the primary antibody, diluted in Antibody Diluent 1:100, at 37°C for 1 h. Samples were washed twice with 1x wash buffer A (Table 24) for 5 min with gentle shaking, then the respectively PLA probe, diluted in Antibody Diluent 1:5, was added and the coverslips were incubated again at 37°C for 1 h. After removing the unlinked PLA probes by washing the cells twice with 1x wash buffer A for 5 min, ligation was started by adding diluted Ligase (1:40) and incubated at 37°C for 30 min. To continue with amplification, the coverslips were washed twice with 1x wash buffer A for 2 min under gentle agitation, the polymerase diluted 1:80 was added onto reaction area and plate was incubated at 37°C for 100 min in the dark. Subsequently, the coverslips were washed twice with 1x wash buffer A for 10 min and with 1x wash buffer B (Table 24) for 1 min with cautious shaking in the dark. After drying the coverslips, the cells were mounted with Duolink® In Situ Mounting Medium already containing DAPI. Finally, the coverslips were placed on slides and sealed with nail polish. Slides were stored at -20°C in the dark until images were taken at the confocal microscope.

5.3.10 Determination of the F-actin to G-actin ratio

Cells were cultured as adherent monolayers in 6 cm cell culture dishes at 37°C and 5 % CO_2 atmosphere. For determination of the F-actin to G-actin ratio the cell fractionation was performed on the plate. The plate to be harvested was put on ice and washed two times with 2 ml ice cold PBS. Subsequently, 1000 µl lysis buffer (Table 26) was added and plate was shaken gently for 2 min at room temperature. The supernatant, Triton-soluble and containing the G-actin fraction, was carefully removed directly into 2-4 x SDS loading buffer. Thereafter, another 1000 µl of lysis buffer was pipetted onto the plate, the Triton-insoluble fraction containing the F-actin fraction was scraped off the plate by a cell scraper and transferred into a further tube containing 2-4 x SDS loading buffer. The cytoskeletal fraction was sonicated for 10 secs to shear the DNA. The samples were boiled at 95°C for 10 min and further loaded on

a 10 % polyacrylamide gel for SDS-PAGE and immunoblotting. Finally, protein bands were analyzed and quantified by the ImageLab Software of BioRad®.

5.4 Chorio-allantoic-membrane assay (CAM assay)

5.4.1 General implementation of CAM assay

Using fertilized chicken eggs, the chorio-allantoic membrane (CAM) assay enabled the *in vivo* investigation of tumor cell growth, migration, and invasion ability. It has been performed as described in literature by Ribatti (Ribatti 2014, 2017). For the *on ovo* experiment, specific pathogen free (SPE) eggs were bred in a 70-80 % humidity chamber at 37°C. On the 8th day of embryo development, a window of approximately 1-2 cm^2 was cut into the flatter pole of the chicken´s eggshell and subsequently sealed by silk tape. Eggs were incubated for another day and ensuing 1x 10^6 cells in 20 µl medium, embedded in 20 µl Matrigel (Corning® Matrigel® Basement Membrane Matrix), were placed on the chicken embryos CAM. Breeding of the eggs was continued until day 14 of embryo development. Thereafter the grown micro-tumors with their surrounding CAM were isolated, fixed in 4 % PFA for 24 h and embedded in paraffin. In parallel, some tumor pellets were removed without CAM and frozen in liquid nitrogen for later RNA or protein isolation. Embryos were decapitated, liver, heart and brain extracted and frozen in liquid nitrogen. Previously volume of tumor pellet was determined by using a mathematical formula for ellipse calculation: tumor volume = pellet length * width * height * 0.52 (Feldman et al. 2009).

5.4.2 RNA, DNA and protein isolation of CAM tumors

RNA, DNA and proteins were isolated parallel by AllPrep® DNA/RNA/Protein Mini Kit of Qiagen. First of all, tumor samples were thawed on ice and RPE lysis Buffer included in the kit was added. To homogenize the lysate, the tip of the TissueRuptor® was placed in the Eppendorf tube with the tumor pellet suspension and operated at full speed (usually 30 secs) until the lysate was homogenous. In the following, RNA, DNA and proteins were successively isolated, purified and highly concentrated via columns according to the manufacturer´s

instruction. DNA and protein samples were stored at -20°C and RNA samples at -80°C until further use.

5.4.3 Immunohistochemistry (IHC) of CAM tumors

Formalin-fixed and paraffin-embedded sections (1-3 µm) of excised CAM tumors were deparaffinized with xylene. Afterwards sections were rehydrated with graded ethanol according to standard procedures. Validated immunohistochemistry (IHC) protocols established at the Institute of Pathology of FAU Erlangen were applied for hematoxylin and eosin (HE), Ki67 and $p16^{INK4a}$ staining. For this purpose, an IHC automat "Ventana BenchMark Ultra instrument" (Ventana Medical Systems, part of Roche Diagnostics, Oro Valley, Arizona, USA) and detection kit "UltraView Universal DAB Detection Kit" (Ventana Medical Systems, part of Roche Diagnostics, Oro Valley, Arizona, USA) were used according to the manufacturer´s instructions. TSPAN5, MKL1, and H3K9me3 were stained manually. For antigen-specific heat-induced antigen retrieval, endogenous peroxidases were first blocked, slides were incubated with the primary antibody (Table 14) overnight at RT and then incubated with the biotinylated secondary antibody. Sections were detected with VECTASTAIN® Elite® ABC Kit (Vector Laboratories, Burlingame, CA, USA) and DAB substrate (Dako, part of Agilent, Santa Clara, CA, USA) and counterstained with hematoxylin.

5.4.4 Scanning of IHC sections

Prepared and stained IHC sections of CAM tumors were scanned by anoramic MIDI system (Camera type: CIS VCCFC60FR19CL; objective: Plan-Apochromat; magnification: 40x; Camera adapter (PanoramicMidi and Panoramic Flash 250, 3D-Histech) magnification: ×1, 3DHISTECH, Budapest Hungary). The scans were viewed and analyzed using CaseViewer software (3DHISTECH, Budapest, Hungary).

5.5 Subcutaneous tumor xenograft

The subcutaneous tumor xenograft model to study the *in vivo* effects of TSPAN5 knockdown by systemic injection of siRNA complexed with polyethylenimine (PEI) was performed as previously described (Aigner 2006; Borchardt et al. 2019; Borchardt et al. 2021; Hampl et al. 2013; Ibrahim et al. 2011; Schäfer et al. 2010). The experiments were approved by the local authorities (Landesdirektion Sachsen), performed in accordance with the EU Directive 2010/63/EU for animal experiments and the national regulations, and complied with the ARRIVE guidelines. Athymic nude mice (Crl:CD1-Foxn1nu, Charles River Laboratories, Sulzfeld, Germany) were kept under special pathogen free conditions in cages with rodent chow and with unrestricted access to water (ssniff, Soest, Germany). In both flanks of 6-week-old female mice, $2*10^6$ HuH7 cells in 150 µl PBS were injected subcutaneously to generate tumors. After solid tumors had formed after 2.5 weeks, the mice were randomized into control and treatment group with 6 animals per group. Mice were intraperitoneally (i.p.) injected with PEI F25-LMW/siRNA complexes containing 10 µg nonspecific or specific siRNA in 150 µl HN buffer 3x per week. Tumor volume has measured daily and calculated according to the formula length * width * width/2. By day 10, some of the tumors were already so large that the experiment had to be terminated. The mice were sacrificed, the tumors were excised and subsequently shock frozen in liquid nitrogen for subsequent RNA and protein preparation.

5.6 Statistical analysis

Unless otherwise indicated, data were analyzed from at least three independent experiments and expressed as mean ± standard deviation (SD). All statistical analyses among two groups were accomplished by using Student´s unpaired t-test and among three or more groups by using One Way Anova test. P-values are *p≤0.05, **p≤0.01, ***p≤0.001.

5.7 Software and databases

GraphPad Prism® (GraphPad Software, La Jolla, CA, USA) was used for calculations and statistical analysis. ImageLab® BioRad (ImageLab Software, Bio-Rad Laboratories, Inc., Hercules, CA, USA) was used to evaluate and quantify the Western blot detections. Research

publications were retrieved from the online database NCBI PubMed (http://www.ncbi.mlm.nih.gov/pubmed) and managed with Citavi 6.0.

6 Results

6.1 Novel target genes induced by DLC1 loss in HCC

6.1.1 Gene expression profiling identifies genes induced by DLC1 loss

To identify novel gene targets induced by DLC1 loss, microarray experiments using Affymetrix oligonucleotide arrays in HepG2 transduced with DLC1 shRNA were performed by C. Mittermeier. The top 5 genes from the list of genes that were upregulated in HepG2 DLC1 knockdown cells were selected and thus Versican (VCAN), Tetraspanin 5 (TSPAN5), Meprin 1A (MEP1A), Histon cluster 1 H2B family member K (HIST1H2BK) and N-Cadherin (CDH2) were identified (Table 44).

Table 44: Selected top 5 genes that were upregulated in performed microarray experiments after DLC1 loss

Gene Symbol	Fold-Change (HepG2 shRNA DLC1 vs. ctrl)	p-Value
VCAN	6.32	0.001515
TSPAN5	4.96	0.001795
MEP1A	4.16	0.002295
HIST1H2BK	3.24	0.003902
CDH2	3.21	0.00091

The upregulation of the DLC1 dependent genes in the HepG2 shDLC1 were already verified by qRT-PCR.

6.1.2 Validation of gene expression profiling via transient knockdown of DLC1

6.1.2.1 Transient knockdown of DLC1 in HepG2 cells

First aim of this thesis was the further validation of an already performed and basically validated microarray. By transfecting HepG2 HCC cells with DLC1 siRNA, we obtained a knockdown efficiency of about 75 % after 48 h. We determined the mRNA expression of the newly identified target genes after 48 h, 72 h and 96 h. As a result, we could show that in

HepG2 cells with transient knockdown of DLC1, CDH2 was most overexpressed after 48 h, TSPAN5 after 72 h and VCAN, MEP1A and HIST1H2KB after 96 h (Figure 12).

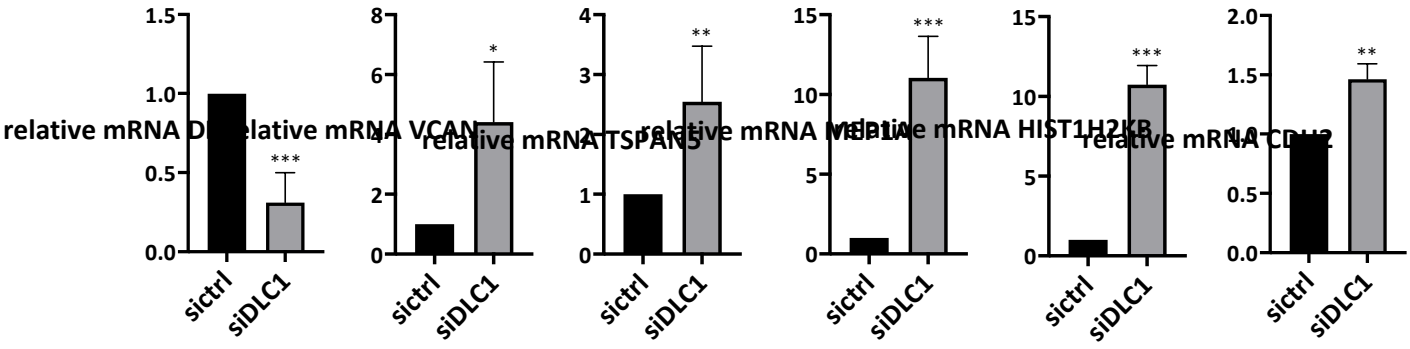

Figure 12: DLC1 knockdown efficiency and DLC1 dependent target gene expression in HepG2 cells. mRNA expression of the indicated target genes in HepG2 cells either expressing control siRNA (sictrl) or DLC1 siRNA (siDLC1) (CDH2 after 48 h, TSPAN5 after 72 h and VCAN, MEP1A and HIST1H2KB after 96 h) as well as knockdown efficiency of DLC1 after 48 h were measured by qRT-PCR. Values are mean ± SD (n=3); *p<0.05, **p<0.01, ***p<0.001.

On protein level, loss of DLC1 after RNA interference and consequent overexpression of VCAN, TSPAN5, and CDH2 were confirmed (Figure 13).

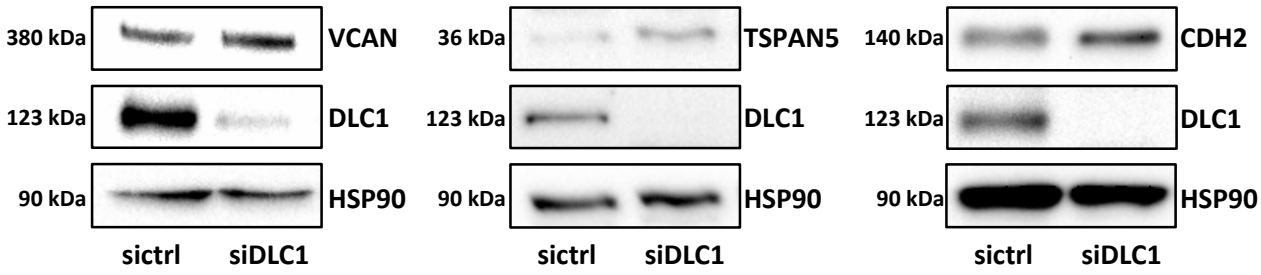

Figure 13: Protein overexpression of DLC1 dependent target genes in HepG2 cells. Immunoblotting of lysates of HepG2 cells either expressing control siRNA (sictrl) or TSPAN5 siRNA (siTSPAN5) with anti-Versican, anti-n-Cadherin, anti-Tetraspanin5 and anti-HSP90 antibody. Lysates were prepared 96 h after siRNA transfection. The blots are representative for three individual experiments.

6.1.2.2 Transient knockdown of DLC1 in Hep3B cells

The same transient knockdown using DLC1 siRNA was performed in Hep3B HCC cells and the mRNA expression was analyzed at equal intervals (Figure 14). The DLC1 expression was

reduced by approximately 75 % in the DLC1 knockdown cells compared to the control cells. The new gene targets TSPAN5, MEP1A and CDH2 were significantly upregulated upon DLC1 loss. TSPAN5 and MEP1A reached the highest upregulation after 96 h, contrary to CDH2, which was already upregulated after 48 h to 72 h and came down to basic level after 96 h again. Thereby, we could show that the upregulation of the gene targets like TSPAN5 or MEP1A determined by microarray analysis is also DLC1 dependent in Hep3B cells. The findings lead to the conclusion that this dependency is a general finding in HCC cell lines and not only cell line specific.

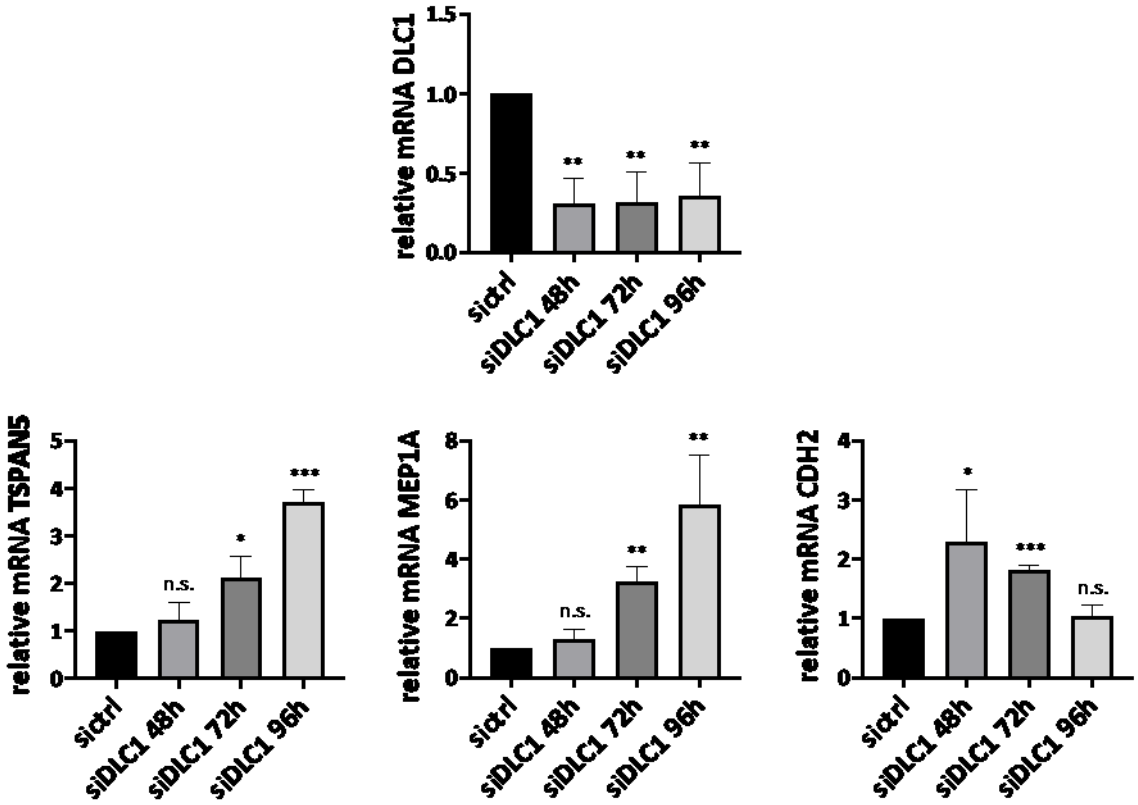

Figure 14: DLC1 knockdown efficiency and target gene upregulation upon DLC1 depletion in Hep3B cells. Expression of the indicated target genes mRNA in Hep3B cells either expressing control siRNA (sictrl) or DLC1 siRNA (siDLC1) was measured by qRT-PCR. Statistical analysis was performed using one-way ANOVA, followed by Tukey´s multiple comparison test. Values are mean ± SD (n=3); *p<0.05, **p<0.01, ***p<0.001, ****p<0.0001. SD of the 48 h, 72 h and 96 h value is always in comparison to the control value.

Analogous to HepG2 cells, protein levels of VCAN, TSPAN5, and CDH2 were each increased in Hep3B cells after DLC1 loss for 96 h (Figure 15).

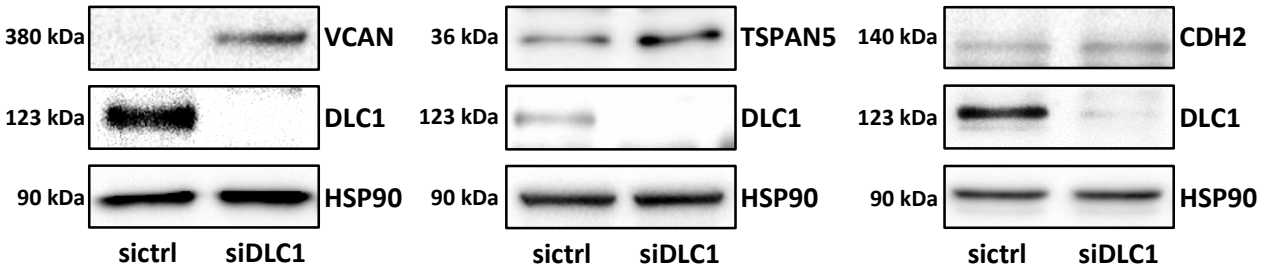

Figure 15: Protein overexpression of DLC1 dependent target genes in HepG2 cells. Immunoblotting of lysates of HepG2 cells either expressing control siRNA (sictrl) or TSPAN5 siRNA (siTSPAN5) with anti-Versican, anti-n-Cadherin, anti-Tetraspanin 5 and anti-HSP90 antibody. Lysates were prepared 96 h after siRNA transfection. The blots are representative for three individual experiments.

6.2 MKL1, FLNA and SRF dependence of novel gene targets

6.2.1 MKL1 and FLNA dependence of the newly identified gene targets

We next investigated whether silencing MKL1/2 or Filamin A (FLNA) expression prevents upregulation of the genes identified by DLC1 loss. Therefore, HepG2 cells were transfected on the one hand only with DLC1 siRNA and on the other hand with DLC1 siRNA and MKL1/2 or FLNA siRNA. Hereby we could show that the knockdown-mediated upregulation of VCAN, TSPAN5 and CDH2 was significantly impaired by additional MKL1/2 siRNA and FLNA siRNA transfection (Figure 16).

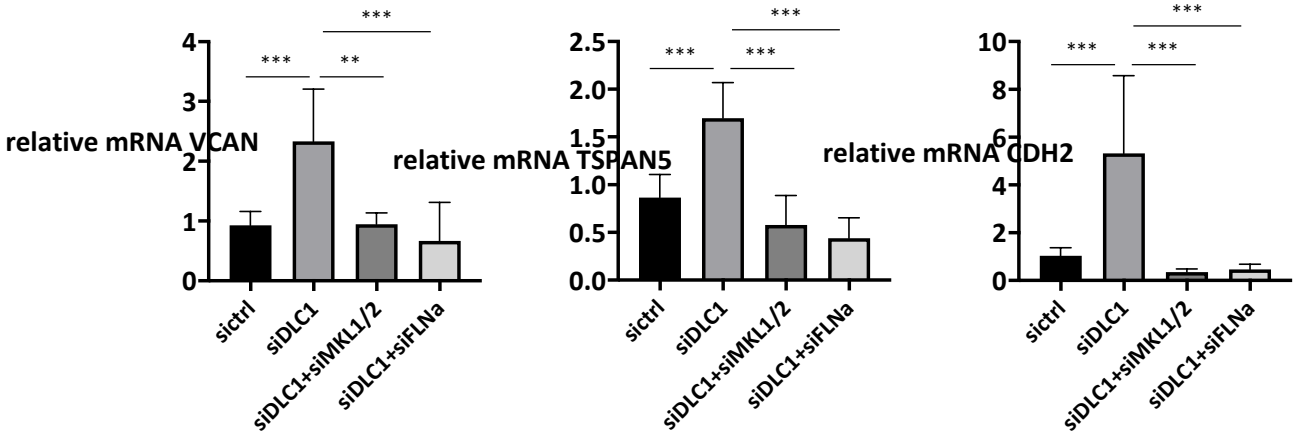

Figure 16: MKL1/2 and FLNA dependence of newly identified target genes upon DLC1 loss. mRNA expression of TSPAN5, VCAN and CDH2 in HepG2 cells, after transfection with control siRNA (sictrl), DLC1 siRNA (siDLC1) and the combination of DLC1 siRNA and MKL1/2 siRNA (siDLC1 + siMKL1/2) or the combination of DLC1 siRNA and FLNA siRNA (siDLC1 + siFLNA) was assessed by qRT-PCR. The respective gene specific primers were used and normalization to the 18S was rRNA carried out. Statistical analysis was performed using one-way ANOVA, followed by Tukey´s multiple comparison test. Values are mean ± SD (n=3); **p<0.01, ***p<0.001.

To validate the assumption of MKL1 and FLNA dependence of the newly found gene targets VCAN, TSPAN5, and CDH2, we performed a chromatin immunoprecipitation (ChIP) assay. For this purpose, we used FLNA positive A7 cells and FLNA negative M2 cells. To activate the co-transcription factor MKL1 and recruit at the transcription factor SRF, we stimulated the cells exactly for 20 min in 20% FBS. To directly analyze the recruitment of MKL1 for the VCAN, TSPAN5 and CDH2 promoters, we performed an MKL1 pulldown on the one hand and additionally an IgG pulldown as a control. We were able to amplify the VCAN, TSPAN5 and CDH2 promoters from MKL1 immunoprecipitates in A7 cells, but not from IgG immunoprecipitates. Additionally, the VCAN, TSPAN5 and CDH2 promoters were enriched only in FLNA-positive (A7) cells, but not in FLNA negative (M2) cells (Figure 17). Based on this experiment we could demonstrate the direct recruitment of MKL1 to the promoters of VCAN, TSPAN5 and CDH2 and therefore the direct transcriptional regulation of the newly identified gene targets upon DLC1 loss. Further, we revealed that the presence of FLNA is indispensable for this process.

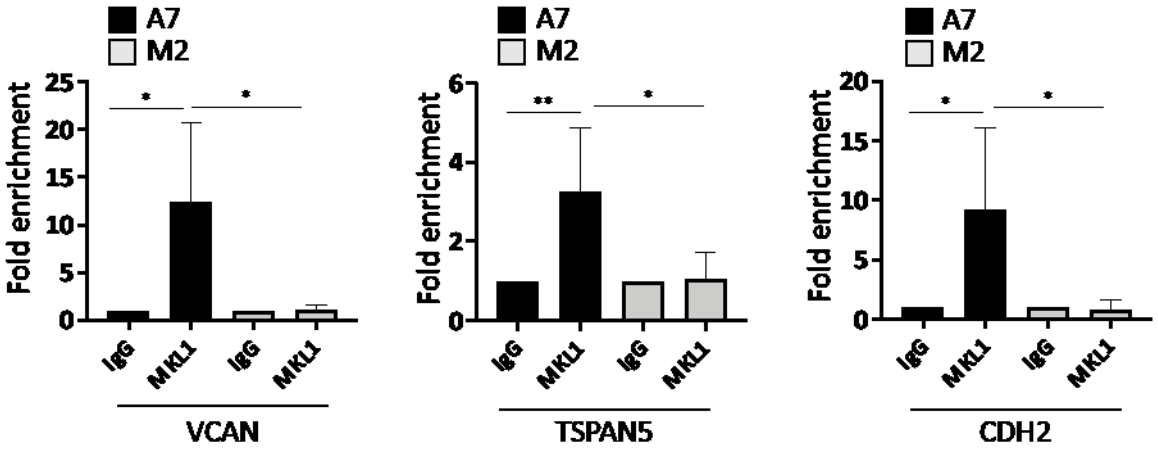

Figure 17: MKL1 recruitment to the VCAN, TSPAN5 and CDH2 promoters. For ChIP assay, A7 and M2 cells were stimulated with 20 % FBS for 20 min, crosslinked with formaldehyde, and quenched with glycine. Finally, the sheared chromatin was immunoprecipitated with a specific MKL1- or IgG-antibody. For qRT-PCR analysis respectively primers for VCAN, TSPAN5 and CDH2 promotors were used. Values are mean ± SD (n=3); *p<0.05, **p<0.01.

6.2.2 MKL1 dependence in DLC1 deficient cell line

Furthermore, we were interested in the extent to which the expression of the newly identified target genes can be regulated by MKL1 alone without primary DLC1 effects. Therefore, we used DLC1 deficient HCC cell line HuH7 and performed MKL1 knockdown and overexpression experiments. The knockdown efficiency of MKL1 was about 80 %, with the additional transfection of the constitutively active MKL1N100 variant we reached basic level of MKL1 mRNA expression again. By overexpressing MKL1N100, we were able to increase MKL1 levels 100-fold (Figure 18). After transient MKL1/2 knockdown via siRNA interference, we demonstrated significant downregulation of newly identified target genes using TSPAN5 or VCAN as examples (Figure 18). The combination of transfecting firstly siMKL1/2 and afterwards MKL1N100 for reconstitution resulted in recovery of gene expression. We detected a strong upregulation of TSPAN5 after MKL1 overexpression via MKL1N100 plasmid transfection. The already known MKL1/2 target gene SM22 behaved analogously as a positive control.

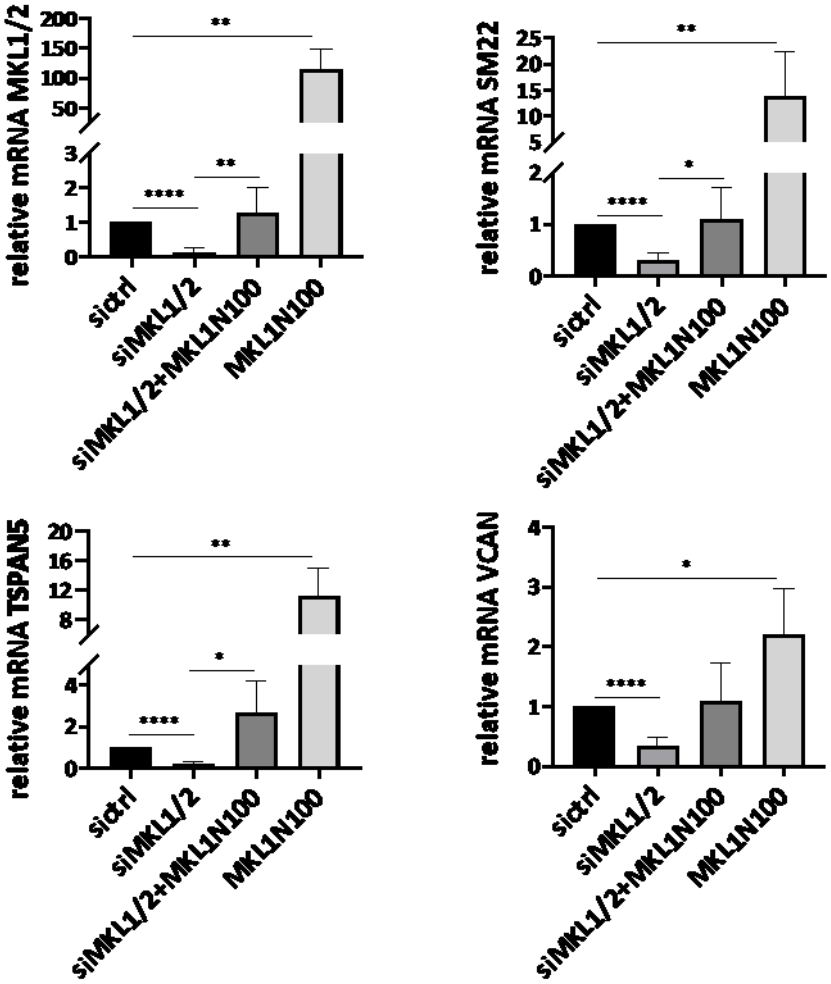

Figure 18: MKL1 dependence of novel target genes compared with known MKL1 dependent target gene SM22. Expression of MKL1, SM22, TSPAN5 and VCAN mRNA in HuH7 cells after MKL1/2 knockdown via RNA interference alone, a followed reconstitution of MKL1N100 and overexpression of MKL1N100 alone, determined by qRT-PCR. The appropriate gene specific primers were used and normalized to 18S primers. Statistical analysis was performed using one-way ANOVA, followed by Tukey´s multiple comparison test. Values are mean ± SD (n=3); *p<0.05, **p<0.01, ***p<0.001, ****p<0.0001.

6.2.3 SRF dependence of newly identified target genes in HCC cells

Next, we sought to investigate whether there is a SRF dependency besides the MKL1 dependency. For this reason, we used HuH7 cells and transfected them with SRF siRNA for 48 h and achieved a knockdown efficiency of 80 %. Thereby we could show evidence, that the mRNA expression of the novel target genes like TSPAN5, VCAN or CDH2 has clearly decreased after silencing SRF gene (Figure 19).

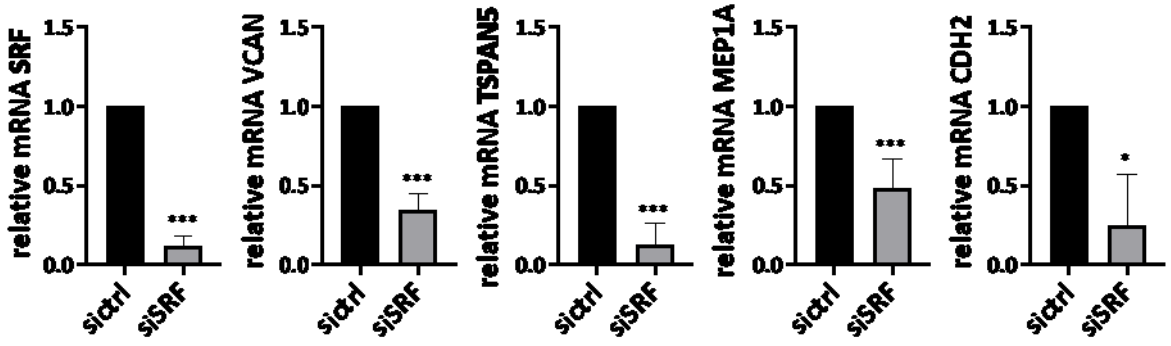

Figure 19: SRF dependence of novel target genes. mRNA expression of SRF and novel target genes in HuH7 cells either expressing control siRNA (sictrl) or SRF siRNA (siSRF) was measured by qRT-PCR using the respective gene specific primers and normalizing to 18S. Values are mean ± SD (n=3); *p<0.05, ***p<0.001, ****p<0.0001.

6.3 Regulation of the target gene TSPAN5 upon inhibitor or stimulant treatment

After pointing out the MKl1/2 and SRF dependency of the newly found target gene TSPAN5, we were interested in whether we could modify the expression level of TSPAN5 by affecting the MKL1/2 signal pathway. Since translocation of MKL1 into the nucleus and thus the activation of MKl1 and SRF is triggered via the RhoA signaling pathway, in our next experiment we wanted to investigate to what extent therefor known inhibitors or stimulants influence the TSPAN5 protein levels (Miralles et al. 2003; Muehlich et al. 2008).

6.3.1 Inhibition of TSPAN5 expression upon Latrunculin B und Y-27632 treatment

The extracellular inhibitor Latrunculin B (LatB) tested by us is known as an inhibitor of actin polymerization and prevents filamentous F-actin polymerization from monomeric G-actin by binding to G-actin monomers (Yarmola et al, 2000). Another inhibitor whose role on TSPAN5 expression we analyzed was Y-27632, which inhibits the Rho associated protein kinase (Rock). We found out that upon LatB and Y-27632 treatment of HuH7 cells, the protein levels of TSPAN5 were reduced compared to the negative control sample (Figure 20).

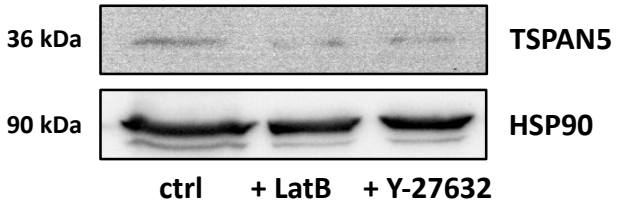

Figure 20: Downregulation of TSPAN5 upon LatB and Y-27632 treatment. Protein level of TSPAN5 was analyzed in lysates of HuH7 cells treated with 0.3 µM LatB (+LatB), 10 µM Y-27632 (+y-27632) or DMSO as control (ctrl) for 45 min each. Equal amounts of total protein were immunoblotted with anti-TSPAN5 antibody and anti-HSP90 antibody was used as loading control. The blots are representative for three individual experiments.

6.3.2 Stimulation of TSPAN5 protein level upon LPA treatment

Contrary to inhibitors inducing downregulation of TSPAN5 levels, we next assessed to what extent substances stimulating the RhoA/actin signal axis can increase the TSPAN5 protein levels. To this end, we treated initially serum-starved HepG2 cells for 2 h with lysophosphatidic acid (LPA), which is an active component of serum and stimulates the RhoA/actin pathway. LPA is a potent signaling molecule that is involved in many cellular processes and regarding to the RhoA/actin signaling pathway it enhances the actin polymerization into F-actin filaments (Lin et al. 2010; Muehlich et al. 2004). In this experiment, HepG2 cells were used because their DLC1 expression negatively regulates RhoA activity. We could demonstrate an upregulation of TSPAN5 expression upon LPA treatment in HepG2 cells (Figure 21).

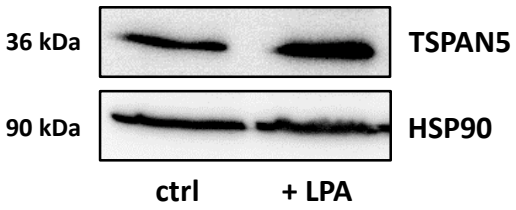

Figure 21: Upregulation of TSPAN5 protein level upon LPA treatment. HepG2 cells were serum-starved for 16 h and subsequently stimulated with either 10 µM LPA (+LPA) or PBS as control (ctrl) for 2 h. Afterwards HepG2 cell lysates were purified and same amounts of total protein content were immunoblotted with anti-TSPAN5 antibody. For loading control anti-HSP90 antibody was used. The blots are representative for three individual experiments.

The results of this chapter proof evidence that the TSPAN5 protein expression can be modulated by activating or inhibiting the RhoA/actin signal axis. This confirms the assumption

that the TSPAN5 expression is also MKL1/SRF dependent, making TSPAN5 itself a MKL1 target gene.

6.4 Effects of novel target genes on HCC growth and tumorigenesis

Because of the dependency of the novel target genes TSPAN5, VCAN and CDH2 on MKL1, FLNA and SRF, we were interested in whether the target genes are able to be transducer of MKL1/2 effects on tumorigenic process. So we next investigated the role of the newly identified target genes for different characteristic tumorigenic properties, like proliferation, migration and invasion of cells or the ability to form spheroids.

6.4.1 TSPAN5 is required for proliferation in HCC cells

One essential property of tumor cells is their tremendous proliferation rate. Therefore, a correlation between proliferation and upregulation of the gene targets upon DLC1 depletion needs to be investigated.

6.4.1.1 TSPAN5 leads to proliferation arrest in DLC1 deficient cells

To search for the target gene(s) that is responsible for HCC growth, we depleted VCAN, TSPAN5 and CDH2 by RNA interference in HuH7 cells with an efficiency of 60 %– 80 % (Figure 22A) and performed proliferation assays for 5 days. By monitoring the HCC proliferation rate we found out that silencing VCAN and CDH2 did not affect HuH7 cell proliferation, but knockdown of TSPAN5 provoked a strong growth arrest (Figure 22B). Already on the third day of counting, the difference between the cell number of HuH7 siTSPAN5 cells and the control cells was significant. In contrast, the numbers of siVCAN and siCDH2 cells were at no time significantly lower than those of the control cells.

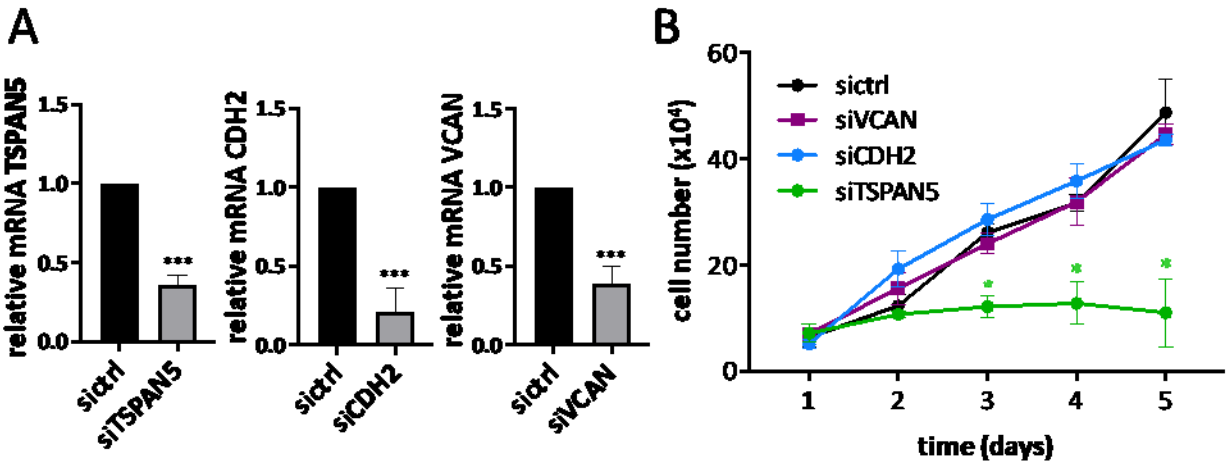

Figure 22: TSPAN5 is required for cell proliferation. (A) HuH7 cells were expressing control siRNA (sictrl) or TSPAN5, CDH2 or VCAN siRNA (siTSPAN5, siCDH2 or siVCAN). Knockdown efficiency of mRNA expression was determined by qRT-PCR at 48 h after transfection. Therefore, the appropriate rRNA primers and 18S rRNA primers for normalization were used. **(B)** Cells were counted daily for 5 days with a Neubauer counting chamber. Values are mean ± SD (n=3); *p<0.05, ***p<0.001.

Furthermore, we were able to reproduce the necessity of TSPAN5 for proliferation in HuH6 cells, another DLC1 deficient cell line. Transient transfection with TSPAN5 siRNA and counting of cells was performed analogously to the experimental setup with HuH7 cells. Only about 10 % of the cells expressed TSPAN5 mRNA after siRNA transfection (Figure 23A). Knockdown of TSPAN5 was arresting the proliferation rate strongly compared to the uninhibited growth of the control cells (Figure 23B). From day three a significant growth arrest could be observed.

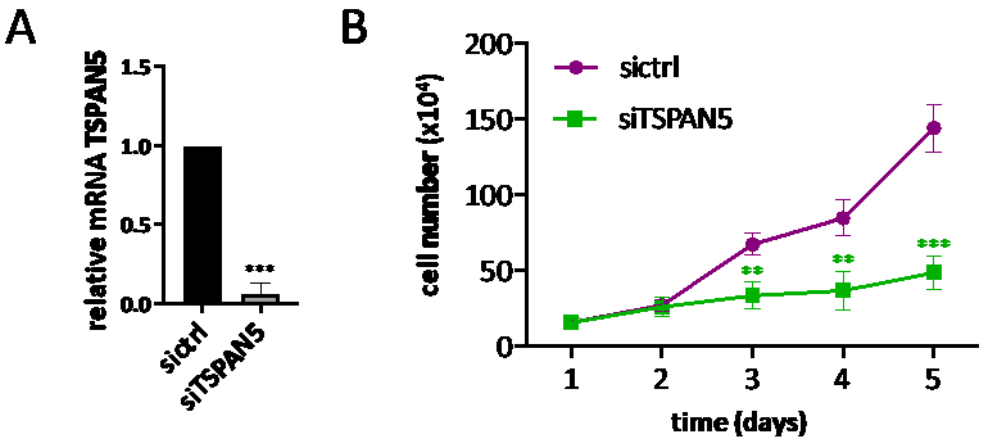

Figure 23: TSPAN5 depletion provoked growth arrest in HuH6 cells. (A) HuH6 cells were transfected with TSPAN5 siRNA (siTSPAN5) and scrambled RNA for control (sictrl). At 48 h post transfection, knockdown efficiency was assessed by qRT-PCR using the gene specific primers and 18S primers for normalization. **(B)** HuH6 proliferation was monitored daily for 5 days by counting with Neubauer counting chamber. Values are mean ± SD (n=3); **p<0.01, ***p<0.001.

To further validate the proliferation arrest due to TSPAN5 loss, we performed the proliferation assay using an alternative TSPAN5 siRNA (siTSPAN5_V2) in addition to another cell line. Again, we observed reasonable knockdown efficiency and strong growth arrest of HuH7 cells with TSPAN5 depletion (Figure 24).

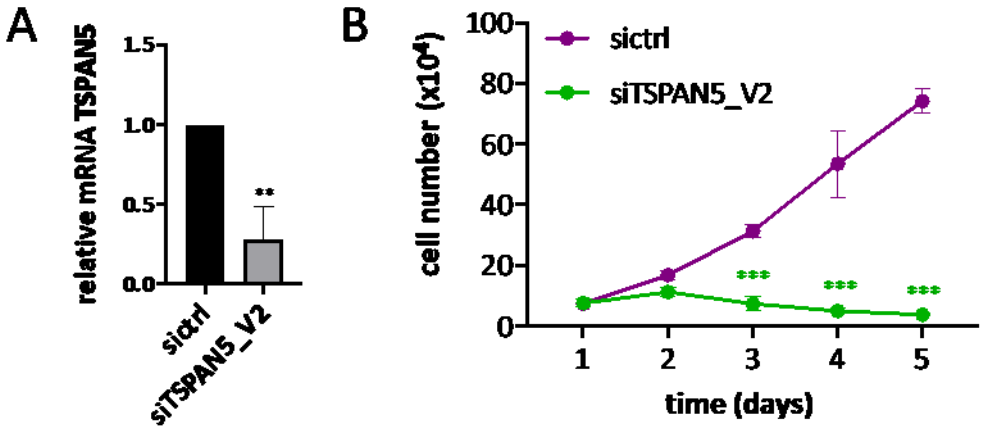

Figure 24: TSPAN5 depletion provokes growth arrest. (A) HuH7 cells were transfected with an alternative TSPAN5 siRNA (siTSPAN5_V2) and scrambled RNA for control (sictrl). At 48 h post transfection, knockdown efficiency was assessed by qRT-PCR using the gene specific primers and 18S primers for normalization. **(B)** HuH7 proliferation was monitored daily for 5 days by counting the cells with Neubauer counting chamber. Values are mean ± SD (n=3); **p<0.01, ***p<0.001.

6.4.1.2 Overexpression of the MKL1N100 mutant attenuates the proliferation arrest

To gain deeper insight into the significance and implications of MKL1 dependence on TSPAN5, we examined in subsequent experiments whether the proliferation arrest caused by TSPAN5 loss could be reduced by overexpression of the constitutively active MKL1 variant (MKL1N100). The MKL1N100 mutant, due to defective actin binding, represents a permanently active MKL1 variant that cannot be shuttled out of the nucleus and thus continuously activates SRF. For this purpose, we used HuH7 cells which were transfected with the plasmid of the MKL1N100 variant or an empty vector after transient TSPAN5 silencing on the following day. By counting the cells daily, we observed that overexpression of the constitutively active MKL1N100 variant could not completely abolish the TSPAN5-induced proliferation arrest, but it mitigated the proliferation rate (Figure 25).

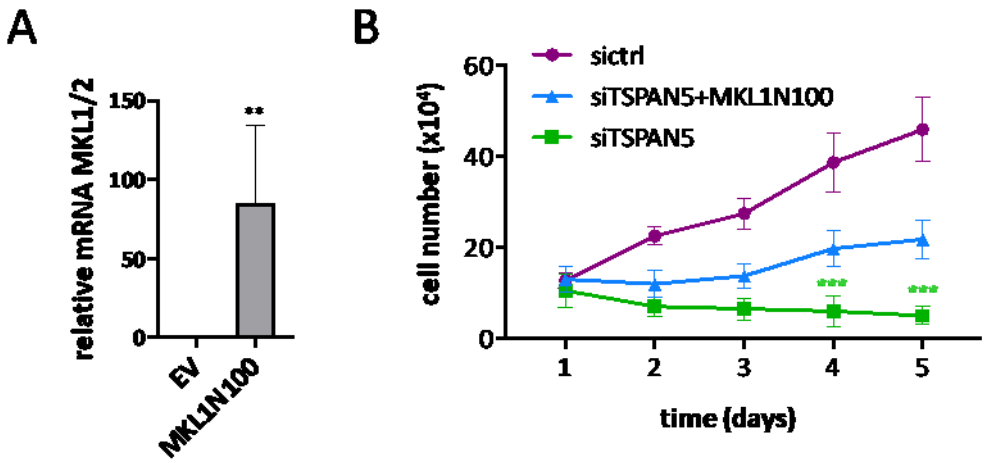

Figure 25: Overexpression of the constitutively active MKL1 variant (MKL1N100) attenuates the proliferation arrest. (A) HuH7 cells were first transiently transfected with TSPAN5 siRNA (siTSPAN5) or scrambled siRNA as control (sictrl) and then subjected to plasmid transfection with MKL1N100 mutant (MKL1N100) or empty vector (EV) the next day. After 48 h transfection efficiency was assessed by qRT-PCR using the gene specific primers and 18S primers for normalization. **(B)** HuH7 proliferation was monitored daily for 5 days by counting the cells with Neubauer counting chamber. Values are mean ± SD (n=3); **p<0.01, ***p<0.001.

6.4.1.3 TSPAN5 is essential in general for proliferation of HCC cell lines

Another point for us was to check whether TSPAN5 depletion also causes a growth arrest in HCC cells with normal physiological DLC1 expression. In this context we additionally wanted to find out to what extent DLC1 itself influences the proliferation behavior of the cells. Therefore, we used HepG2 cells in which TSPAN5 expression was silenced via RNA interference. In further approaches, DLC1 and also the combination DLC1 and TSPAN5 were switched off by transfecting appropriate siRNAs. Cells after DLC1 knockdown grew significantly faster than control cells from day 5 onward (Figure 26). After TSPAN5 depletion the proliferation of HepG2 cells was prevented both with and without DLC1 expression.

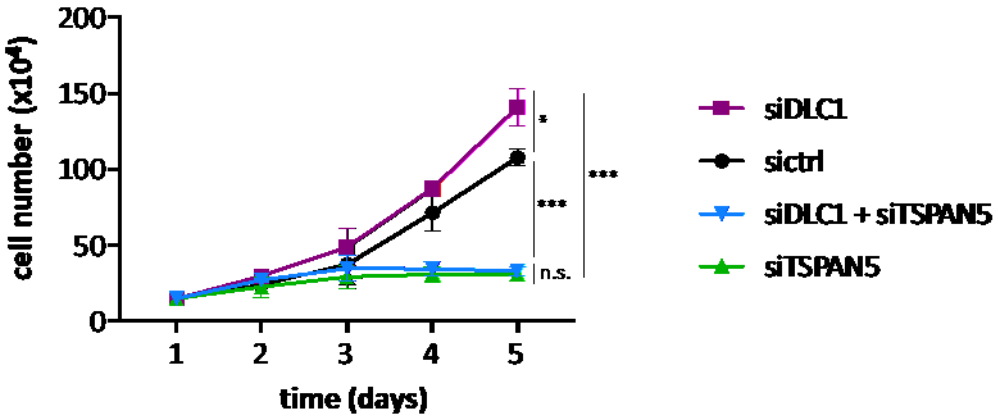

Figure 26: TSPAN5 knockdown via RNA interference provokes a growth arrest of HepG2 DLC1 KD cells. Genes were silenced with appropriate DLC1 or/and TSPAN5 siRNA (siDLC1, siTSPAN5) and scrambled RNA (sictrl) was used for control cells, each transfected with Lipofectamin RNAiMAX. Cell proliferation was monitored by counting the cells daily for 5 days with Neubauer counting chamber. Values are mean ± SD (n=3); *p<0.05, ***p<0.001.

As a next step, we were interested in how the proliferation rates after complete and permanent DLC1 knockout via CRISPR Cas9 (HepG2 DLC1 KO) differ from those with only transient knockdown via RNA interference. TSPAN5 was still switched off by siRNA transfection. Cell proliferation was determined by counting the cells daily for 6 days with a Neubauer counting chamber. HepG2 DLC1 KO cells proliferated analogous to the transient knockdown HepG2 cells significantly faster than the corresponding control cells (Figure 27). The remaining proliferation behavior of the CRISPR Cas9 KO cells was also very consistent to the transient knockdown cells. In particular, the knockdown of TSPAN5 by siRNA was able to arrest the proliferation of DLC1 positive as well as DLC1 negative cells.

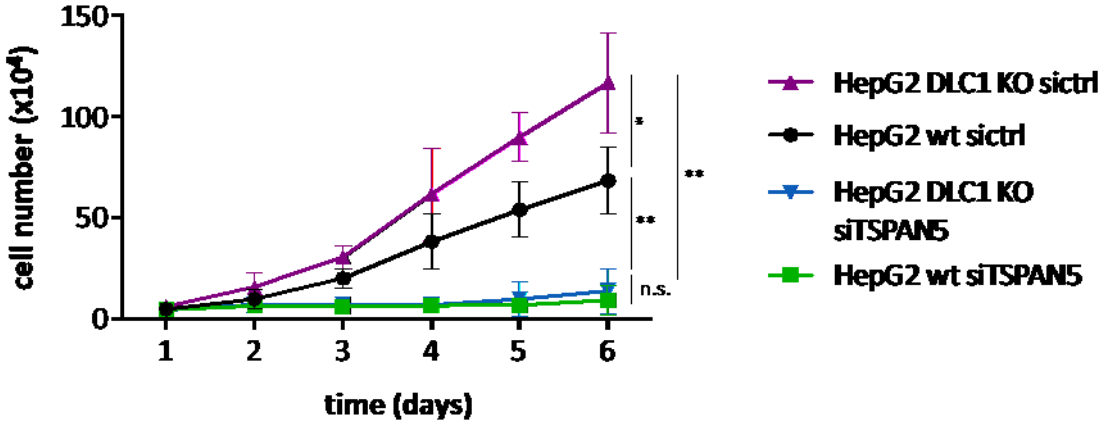

Figure 27: TSPAN5 depletion leads to proliferation arrest in DLC1 positive and negative HepG2 CRISP Cas9 KO cells. The proliferation rate of HepG2 DLC1 KO and wild type (wt) cells either expressing control siRNA (sictrl) or TSPAN5 siRNA (siTSPAN5) was monitored by counting the cells daily with Neubauer counting chamber for 6 days. Values are mean ± SD (n=3); *p<0.05, **p<0.01.

6.4.2 TSPAN5 depletion leads to decreased migration

In addition to proliferation, migration also plays an important role in tumorigenesis. Against this background, we analyzed the migration behavior of DLC1 deficient HCC cells after depletion of TSPAN5, VCAN or CDH2 compared to control cells. Knockdown of the different target genes was carried out via RNA interference with the respectively siRNA. The ability of cell migration after loss of the several genes was determined by scratch-wound assay (Figure 28). We could show that HuH7 control cells closed the wound gap 48 h post scratch generation, analogous behavior could be detected after VCAN depletion. The situation was completely different after TSPAN5 knockdown, since not a single cell was able to migrate into scratched gap. Silencing of CDH2 slowed down the migration, as the gap was not completely closed after 48 h. Evaluation by counting the migrated cells showed that the migration ability decreased significantly after TSPAN5 depletion, but also after CDH2 depletion.

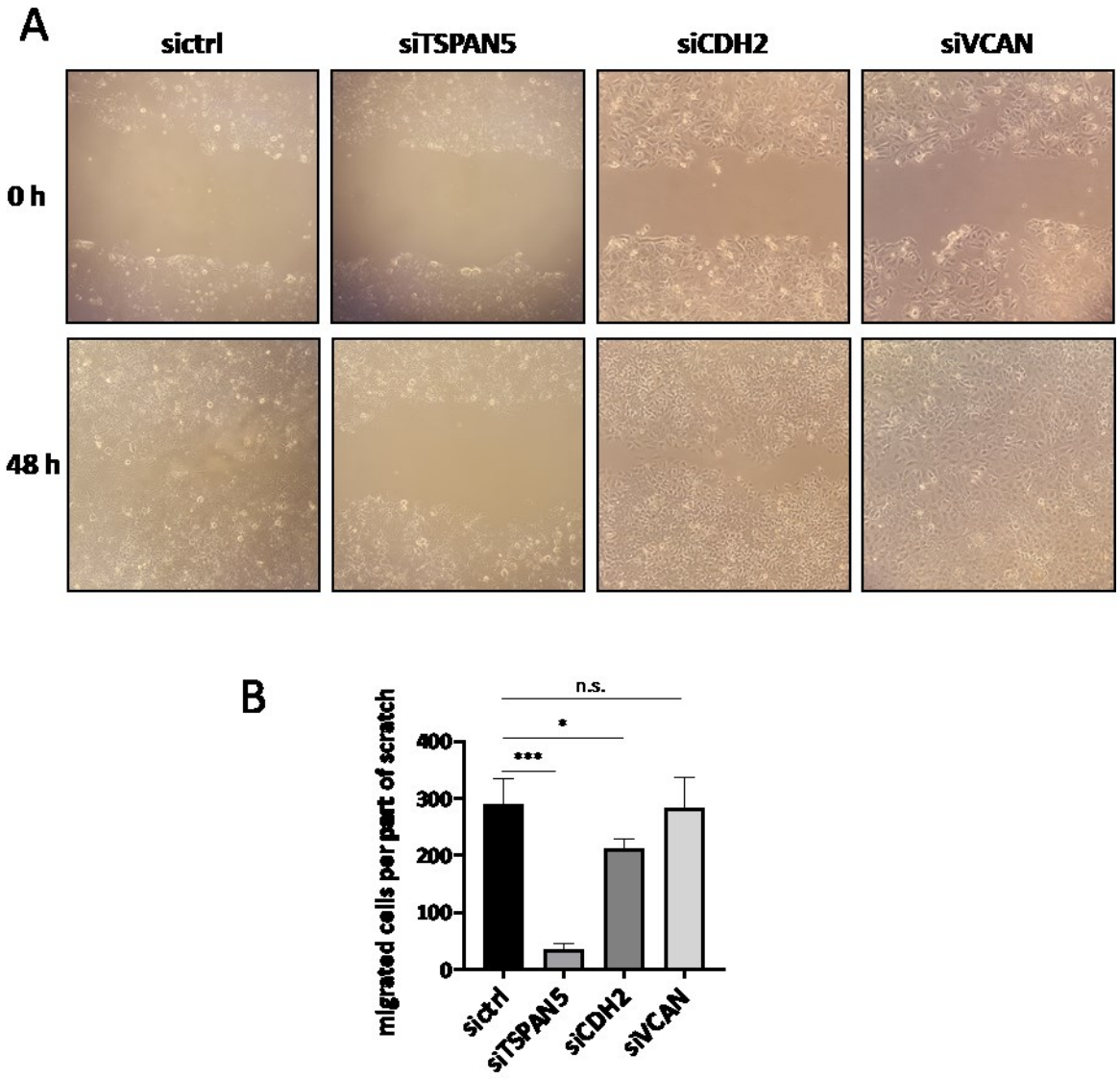

Figure 28: TSPAN5 and CDH2 depletion inhibits cell migration assessed by scratch-wound assay. HuH7 cells were transfected with indicated siRNAs (siTSPAN5, siCDH2 or siVCAN) and scrambled RNA (sictrl) was used for HuH7 control cells. 48 h post scratch creation, progress in closing the gap by migrated cells has been determined microscopically, recorded on images **(A)** and migrated cells per part of scratch were counted **(B)**. Values are mean ± SD (n=3); *p<0.05, ***p<0.001.

Consistent results were obtained after TSPAN5 knockdown for 48 h in HuH6 cells. Cell migration was reduced again in a statistically significant manner (Figure 29).

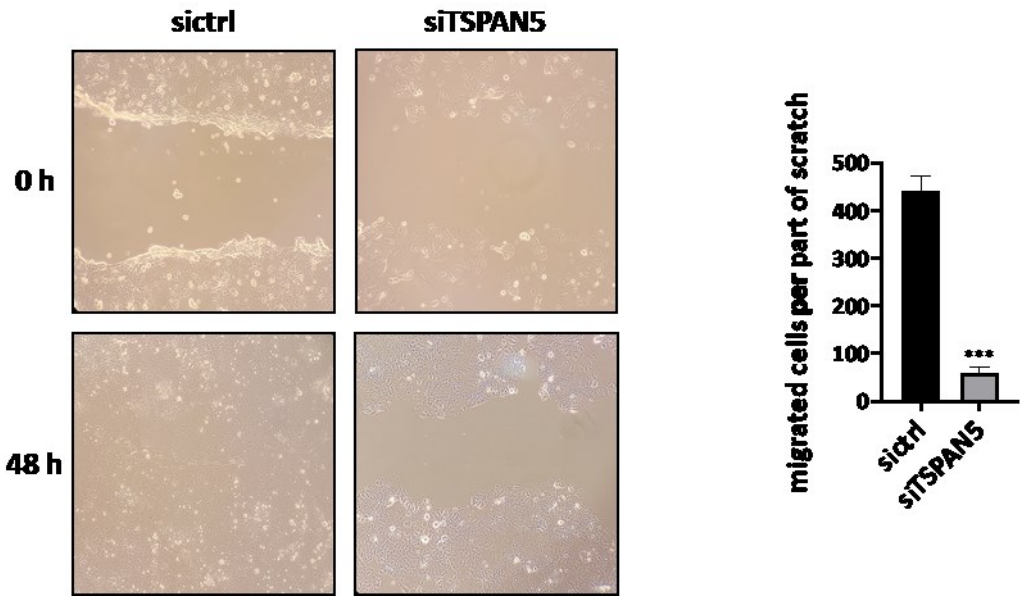

Figure 29: TSPAN5 depletion provokes migration stop in HuH6 cells. Silencing of TSPAN5 was performed by RNA interference (siTSPAN5) and scrambled RNA (sictrl) was used for control cells. Cell migration was determined by using the scratch-wound assay, in which cells migrating into the gap were monitored and counted. Values are mean ± SD (n=3); ***p<0.001.

6.4.3 TSPAN5 depletion results in decreased invasion

A further meaningful property of tumor cells is their ability to invade. Therefore, we analyzed the invasive behavior of HuH7 cells after TSPAN5 depletion compared to control cells. Cells were transfected with negative control or TSPAN5 siRNA, where we obtained a knockdown efficiency of about 75 % (Figure 30A). A Matrigel invasion assay was performed and we observed a significant decrease of invasive cells due to TSPAN5 silencing by counting the invaded cells after 48 h (Figure 30B). These findings suggest that TSPAN5 is not only required for proliferation and migration, but also for invasion.

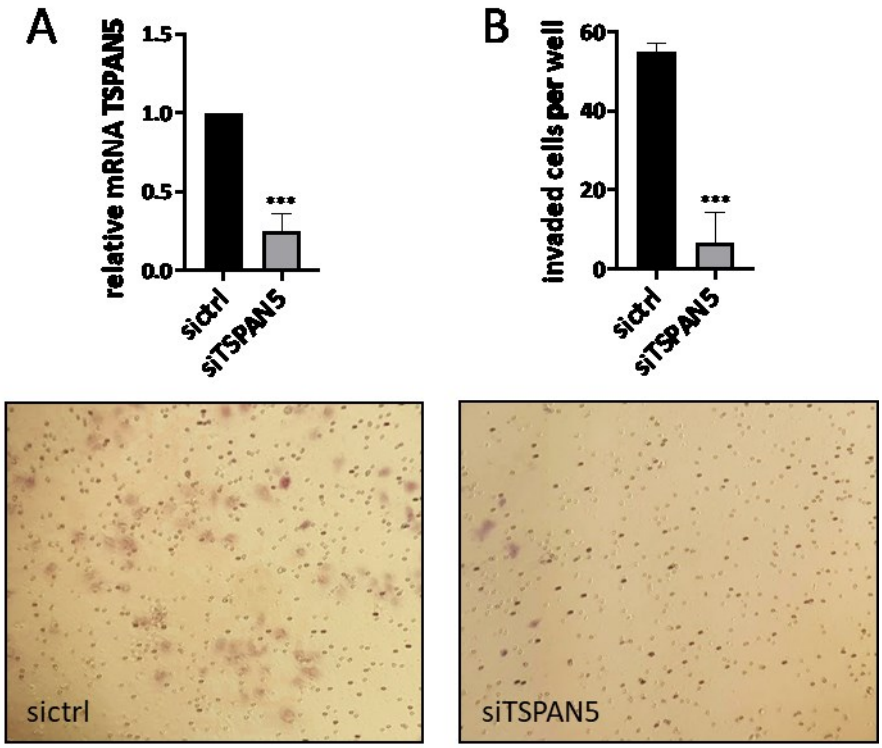

Figure 30: Decreased invasion of HuH7 cells upon TSPAN5 depletion. (A) HuH7 cells were transfected with TSPAN5 siRNA (siTSPAN5) and scrambled RNA (siCtrl). Knockdown efficiency was determined by qRT-PCR with TSPAN5 and 18S rRNA primers for normalization at 48 h post transfection. **(B)** Transfected HuH7 cells were subjected to Matrigel invasion assay chambers and invaded cells were stained by crystal violet and counted after 48 h. Values are mean ± SD (n=3); ***p<0.001.

6.4.4 TSPAN5 depletion prevents spheroid formation

As another important property of tumorigenesis, we investigated to what extent HCC cells are able to form spheroids after TSPAN5, CDH2 or VCAN loss. Therefore, the respective gene was silenced by RNA interference in HuH7 cells and knockdown efficiencies between 60-80 % were reached (Figure 31A). Knockdown and control cells were transduced to a dedicated spheroid assay plate and spheroid formation was monitored daily for 11 days. Two days after seeding the cells an onset of small cell formations could be observed in each experimental set. A maximum spheroid formation was noted in HuH7 control cells on day 11 (Figure 31B). These control spheroids have significantly grown to a size of about 160 µm. While silencing of VCAN and CDH2 did not affect HuH7 spheroid formation, knockdown of TSPAN5 provoked the building of spheroids completely (Figure 31C).

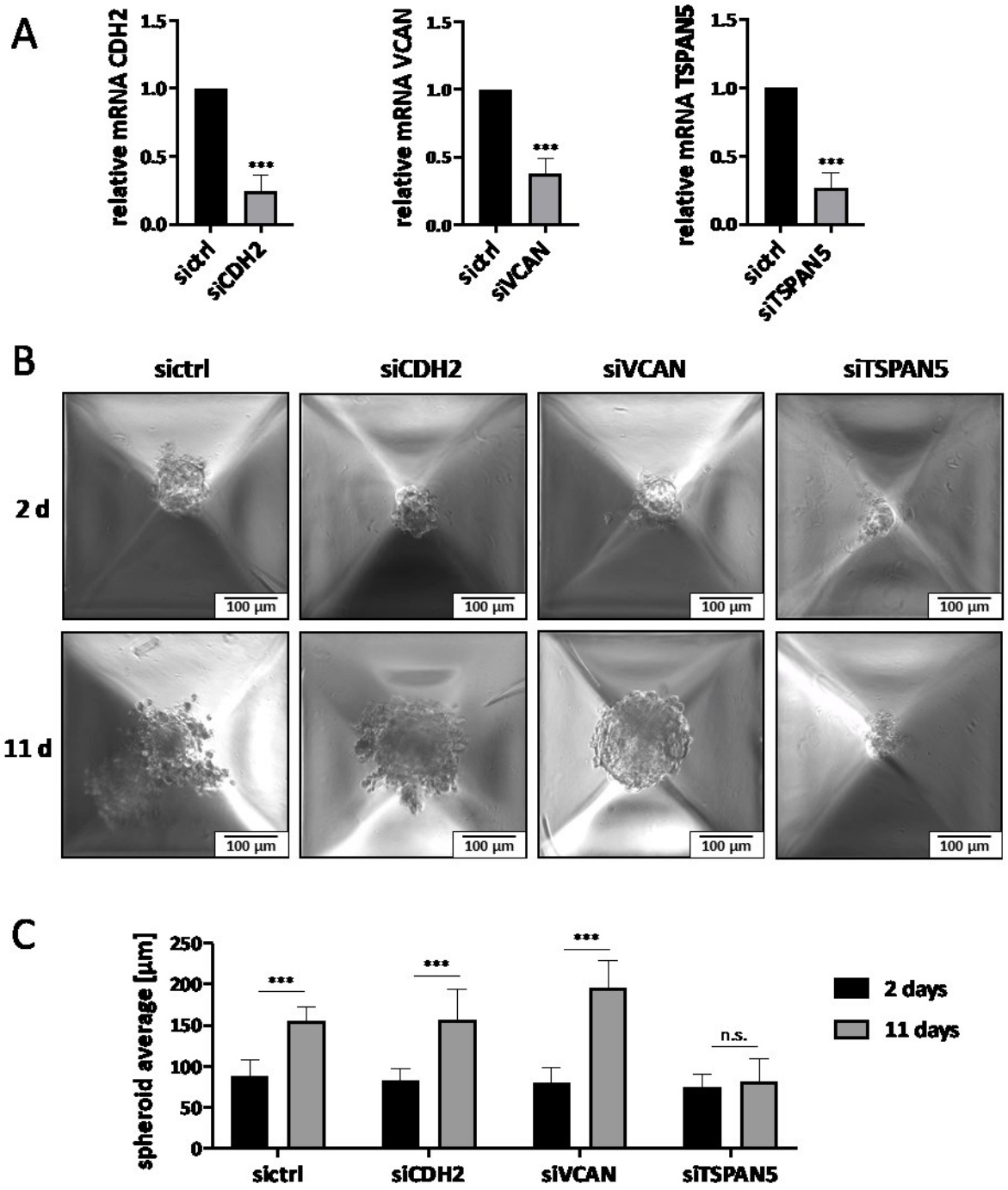

Figure 31: Inhibited spheroid formation upon TSPAN5 depletion. (A) Spheroid assay was performed in HuH7 control (sictrl) and knockdown cells in which CDH2, VCAN or TSPAN5 were switched off in single approaches using RNA interference (siCDH2, siVCAN, siTSPAN5). For knockdown efficiency mRNA expression of the silenced gene was assessed by qRT-PCR and normalized to 18S. **(B)** Transfected HuH7 cells were transduced to a special spheroid plate and incubated for 11 days at 37°C. Spheroid formation was monitored daily and pictures were taken with an optical microscope at the beginning and the end of spheroid building. **(C)** The spheroid averages were measured every day and those of day two and day 11 were compared to the same condition. Values are mean ± SD (n=3); ***p<0.001.

All these results show that the expression of the novel target gene TSPAN5 is required for characteristic properties of a tumor cell such as proliferation, migration, invasion and the ability to form spheroids. While silencing of CDH2 and VCAN did not affect the features of a tumor cell, TSPAN5 depletion was able to inhibit tumorigenic properties. Taking into account these results, it can be hypothesized that TSPAN5 is able to be a transducer of the MKL1/2 effects regarding tumorigenesis and tumor growth.

6.5 Tumorigenic characteristics of TSPAN5

Due to the findings above that TSPAN5 is required for cell proliferation, migration and invasion, we selected TSPAN5 as the target gene of interest and wanted to learn more about its tumorigenic characteristics. Therefore, we wanted to investigate the influence of TSPAN5 on hallmarks for cancer cells and induction of senescence.

6.5.1 TSPAN5 depletion induces senescence

Based on the fact that MKL1/2 loss inhibits HCC xenograft growth by inducing senescence (Hampl et al. 2013), we determined the possibility of senescence induction upon TSPAN5 depletion. Therefore, we performed a senescence-associated ß-galactosidase (SA-ß-gal) staining in DLC1 deficient HuH7 cells, transfected with TSPAN5 siRNA and scrambled RNA for control. The blue colored cells in each experimental approach were counted and compared (Figure 32). In doing so we noticed a significant induction of senescence in cells with TSPAN5 loss.

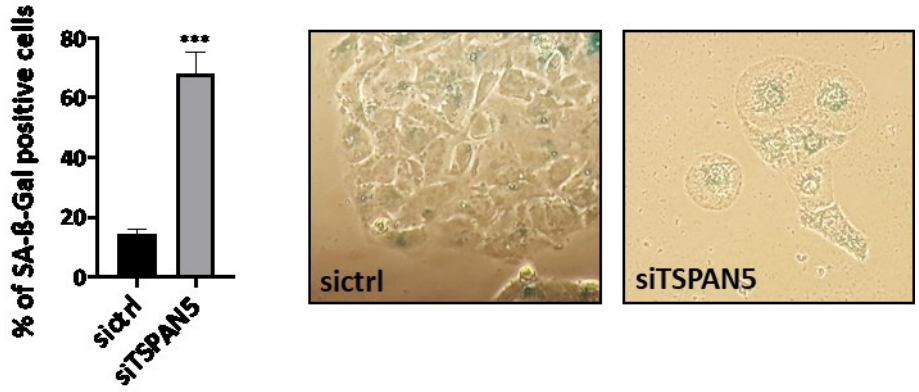

Figure 32: Induction of cellular senescence upon TSPAN5 depletion. Senescence-associated ß-galactosidase staining was performed in HuH7 cells 5 days after transfection with TSPAN5 siRNA (siTSPAN5) or scrambled RNA (sictrl). SA-ß-gal positive and thereby blue colored cells were counted and put into relation. Values are mean ± SD (n=3); ***p<0.001.

We succeeded in reproducing the results of senescence induction in HuH6 cells. Again, a significant increase in senescence induction was observed after TSPAN5 loss (Figure 33).

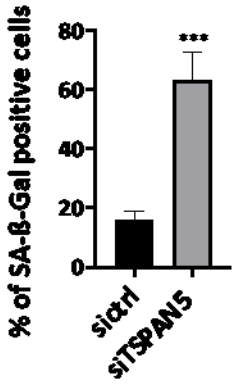

Figure 33: Induction of cellular senescence upon TSPAN5 loss. Senescence evidence in HuH6 cells either expressing control siRNA (sictrl) or TSPAN5 siRNA (siTSPAN5) was carried out by senescence associated ß-galactosidase staining. The blue colored SA-ß-gal positive cells were counted and compared. Values are mean ± SD (n=3); ***p<0.001.

We obtained further evidence of senescence induction through the evaluation of senescence-associated heterochromatin foci (SAHF) (Di Micco et al. 2011; Narita et al. 2003). Therefore, we performed immunoblotting in HuH7 cells previously transfected with TSPAN5 siRNA and subsequently incubated for 6 days. We could observe an accumulation of Histone H3 methylated on lysine 9 (H3K9me3) in SAHF upon TSPAN5 depletion (Figure 34A). We also

detected a slight increase in levels of H3K9me3 after TSPAN5 knockdown in HuH6 cells (Figure 34B).

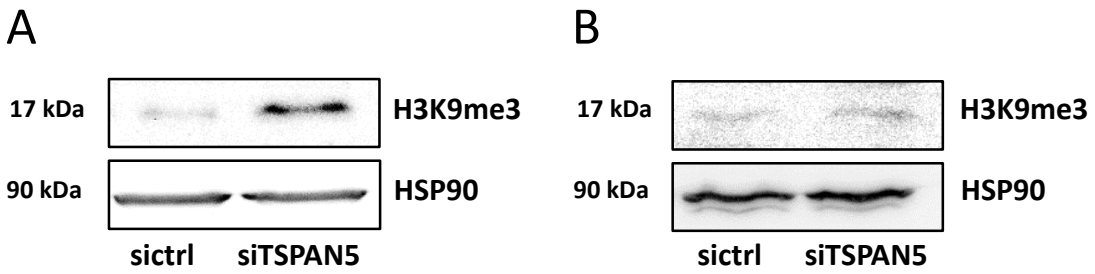

Figure 34: Accumulation of Histone H3 methylated on Lysine 9 upon TSPAN5 depletion. Lysates of **(A)** HuH7 and **(B)** HuH6 cells either expressing negative control RNA (sictrl) or TSPAN5 siRNA (siTSPAN5) for 6 days were immunoblotted with anti-H3K9me3 and anti-HSP90 antibodies as loading control.

6.5.2 TSPAN5 depletion induces oncogene-induced senescence

After demonstrating a senescence-inducing effect after TSPAN5 depletion revealed by ß-galactosidase staining and accumulation of methylated Histone H3, we sought to find out whether TSPAN5 loss also leads to oncogene-induced senescence (OIS) as knockdown of MKL1/2 does (Hampl et al. 2013). To figure out the contribution of TSPAN5 depletion to the induction of OIS, we examined established markers for OIS such as phosphorylation of ERK1/2, accumulation of $p16^{INK4a}$, hypophosphorylation of retinoblastoma protein (Rb), an accumulation of nuclear promyelocytic leukemia (PML) protein bodies and expression of *CXCL10* or *TNFSF10* upon silencing TSPAN5.

6.5.2.1 Activation of ERK1/2 upon TSPAN5 depletion

Due to the fact that ERK is a downstream effector of Ras and OIS is induced via Ras, we were interested in whether loss of TSPAN5 could also activate ERK1/2 (Hampl et al. 2013). To finally test the activation of ERK, we determined the phosphorylation status of ERK1/2 by immunoblotting (Crews and Erikson 1993). Thereby we could show a strong increase of phosphorylated ERK1/2 in DLC1 deficient HuH7 cells as well as in HuH6 cells after TSPAN5 knockdown by siRNA (Figure 35).

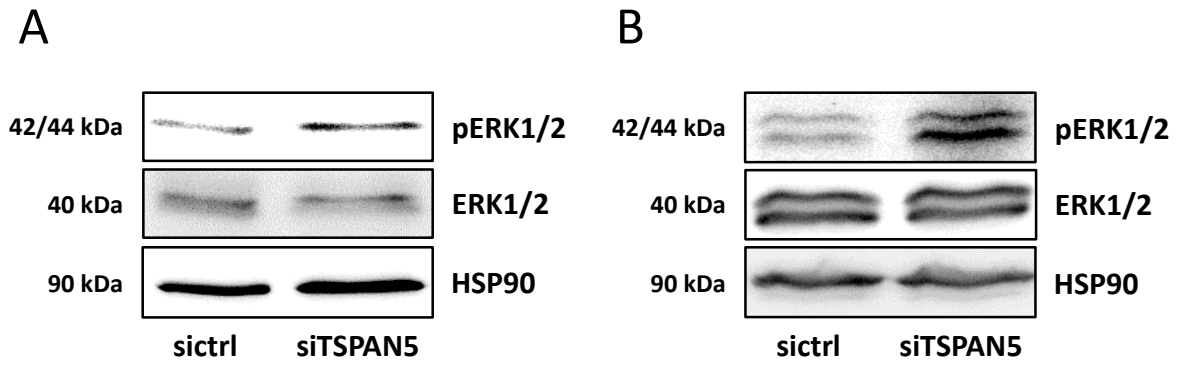

Figure 35: Activation of ERK1/2 by phosphorylation upon TSPAN5 loss. Protein lysates of **(A)** HuH7 cells and **(B)** HuH6 cells transfected with scrambled RNA (sictrl) or TSPAN5 siRNA (siTSPAN5) were prepared and measured. Same amounts of total protein were subjected to immunoblotting. pERK was detected by using anti-ERK$^{pT202/pY204}$ antibody and afterwards total anti-ERK antibody. For loading control anti-HSP90 antibody was used.

6.5.2.2 Accumulation of p16^{NKk4a} expression in HCC cells after TSPAN5 depletion

It is a well-established fact that p16^{INK4a}, operating as a tumor suppressor, is enhanced expressed in senescent cells (Alcorta et al. 1996; Hara et al. 1996; Sherr and Roberts 1999). We determined the expression levels of p16^{INK4a} in lysates of HuH7 cells after TSPAN5 was silenced via RNA interference by immunoblotting. We found out that the protein expression of p16^{INK4a} was accumulated in DLC1 deficient HuH7 cells upon TSPAN5 depletion (Figure 36).

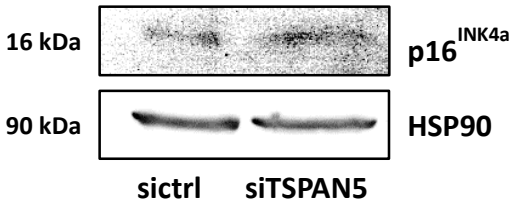

Figure 36: Accumulation of p16^{INK4a} protein expression upon TSPAN5 depletion. Immunoblotting of lysates of HuH7 cells either expressing control siRNA (sictrl) or TSPAN5 siRNA (siTSPAN5) for 6 days. Equal amounts of total protein were applied to immunoblotting and anti-p16^{INK4a} and anti-HSP90 antibodies were used for detection.

6.5.2.3 Hypophosphorylation of the retinoblastoma protein upon TSPAN5 knockdown

In order to obtain more information about the induction of oncogene-induced senescence after TSPAN5 loss, we tested further characteristic OIS markers such as retinoblastoma protein (Rb), which is converted to the active state by downregulation of the phosphorylation status.

Immunoblotting was determining a strong decrease of phosphorylated Rb expression in HuH7 (Figure 37A) und HuH6 (Figure 37B) cells after TSPAN5 knockdown. This in turn indicated a strong hypophosphorylation of Rb providing evidence for OIS upon TSPAN5 depletion.

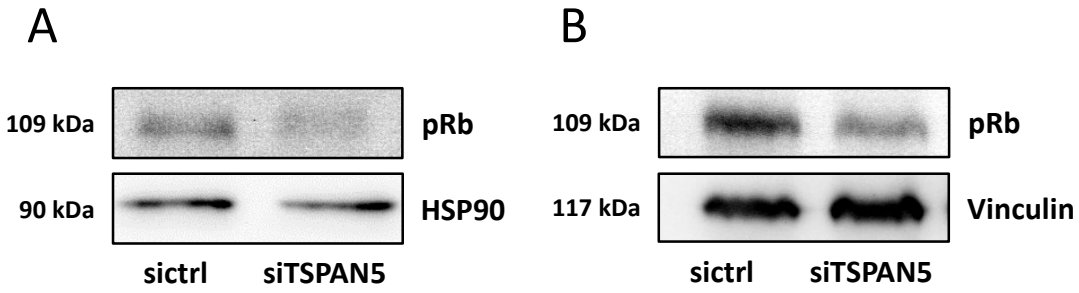

Figure 37: Hypophosphorylation of retinoblastoma protein after TSPAN5 depletion. Lysates of HuH7 **(A)** and HuH6 **(B)** cells either expressing control siRNA (sictrl) or TSPAN5 siRNA (siTSPAN5) were immunoblotted with anti-pRb antibody. For loading control anti-HSP90 **(A)** or anti-Vinculin **(B)** antibodies were used.

6.5.2.4 Accumulation of nuclear PML bodies upon TSPAN5 depletion

We next wanted to examine whether there is an accumulation of promyelocytic leukemia (PML) protein bodies in the nucleus after TSPAN5 loss. Increased expression of PML leads to cell cycle arrest and is therefore important for a senescent response (Bischof et al. 2002; Ferbeyre et al. 2000; Pearson et al. 2000). Further, PML expression is often lost in human cancers (Gurrieri et al. 2004). Using immunofluorescence, we demonstrated that there is significant accumulation of PML nuclear bodies in HuH7 cells after 72 h of TSPAN5 loss (Figure 38).

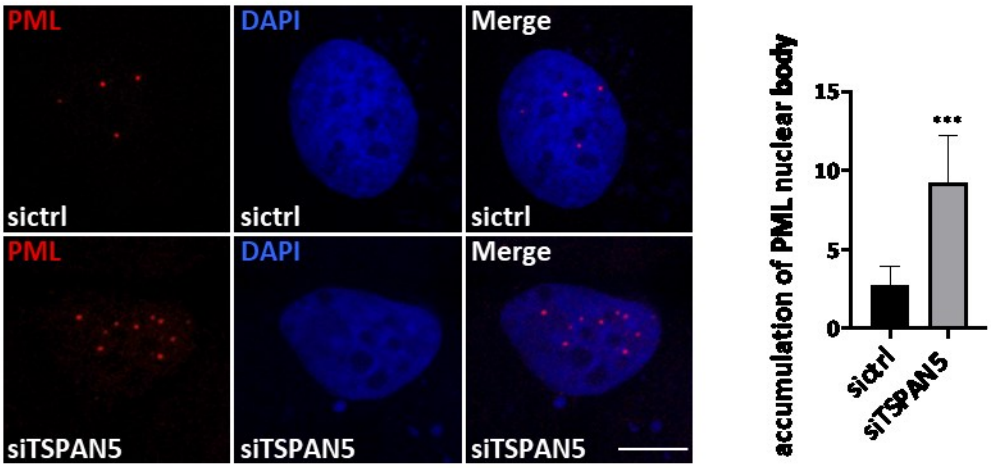

Figure 38: Accumulation of PML nuclear bodies after TSPAN5 depletion. Immunofluorescence of HuH7 cells after silencing TSPAN5 by RNA interference (siTSPAN5) for 72 h. Cells were fixed and followed immunostained with anti-PML antibody for 1 h. Nuclei were counterstained with DAPI. Three independent experiments were performed, and representative images are shown. Scale bar, 8 µm. Quantification of PML nuclear body accumulation by counting the red spots in 50 cells per condition. Data are means ± SD (n=3); ***p<0.001.

6.5.2.5 Induction of CXCL10 and TNFSF10 expression upon TSPAN5 loss

To investigate further OIS markers like C-X-C motif chemokine 10 (CXCL10) and tumor necrosis factor superfamily member 10 (TNFSF10), both senescence messaging secretome (SMS) factors, we silenced TSPAN5 via RNA interference in HuH7 cells (Braumüller et al. 2013; Coppé et al. 2010; Kuilman and Peeper 2009). We reached a knockdown efficiency of 60 % (Figure 39A), and after 6 days of incubation to enable senescence induction, the expression levels of the senescence markers were analyzed. We found a significant upregulation of the *CXCL10* and *TNFSF10* mRNA expression upon TSPAN5 depletion compared to the negative control cells. The result of increased *CXCL10* mRNA expression after TSPAN5 loss could be reproduced in HuH6 cells with an 80 % TSPAN5 knockdown rate (Figure 39B).

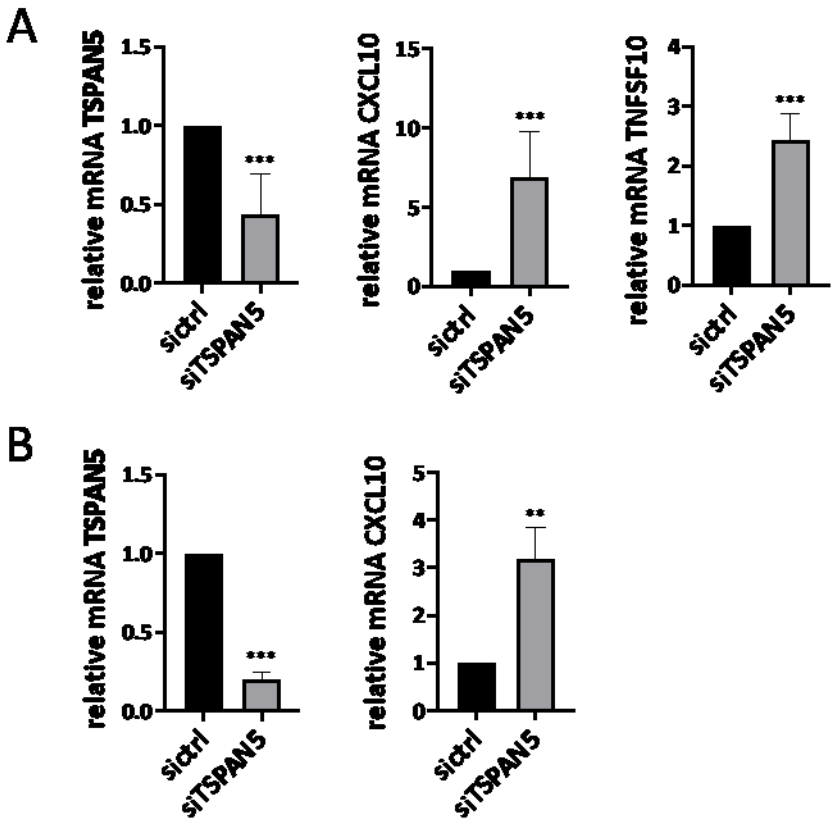

Figure 39: Induction of CXCL10 and TNFSF10 expression upon TSPAN5 depletion. (A) HuH7 cells were transfected with negative control RNA (sictrl) or TSPAN5 siRNA (siTSPAN5). Knockdown efficiency was determined by qRT-PCR after 48 h with TSPAN5 and 18S primers for normalization. CXCL10 and TNFSF10 mRNA expression were subjected by qRT-PCR with respective CXCL10, TNFSF10 and 18S primers for normalization 6 days after transfection. **(B)** HuH6 cells were transfected with negative control RNA (sictrl) or TSPAN5 siRNA (siTSPAN5). Knockdown efficiency was determined by qRT-PCR after 48 h with TSPAN5 and 18S primers for normalization. CXCL10 and TNFSF10 mRNA expressions were subjected by qRT-PCR with respective CXCL10, TNFSF10 and 18S primers for normalization 4 days after transfection. Values are mean ± SD (n=3); **p<0.01, ***p<0.001.

Summarizing the results in this chapter, we could demonstrate that established OIS markers like phosphorylation of ERK1/2, accumulation of $p16^{Ink4a}$, hypophosphorylation of Rb, accumulation of nuclear PML bodies and elevation of *CXCL10* and *TNFSF10* were confirmed after knocking down TSPAN5. All these facts are indicating that TSPAN5 depletion mediates the reduced tumorigenic cell properties like proliferation arrest or invasion stop by inducing oncogene-induced senescence.

6.5.3 TSPAN5 depletion inhibits epithelial-mesenchymal transition

Since the multistep process of epithelial to mesenchymal transition (EMT) plays a fundamental role in tumor progression and especially in the early stages of metastasis, we were interested in a possible role of TSPAN5 in this process (Giannelli et al. 2016). Precisely because TSPANs, as transmembrane proteins and in the context of TEMs, have a strong influence on cell adhesion, migration and invasion, we hypothesized that a TSPAN5 knockdown would affect specific EMT markers (Hemler 2005; Peñas et al. 2000; Yáñez-Mó et al. 2009). Regarding this, we examined different EMT markers in dependence of TSPAN5 loss by RNA interference using an epithelial-mesenchymal transition sampler kit according to the manufacturer's instructions. We found that as early as 24 h after transient siTSPAN5 transfection, there is an increase in epithelial-cadherin (E-Cadherin) and Zonula occludens-1 (ZO-1) protein levels in HuH7 cells compared to control cells. This increase continues until 72 h for E-Cadherin and 48 h for ZO-1 after transfection (Figure 40). E-Cadherin and ZO-1 are both very characteristic markers. E-Cadherin has been shown to have tumor suppressive properties and its loss has been associated with increased metastasis and a worsened prognosis for patients in many studies (Derycke and Bracke 2004; Gan et al. 2016; Li and Herlyn 2000; Mareel and Leroy 2003; Tomita et al. 2000). ZO-1 is linked to the function of tight and adherens junctions and is thought to play a critical role in prevention of HCC progression by inhibiting migration and invasion (González-Mariscal et al. 2000; Nagai et al. 2016). Further, after a 24 h knockdown of TSPAN5, we detected a sustained decrease in vimentin protein levels (Figure 40). Vimentin has been recognized as an EMT marker in recent years, and its overexpression in cancers is associated with tumor growth and metastasis (Satelli and Li 2011). 72 h after TSPAN5 silencing, we also observed a decrease in SLUG proteins, a zinc-finger transcription factor that is overexpressed in various cancers (Figure 40) (Meng et al. 2019).

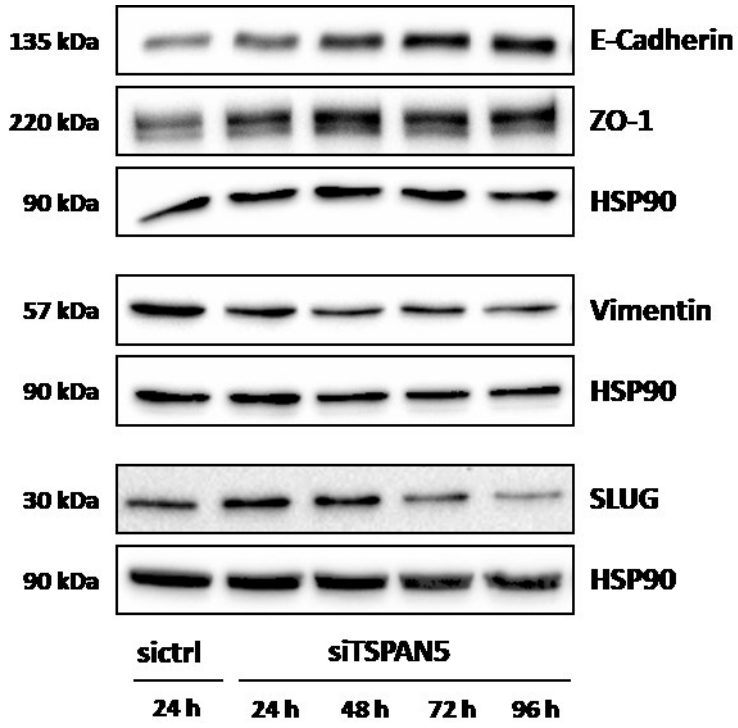

Figure 40: TSPAN5 loss inhibits EMT. HuH7 cells were either expressing control siRNA (sictrl) or TSPAN5 siRNA (siTSPAN5). Cell lysates were generated after 24 h, 48 h, 72 h and 96 h and afterwards immunoblotted with anti-E-Cadherin, anti-ZO-1, anti-Vimentin, anti-SLUG and anti-HSP90 antibodies as loading control.

6.6 Effects of TSPAN5 depletion on MKL1/SRF signaling pathway

Our next point of interest was the consideration whether TSPAN5 itself has a role in the MKL1/SRF signaling pathway and can affect it. For this study, we silenced TSPAN5 transient in HuH7 cells, which possess a permanently active RhoA/actin signaling pathway and thus active MKL1/SRF gene expression, and investigated several aspects of this pathway.

6.6.1 Depletion of TSPAN5 reduces RhoA activity

As an initiating step in the RhoA pathway, we first tested the activity of RhoA itself for changes regarding a TSPAN5 knockdown. For this reason, we performed a RhoA assay in HepG2 DLC1 CRISP Cas9 KO cells that have a permanently active RhoA due to the DLC1 loss. Additional silencing of TSPAN5 by RNA interference resulted in a reduced amount of GTP-loaded and thus active RhoA, which we found out by immunoprecipitation with an antibody that specifically recognizes GTP-loaded RhoA (Figure 41).

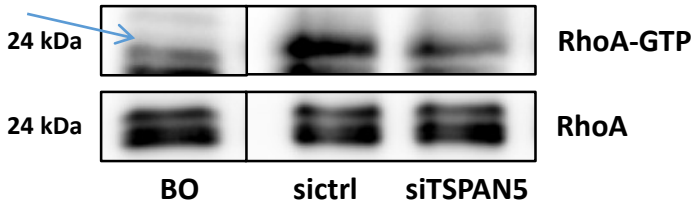

Figure 41: Inactivation of RhoA upon TSPAN5 depletion. HepG2 DLC1 CRISP Cas9 KO cells were additionally transfected with TSPAN5 siRNA (siTSPAN5) and scrambled RNA (sictrl) for control. Lysed cells were immunoprecipitated with anti-active RhoA antibody. The magnetic-beads only control (BO) was prepared analogously, but no antibody was added. Lysates with equal amount of total protein were directly immunoblotted with anti-RhoA antibody.

6.6.2 Downregulation of F-actin upon TSPAN5 depletion

We were next interested in whether there were also alterations in the cytoskeleton due to the reduced activity of RhoA upon TSPAN5 loss. Especially we hypothesized changes in the polymerization of monomeric G-actin to filamentous F-actin, since this is induced by activation of RhoA via Rho Kinase and mDia (Copeland and Treisman 2002; Sotiropoulos et al. 1999). Therefore, we analyzed the actin cytoskeleton by F- and G-actin fractionation in HuH7 (Figure

42A) and HuH6 (Figure 42B) cells with each silenced transiently TSPAN5. We were able to show that the ratio of F-actin to G-actin became smaller compared to the control cells after TSPAN5 was silenced. This indicates a strong decrease in the mean cellular content of F-actin.

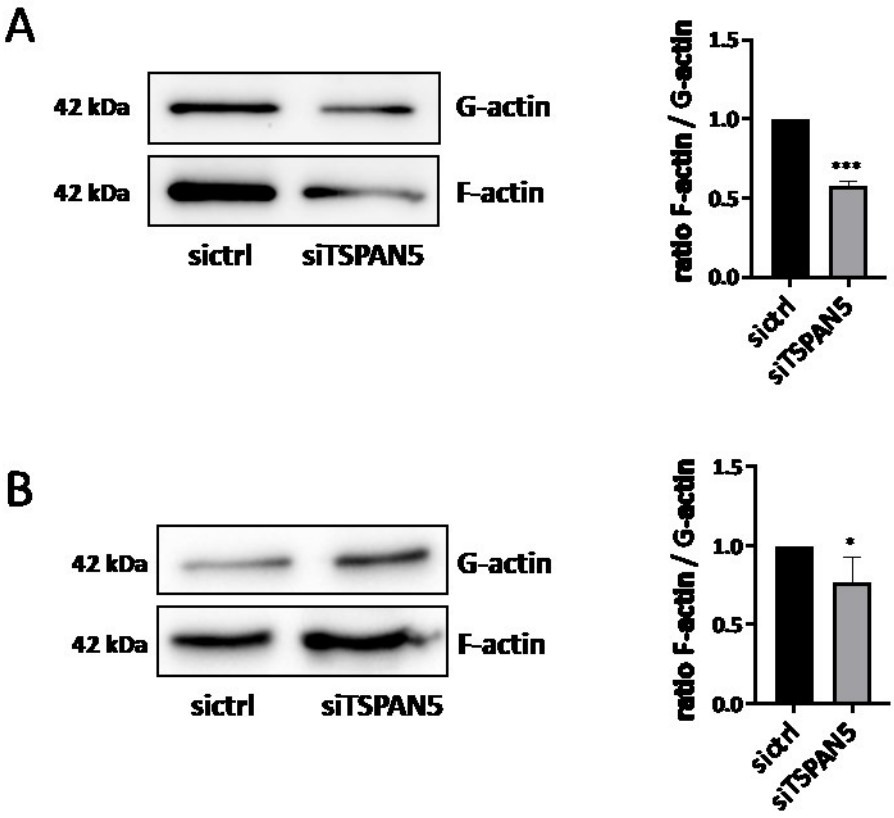

Figure 42: Decrease in cellular F-actin upon TSPAN5 depletion. TSPAN5 was transient depleted by RNA interference (siTSPAN5) in HuH7 **(A)** and HuH6 **(B)** cells. F- and G-actin fractions were separated and immunoblotted using anti-Actin antibody. Quantification was done with BioRad ImageLab software. Values are mean ± SD (n=3); *p<0.05; ***p<0.001.

6.6.3 Reduced actin stress fibers upon TSPAN5 depletion

Taking into account the results of the actin fractionation, it was in our interest to investigate the cytoskeleton in more detail after the loss of TSPAN5. In the course of this we transfected HuH7 cells with control siRNA (sictrl) and TSPAN5 siRNA (siTSPAN5) and performed an immunofluorescence analysis using a fluorescent α-Phalloidin conjugate for actin staining. By fluorescence microscopy we observed a reduction in the actin stress fibers after TSPAN5 loss. The α-Phalloidin staining also showed that after TSPAN5 silencing the actin network was increasingly reorganized from the nucleus and the perinuclear region towards the cell

membrane (Figure 43, left panel). Analyzing the MKL1 staining in the control cells compared to TSPAN5 knockdown cells, it is at least partially noticeable that in some cells upon TSPAN5 depletion MKL1 is not as strongly localized in the nucleus as it is usual for untreated HuH7 (Figure 43, middle panel).

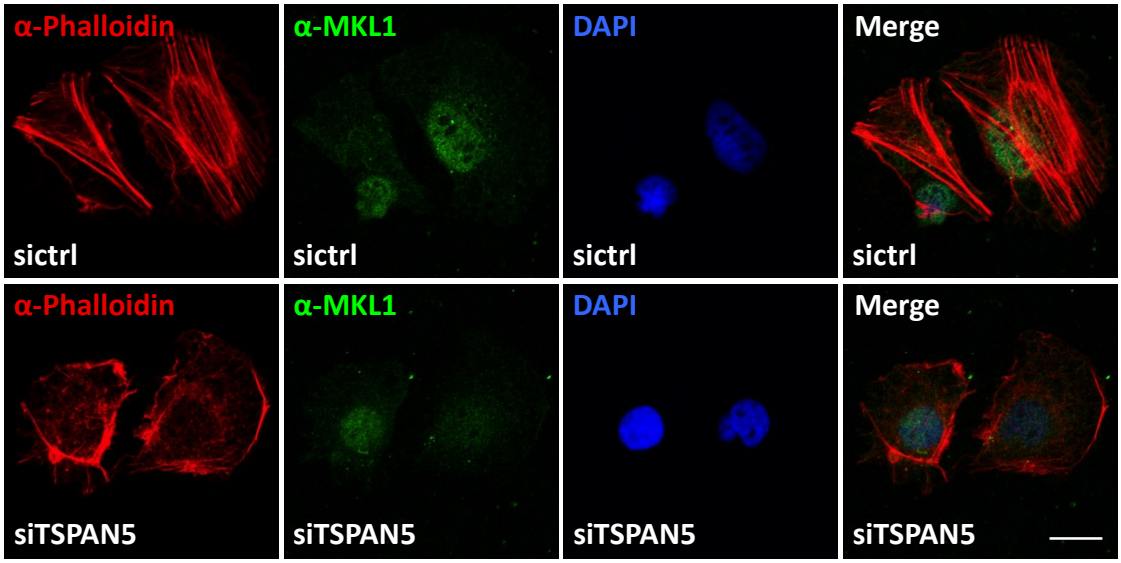

Figure 43: Reduced and reorganized actin skeleton upon TSPAN5 knockdown. Immunofluorescence analysis of HuH7 cells either expressing control siRNA (sictrl) or TSPAN5 siRNA (siTSPAN5). Cells were fixed, subsequently Phalloidin was stained by α-Phallotoxin A555 and MKL1 was immunostained with anti-MKL1 antibody. Nuclei were counterstained with DAPI. Three independent experiments were performed, and representative images are shown. Scale bar, 10 µm.

6.6.4 Abrogation of MKL1-FLNA interaction upon TSPAN5 knockdown

The finding that loss of TSPAN5 results in a percentage decrease in F-actin may indicate that there is now relatively more G-actin in the cell. This could prevent MKL1 from translocating into the nucleus as a complex with Filamin A (FLNA) and F-actin that could be reflected by an increased complexation of MKL1 with G-actin (Kircher et al. 2015). This allows us to theorize whether the FLNA-MKL1 complex, which is important for the activation of MKL1/SRF, also decreases if MKL1 is complexed to monomeric G-actin. Accordingly, we analyzed the interaction between endogenous MKL1 and FLNA by proximity ligation assay (PLA) in HuH7 cells after TSPAN5 knockdown compared to negative control cells. We could determine an abrogation of MKL1-FLNA complexes upon TSPAN5 depletion in HuH7 cells (Figure 44A) as well as in 3T3 cells (Figure 44B). Murine 3T3 cells were used to visualize the interactions before and after TSPAN elimination particularly well under the confocal microscope.

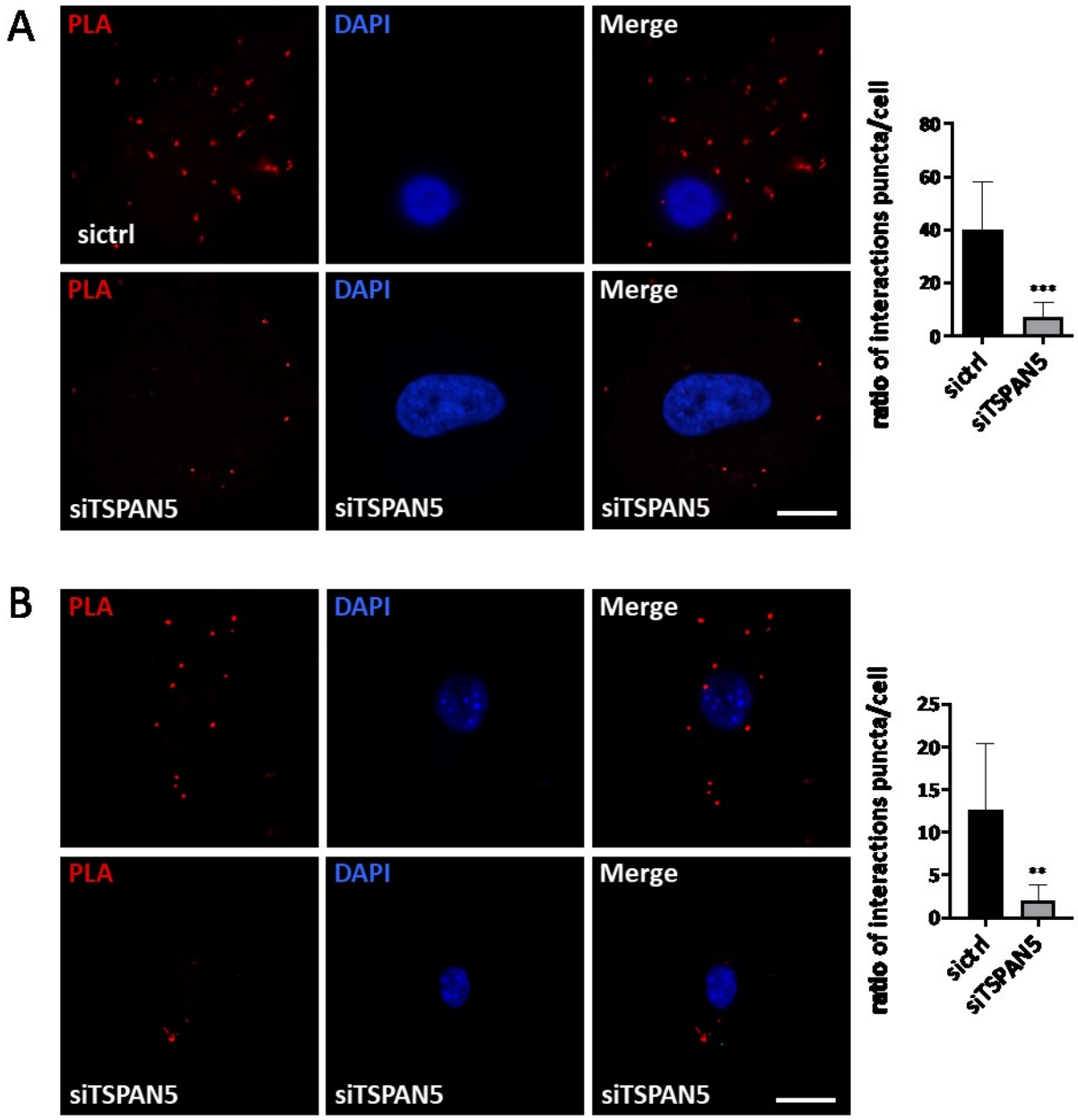

Figure 44: Abrogation of MKL1-FLNA interactions upon TSPAN5 knockdown. Immunofluorescence analysis and quantification of proximity ligation assay (PLA) for endogenous MKL1 and FLNA in HuH7 **(A)** and 3T3 **(B)** cells either expressing control siRNA (sictrl) or TSPAN5 siRNA (siTSPAN5). Proximity ligation assay was performed by using anti-Filamin A antibody (Millipore) and anti-MKL1 antibody (SantaCruz). Scale bar, 10 µm. PLA signals were counted in 8 cells per condition.

6.6.5 Decreased expression of MKL1/SRF target genes upon TSPAN5 depletion

As shown in the upper chapters, TSPAN5 elimination leads to a significantly reduced number of MKL1-FLNA interactions. Considering that the MKL1-FLNA complex is a prerequisite for the translocation of MKL1 into the nucleus, and has been shown to be essential for the expression

of MKL1/SRF dependent target genes, we sought to determine whether depletion of TSPAN5 also decreases MKL1/SRF target gene expression (Kircher et al. 2015). To figure this out, we transfected HuH7 and HuH6 cells with scrambled or TSPAN5 siRNA with knockdown efficiency of 80 % and determined the MKL1/SRF target gene mRNA expression via qRT-PCR. It was revealed that after TSPAN5 loss there is a significant reduced gene expression of smooth muscle protein 22 (*SM22*), glioma pathogenesis-related protein 1 (*GLIPR1*) and transforming growth factor beta 1 (*TGFß1*) in HuH7 cells (Figure 45A) as well as in HuH6 cells (Figure 45B).

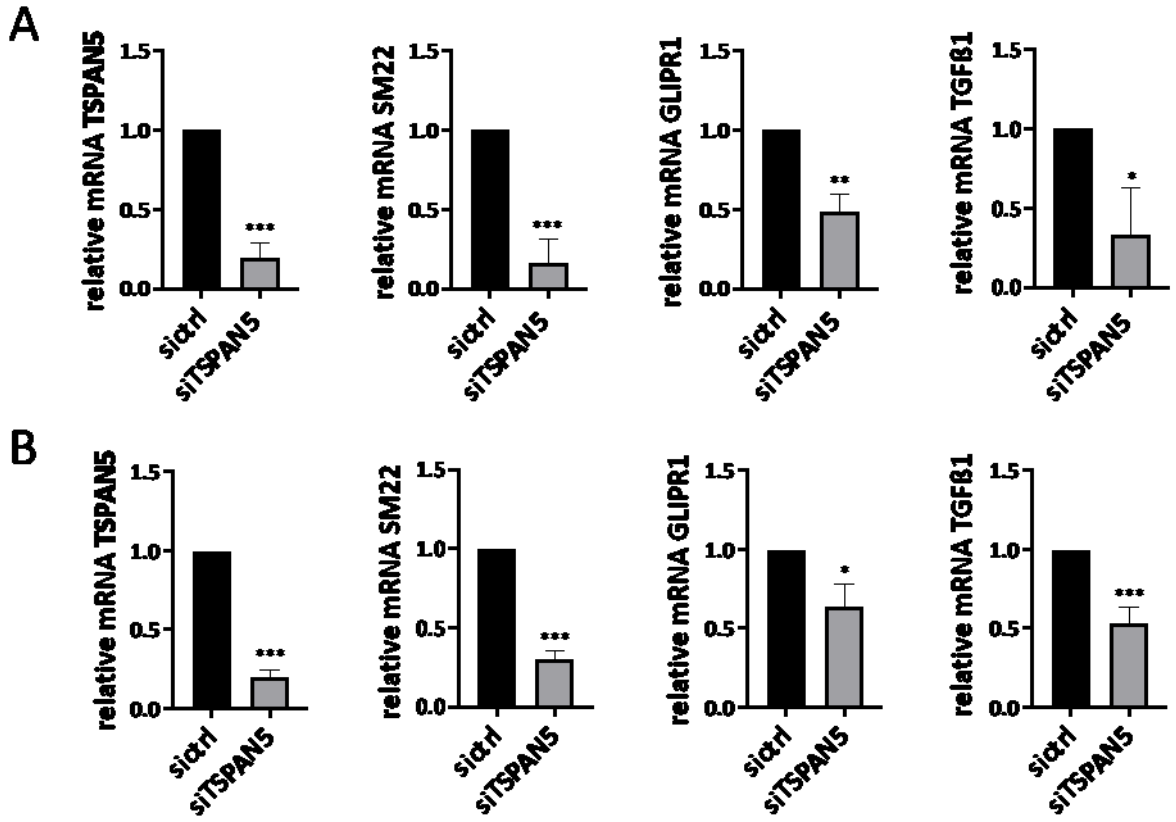

Figure 45: Downregulation of MKL1/SRF target genes upon TSPAN5 depletion. Knockdown efficiency of HuH7 **(A)** and HuH6 **(B)** cells either expressing control siRNA (sictrl) or TSPAN5 siRNA (siTSPAN5) was determined by qRT-PCR. mRNA expression of MKL1 target genes was analyzed via qRT-PCR using the appropriate gene specific primers and 18S rRNA primers for normalization in HuH7 cells **(A)** as well as in HuH6 cells **(B).** Values are mean ± SD (n=3); *p<0.05, **p<0.01, ***p<0.001.

The downregulation of MKL1/2 target genes after TSPAN5 loss can be shown not only on mRNA but also on protein levels. For this purpose, we transfected HuH7 cells with TSPAN5 siRNA for 96 h and finally immunoblotted the proteins, separated by SDS-PAGE. We were able

to show a strong decrease in protein expression for Myoferlin (MYOF), GLIPR1 and SM22 compared to control cells along with TSPAN5 silencing (Figure 46).

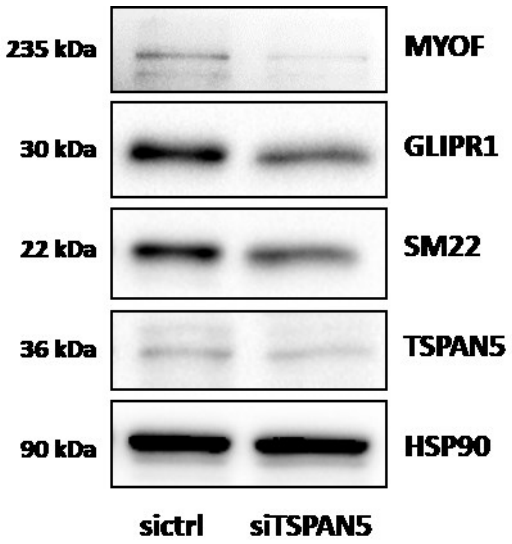

Figure 46: Downregulation of SM22 upon TSPAN5 knockdown. Lysates from HuH7 cells either expressing control siRNA (sictrl) or TSPAN5 siRNA (siTSPAN5) for 96 h were prepared and equal amounts of total protein were analyzed by immunoblotting using anti-Myoferlin, anti-GLIPR1, anti-Transgelin (SM22) anti-TSPAN5 and anti-HSP90 antibodies. Three independent experiments were performed and representative images are shown.

6.6.6 Reconstitution of TSPAN5 induces re-expression of MKl1 target genes

To ultimately prove the link between TSPAN5 and MKL target gene expression, we examined whether TSPAN5 reconstitution by plasmid transfection can reverse the downregulation of MKL1 target genes caused by previous TSPAN5 knockdown. In the course of this attempt, HuH7 cells were first transfected with respective siRNA to suppress TSPAN5 expression. The following day, TSPAN5 was reconstituted by plasmid transfection (Figure 47A). By analyzing the mRNA expression of MKL1 dependent target genes, we figured out that a prior knockdown of TSPAN5 provokes a significant decrease of genes like *SM22*, *GLIPR1* or *TGFß1* and moreover, an additional reconstitution of TSPAN5 abolished the downregulation (Figure 47B).

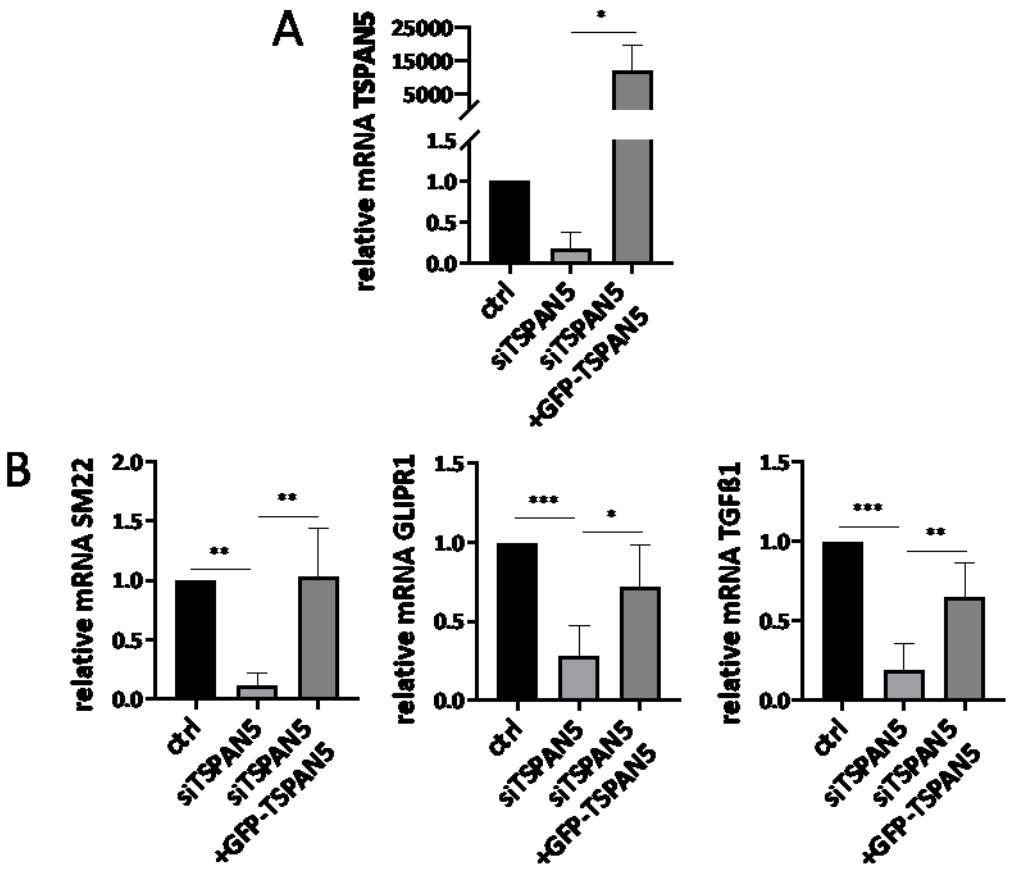

Figure 47: TSPAN5 reconstitution abolishes downregulation of MKL1 dependent target genes induced by prior TSPAN5 loss. TSPAN5 was switched off by RNA interference (siTSPAN5) in HuH7 cells and then re-expressed by plasmid transfection using 4 µg of GFP-TSPAN5 plasmid (GFP-TSPAN5). Control cells were transfected with scrambled siRNA and afterwards with GFP-empty vector (ctrl). mRNA expression of TSPAN5 **(A)** to determine transfection efficiency as well as of the MKL1 target genes SM22, GLIPR1 and TGFß1 **(B)** was analyzed by qRT-PCR using gene specific primers. The amount of each RNA sample was normalized to the endogenous housekeeping gene 18S rRNA. Statistical analysis was performed using one-way ANOVA, followed by Tukey´s multiple comparison test. Values are mean ± SD (n=3); *p<0.05, **p<0.01, ***p<0.001.

6.7 Decreased tumorigenicity upon TSPAN5 depletion in the CAM model

6.7.1 Decreased tumor proliferation after TSPAN5 loss in CAM model

In previous experiments we could show important findings regarding a reduced proliferation, migration and invasion after TSPAN5 loss. Hence it was of particular importance to continue our research to determine whether TSPAN5 could act as a new target in tumor therapy of HCC. Therefore, we sought to find out if TSPAN5 loss can also inhibit tumor growth *in vivo*. For this purpose, we used the chicken chorio-allantoic-membrane assay (CAM assay) and performed it in collaboration with Prof. Schneider-Stock of the "Tumor Pathology of the University of Erlangen" as described by Ribatti (Ribatti 2014, 2017). In the process transfected HuH7 cells were placed on the CAM of fertilized chicken eggs and the growth of the tumor pellet could be observed and analyzed *on ovo*. More specifically, HuH7 cells were transfected with scrambled or TSPAN5 siRNA to generate negative control and TSPAN5 silenced cells. These transfected cells were formed into pellets with Matrigel next to untransfected (mock) HuH7 cells (mock cells as a further control to account for the influence of siRNA transfection on the CAM assay) and placed on the CAM for 5 days. When excising the tumors with the surrounding CAM on day 8 of embryonic development, it was already noticeable during macroscopic examination that the CAM-tumors formed from control cells were visibly bloodier and bigger than the CAM-tumors with TSPAN5 loss (Figure 48A). When measuring and calculating the volume of the tumors, the HuH7 tumor pellets showed no significant difference between the mock and siRNA controls. A strong difference in volume could be calculated for pellets with TSPAN5 depletion compared to the siRNA control cells (Figure 48B). Similar results were obtained in the parallel experiment with HepG2 clone 5 cells. The HepG2 clone 5 represents a more aggressive variant of the conventional HepG2 cells and was provided to us by Muenzner and colleagues (Muenzner et al. 2018). Also in this experimental set, a significantly smaller tumor cell pellet could be measured in the group with TSPAN5 loss compared to the one with scrambeld siRNA. However, the tumor pellet measurement also revealed that the siRNA control samples were slightly smaller than the mock samples (Figure 48C).

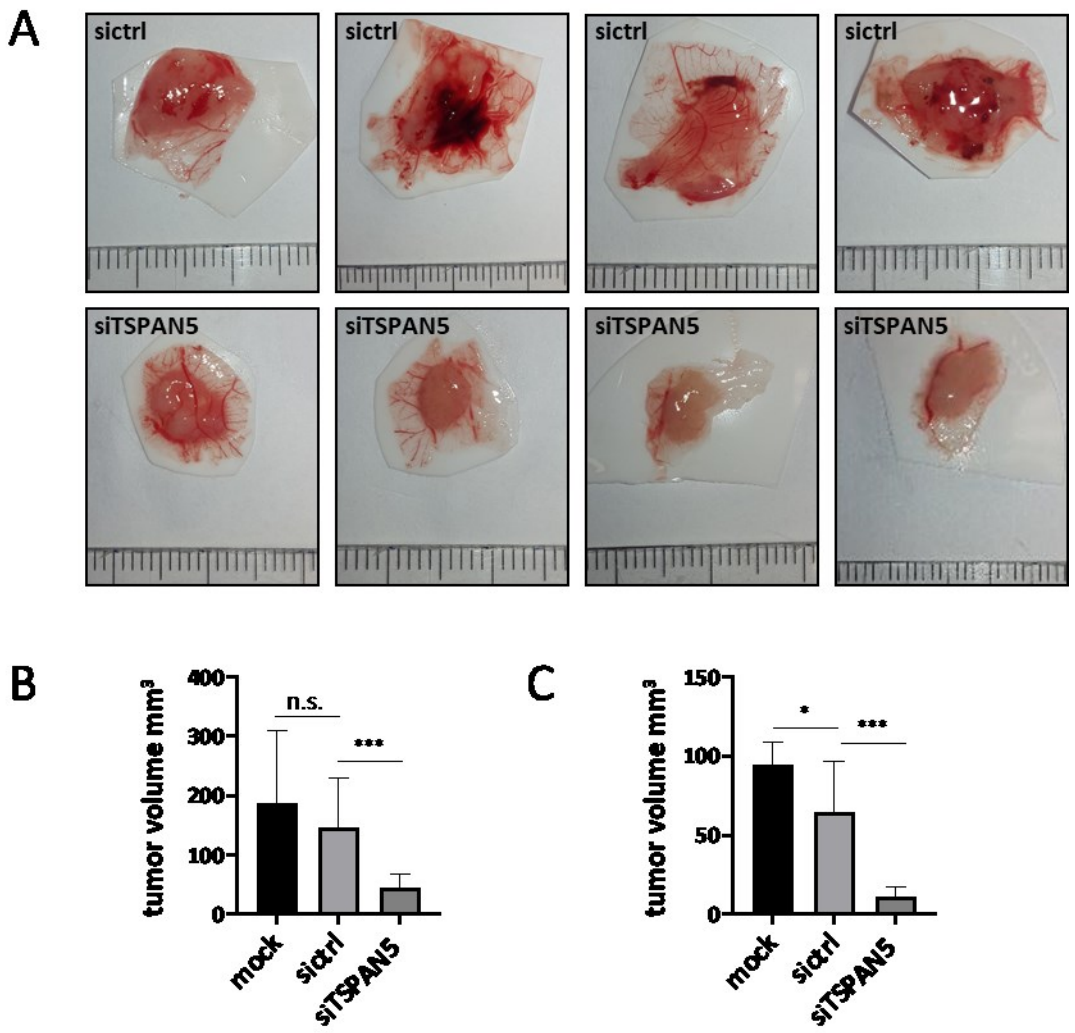

Figure 48: Anti-tumor effects of TSPAN5 knockdown in CAM assay. (A) HuH7 cells were either expressing control siRNA (sictrl) or TSPAN5 siRNA (siTSPAN5) or no siRNA (mock). At 48 h after transfection Matrigel pellets with $1*10^6$ cells per pellet were prepared and transferred to the CAM of fertilized chicken eggs**.** 5 days after transferring the cells embedded in Matrigel on the CAM, tumor pellets of HuH7 cells were extracted and *ex ovo* images of micro-tumors were taken. Each tumor pellet of HuH7 **(B)** or HepG2 clone 5 **(C)** was measured in length, width and height and thereby the tumor volume calculated. Data are presented with means ± SD and statistical analysis was performed using one-way ANOVA following Tukey´s multiple comparison test; (HuH7 mock n=11, sictrl n=17, siTSPAN5 n=21; HepG2 clone 5 mock n=7, sictrl n=15, siTSPAN5=15); *p<0.05, **p<0.01, ***p<0.001.

In addition, we wanted to control the knockdown efficiency of the previous siRNA transfection and verify the proliferation inhibition, which has already been identified macroscopically, on the basis of the mRNA expression of *Ki67*. Significantly decreased mRNA levels of Ki67 indicate reduced mitosis and proliferation rate of tumor cells. For this purpose, RNA was isolated from HuH7 and HepG2 clone 5 CAM-tumors and subsequently the mRNA was quantified by qRT-PCR. This enabled us to demonstrate successful TSPAN5 knockdown in CAM model, and

furthermore, the reduced Ki67 mRNA expression indicates a significant decrease in mitosis and proliferation rate in microtumors of Huh7 cells (Figure 49A) as well as HepG2 clone 5 cells (Figure 49B).

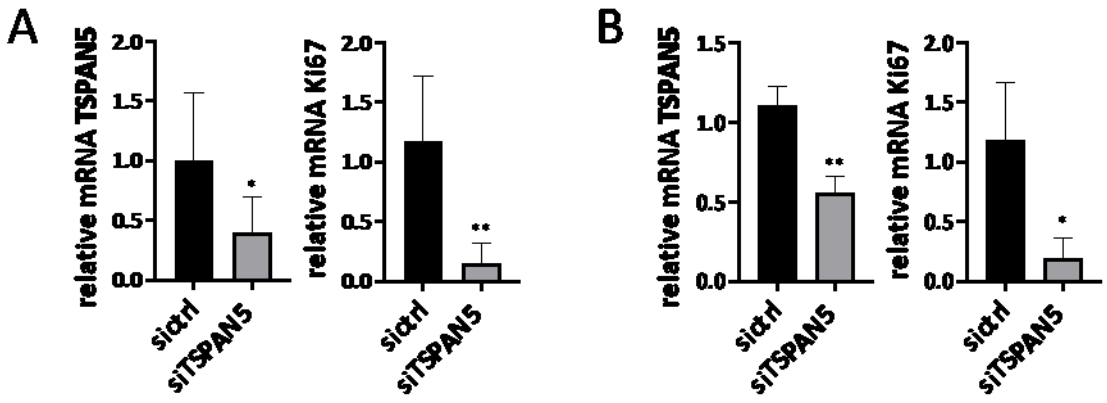

Figure 49: Decreased Ki67 mRNA level upon TSPAN5 depletion *on ovo*. RNA was isolated and purified from extracted and frozen CAM-tumors of **(A)** Huh7 cells and of **(B)** HepG2 clone 5 cells. cDNA was prepared and then mRNA expression of TSPAN5 for knockdown efficiency and Ki67 was determined by qRT-PCR using the respective RNA primers and 18S rRNA as endogenous housekeeping gene for normalization. Data are presented with means ± SD and statistical analysis was performed using students t-test; (HuH7 mock n=11, sictrl n=17, siTSPAN5 n=21; HepG2 clone 5 mock n=7, sictrl n=15, siTSPAN5=15); *p<0.05, **p<0.01.

This finding can also be shown by conventional hematoxylin-eosin (HE)-staining. Here, a very dense and aggressive growth can be seen in HuH7 control cells, Matrigel was completely consumed and also the CAM was almost completely displaced by tumor cells. In addition, necrosis with typically recognizable pyknosis were formed in the control cells due to the extremely rapid growth in part of the tumors (Figure 50). In contrast, the TSPAN5 knockdown cells show a very loose and broken growth with nests, which indicates a disintegration of the tumor. Moreover, large parts of the Matrigel are still present and the CAM is intact. These observations regarding proliferation are also confirmed by Ki67-staining. Especially the single nests of the HuH7 siTSPAN5 sections show hardly any Ki67 activity (Figure 50B, left panel). Regarding the TSPAN5-staining it can be observed that it is slightly brighter in the slides of siTSPAN5 tumors, especially in the nuclear and intercellular regions. This result is also reflected by MKL1, so that the MKL1-staining in CAM-tumors with siTSPAN5 depletion is brighter and an increased MKL1 redistribution from the nucleus towards the cytoplasm can be detected (Figure 50B, right pane, arrowheads).

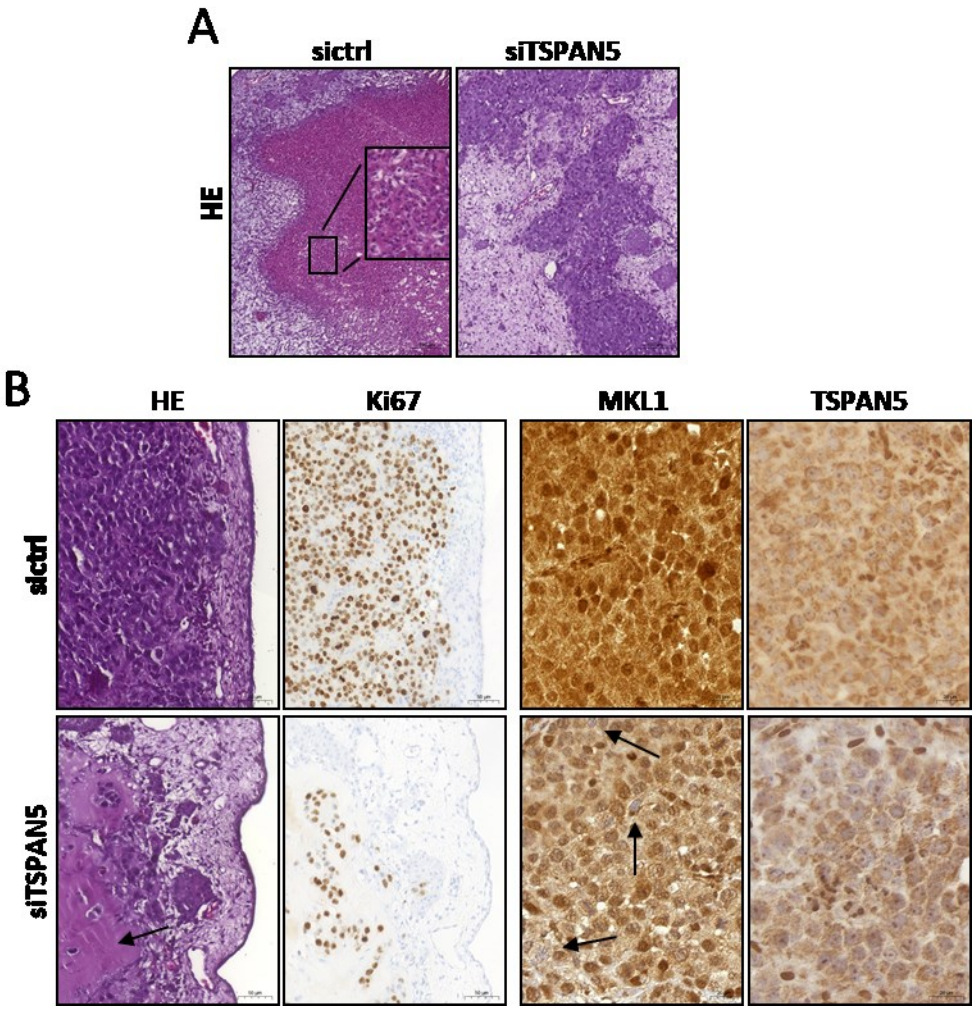

Figure 50: Histological changes after TSPAN5 silencing in CAM model. (A) Representative photomicrographs of hematoxylin-eosin (HE) stained paraffin sections of HuH7 sictrl and siTSPAN5 CAM-tumors. Scale bar = 100 µm. **(B)** Left panel: Characteristic photomicrographs of hematoxylin-eosin (HE) and Ki67 stained paraffin sections of HuH7 CAM-tumors. Arrowhead: Undigested Matrigel. Scale bar = 50 µm. Right panel: More magnified images of MKL1 and TSPAN5 stained paraffin sections of HuH7 micro-tumors. Arrowhead: Cytoplasmic MKL1 staining and unstained nucleus. Scale bar = 20µm.

The immunohistochemically results of HE-staining, as well as TSPAN5-staining could be reproduced in the more aggressive HepG2 clone 5 cells. Again, in the sections of siTSPAN5 CAM-tumors, cell growth appears looser and CAM was not completely displaced by tumor cells (Figure 51, left panel). The successful TSPAN5 knockdown is confirmed by the significantly brighter TSPAN5-staining in the treatment group (Figure 51, middle panel). Interestingly, in the immunohistochemistry (IHC)-sections, more E-cadherin can be stained in the membranes after TSPAN5 loss, which, in agreement with previous results, suggests less migration, invasion

and spheroid formation ability (Feng et al. 2018; Gan et al. 2016; Kaszak et al. 2020) (Figure 51, right panel).

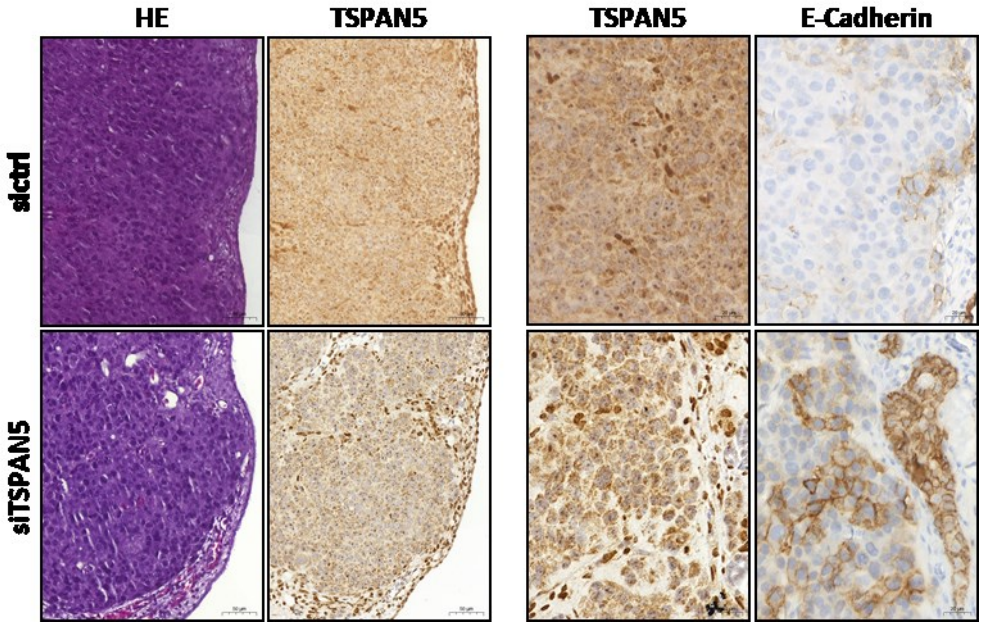

Figure 51: Increased E-Cadherin expression after TSPAN5 loss in HepG2 clone 5 CAM-tumors. Left panel: Characteristic images of immunohistochemistry analysis with HE and TSPAN5 stained paraffin sections of HepG2 clone 5 CAM-tumors. Scale bar = 50 µm. Right panel: Photomicrographs of TSPAN5 and E-Cadherin stained paraffin sections of HepG2 Clone 5 CAM-tumors. Scale bar = 20 µm.

6.7.2 Reduced MKL1 target gene expression upon TSPAN5 depletion in CAM assay

Besides, it was of major interest to us to investigate whether the MKL1/SRF target genes also exhibit reduced expression in the *in vivo* CAM model after TSPAN5 loss. To this end we isolated and purified RNA from the HuH7 (Figure 52A) and HepG2 clone 5 (Figure 52B) CAM-tumors and determined the mRNA expression by qRT-PCR. Our analysis revealed that, especially in HuH7 cells, mRNA expression of MKL1/SRF target genes such as *GLIPR1, TGFß1,* connective tissue growth factor *(CTGF)* and calponin 1 *(CNN1*) was decreased (Hermanns et al. 2017; Muehlich et al. 2007; Muehlich et al. 2008).

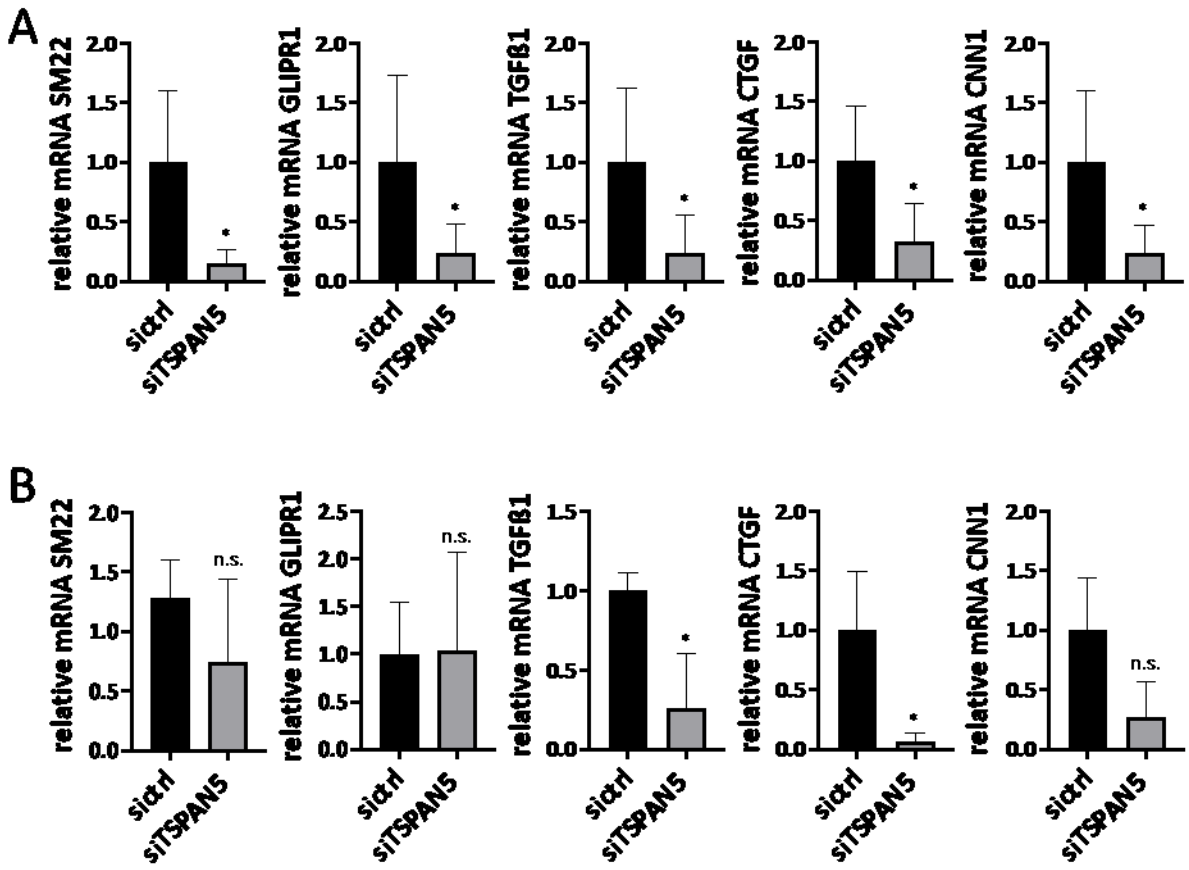

Figure 52: Decreased mRNA expression of MKL1 target genes upon TSPAN5 depletion *in vivo*. RNA was isolated and purified from extracted and frozen CAM-tumors of HuH7 **(A)** and HepG2 clone 5 **(B)** cells either expressing control siRNA (sictrl) or TSPAN5 siRNA (siTSPAN5). cDNA was prepared and then mRNA expression of MKL1 specific genes was analyzed as well by qRT-PCR as described above. Values are mean ± SD (HuH7 sictrl n=3, siTSPAN5=6; HepG2 Clone 5 sictrl n=3, siTSPAN5 n=3); *p<0.05.

Furthermore, reduced protein levels, as shown here for GLIPR1, were detected in HuH7 CAM-tumors after TSPAN5 silencing (Figure 53).

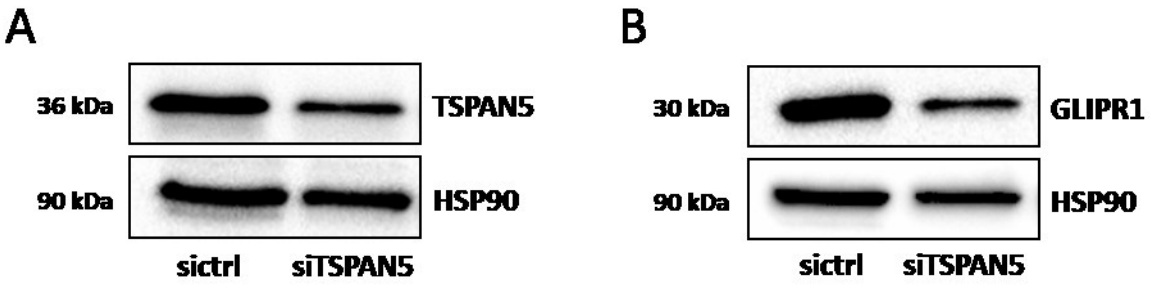

Figure 53.: Decreased protein level of MKL1 target gene GLIPR1 after TSPAN5 loss *in vivo*. Purified lysates from excised micro-tumors, grown from HuH7 cells expressing control siRNA (sictrl) or TSPAN5 siRNA (siTSPAN5) *on ovo* for 5 days, were prepared and immunoblotted with anti-TSPAN5 antibody **(A)**, anti-GLIPR1 antibody **(B)** and anti-HSP90 antibody as loading control.

6.7.3 Senescence induction in CAM assay after TSPAN5 knockdown

In order to prove whether the regression of CAM-tumors is associated with senescence, we determined senescence markers, detecting phosphorylation of ERK1/2 in HuH7 tumor lysates (Figure 54A). Furthermore, we noted an accumulation of Histone H3 methylated on lysine 8 in SAHF in HuH7 tumor lysates as well as in immunohistochemically sections of HepG2 clone 5 cells (Figure 54B and C, left panel). In addition, accumulation of $p16^{INK4a}$ was confirmed by p16-staining in HepG2 clone 5 IHC tumor sections (Figure 54C, right panel).

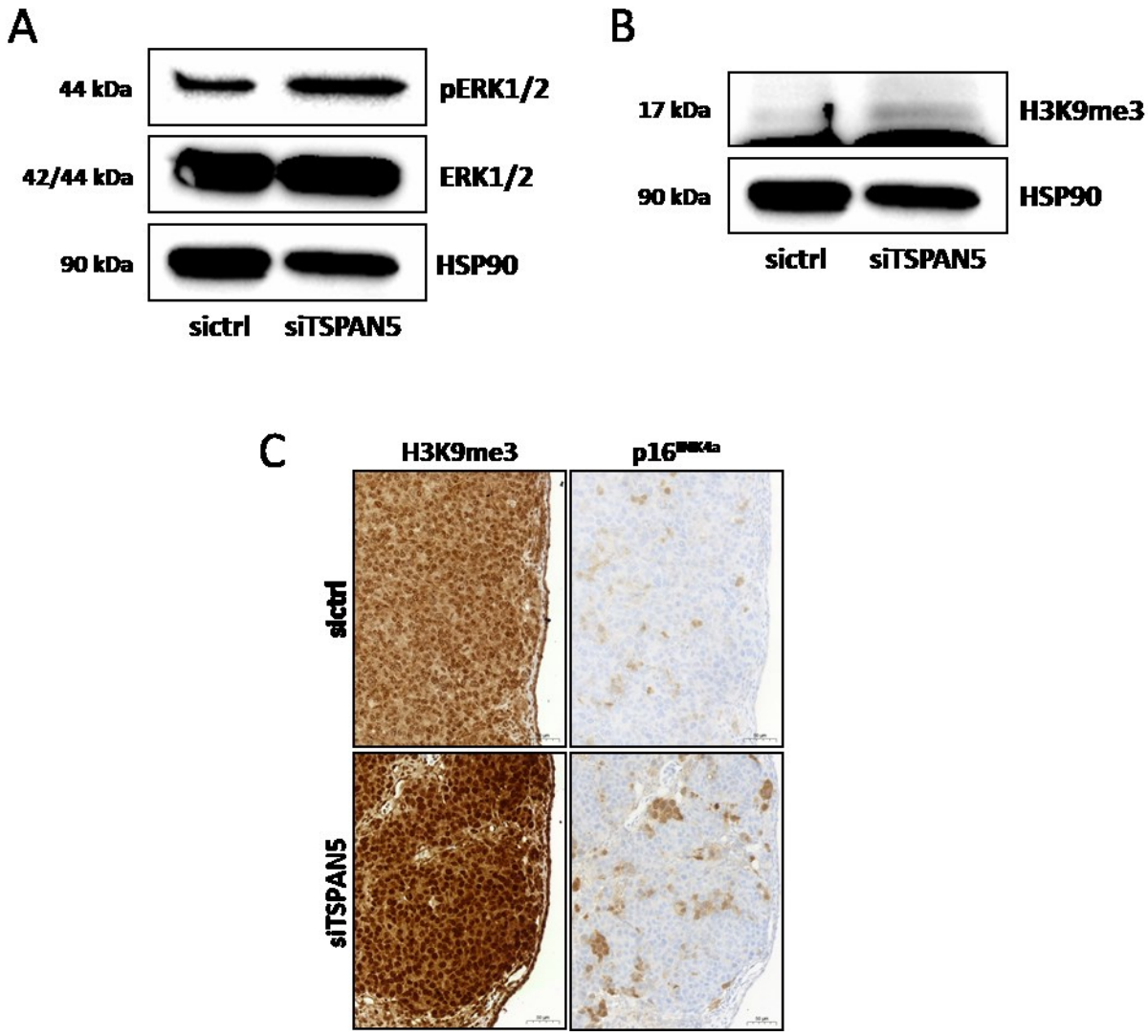

Figure 54: Positive senescence markers after TSPAN5 depletion *in vivo*. (A) Lysates from extracted HuH7 CAM-tumors either expressing control siRNA (sictrl) or TSPAN5 siRNA (siTSPAN5) were prepared and immunoblotted with anti-$ERK^{pT202/pY204}$ antibody (for detecting pERK), anti-ERK antibody and anti-HSP90 antibody. **(B)** Lysates from excised HepG2 clone 5 CAM-tumors either expressing control siRNA (sictrl) or TSPAN5 siRNA (siTSPAN5) were prepared and immunoblotted with anti-H3K9me3 antibody and anti-HSP90 antibody. **(C)** Characteristic images of paraffin sections of HepG2 clone 5 sictrl and siTSPAN5 CAM-tumors stained with anti-H3K9me3 antibody (left side) and anti-$p16^{INK4a}$ antibody (right side). Scale bar = 50 µm.

6.8 TSPAN5 overexpression in human HCC

To investigate to what extent the previous data have clinical relevance, we were eager to find out whether human patients diagnosed with HCC also show changes in TSPAN5 expression. For this purpose, tissue samples of patients from an existing database were examined in collaboration with pathologist Professor Singer from the University of Tübingen (Table 45). The tissue samples were prepared in such a way that proteins could be isolated, separated by SDS-PAGE and finally immunoblotted. We found that patients with HCC have on average a 2.5-fold higher protein concentration of TSPAN5 than patients with healthy tissue (Figure 55). Examining the human data in more detail, it can be seen that in approximately 25 % of the samples examined, there is a significantly higher TSPAN5 overexpression in the range of 20-fold increase in TSPAN5 protein levels compared to the general average increase.

Table 45: Patient characteristics including age, gender, grading, staging, lymphangiosis and hemangiosis carcinomatosa, R-status and tumor size

Patient characteristics		HCC
Age (years)	Mean ± SD	69.8 ± 7.5
	Range	61 - 89
Gender	F	-
	M	11
Grading	G1	5
	G2	6
Stage (7th edition UICC)	T1	6
	T2	3
	T3	1
	unknown	1
Lymphangiosis	yes	-
	no	9
	unknown	2

Hemangiosis	yes	3
	no	7
	unknown	1
R-Status	R0	10
	R1	-
	unknown	1
Tumour size cm (n=10)	Mean ± SD	5 ± 5
	Range	2 – 19

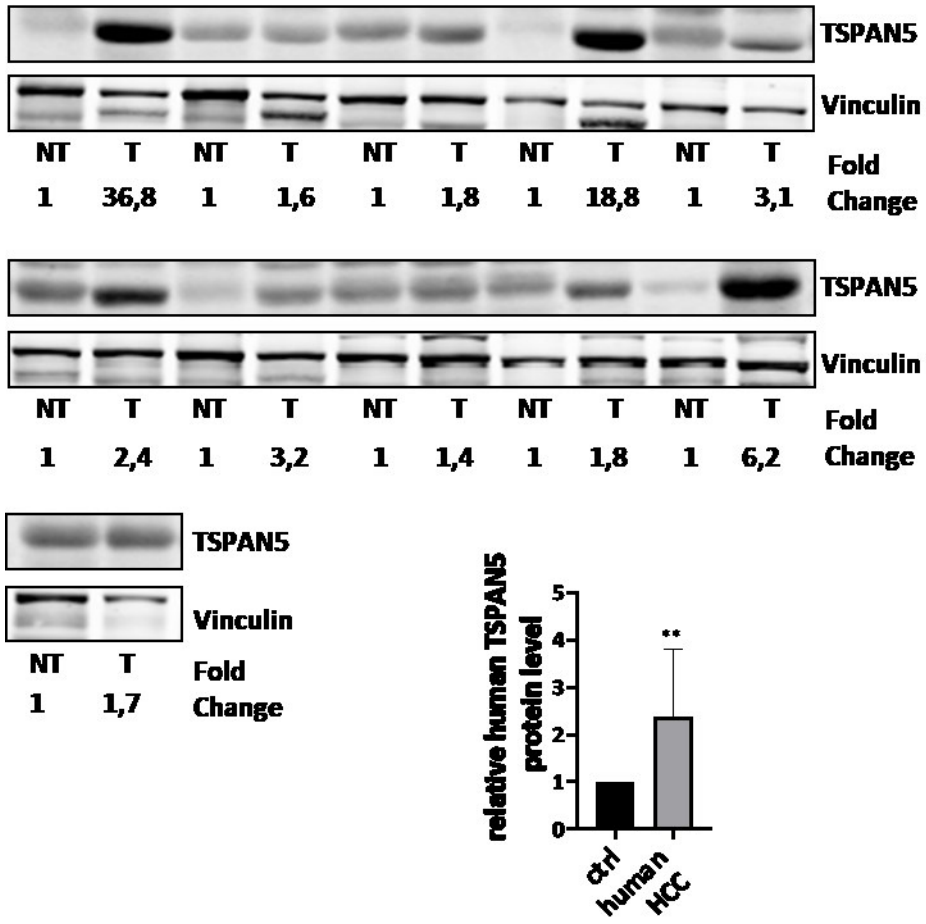

Figure 55: TSPAN5 overexpression in human HCC tissue samples. Tissue samples of human patients were prepared and lysates for Western Blot generated. Lysates were immunoblotted with anti-TSPAN5 antibody and anti-vinculin antibody as loading control. Images of the detections are shown. Statistical analysis was performed using students t-test. Values are mean ± SD (ctrl n = 11, human HCC = 11); **p<0.01.

6.9 Anti-tumor effects of TSPAN5 depletion in HCC Xenograft

6.9.1 Reduced tumor growth after TSPAN5 depletion *in vivo*

Results to date suggest that TSPAN5 is a potential target in the treatment of DLC1 deficient HCCs. To evaluate the therapeutic efficacy of a TSPAN5 knockdown *in vivo*, we used a xenograft model in collaboration with Professor Aigner from University of Leipzig. For this purpose, subcutaneous tumor xenografts were first generated by injecting HuH7 cells into athymic mice. As an efficient tool to ensure *in vivo* siRNA delivery, we used polyethyleneimine (PEI) complexation with TSPAN5 or scrambled siRNA (Aigner 2006; Hampl et al. 2013; Ibrahim et al. 2011; Schäfer et al. 2010). After solid and roughly equal-sized tumors had formed, the mice were treated systemically by intraperitoneal (i.p.) injection of PEI/siRNA complexes three times per week. After day 3, tumor growth was increasingly inhibited in the siTSPAN5 treatment group (Figure 56). On the 10th day of treatment, the tumors had to be excised, otherwise the tumors of the control group would have become too large.

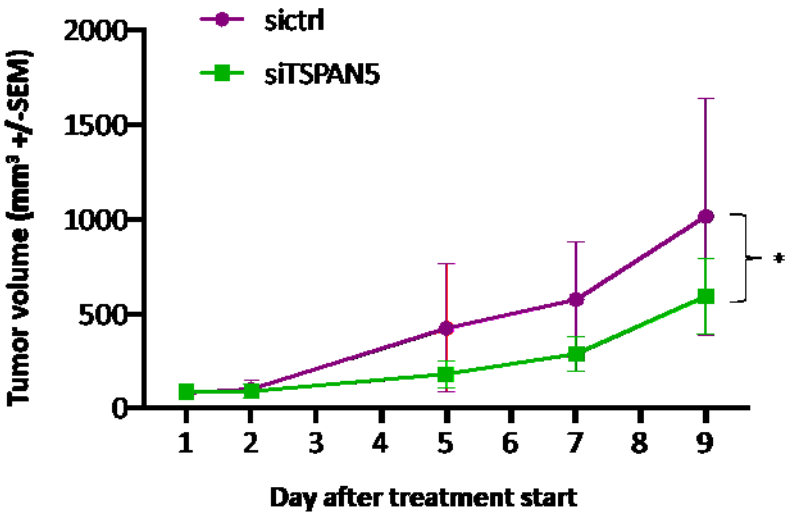

Figure 56: TSPAN5 depletion reduces tumor growth in mice xenograft *in vivo*. HCC xenograft mice were treated on day 0, 2, 4, 6 and 8 with polymeric nanoscale complexes containing either control siRNA (sictrl) or TSPAN5 siRNA (siTSPAN5). Tumor growth was measured manually. Means of tumor sizes are shown for control and treated group over the entire treatment period. Statistical analysis was performed using the unpaired t-test. Data are presented with means ± SD (n=6 mice per group)

Further examination of excised xenograft tumors shows decreased proliferation and mitotic rates due to diminished *Ki67* mRNA expression in the siTSPAN5 treatment group. Successful

TSPAN5 knockdown in the treatment group compared to the control group was demonstrated at both mRNA (Figure 57A) and protein (Figure 57B) levels.

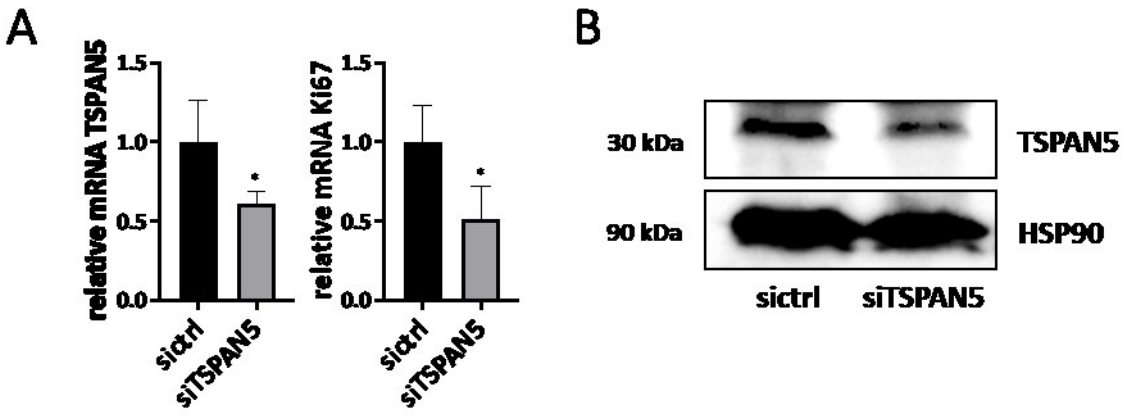

Figure 57: TSPAN5 knockdown inhibits proliferate *in vivo*. (A) TSPAN5 knockdown efficiency and Ki67 mRNA expression in HCC xenografts after treatment with PEI/TSPAN5 siRNA (siTSPAN5) or PEI/control siRNA (sictrl) i.p. three times per week, determined by qRT-PCR using the respective RNA primers and 18S rRNA as endogenous housekeeping gene for normalization. **(B)** Immunoblotting of corresponding lysates of HCC xenografts treated as described above with anti-Tetraspanin 5 and anti-HSP90 antibody as loading control. All data are means ± SD (n=5); *p<0.05.

6.9.2 Decreased MKL1 target gene expression after TSPAN5 loss *in vivo*

Further investigations related to the expression of MKL1 target genes revealed a significant decrease in MKL1 target genes, consistent with the previous results. These findings could be observed on the mRNA (Figure 58A) as well as on the protein (Figure 58B) level.

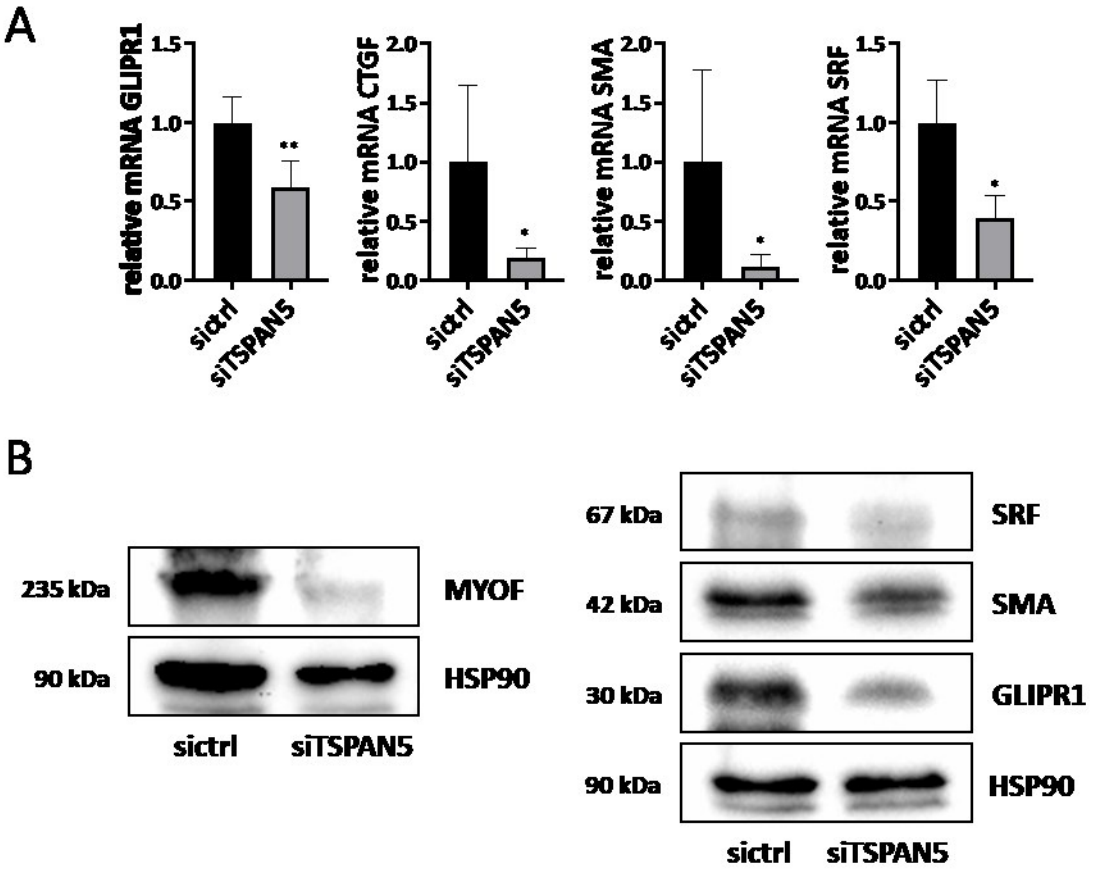

Figure 58: TSPAN5 depletion reduces MKL1 target genes *in vivo*. (A) MKL1 target gene expression of *GLIPR1*, *CTGF*, *SMA* and *SRF* in HCC xenografts after treatment with PEI/TSPAN5 siRNA (siTSPAN5) or PEI/control siRNA (sictrl) i.p. three times per week, determined by qRT-PCR using the respective RNA primers and 18S rRNA as endogenous housekeeping gene for normalization. **(B)** Immunoblotting of corresponding lysates of HCC xenografts treated as described above with anti-Myoferlin antibody, anti-SRF antibody, anti-SMA antibody, anti-GLIPR1 antibody and respectively anti-HSP90 antibody as loading control. All data are means ± SD (n=5); *p<0.05, **p<0.01.

6.9.3 Senescence induction upon TSPAN5 depletion *in vivo*

Also, we analyzed phosphorylation of ERK1/2 in order to confirm that the regression of xenografts treated with TSPAN5 siRNA is associated with Ras-induced senescence. We were able to demonstrate an increase in phosphorylation of ERK1/2 and, in addition, hypophosphorylation of retinoblastoma (Figure 59).

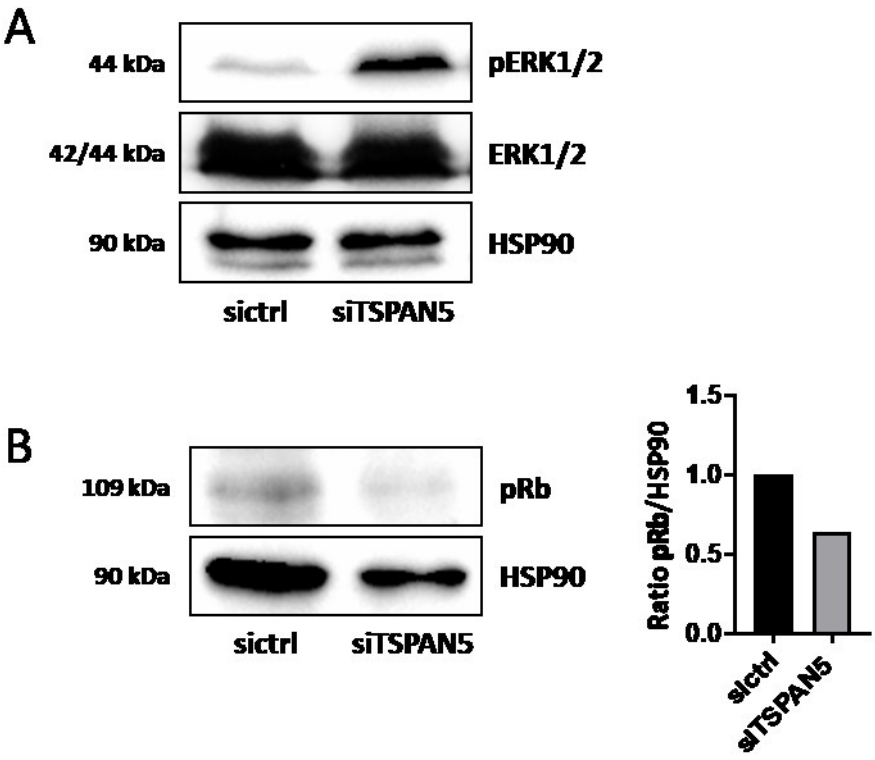

Figure 59: Positive senescence markers upon TSPAN5 depletion in HCC xenograft *in vivo*. Immunoblotting of corresponding lysates of HCC xenografts treated as described above with anti-ERK$^{pT202/pY204}$ antibody, anti-ERK antibody **(A)**, anti-pRB antibody **(B)** and respectively anti-HSP90 antibody as loading control.

All these findings *in vitro* and *in vivo* suggest that TSPAN5 plays a major role in the development and growth of HCC. The results further describe that silencing TSPAN5 in HCC can reduce tumorigenic properties through an oncogene-induced senescence response.

7 Discussion

7.1 DLC1 loss-dependent expression of novel gene targets in HCC

One aim of this PhD thesis was to validate the novel gene targets identified after DLC1 loss in HCC and to distinguish the gene that is responsible for HCC growth and other tumorigenic characteristics. Because DLC1 functions as a tumor suppressor by regulating and controlling the RhoA cascade, its loss or mutation results in an increased likelihood of HCC development (Xue et al. 2008; Yuan et al. 1998). Further, DLC1 expression leads to an induction of senescence in HCC cells, which acts as a tumor suppressive mechanism in liver tumorigenesis (Hampl et al. 2013). After DLC1 loss, this protective mechanism is also lost, so it is of great interest to investigate and elucidate the changes in gene expression and its effects on the signaling pathways of a DLC1 deficient cell. Previous microarray analyses by C. Mittermeier examined the transcriptome of HepG2 cells depleted of DLC1 by shRNA interference compared to control cells which led to the discovery of several novel DLC1 loss-dependent gene targets. The top 5 genes that were upregulated in HepG2 DLC1 knockdown cells by a factor of 3.0 compared to the control cells were selected and so the following 5 novel DLC1 dependent genes were identified: Versican (VCAN), Tetraspanin 5 (TSPAN5), Meprin 1A (MEP1A), Histon cluster 1 H2B family member K (HIST1H2BK) and N-cadherin (CDH2). The DLC1 dependency of the newly found gene targets in the microarray could be validated in several HCC cell lines both at the mRNA and protein level. The genes are already known to have multiple properties in other cell lines and tissues, so that their overexpression in HCC - depending on the tumorigenic characteristic of the gene - may open up new targets in HCC treatment (Tanaka et al. 2016). Versican (VCAN) is a large (>1000 kDa) extracellular matrix proteoglycan of which 5 splice isoforms have been described and which interacts with various extracellular matrix (ECM) components such as hyaluronan (Iozzo 1998; Kischel et al. 2010; Wight 2002, 2017). VCAN plays an important role in organ development such as the heart and in inflammatory processes but also in cancer development by contributing to cell adhesion, proliferation and migration (Gao et al. 2012b; Mjaatvedt et al. 1998; Zhang et al. 2012). In this context, VCAN is increasingly expressed both in the tumor cells themselves and in the surrounding stromal cells and contributes to tumor invasion and metastasis through its influence on cell adhesion, migration and angiogenesis (Ricciardelli et al. 2009). Upregulation

of VCAN has been demonstrated in various tumors such as breast, brain, bone, ovarian or liver tumors and correlated with reduced survival (Nara et al. 1997; Nikitovic et al. 2006; Paulus et al. 1996; Ricciardelli et al. 2002; Voutilainen et al. 2003). For example, VCAN is expected to induce mesenchymal to epithelial transition (MET) of metastatic tumor cells, thus accelerating metastasis (Gao et al. 2012a; Sheng et al. 2006). More specifically, Goa and colleagues found in a mouse model of spontaneous breast cancer, that myeloid progenitor cells express increased levels of VCAN in the pre-metastatic lung. An *in vivo* knockdown of VCAN significantly affected lung metastases. In addition, analysis of clinical samples also showed increased VCAN expression in the metastatic lung of patients with breast cancer (Gao et al. 2012a). Not only in lung metastases, but also in primary breast cancer tissue itself, a significant overexpression of all five VCAN isoforms could be shown on mRNA level as well as on protein level (Kischel et al. 2010). Since DLC1 is also active as a tumor suppressor in lung and breast tissue, it would be quite conceivable and tempting to speculate whether it is the DLC1 loss that preceded breast cancer and lung metastases in these cases and promoted overexpression of VCAN. Furthermore, the impact of VCAN overexpression, due to increased expression of Sharpin, on tumor progression and invasion has already been shown in HCC cells. Sharpin (Shank-associated RH domain-interacting protein) is a multi-functional protein that promotes tumor progression in various types of cancer by activating nuclear factor-κB signaling and inhibiting tumor suppressors. By microarray analysis, Tanaka and colleagues found that Sharpin overexpression in HCC tissues correlates with VCAN overexpression and that this combination of overexpression plays a significant role in tumor progression and invasion (Tanaka et al. 2016). Using proteomic approaches, Naboulsi and colleagues analyzed patient HCC samples as well as non-tumorigenic tissue samples and found that VCAN is already significantly overexpressed in well-differentiated and low-stage HCCs. These results provide the opportunity to use VCAN as a potential biomarker for early HCC diagnosis (Naboulsi et al. 2016). Recent studies suggest that the expression of VCAN isoform V1 (VCAN V1), the only isoform of VCAN expressed in the liver, is regulated by Linc01225, an oncogenic noncoding RNA that promotes occurrence and metastasis of HCC (Cattaruzza et al. 2002; Wang et al. 2016c; Zhangyuan et al. 2020). The authors Zhangyan and colleagues published a possible mechanism by which VCAN V1 promotes HCC proliferation and metastasis. They suggest that VCAN triggers the “epidermal growth factor receptor (EGFR) - Phosphoinositide 3-kinase

(Pi3K) - protein kinase B (AKT)" pathway via an EGF-like motif and discovered a direct interaction between VCAN and the EGF receptor (Zhangyuan et al. 2020). In addition to the EGFR-Pi3K-AKT signaling pathway, sustained activation of EGFR can also lead to increased cell proliferation via additional activation of the Ras-Raf-Mek-ERK signaling pathway (Gale et al. 1993). This is also in agreement with results from our group, in which Hermanns and colleagues demonstrate that myoferlin, a MKL1 target gene, mediates its effect on oncogene-induced senescence (OIS) via modulation of the EGFR signaling pathway and thus plays an essential role for HCC growth (Hermanns et al. 2017). Indeed, aberrant activation of the Ras-Raf-Mek-ERK pathway is a consistent finding in numerous cancers and has also been associated with cell proliferation, cell survival, and metastasis (Roberts and Der 2007). Analogously, an overexpression of VCAN induced by DLC1 loss could contribute to HCC development and growth via the two signaling pathways just mentioned. At the same time, activation of the EGFR-Ras-Mek-ERK pathway in DLC1 deficient HCC also leads to an oncogene-induced senescence response that counteracts tumor growth and provides a protective mechanism upon loss of e.g. tumor suppressors (Hampl et al. 2013).

The MEP1A gene, which encodes the zinc metalloprotease MEP1A, modulates the activity of proteins and inflammatory cytokines in various diseases (Gao et al. 2020). For example, MEP1A affects the inflammatory response, fibrosis and cardiac remodeling by regulating inflammatory cytokine expression. Mechanistic studies by Ge and colleagues showed that activation of ERK1/2 in cardiac myocytes, fibroblasts and macrophages underlies also cardiac remodeling induced by MEP1A (Ge et al. 2020). Similar to VCAN overexpression, MEP1A overexpression also involves activation of the ERK pathway, suggesting involvement of MEP1A in tumorigenesis. Indeed, MEP1A expression is associated with colorectal and breast cancer, osteosarcoma and HCC (Matters and Bond 1999; Matters et al. 2005; OuYang et al. 2016). In the case of colorectal cancer, for example, it has been shown that MEP1A not only functionally promotes proliferation, migration, and invasion of tumor cells, but may also serve as an important and uniquely bioindicator of prognostic outcome of colorectal carcinoma. This is indicated by the fact that both mRNA and protein levels of MEP1A were increased in colorectal cancer tissue samples (Wang et al. 2016d). Analogously, similar findings can be shown in HCC by OuYang and colleagues. They demonstrated by *in vitro* and *in vivo* assays that MEP1A promotes HCC cell proliferation, migration and invasion and that patients with positive MEP1A

expression in tissue samples show poorer prognosis and survival after curative resection (OuYang et al. 2016). Since DLC1 also acts as a tumor suppressor not only in HCC but also in colorectal cancer, it can be hypothesized that the oncogenic properties of MEP1A are also associated with a previous loss of DLC1, further worsening the course and prognosis of the tumor disease (Wu et al. 2015).

Moreover, increased levels of HIST1H2BK can also be detected in various tumors such as glioma, lung adenocarcinoma, ovarian and breast cancer and high expression levels of HIST1H2BK can be correlated with a worse prognosis for the patients (Han et al. 2019; Li and Zhan 2019; Liu et al. 2020; Zeng et al. 2021). Interestingly, an increased expression of HIST1H2BK was detected specifically in breast cancer cells resistant to doxorubicin. Doxorubicin resistance is next to the “Leukemia inhibitory factor receptor (LIFR) - Januskinase 1 (JAK1) – Signal transducer and activator of transcription 3 (STAT3)” signaling pathway, for example, with the Ras-Raf-Mek-ERK or the Pi3K-AKT signaling pathways associated. It is tempting to speculate that DLC1 loss also plays an additional role here and at least partially contributes to the overexpression of HIST1H2BK in breast cancer cells or whether an additional expression of MEP1A or VCAN may be involved in the resistance of breast cancer cells.

Neural-Cadherin (N-cadherin or CDH2) is a calcium-dependent single-chain transmembrane glycoprotein that is mainly responsible for cell-cell adhesion, migration and invasion (Cao et al. 2019). Therefore, it is a key molecule for neural crest development, but also for the development of other organs such as brain, heart or skeletal muscle, especially in embryogenesis (Cao et al. 2019; Derycke and Bracke 2004). By interacting with other proteins, N-cadherin has a reciprocal influence on the regulation of various signaling pathways such as the RhoA cascade and function in tyrosine kinase signaling (Derycke and Bracke 2004). For example, the adhesive activity of N-cadherin is also subject to the regulation of RhoGTPases, reinforcing its dependence on DLC1. Furthermore, its interaction with ß-catenin also provides a link to the Wnt-ß-catenin pathway (Derycke and Bracke 2004). Besides, it is already known that N-cadherin is frequently upregulated in various types of cancers such as lung cancer, breast cancer, liver cancer and prostate cancer (Drivalos et al. 2016; Saadatmand et al. 2013; Seo et al. 2008). In this context, it acts as an invasion and metastatic promoter and is associated with malignant tumor progression. Moreover, upregulation of N-cadherin

expression was observed in 67 % of HCC tissues by Seo and colleagues and identified as a predictive marker for early recurrence in HCC (Seo et al. 2008). Interestingly, it has been shown that VCAN isoform V1 promotes a switch in the expression of N- to E-cadherin (Sheng et al. 2006). Increased N-cadherin can promote tumor progression, while E-cadherin, which normally acts as an invasion suppressor, is repressed and downregulated in most tumors (Derycke and Bracke 2004; Kanai et al. 1997; Li and Herlyn 2000; Mareel and Leroy 2003; Tomita et al. 2000). Thus, N-cadherin expression is additionally regulated by VCAN, which itself has also been described as tumor-promoting in literature. However, the data of Shen and colleagues suggest that overexpression of both genes, VCAN isoform V1 and N-cadherin, do not necessarily have synergistic effects on tumorigenesis and progression, but rather that VCAN isoform V1 inhibits the expression of N-cadherin and promotes that of the more tumor-suppressive E-cadherin (Sheng et al. 2006). Transforming growth factor-ß (TGFß) is known to be an inducer of EMT, where N-cadherin expression is significantly upregulated and that of E-cadherin is downregulated. It has been demonstrated in several studies that TGFß promotes the upregulation of N-cadherin and thus tumor progression by binding to the N-cadherin promoter region (Diamond et al. 2008; Nuessle et al. 2011; Yang et al. 2015). It is also interesting to note that TGFß1 itself is a MKL1/SRF target gene that is increasingly expressed by RhoA stimulation (Hampl et al. 2013). Due to the loss of the RhoGAP DLC1 which in turn leads to a permanent activation of RhoA, one could assume a mechanistic link via an increased TGFß and thereby increased N-cadherin expression after DLC1 loss, that triggers EMT, migration and metastasis.

The last DLC1 dependent gene target, which is the primary focus of this thesis, and which is strongly upregulated after DLC1 loss, is Tetraspanin 5 (TSPAN5). As very little is known about TSPAN5 itself, especially in the field of carcinogenesis and cancer development, its contribution remains to be investigated. Previous studies showed that TSPAN5 plays an important role in the differentiation of neurons during brain development and osteoclast formation (García-Frigola et al. 2000; Iwai et al. 2007; Juenger et al. 2005; Zhou et al. 2014). Nevertheless, since many TSPANs have already been shown to be involved in tumorigenesis and tumor development, for example in blood, liver or gastric cancer, it is essential to investigate the role of TSPAN5 in tumorigenesis and progression (Boucheix et al. 1985; Ke et al. 2009; Zöller 2009). The special role and involvement of TSPAN5 in HCC development and

growth will be discussed in more detail in the following chapters (chapters 7.3 - 7.5). In this thesis, we show that the newly identified gene targets are overexpressed at both mRNA and protein level upon DLC1 loss in various HCC cell lines such as HepG2 and Hep3B. Interestingly, all newly identified genes are involved in the carcinogenesis or progression of different tumors and partly even in that of HCC, whereas the individual signaling pathways are unfortunately largely unknown. Work from our laboratory showed that DLC1 has an effect on cellular senescence and the loss of DLC1 triggers MKL1/2 activity, but the associated molecular mechanism is still unknown, it is of great importance to study it in more detail (Hampl et al. 2013; Muehlich et al. 2012; Xue et al. 2008). Microarray-based characterization of novel DLC1 dependent genes opens up the possibility of identifying the target gene(s) that promote HCC growth.

7.2 MKL1- and Filamin A dependency of newly identified DLC1 dependent genes

After loss of DLC1, which acts as a RhoGAP and thus converts active RhoA back to the inactive state, a permanently active RhoA signaling cascade occurs (Tcherkezian and Lamarche-Vane 2007). This permanently active state of RhoA leads to an increased polymerization of monomeric G-actin to polymeric F-actin by Rho kinases (Sotiropoulos et al. 1999). Due to these changes in the actin cytoskeleton, the coactivator MKL1 is now able to form a complex with Filamin A (FLNA), which is ultimately required to express the SRF/MKL1-dependent target genes (Hermanns et al. 2017; Kircher et al. 2015). FLNA, as an actin-binding protein, is essential for the crosslinking of actin filaments, the stabilization of the orthogonal actin network and its attachment to cellular membranes (Flanagan et al. 2001; van der Flier and Sonnenberg 2001; Stossel et al. 2001). In addition, FLNA is also able to interact directly with the RhoA signaling cascade via binding to GTPases of the Rho family (Stossel et al. 2001). Considering that for SRF-dependent target gene expression, which involves tumorigenic properties such as increased cell proliferation, FLNA is indispensable in addition to the coactivator MKL1, the goal to characterize DLC1 dependent genes not only for their SRF dependence but also for MKL1 and FLNA dependence is obvious.

In this thesis, we demonstrated that the upregulation of gene targets mediated upon DLC1 loss after additional knockdown of MKL1 or FLNA was suppressed for VCAN, TSPAN5, and n-

CDH2, but not for MEP1A or HISTK21A. These findings could be confirmed by MKL1 re-expression experiments with an MKL1N100 mutant that is constantly located in the nucleus and thus acts permanently as a coactivator of SRF (Muehlich et al. 2008). Further, VCAN, TSPAN5, n-CDH2 as well as MEP1A show a strong dependence of the transcriptional activator serum response factor (SRF). To our knowledge, DLC1 dependent genes have not been linked so far to the transcriptional activator SRF or its coactivator MKL1. For the first time, we publish data on VCAN, TSPAN5 and CDH2 and their dependence on MKL1 and SRF in this thesis.

For VCAN, however, it has been found, for example in heart disease, that metalloprotease-induced VCAN cleavage is required for normal expression of the cytoskeletal proteins FLNA and smooth muscle alpha-actin (a-SMA) (Dupuis et al. 2013). Accumulation of VCAN leads to a reduction of FLNA and a-SMA, which in turn affects the TGF-ß signaling pathway (Dupuis et al. 2013). In addition to the previously known signaling pathway of SMAD and FLNA interaction, which regulates the TGFß signaling, it is conceivable that the further TGFß mediated pathways are also influenced by the FLNA dependent MKL1/SRF-mediated target gene expression of e.g. TGFß1 (Hermanns et al. 2017; Kircher et al. 2015; Sasaki et al. 2001). Studies with SRF overexpression, on the other hand, indeed have illustrated increased expression levels of N-cadherin, which have already been associated with increased cell migration and invasiveness of HCC cells (Kwon et al. 2010). Furthermore, the authors Kwon and colleagues have shown a correlation between SRF overexpression and subsequent Wnt/ß-catenin pathway activation, which is also one of the most important signaling pathways in HCC progression (Kwon et al. 2010). This study suggests a possible cross-link from the MKL1/SRF signaling pathway to Wnt/ß-catenin signaling pathway due to the increased expression of N-cadherin itself caused by SRF overexpression. This can be substantiated by the fact that N-cadherin, as an important interaction partner of ß-catenin, shows influence on the Wnt/ß signaling pathway. Using chromatin immunoprecipitation (ChIP), we further confirmed the findings of MKL1 and FLNA dependence of the DLC1 dependent genes VCAN, TSPAN5 and n-CDH2. Thus, we were able to amplify the VCAN, TSPAN5 and CDH2 promoters from MKL1 immunoprecipitates in A7 cells, but not from IgG immunoprecipitates as negative control. Moreover, the VCAN, TSPAN5 and CDH2 promoters were enriched only in FLNA-positive (A7) cells, but not in FLNA negative (M2) cells.

Inhibition and stimulation experiments show that TSPAN5 is not only dependent on FLNA/MKL1/SRF, but is also regulated via the RhoA/actin signaling pathway, which is permanently active after DLC1 loss and ensures permanent nuclear localization and thus activation of MKL1. Thus, by inhibiting different steps of the RhoA/actin signaling pathway TSPAN5 expression was decreased. For example, the actin-polymerization inhibitor Latrunculin B (LatB), which prevents polymerization to F-actin and thus the assembly of the actin cytoskeleton by binding to monomeric G-actin, had the same inhibitory effect on TSPAN5 expression as the Rho associated protein kinase (Rock) inhibitor Y-27632 (Yarmola et al. 2000). In addition, preliminary data show that inhibition of the recently implicated RhoA/actin pathway transient receptor potential cation channel TRPM7 with NS8593 also results in significant downregulation of TSPAN5 (Voringer et al. 2020). TRPM7 is able to phosphorylate and thus activate RhoA after TRPM7 channel mediated Mg^{2+} influx by means of its kinase domain (Voringer et al. 2020). The regulation of TSPAN5 expression by the RhoA/actin signaling pathway was confirmed analogously by stimulation with lysophosphatidic acid (LPA) and thus activation of the RhoA signaling cascade and consequent overexpression of TSPAN5. LPA mimics serum stimulation as a potent signaling molecule and enhances actin polymerization to F-actin filaments via activation of the RhoA/actin cascade (Lin et al. 2010; Muehlich et al. 2004). These results are consistent with the finding of TSPAN5 overexpression after DLC1 loss, which is associated with a permanently active RhoA and thus RhoA/actin signaling cascade. Our data on the dependence of VCAN, TSPAN5 and n-CDH2 on MKL1 and SRF, as well as the influence of TSPAN5 expression by modulating the Rho/actin signaling pathway, suggest first and foremost TSPAN5 as a novel MKL1/SRF-dependent target gene. This finding, in turn, reveals new potential targets in the MKL1/SRF signaling cascade for the treatment of DLC1 deficient cancers in which TSPAN5 is overexpressed.

7.3 Effects of TSPAN5 on the tumorigenicity of HCC cells

7.3.1 Functional effects of TSPAN5 on HCC cells

Previous studies performed by our group revealed that DLC1 loss is associated with nuclear accumulation and thus persistently active MKL1 in primary human HCC *in vitro* and *in vivo* (Muehlich et al. 2012). Furthermore, these findings are accompanied by an increased

expression of the proliferation marker Ki67, whose expression directly correlates with cell proliferation and tumor progression (Muehlich et al. 2012). Thus, Ki67 expression can be detected in all active phases of the cell cycle, but not in resting cells (Scholzen and Gerdes 2000). Given that the tumor suppressor DLC1 is frequently deleted in human HCC, which is one of the most common cancers with poor prognosis, it was of great interest to study the genes upregulated after DLC1 depletion. With the new microarray results, which demonstrate the previously unknown upregulation of new gene targets after DLC1 loss, we focused on the impact of the additional MKL1- and FLNA-dependent genes VCAN, TSPAN5, and n-CDH2 on HCC growth.

Our study highlights for the first time that RNA-mediated downregulation of TSPAN5 expression, but not of VCAN or n-CDH2 expression, completely abolished the proliferation of human HCC cells. Interestingly, the proliferation was not only inhibited in DLC1 deficient cells such as HuH7 or HuH6 cells, but also in DLC1 expressing cells such as HepG2 cells. Further, increased proliferation in HepG2 cells upon additional silencing of DLC1 expression could also be completely suppressed by TSPAN5 knockdown. This indicates that TSPAN5 plays an essential role in proliferation of HCC tumor cells in general. Publications on TSPAN CD9, for example, state that TSPANs are not only involved in tumor cell proliferation, but in cell proliferation in general. It has been shown that de novo expression of CD9 in parietal epithelial cells causes the cells to invade glomerular capillaries, thereby promoting kidney injury and failure (Lazareth et al. 2019). However, our data suggest that TSPAN5 expression is in a delicate equilibrium and that overexpression upon DLC1 loss triggers proliferation of tumor cells. Consistent with this, similar studies show that other TSPANs such as TSPAN CD81 promote the growth of osteosarcoma or that overexpression of TSPAN CD9 increases the proliferation of human lymphoma cells (Herr et al. 2014a; Mizoshiri et al. 2019). Further, all our data show that TSPAN5 knockdown is not only able to inhibit proliferation, but also suppress other tumorigenic properties such as migration, invasion or the ability to form spheroids. Migration and invasion properties of tumor cells are essential for the tumor in terms of its ability to metastasize. For example, migrating and invading cells can reach and penetrate blood vessels in order to establish metastatic foci elsewhere in the organism. The ability to form spheroids is also associated with angiogenesis, which enables the tumor to grow and progress by improving the blood supply (Hanahan and Weinberg 2000; Zahra et al.

2019). Amongst the other gene targets identified in our microarray, we modulated neither proliferation nor migration inhibition by silencing the appropriate gene expression, while the loss of n-CDH2 at least resulted in reduced migratory capacity. In agreement with the fact that n-CDH2 serves as an indicator for ongoing EMT, which promotes migration and ultimately invasion of tumor cells, has been released in several publications and agrees with our results on migration inhibition after n-CDH2 silencing via RNA interference (Derycke and Bracke 2004; Wang et al. 2016b). Furthermore, increased n-CDH2 expression has been correlated with the development of different types of carcinomas (Hui et al. 2013; Hulit et al. 2007; Jennbacken et al. 2010). Consistent with our novel findings that targeted TSPAN5 knockdown inhibits tumorigenic properties such as proliferation, migration or invasion, publications regarding other members of the TSPAN superfamily show a similar influence of different TSPANs on tumorigenesis and progression. For example, inhibition of TSPAN CD81 expression has been shown to reduce lung metastasis by osteosarcoma cells (Mizoshiri et al. 2019). Further studies show that TSPAN2 is overexpressed in lung cancer cells, for example, and that invasiveness and motility are reduced after TSPAN2 knockdown (Yaseen et al. 2017). In the mouse model, the results were confirmed by a reduction of lung metastasis after TSPAN2 knockdown (Otsubo et al. 2014). TSPAN8 overexpression has previously been correlated with increased metastasis in HCC due to its invasion- and metastasis-enhancing properties (Kanetaka et al. 2001; Kanetaka et al. 2003). It is interesting to note that a previous microarray from our group in HuH7 cells stably expressing shRNA against MKL1/2 revealed under-expression of TSPAN8 after MKL1 loss, among other genes (Hermanns et al. 2017). This suggests that TSPAN8, for which tumor enhancing properties have been demonstrated by Kanetaka and colleagues, is an MKL1-dependent target gene and thus is (at least partially) expressed in a regulated manner via the RhoA signaling pathway and MKL1/SRF activation. Moreover, using TSPAN CD151 knockdown mice, it was shown that the promotion of tumor growth by angiogenesis *in vivo* is dependent on CD151 (Takeda et al. 2007). Among the VCAN, TSPAN5 and n-CDH2 genes overexpressed as a result of DLC1 loss, only TSPAN5 depletion manifests a strong effect on proliferation arrest. Since proliferation is one of the first degenerate features of tumor cells in tumorigenesis, which should accordingly be addressed as early as possible in tumor control, we were interested in uncovering the mechanism of proliferation inhibition after TSPAN5 knockdown.

7.3.2 Induction of oncogene-induced senescence due to TSPAN5 depletion

The proliferation arrest described in the previous chapter, which is due to TSPAN5 depletion and serves as a tumor evasion strategy for the cell, may result from an induced apoptotic or senescent signaling pathway (Wyllie et al. 1980; Wynford-Thomas 1999). On this basis, we next investigated whether the cells after TSPAN5 loss indicated cellular senescence. For this purpose, we analyzed HCC cells, such as HuH7 or HuH6 cells, after TSPAN5 knockdown by using ß-galactosidase staining, which is known to be a well-established marker for senescent cells (Debacq-Chainiaux et al. 2009; Dimri et al. 1995). In agreement with the results of Hampl and colleagues that MKL1/2 knockdown causes senescence induction, we were able to show that analogously after loss of TSPAN5, which is dependent on MKL1 as shown above, there is a significant senescence induction compared to control cells (Hampl et al. 2013). Whereas MKL1 and SRF have already been shown to be modulators of an induction of a senescence response in several studies, for example in HCC cells, but also in smooth muscle cells (SMCs) of mice or in mouse muscles themselves, a correlation of TSPAN5 with cellular senescence was observed for the first time in HCC cells (Angstenberger et al. 2007; Hampl et al. 2013; Lahoute et al. 2008). In view of the background that proliferation arrest can be triggered by senescence induction, we were next interested in the more precise molecular mechanism leading to the senescence response.

Since the Raf/Mek/ERK signaling pathway downstream of Ras is one of the most relevant for senescence induction, proliferation arrest and also plays an important role in the senescence response after MKL1 depletion, we first wanted to investigate whether senescence is also induced via this pathway after TSPAN5 loss (Hampl et al. 2013; Lin et al. 1998; Zhu et al. 1998). By analyzing the phosphorylation levels of ERK in TSPAN5 deficient HCC cells compared to control cells, we were able to detect an activation of ERK. These results point to the Ras/Raf/Mek/ERK signaling pathway as a senescence inducing pathway upon TSPAN5 loss (Crews and Erikson 1993). In the context of oncogenic Ras expression, Serrano and colleagues postulated for the first time premature senescence, which cannot be attributed to a finite number of cell doublings depending on telomere length like previously known replicative senescence (Serrano et al. 1997). The existence of this premature or so-called oncogene-induced senescence (OIS) is due to the activation of oncogenes and thus represents a very efficient cellular tumor suppressor mechanism that counteracts the cell transforming

properties of sustained Ras activation (Lin et al. 1998; Michaloglou et al. 2005; Serrano et al. 1997). Consistent with several studies that the Raf/Mek/ERK signaling pathway causing oncogene-induced senescence is, among others, controlled by $p16^{INK4a}$, by inducing a G1-cell cycle arrest, we demonstrated an accumulation of $p16^{INK4a}$ in HCC cells after TSPAN5 loss (Lin et al. 1998; Serrano et al. 1997; Sherr and Roberts 1999). Furthermore, analogous studies in HCC cells after MKL1 loss as well as loss of the MKL1 target gene myoferlin (MYOF) showed activation of ERK followed by an accumulation of $p16^{INK4a}$, which triggers the senescence response (Hampl et al. 2013; Hermanns et al. 2017). As early as 1996, an upregulation of $p16^{INK4a}$ expression in senescent cells and its ability to trigger the senescence response was found, underscoring an impact of TSPAN5 on the induction of oncogene-induced senescence response (Alcorta et al. 1996; Hara et al. 1996). The fact that $p16^{INK4a}$ is expressed in many different tumor cell lines at very low levels or in a mutated and thus functionless form highlights the important role of $p16^{INK4a}$ as a tumor suppressor (Bennett 2003; Grant et al. 2016; LaPak and Burd 2014; Liggett, JR and Sidransky 1998). Furthermore, as a CDK inhibitor protein, $p16^{INK4a}$ regulates CDK4/6 activity, which provokes G1 cell cycle arrest and consequently prevents phosphorylation of the retinoblastoma (Rb) protein (Alcorta et al. 1996; Hara et al. 1996; Serrano et al. 1997). Therefore, the accumulation of $p16^{INK4a}$ maintains the Rb protein in its hypophosphorylated and thus active state, which hinders cell cycle progression from G1 to S phase and thereby promotes senescence induction (Chicas et al. 2010; Peeper et al. 1994; Weinberg 1995). Given these facts, we found that the phosphorylation status of Rb was strongly decreased after TSPAN5 depletion in both HuH7 and HuH6 cells. Thus, the absence of TSPAN5 leads to the induction of an OIS response via an active, hypophosphorylated Rb protein, which, through association with the transcription factors of the E2F family, prevents the transcription of cyclins E and A. These cyclins are essentially required for the G1 to S phase transition (Burkhart and Sage 2008; Serrano et al. 1997). Thus, our results show that silencing of TSPAN5 activates the Ras/Raf/Mek/ERK signaling pathway and thereby triggers the $p16^{INK4a}$/Rb tumor suppressor pathway, which prevents cell cycle progression and eventually induces the OIS response. In summary, therefore, both the Ras/ERK and $p16^{INK4a}$/Rb signaling pathways are involved and responsible for the TSPAN5 mediated senescence response. Ferbeyre and colleagues found by differential gene expression screens of cells with *Ras*-induced senescence compared with cells with

quiescent-like arrest that promyelocytic leukemia (PML) is significantly overexpressed in the cells with oncogenic *Ras* (Ferbeyre et al. 2000). Their results imply that PML modulates and acts with the Rb tumor suppressor pathway, thereby promoting and maintaining ras-induced senescence (Ferbeyre et al. 2000). PML, a RING (Really Interesting New Gene) finger protein, is localized in large nuclear structures called promyelocytic oncogenic domains (PODs) or PML nuclear bodies and accumulates in *Ras*-arrested cells in the nucleus (Zhong et al. 2000). The accumulation of such PML nuclear bodies after TSPAN5 knockdown compared to control cells further strengthened the hypothesis that oncogenic *Ras* triggers activation of the Ras/Raf/Mek/ERK signaling pathway, leading to an overexpression of PML and a maintaining senescence response via the $p16^{INK4a}$/Rb signaling pathway (Ferbeyre et al. 2000).

To further investigate the impact of TSPAN5 loss on the oncogene-induced senescence response, we analyzed the cells for remodeling of chromatin structure in response to TSPAN5 expression. Senescent cells show the formation of facultative heterochromatin structures termed senescence-associated heterochromatin foci (SAHF), which contain increased levels of characteristic heterochromatin structures such as histone 3 trimethylated on lysine 9 (H3K9me3) (Narita et al. 2003). The accumulation of SAHF induces, for example, the recruitment of Rb, which in turn prevents the expression of E2F-dependent target genes essential for cell cycle progression and thus promotes OIS development (Adams 2007; Narita et al. 2003). Again, our results showed that cells lacking TSPAN5 significantly accumulated H3K9me3, further supporting the hypothesis of OIS and additionally paralleling senescence development after MKL1 loss.

To further strengthen the finding that TSPAN5 knockdown leads to OIS induction, we analyzed other OIS markers that are characteristic signs of senescent cells in addition to those already studied ranging from ß-galactosidase activity to the $p16^{INK4a}$/Rb pathway to accumulation of H3K9me3. Thus, senescent cells secrete a number of different interleukins, growth factors, matrix remodeling factors and cytokines, which are collectively referred to as the senescence-messaging secretome (SMS) or the senescence-associated secretory phenotype (SASP) (Coppé et al. 2010; Cristofalo and Pignolo 1996; Kuilman and Peeper 2009). These changes in the secretome of the cells, which are also accompanied by changes in the factors associated with the extracellular matrix (ECM), are important key processes in the development of senescence (Cristofalo and Pignolo 1996; Kuilman and Peeper 2009). The expression of chemokine (C-S-C

motif) ligand 10 (CXCL10) and tumor necrosis factor (ligand) superfamily member 10 (TNFSF10), both of which promote senescence response in human tumors, significantly increases after TSPAN5 loss in human HuH7 cells (Braumüller et al. 2013; Dabrowska et al. 2011). The fact that CXCL10 and TNFSF10 are secreted by senescent cells and thereby promote senescence induction, supports previous findings that silencing of TSPAN5 initiates the senescence response.

Here, one might speculate that TSPAN5, as an MKL1-dependent gene, plays a role in senescence induction not only after its own loss but also after MKL1 depletion, in addition to the direct MKL1 target gene Myoferlin or MKL1 itself (Hampl et al. 2013; Hermanns et al. 2017). Considering that Hampl and colleagues found out that the loss of MKL1 leads to an induction of senescence only in DLC1 deficient cells, one could see a putative correlation here, since DLC1 loss overexpresses TSPAN5. Furthermore, just as direct knockdown of overexpressed TSPAN5 triggers a proliferation arrest by OIS induction, MKL1 knockdown analogously decreases TSPAN5 expression, which could promote senescence induction upon MKL1 loss in DLC1 deficient cells, in addition to myoferlin as another MKL1 target gene. Proliferation experiments with overexpression of a constitutively active MKL1 variant (MKL1N100) on a previous TSPAN5 depletion also demonstrate, by attenuating the proliferation arrest, the inhibitory role of MKL1 on senescence induction and thus proliferation.

Summarizing the collected data, these results show for the first time that TSPAN5 is directly involved in the OIS response in HCC cells. Thus, reduction of TSPAN5 expression by RNA interference increased senescence-associated ß-galactosidase activity and resulted in activation of the MAPK signaling cascade indicated by increased ERK1/2 phosphorylation. PML accumulation and $p16^{INK4a}$/Rb pathway activation ultimately trigger the OIS response, which is further indicated by increased expression of CXCL10 and TNFSF10. In this way, we identified that the overexpression of the gene target TSPAN5 due to DLC1 loss mediates the effects of OIS in HCC cells. Thus, TSPAN5 serves as a promising therapeutic target to prevent or eliminate hepatocarcinogenesis by OIS induction in DLC1 deficient cancers.

7.4 Depletion of TSPAN5 affects the actin cytoskeleton, epithelial transition and MKL1 signaling pathway

7.4.1 Depletion of TSPAN5 affects the actin cytoskeleton

Since TSPANs impacts the cytoskeleton through their interaction with integrins, we sought to focus on their potential influence on the Rho/actin signaling pathway in the next part of this thesis (Hemler 2005; Zhang et al. 2001). For this purpose, we first examined the effect of TSPAN5 depletion on RhoA activity. As a result, we found a decrease in RhoA activity in HepG2 CRISP Cas9 DLC1 KO cells after additional TSPAN5 knockdown. This suggests, for example, a direct interaction of TSPAN5 itself or as a member of the tetraspanin enriched microdomains (TEMs) and the membrane associated RhoA protein. Similarly, it was shown that TSPAN CD151 has regulatory properties for RhoA activation (Johnson et al. 2009). Analogous to our findings that loss of TSPAN5 leads to decreased RhoA activity, diminished levels of active RhoA protein were found upon TSPAN CD9 deficiency (Herr et al. 2014b). Another assumption is that TSPAN5, like the TSPANs CD9, CD81, CD82, or CD151, also interacts with protein kinase C (PKC) and is thereby involved in the regulation of the phosphorylation status and thus the activity of the RhoA protein (Knezevic et al. 2007; Kuribayashi et al. 2007; Sabbatini and Williams 2013; Zhang et al. 2001). Due to the interaction of TSPANs with integrins or even with PKCs and in particular due to their influence on RhoA activity, it remains to be investigated whether TSPAN5 is involved in the organization of the actin cytoskeleton. To gain insight into TSPAN5-induced changes in the actin cytoskeleton, we first analyzed whether there were changes in the proportion of monomeric G-actin and polymeric F-actin and in the formation of stress fibers. As expected, the balance of G- and F-actin in TSPAN5 knockdown cells shifted toward increased monomeric G-actin compared to control cells. This reflects the effect of decreased RhoA activity after TSPAN5 loss and consequently the inhibition of the downstream effectors diaphanous-related formin (mDia) and Rho-associated kinase (Rho-kinase, Rock), which regulate the polymerization of monomeric G-actin to polymeric F-actin filaments (Copeland and Treisman 2002; Ishizaki et al. 1996; Leung et al. 1995; Matsui et al. 1996). In activated Rho cascade, mDia promotes actin nucleation as well as its elongation from G-actin to F-actin by interacting with the barbed ends of actin (Baarlink et al. 2013; Watanabe et al. 1999). Rock additionally phosphorylates Lim-kinase in the activated state, which in turn phosphorylates

the actin depolymerization factor cofilin and thus inactivates it. In this way, Rock stabilizes the filamentous F-actin (Sotiropoulos et al. 1999). The enhancing effect that mDia exerts on the nuclear localization of MKL1 through the polymerization of actin and thus on SRF target gene expression was confirmed by Hermanns and colleagues using mDia overexpression experiments (Hermanns et al. 2017; Staus et al. 2007; Staus et al. 2014). Moreover, studies show that mDia also has a positive effect on nuclear actin assembly, which, according to Baarlink and colleagues, further supports SRF target gene expression by facilitating nuclear MKL1 accumulation and thus increased SRF activity (Baarlink et al. 2013). These data may imply that the increased expression level of TSPAN5 in a DLC1 deficient carcinoma also has an impact on the expression of mDia and thus supports the nuclear assembly of actin and SRF target gene expression. This hypothesis should be further investigated in future studies to uncover the influence of TSPAN5 on additional signaling pathways and their effectors. That elevated RhoA levels are found in many various types of cancer and promote tumor growth has been shown in several studies (Del Gómez Pulgar et al. 2005). However, the underlying mechanism of RhoA activation is still not well understood. Our data led us to hypothesize that elevated TSPAN5 levels, possibly through direct or indirect interaction via TEMs with RhoA, may be partly responsible for its increased activity and exert a supporting effect on RhoA activity alongside the loss of RhoGAP DLC1. Furthermore, in cells with silenced TSPAN5, we observed a decrease in actin stress fibers just in the nuclear and perinuclear regions, as well as an increased reorganization of the actin network in the cortical regions of TSPAN5 knockdown cells, which is associated with a more rounded cell morphology. This led us to hypothesize that TSPAN5 loss counteracts tumorigenic properties by inhibiting RhoA and affecting actin cytoskeleton and cellular stress fibers. Our findings are consistent with other studies using, for example, TSPAN CD9 knockdown cells, in which morphological changes, a lack of parallel actin arrangements and a resulting reduction in cell contractility were similar to our results (Herr et al. 2014b). Furthermore, Lee and colleagues observed overexpression of TSPAN TM4SF5 in human hepatocarcinoma tissue, which they correlated with increased RhoA activity and a consequently aberrant cell growth (Lee et al. 2008). Moreover, they maintained that TSPAN TM4SF5 mediated effects led to epithelial-mesenchymal transition (EMT) via loss of E-cadherin expression and a subsequently aberrant cell growth (Lee et al. 2008). Such changes in RhoA activity and concomitant changes in the organization and

formation of the actin cytoskeleton appear to be fundamental mechanisms for TSPAN5-loss-induced proliferation arrest as well as loss of migratory and invasive capacity in TSPAN5 knockdown cells (Bersini et al. 2020; Peng et al. 2018; Svitkina 2018). In HCC, for example, it was recently found that the EMT, which is essential for cancer invasion and metastasis, can be triggered by actin cytoskeleton remodeling and is prevented by proteins that inhibit actin polymerization (Peng et al. 2018). Our results show that the expression level of TSPAN5 can influence not only the RhoA activity itself, but also the downstream processes such as actin polymerization and stress fiber formation. In further experiments, based on the results of Peng and colleagues, it was of interest whether TSPAN5 knockdown, which has an inhibitory effect on actin polymerization, can also affect EMT.

7.4.2 Depletion of TSPAN5 affects the epithelial-mesenchymal transition (EMT)

In subsequent studies, we were able to show a direct influence of TSPAN5 on EMT by knockdown experiments. In this way, the protein levels of specific EMT markers changed after TSPAN5 silencing in DLC1 deficient cells. We demonstrated for the first time that E-cadherin, a protein with tumor suppressive properties, whose loss is associated with enhanced metastasis, is increasingly expressed after TSPAN5 loss. Silencing of TSPAN5 in HCC cells could thus also improve the worsened prognosis for patients lacking E-cadherin. In addition to downregulation of E-cadherin expression, concomitant elevated levels of N-cadherin (CDH2), which enhance tumor progression by promoting migration, are typical of EMT (Diamond et al. 2008; Nuessle et al. 2011; Yang et al. 2015). These inducing EMT processes are consistent with our microarray results in DLC1 deficient HCC cells, in which CDH2 in addition to TSPAN5 is strongly elevated in expression, strongly supporting EMT with regard to progressive tumor progression with migratory and invasive properties. Our results suggest that TSPAN5 knockdown can shift the balance of EMT lying on the side of CDH2 by increasing E-cadherin levels such that EMT-induced tumor progression is diminished. Another EMT marker is Zonula occludens-1 (ZO-1), whose function has been linked to tight and adherens junctions and its decreased expression plays a critical role in HCC progression by promoting migration, invasion and metastasis (González-Mariscal et al. 2000; Nagai et al. 2016). ZO-1 is not only associated with the prognosis of HCC and lung cancer, but it has also been convincingly shown in HCC cell

lines that an increasing ZO-1 expression inhibits their invasive capacity (Hsu et al. 2017; Zhang et al. 2019). Silencing of TSPAN5 has been shown to increase expression of ZO-1, which may inhibit the EMT and thus the tumorigenic properties of the cells and thereby improve the prognosis of HCC patients. In addition to an increase of E-cadherin and ZO-1 with their tumor suppressive properties, we also observed a decrease of the tumor promoting proteins vimentin and SLUG upon TSPAN5 depletion. The EMT marker vimentin is a cytoskeletal protein whose increased expression is associated with higher tumor cell proliferation, invasion and metastasis as well as a poorer prognosis (Mendez et al. 2010; Meng et al. 2018; Shibue and Weinberg 2017). This deregulation of vimentin expression in tumor tissue is associated with metastasis of various types of cancer such as prostate carcinoma, gastrointestinal and breast tumors (Fuyuhiro et al. 2010; Gilles et al. 2003; Lang et al. 2002; Takemura et al. 1994; Zhao et al. 2008). Furthermore, there is also evidence that overexpression of vimentin is associated with drug resistance (Huo et al. 2016; Kanakkanthara et al. 2012). TSPAN5 depletion is capable of lowering vimentin protein levels and may thereby counteracts progressive tumor growth and metastasis. The fact that TSPAN5 may cooperate indirectly or directly with cytoskeleton or its components such as vimentin via the TEMs underscores this finding. Also, the studies on drug resistance associated with vimentin overexpression opens up the possibility to further investigate and ultimately counteract it by TSPAN5 knockdown in HCC (Huo et al. 2016; Kanakkanthara et al. 2012). Another hallmark of EMT development is SLUG (Meng et al. 2019). SLUG is a zinc-finger transcription factor that represses E-cadherin expression, thereby counteracting tumor protection (Hajra et al. 2002). SLUG is aberrantly expressed in various types of cancer, and contributes to proliferation and cell survival, as well as tumor cell invasion and metastasis (Barrallo-Gimeno and Nieto 2005; Dhasarathy et al. 2011; Emadi Baygi et al. 2010; Kurrey et al. 2005; Turner et al. 2006; Uygur and Wu 2011). Thus, TSPAN5 loss not only lowers SLUG protein levels, which manifest antitumorigenic effects, it further prevents transcription of the tumor-suppressive E-cadherin from being repressed.

In summary, our data add another twist to this story, suggesting that TSPAN5 knockdown can interrupt or even reverse the epithelial-mesenchymal transition to the so-called mesenchymal-epithelial transition (MET), thus inhibiting tumor progression in terms of invasion and metastasis.

7.4.3 Depletion of TSPAN5 affects the MKL1/SRF target gene expression

Since TSPANs regulate integrins in the context of TEMs, which in turn interact with actin cytoskeleton, which also affects MKL1/FLNA signaling via F- and G-actin, it seemed to us very likely that TSPAN5 itself effects MKL1/SRF target gene expression. More precisely, since the actin/RhoA signaling pathway in turn influences the MKL1/FLNA signaling cascade, which ultimately leads to activation of the transcription factor SRF and corresponding pro-proliferative target gene expression, our next goal was to investigate the influence of TSPAN5 on the MKL1/SRF signaling pathway. For this purpose, we first examined whether the MKL1-FLNA interaction, which is G- and F-actin-dependent and ultimately essential for SRF target gene expression, is affected by TSPAN5 depletion. Indeed, TSPAN5 deficiency causes abrogation of the MKL1-FLNA complex not only in human HCC cells but also in murine 3T3 cells (embryonic fibroblasts). Moreover, we determined that the MKL1/SRF target genes are also significantly diminished upon TSPAN5 knockdown both at the mRNA level and at the protein level. Additionally, re-expression of TSPAN5 reverses the MKL1/SRF target gene downregulation. These findings suggest that the proliferation, migration and invasion arrest caused by TSPAN5 loss is not only due to direct changes in the actin cytoskeleton, but also to an actin-related inhibition of the MKL1/FLNA signaling pathway. These very interesting results indicate that there is obviously a kind of positive feedback loop, as TSPAN5, identified as an MKL1-dependent gene, itself influences the MKL1 signaling cascade.

7.5 *In vivo* anti-tumor effects of TSPAN5 depletion

7.5.1 Anti-tumor effects of TSPAN5 silencing in CAM assay

To obtain first evidence for anti-tumorigenic effects upon TSPAN5 depletion *in vivo* we utilized chorioallantoic membrane (CAM) assay. CAM assays allow the assessment of tumor cell growth and aggressiveness *on ovo*, providing a reliable and ideal pre-test to conventional *in vivo* mouse xenografts (Nowak-Sliwinska et al. 2014; Ribatti 2014). For our study to analyze the micro-tumors after TSPAN5 knockdown in comparison to control micro-tumors, we used HuH7 cells on the one hand, analogous to the previous experiments, and on the other hand an aggressive HepG2 clone 5 (Muenzner et al. 2018). The HepG2 clone 5 cell line is a cancer stem cell (CSC) enriched sub-cell line of the established HCC cell line HepG2 generated by

Muenzner and colleagues by spheroid formation and single-cell cloning. It is characterized by a high migratory and invasive potential *in vitro* and an enhanced tumor aggressiveness *in vivo* (Muenzner et al. 2018). By excising the tumors that manifested after transplantation of the corresponding cells on chicken CAM, tumors with TSPAN5 depletion showed significantly smaller volume compared with control tumors. This macroscopic finding of growth arrest after TSPAN5 knockdown was confirmed by decreased Ki67 mRNA and protein expression as well as conventional HE staining showing only loose and broken-up tumor growth. These results were obtained not only for HuH7 tumors but also for HepG2 clone 5 tumors, further confirming the anti-tumorigenic effects of TSPAN5 depletion. Especially, the finding that TSPAN5 depletion can also inhibit the growth of the CSC enriched cell line HepG2 clone 5 is of utmost importance for the consideration of TSPAN5 as a pharmacological target. HCC tumors, like many other types of cancer, are thought to arise from so-called CSCs, which represent a small subunit of the cancer cells and have stem cell-like properties (Castelli et al. 2017; Chiba et al. 2007; Flores-Téllez et al. 2017; Ma et al. 2007a; Rich 2016; Zhang et al. 2017). These stem cell-like characteristics allow the tumor cells to have unlimited self-renewal capacity and differentiation capabilities for multiple tumor heterogeneities responsible for tumor initiation, growth and metastasis (Castelli et al. 2017; Flores-Téllez et al. 2017; Zhang et al. 2017). In addition, hepatic CSCs are resistant to conventional chemotherapy and radiotherapy and often remain in healthy tissue after surgical resection of the primary tumor, severely increasing the likelihood of HCC recurrence (Sun et al. 2016; Zhu et al. 2015). The generated results of the CAM assay suggest that TSPAN5 depletion can also prevent tumors with enriched CSCs from growing and may inhibit the proliferation of the CSCs themselves. If TSPAN5 depletion could be used to attack and inhibit these CSCs as part of tumor therapy, the incidence of tumor relapse would be reduced.

Another finding raised in this thesis is that TSPAN5 loss in the CSC enriched subclones of HepG2 clone 5 can prevent migration, and thus an essential process for metastasis, in addition to proliferation. Inhibition of migration in TSPAN5 knockdown cells is suggested by a marked increase in E-cadherin by IHC staining. EMT changes, which are characterized by transcriptional reprogramming of epithelial cells, are often accompanied by an increase in E-cadherin and a decrease in N-cadherin as well as they are typical signs of a decreased migratory capacity of the cells (Gheldof and Berx 2013; Petrova et al. 2016). It would be a

significant advance and prognosis-improving if the migratory ability of CSCs could be inhibited. In case that the migration of CSCs into healthy tissue would be prevented, the associated survival of CSCs, for example after surgical removal of the primary tumor, would also be eliminated.

Analogous to our *in vitro* experiments, we examined typical oncogene-induced senescence markers as the cause of proliferation arrest *on ovo*. Consistent with the important role of oncogenic Ras in OIS, increased phosphorylation levels of ERK allowed us to demonstrate the Ras/Raf/Mek/ERK pathway as a senescence-inducing pathway in HuH7 siTSPAN5 knockdown tumors *in vivo* (Crews and Erikson 1993; Lin et al. 1998; Serrano et al. 1997). In order to test the hypothesis whether TSPAN5 loss co-regulates the Raf/Mek/ERK signaling via the $p16^{INK4a}$ /Rb pathway also *in vivo*, we examined $p16^{INK4a}$ levels (Lin et al. 1998; Serrano et al. 1997; Sherr and Roberts 1999). Our revealed unequivocal results in the HepG2 clone 5 micro-tumors demonstrated $p16^{INK4a}$ accumulation and thus the involvement of the $p16^{INK4a}$/Rb pathway in senescence induction (Chicas et al. 2010; Peeper et al. 1994; Weinberg 1995). This provides initial evidence that senescence induction in tumor areas with enriched CSCs may even have an anti-proliferative effect on CSCs themselves. Since OIS gains importance for HCC therapy, this approach holds the promises to be an option in tumor therapy of resistant and recurrent tumors and should be further explored (Kang et al. 2011). Besides, accumulation of H3K9me3 is consistent with previous *in vitro* experiments and supports the assumption of proliferation arrest induced by OIS upon TSPAN5 depletion *in vivo*.

When analyzing the MKL1-dependent target gene expression of the harvested CAM tumors, we found that there is explicitly a significant downregulation of MKL1 target genes in the HuH7 tumors after TSPAN5 loss. In contrast, there was only a partial decrease in MKL1 target gene expression in the HepG2 clone 5 tumors upon TSPAN5 loss. This may be due to the partially observed redistribution of the coactivator MKL1 from the nucleus to the cytosol, which only occurs in the HuH7 micro tumors upon TSPAN5 depletion. One reason for this could be that MKL1 is already actively present in the nucleus in unstimulated HuH7 cells, but not in HepG2 clone 5 cells. This leads to an increased expression of MKL1/SRF-dependent target genes in HuH7 cells but not in HepG2 clone 5 cells (Hampl et al. 2013; Muehlich et al. 2012). Despite this discrepancy, our collected results reveal tumorigenic characteristics of TSPAN5 in HuH7 as well as HepG2 clone 5 cells in CAM assay *in vivo*, which are repressed by TSPAN5 silencing.

In the next steps, it was therefore of great importance to investigate whether in human liver tissue samples, a manifestation of HCC correlates with TSPAN5 overexpression. Moreover, we could demonstrate the efficacy of TSPAN5 depletion to inhibit tumor growth in a more complex *in vivo* model with established tumors by adequate siTSPAN5 application.

7.5.2 Evaluation on TSPAN5 as a novel anti-tumor target in HCC-xenograft

Using CAM-assay, we obtained preliminary evidence that a TSPAN5 loss exerts repressive properties on tumor development and growth by OIS induction *in vivo*. In view of a therapeutic use of TSPAN5 silencing, it was of interest to verify our previous findings in a more complex *in vivo* model such as an HCC xenograft and, furthermore, to test the delivery and the effect of siTSPAN5 on already manifested tumors *in vivo*. In order to achieve a therapeutic effective TSPAN5 knockdown in established subcutaneous HCC xenografts derived from DLC1 deficient HuH7 cells, we combined TSPAN5 siRNA with polymer-based nanoparticles (Aigner 2006; Hampl et al. 2013; Ibrahim et al. 2011; Schäfer et al. 2010). Due to their higher relevance in a therapeutic setting, we chose systemic delivery of complexed siRNAs by intraperitoneal injection (i.p.) instead of intratumoral injection. Systemic i.p. application of TSPAN5 siRNA complexed with polyethylenimine PEIF25-LMW (PEI) to ensure drug delivery was performed 3x per week (Höbel and Aigner 2013). Initial differences in tumor size were evident as early as day 5, and by day 7 after treatment initiation, tumors in the treatment group were significantly smaller, indicating a tumor growth inhibitory effect of TSPAN5 interference in the HCC xenograft. However, overall, the HuH7 tumors grew so rapidly that the experiment had to be terminated on day 10. Since we used comparatively low siRNA amounts of 10 µg and HuH7 tumors grew extremely fast, it cannot be excluded that we could have achieved even more significant results with higher siRNA amounts. Also, the fact that no adverse side effects were observed by systemic therapy with complexed PEI-siRNAs targeting TSPAN5 opens up the possibility in further studies to increase the amount of siRNA administered to achieve even stronger effects. TSPAN5 is not the only TSPAN that has been shown to play a role in tumorigenesis and growth. More and more studies are recognizing that TSPANs with their large variety of biological processes also have an influence on many different types of cancer and their development, so they are now being studied in more detail in several *in vivo* studies.

For example, in TSPAN CD9-KO mice a decreased lymph node metastasis and tumor lymph angiogenesis was shown (Iwasaki et al. 2013). Mizoshiri and colleagues could show that mice transplanted with TSPAN CD81 knockout cells exhibited less tumor formation and lung metastasis than the mice of the control group (Mizoshiri et al. 2019). Furthermore, CD151-null mice, for example, also showed impaired pathologic angiogenesis or ablation of TSPAN12 in human MDA-MB-231 cells significantly reduced primary tumor xenograft growth (Knoblich et al. 2014; Takeda et al. 2007). In addition to decreased expression of Ki67 mRNA in the treatment group, indicating inhibited tumor cell proliferation, we also detected, in accordance with our *in vitro* experiments and *in vivo* CAM assay, decreased expression levels of MKL1 target genes at both mRNA and protein levels. This finding is consistent with similar MKL1 interference xenograft experiments performed by our group, which similarly resulted in the suppression of tumor relevant MKL1 target gene expression and confirms that TSPAN5 inhibits tumor growth via MKL1 (Hampl et al. 2013). The question arose whether in xenograft model the inhibition of tumor growth upon TSPAN5 depletion is also related to senescence response. Initial evidence for this is provided by a strong decrease in the MKL1/SRF dependent target gene myoferlin (MYOF) (Hermanns et al. 2017). MYOF mediates its effect on oncogene-induced senescence by modulating the activation state of EGFR and the downstream MAPK and $p16^{INK4a}$/Rb signaling pathway (Hermanns et al. 2017). Decreased expression of MYOF in this xenograft study, triggered by TSPAN5 knockdown, induces OIS, which is responsible for suppressing proliferation. The continued evaluation of OIS markers in HCC xenografts treated with TSPAN5 siRNA strengthened the senescence induction via a MYOF decrease due to TSPAN5 knockdown and revealed a significant accumulation of phosphorylated ERK. Increased phosphorylation levels of ERK1/2 indicate an activated Raf/Mek/ERK signaling pathway known to cause OIS (Crews and Erikson 1993; Serrano et al. 1997). The hypothesis is further supported by the finding that there is a strong hypophosphorylation of Rb in the siTSPAN5 treatment group. An active, hypophosphorylated Rb protein indicates an active $p16^{INK4a}$/Rb signaling pathway that provokes G1 cell cycle arrest by inhibiting CDK4/6 activity, ultimately promoting senescence induction (Alcorta et al. 1996; Chicas et al. 2010; Hara et al. 1996; Peeper et al. 1994; Serrano et al. 1997; Sherr and Roberts 1999; Weinberg 1995). In summary, we corroborated the new identified drug effective target TSPAN5 in the *in vivo* xenograft

model and tested a first possibility for a direct therapeutic approach of TSPAN5 siRNA complexed in PEI nanoparticles.

7.5.3 Comparison of *in vivo* models used: chicken CAM assay versus mouse xenograft model

Comparing the two *in vivo* methods used -CAM and xenograft-, we determined that especially the CAM assay is a well suited and uncomplicated method with few hurdles to transfer obtained *in vitro* data into a first *in vivo* model (Ribatti 2014). In addition, the use of the CAM assay supports the efforts to reduce animal experiments such as xenograft to an indispensable minimum. Especially for testing mechanistic correlations and first possible therapy options in the early stages, the CAM model provides promising, reproducible and accurate results (Tamanoi 2019). Also, because the CAM assay is a very sensitive method, in which hypotheses can be confirmed with the same treatment as in the cell culture experiments, initial *in vivo* testing by means of CAM assay is recommended (Ribatti 2014; Tamanoi 2019). Furthermore, the CAM model is a relatively simple, inexpensive and rapid assay that allows a large number of samples to be screened in a short period of time (Ribatti 2017). Moreover, no administrative procedures are required to obtain the approval of the ethics committee for animal experiments (Ribatti 2017). However, *in vivo* animal experiments such as the xenograft remain indispensable in order to test possible therapeutic options in further steps, which can also find direct application to humans. Only in a fully developed organism can the influence of drug candidates on delivery, distribution, metabolism and elimination be observed, studied and potential side effects detected (Sharpless and DePinho 2006; Zitvogel et al. 2016). Thus, in our xenograft experiment, complexation of siRNA with polyethyleneimines to form nanoparticles is necessary to allow the siRNA to arrive at the site of pharmacological action at all (Ewe et al. 2017; Höbel and Aigner 2013; Schiffelers et al. 2004). In contrast, pharmacokinetic aspects are not elucidated in the CAM assay, but only the result of the pharmacological effect is considered. Our comparison xenograft versus CAM assay showed that CAM models are important alternatives to conventional animal experiments and should be used more frequently, especially in basic studies. Nevertheless, the use of animal experiments cannot be completely avoided, since only in this way can pharmacokinetic and potential toxic effects and

problems be identified and important indications of possible side effects be obtained. Moreover, it would be of enormous scientific importance to investigate and evaluate exactly this comparison or the possible interchangeability of CAM assay and xenograft in more detail in future studies.

7.5.4 Summary model of tumorigenic effects of TSPAN5 and anti-tumorigenic effects of TSPAN5 depletion

HCC tumors are still often inadequately treated. Thus, there is an urgent need to develop new therapeutic intervention strategies in the field of personalized medicine that directly target aberrant molecular mechanisms leading to HCC development. To this end, one aim of my thesis was to identify novel gene targets induced by loss of the tumor suppressor DLC1 that have effects on HCC growth. As already published by Hampl and colleagues, DLC1 loss in human HCC cells provokes constitutive RhoA activation (Hampl et al. 2013). This leads to a nuclear accumulation of MKL1 and SRF, which causes a permanent activation of the MKL1/SRF target gene expression (Hampl et al. 2013). A microarray of shDLC1 HepG2 cells performed by our group revealed, among others, TSPAN5 as a novel DLC1 loss upregulated gene target. Based on this, the data in this thesis show that TSPAN5 is also an MKL1-dependent target gene and its overexpression promotes tumorigenic properties such as proliferation, migration and invasion (Figure 60, left panel).

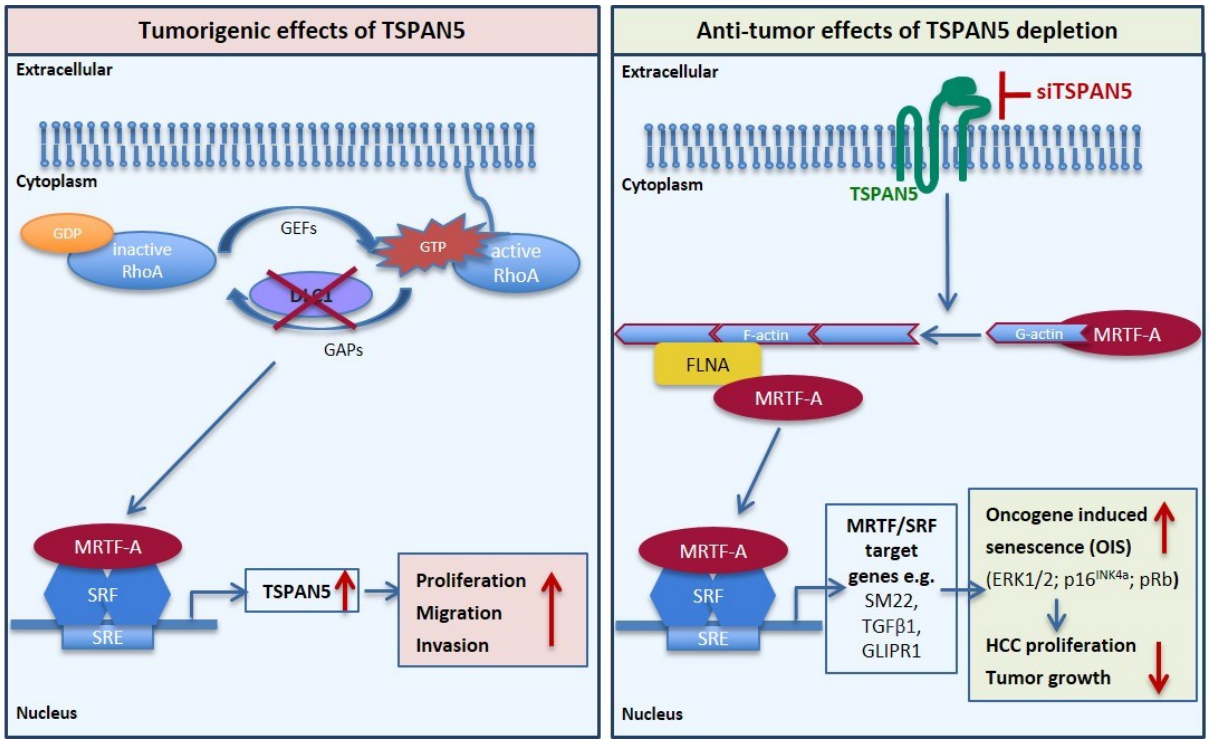

Figure 60: Model for the tumorigenic effects of TSPAN5 and the anti-tumorigenic effects of TSPAN5 depletion. DLC1 loss leads to increased TSPAN5 expression via MRTF-A transcriptional activation (left panel). Therapeutic knockdown of TSPAN5 results in OIS-induced inhibition of HCC growth via decreased actin polymerization and reduced MRTF/SRF target gene expression (right panel).

In summary, all these results reveal that TSPAN5 silencing via RNA interference inhibits the polymerization of G-actin to filamentous F-actin and thus prevents complex formation of FLNA and MKL1. Consequently, the accumulation of the transcriptional coactivator MKL1 with SRF and thus the activation of the transcription factor SRF and the expression of MKL1/SRF target genes is prevented. As a result, TSPAN5 knockdown ultimately enforces a strong arrest of proliferation, migration and invasion by induction of OIS. (Figure 60, right panel). These findings can be confirmed *in vitro*, *on ovo* by CAM assay and *in vivo* by xenograft model and highlight TSPAN5 as a new promising target for personalized treatment of DLC1 deficient HCCs which occurs in 50% of all liver cancers (Xue et al. 2008).

7.6 TSPAN5 overexpression in human HCC and possible therapeutical approaches

7.6.1 TSPAN5 overexpression in human HCC tissue samples

The preceding data show the important role of TSPAN5 overexpression due to DLC1 loss in the development and growth of HCC *in vitro* and *in vivo*. In a further step, it was of great interest to find out whether the fact of TSPAN5 overexpression also applies to human patients with HCC. This was investigated by processing tissue samples taken from patients with HCC and a healthy control group. It was clearly demonstrated that there is a strongly increased TSPAN5 expression in the HCC tissue samples. In our study, there is on average a 2.5-fold increase, but if we look at the 6 of the 11 cases with an extreme TSPAN5 overexpression individually, a 10-fold increase is recognizable. This shows that in some patients there is a strong individual overexpression of TSPAN5, which should be taken into account in therapy planning and also opens up opportunities for particularly effective personalized medicine. Consistent with our results, recent analyses of the Oncomine public database showed that TSPAN5 is highly expressed not only in liver but also in colon cancer (Qi et al. 2020). It is likely that TSPAN5 overexpression is also associated with the loss of the tumor suppressor DLC1 in human tissue samples, which is a characteristic of many HCC diseases and of colon cancers (Wang et al. 2020; Wu et al. 2009; Xue et al. 2008; Zender et al. 2006). However, this remains to be proven in further studies in order to ultimately translate the performed microarray with DLC1 knockdown cells and the resulting TSPAN5 overexpression from bench to bedside.

Summarizing the results, the proposed model of DLC1 dependent TSPAN5 overexpression reveals several novel options for the pharmacological treatment of DLC1 deficient HCC.

7.6.2 Potential therapeutical approaches to target TSPAN5 overexpression in HCC

7.6.2.1 Targeting the signaling pathways affecting TSPAN5 expression

Besides the possibility to address TSPAN5 itself, there is on the one hand the possibility of targeting the signaling pathway that leads to TSPAN5 expression. Owing the loss of DLC1, RhoA is permanently active and leads to increased TSPAN5 expression via the RhoA/actin/MKL1 signaling pathway (Hampl et al. 2013; Miralles et al. 2003; Muehlich et al. 2012). By attacking

the individual signaling pathway intermediates, as shown by our *in vitro* experiments, TSPAN5 protein levels can be significantly reduced. In this regard, inhibition of polymerization of G-actin to filamentous F-actin by Latrunculin B (LatB) and inhibition of Rho associated protein kinase (Rock) by Y-27632 reduced TSPAN5 levels (Coué et al. 1987; Itoh et al. 1999; Uehata et al. 1997; Yarmola et al. 2000). Compounds such as LatB, which target actin filaments in cells, are being tested in various studies, in some cases already in clinical trials Phase 1, with regard to different applications for use in humans (Rasmussen et al. 2014). The agent CK-636, which acts as an actin related protein inhibitor, is also being investigated in preclinical studies for potential therapeutic applications in humans (drug repurposing hub 2021). For instance, Weeks and colleagues have found that inhibition of actin-related protein (ARP) 2/3 by CR-636 inhibits actin polymerization and thus cell migration of prostate cancer cells (Weeks et al. 2016). While no Rock inhibitors are currently in use for patient treatment in the area of cancer therapy, the Rock inhibitor Fasudil is clinically approved for the treatment of non-traumatic subarachnoid hemorrhage, but also shows positive effects in other neurological diseases such as Alzheimer's disease or amyotrophic lateral sclerosis (ALS) (EMA 2021; Feng et al. 2016; Hamano et al. 2020; Nizamudeen et al. 2018; Vennin et al. 2020). However, in various *in vitro* studies, both Y-27632 and Fasudil show tumor inhibitory effects, such as reduced proliferation, migration or invasion ability of ovarian, lung, colon and breast cancer, as well as HCC cell lines (Jeong et al. 2019; Liu et al. 2009; Mikuriya et al. 2015; Ogata et al. 2009; Peng et al. 2012; Toledo et al. 2012; Zhu et al. 2011). Another rock inhibitor is Netarsudil, which is used in clinical patients with glaucoma or ocular hypertension, but not in cancer patients (Lee et al. 2019). Even blockade of the transient receptor potential cation channel TRPM7 by NS8593, which affects RhoA activity, strongly decreased TSPAN5 expression (Voringer et al. 2020). Inhibition of TRPM7, on the one hand, stops the channel mediated Mg^{2+} influx, on the other hand, inhibition of the TRPM7 kinase domain prevents the phosphorylation and activation of RhoA. Inhibition of RhoA subsequently prevents actin polymerization, MKL1-FLNA complexation and finally nuclear translocation of MKL1 and thus ultimately MKL1/SRF target gene expression (Voringer et al. 2020). Consequently, the expression of the proliferation-promoting TSPAN5, which is MKL1-dependent as shown in this thesis, is also diminished. In this regard, our findings show that targeted intervention in the RhoA signaling pathway can reduce tumor-promoting overexpressed TSPAN5 levels.

On the other hand, there is also the possibility to therapeutically target and regulate the MAPK cascade, which is influenced by TSPAN5 overexpression. Precisely because this signaling pathway is very often involved in HCC formation and progression, for example through upregulated corresponding genes such as Mek or ERK or mutations such as K-Ras or H-Ras, which permanently activates the small GTPase Ras, cancer research is trying to regulate this signaling pathway medicamentous (Asati et al. 2016; Liu et al. 2006; Wang et al. 2016e; Zuo et al. 2012). When considering the MAPK signaling pathway, it is important to note that it is this oncogenic H-Ras itself, as well as individual oncogenic variants of the Ras signaling cascade such as Raf, Mek, or Braf, that trigger precisely the desired OIS response (Lin et al. 1998; Michaloglou et al. 2005; Serrano et al. 1997; Zhu et al. 1998). Consistent with our assumption on TSPAN5 loss and senescence induction, Hampl and colleagues exhibited that loss of MKL1 induces a Ras mediated OIS response (Hampl et al. 2013). Further, Hermanns and colleagues also demonstrated the strong influence of Ras activation on OIS induction and the resulting proliferation arrest. They revealed that Myoferlin (MYOF) functions not only as an MKL1 target gene, but also as a negative regulator of EGFR in *in vitro* as well as *in vivo* experiments. EGFR becomes increasingly phosphorylated upon MKL1 or MYOF depletion, which activates the Ras/Raf/Mek/ERK signaling pathway. However, this activation does not result in enhanced tumor progression, but via Ras as a trigger to an OIS response that effectively inhibits tumorigenic properties such as HCC cell proliferation (Hermanns et al. 2017). Thus, with the development of specific kinase inhibitors, the tumorigenic effect of the oncogenic mutated kinases could be inhibited, while at the same time the trigger of an endogenous OIS response, which is supposed to be initiated by TSPAN5 depletion, is suppressed. These two potential aspects of kinase inhibitors should be considered and taken into account in their development and human application.

Nevertheless, is the development of selective inhibitors of the various kinases one promising approach in tumor therapy development. For example, Sorafenib is one of the first kinase inhibitors approved for use in HCC and suppresses Raf-1 (Llovet et al. 2008). Sorafenib has been reported to inhibit HCC cell proliferation, tumor growth and also angiogenesis due to impaired Ras/Raf/Mek/ERK and to prolong survival of patients with advanced HCC, albeit by only about three months compared to the placebo group (Gedaly et al. 2010; Lee et al. 2015; Liu et al. 2006; Llovet et al. 2008). In addition to Sorafenib, newer approved kinase inhibitors

such as Lenvatinib, Cabozantinib and Regorafenib are also available, although only Lenvatinib was shown to be non-inferior to Sorafenib after treatment failure of Sorafenib (Al-Salama et al. 2019; Ettrich and Seufferlein 2018; Faivre et al. 2020; Personeni et al. 2019). However, in some cases of HCC therapy with sorafenib or other kinase inhibitors, drug resistance develops after a certain time (Zhu et al. 2017). Future studies should investigate whether the OIS response, which is triggered by the oncogenic kinases, is lost by the use of kinase inhibitors and thus supports possible resistance symptoms. The development of new kinase inhibitors, e.g., targeting the MAPK pathway and, in the best case, do not affect endogenous OIS response, should be pursued to further improve the treatment of HCC.

7.6.2.2 HCC therapy by targeting TSPAN5 at the mRNA or protein level

The most obvious approach and in line with personalized medicine is to suppress TSPAN5 itself. One possibility is to silence TSPAN5 at the RNA level by means of RNA interference, as was already tested in the xenograft. This, of course, would require optimization of the delivery concentration, further improvement of the delivery system for human and target-specific effects and consideration or exclusion of potential side effects. Nevertheless, individual drugs whose effect is based on the use of RNA interference by means of siRNA are already approved and are on the market. Patisiran, for example, is a siRNA encapsulated in a lipid nanoparticle specifically designed for uptake by hepatocytes, where it suppresses the synthesis of transthyretin for the treatment of hereditary transthyretin amyloidosis or initial stages of polyneuropathy (Adams et al. 2018; Hoy 2018). Another example is Givosiran, which suppresses the synthesis of hepatic δ-aminolevulinic acid synthase 1 (ALAS1) by RNA silencing. Thus, Givosiran improves acute attacks and chronic symptoms of acute hepatic porphyria by counteracting upregulation of ALAS1 with resultant accumulation of δ-aminolevulinic acid (ALA) (Balwani et al. 2020; Scott 2020). Lumasiran also has its RNA interfering effect in the liver region. Here it reduces oxalate overproduction in patients with the rare genetic disease primary hyperoxaluria type 1 (PH1) by targeting glycolate oxidase. By inhibiting oxalate overexpression, negative consequences such as kidney stones, nephrocalcinosis, kidney failure and systemic oxalosis are alleviated (Garrelfs et al. 2021; Scott and Keam 2021). Inclisiran was developed for the treatment of heterozygous familial hypercholesterolemia and

inhibits hepatic synthesis of the proprotein convertase subtilisin-kexin type 9 (PCSK9) by RNA silencing. This decreases the elevated level of low-density lipoprotein (LDL) with the aim of reducing the enormously increased risk of atherosclerotic cardiovascular disease (Raal et al. 2020; Ray et al. 2020). All siRNA therapeutics listed in the previous text and approved in Germany have the pharmacokinetic goal of being taken up by hepatocytes. By coupling siRNA with three sugar residues (triantennary N-acetylgalactosamine), a specific binding to the asialoglycoprotein receptor is achieved, which is almost exclusively expressed on hepatocytes. This results in targeted uptake into the cytoplasm of hepatocytes and, in animal experiments, a primary distribution into the liver (Bissell et al. 2017; Raal et al. 2020; Ray et al. 2020; Scott 2020). For example, such or similar coupling could also allow targeted uptake of therapeutic TSPAN5 siRNA by hepatocytes to minimize adverse systemic effects.

Another possibility to directly target the TSPAN5 protein is by monoclonal antibodies (mAbs), which are already more widespread and established compared to siRNA therapy. Meanwhile, monoclonal antibody therapy is one of the most important pillars of personalized medicine and one of the most effective therapeutic regimens against cancer. For TSPAN CD151, which is frequently overexpressed in cancer cells and functionally associated with cancer metastasis, anti-CD151 mAbs were shown to have growth, migration and metastasis inhibitory function in various CAM and xenograft cancer models (Haeuw et al. 2011; Zijlstra et al. 2008). The generated data suggest, that CD151 is an innovative target in oncology whose inhibition by monoclonal antibodies could be successful in several cancer stages (Haeuw et al. 2011; Zijlstra et al. 2008). Analogously, overexpression of TSPAN8 also plays a driving role in the progression and metastasis of multiple types of cancer (Anami et al. 2016; Fang et al. 2016; Lin et al. 2019; Park et al. 2016; Zhu et al. 2019). Heo and Lee's experiments with murine and human TSPAN8 antibodies have provided evidence that antibody-based targeting of TSPAN8 is an effective strategy to suppress tumor progression and metastasis (Heo and Lee 2020). Promising initial *in vivo* results are also available for TSPAN CD9 and CD63, which are determining proteins of cancer-derived extracellular vesicles (EV) and thus contribute to breast cancer metastasis (Nishida-Aoki et al. 2017). Accordingly, after treatment with appropriate anti-CD9 or anti-CD63 antibodies, metastasis to lung, lymph nodes and thoracic cavity was significantly reduced, although no obvious effect on primary xenograft tumor growth was observed

(Nishida-Aoki et al. 2017). In addition, xenografts with gastric cancer cells and anti-CD9 antibody treatment show inhibited tumor progression via anti-proliferative and anti-angiogenic effects (Nakamoto et al. 2009). By generating a specific and high affinity antibody against TSPAN5, similar to what Saint-Pol and colleagues have done to study the role of TSPAN5 in more detail, there is a promising chance to develop new therapeutic options for personalized medicine targeting the overexpression of TSPAN5 in DLC1 deficient HCC and thus inhibiting HCC progression (Saint-Pol et al. 2017).

7.6.3 TSPAN5 as a diagnostic marker for HCC

Another potential area of application opened up by DLC1 absence induced overexpression of TSPAN5 is diagnostics. The prognosis of many types of cancer, especially liver cancer, is very poor due to limited and usually late diagnosis. Therefore, it is also a very important approach to investigate potential targets such as TSPAN5 for their use as diagnostic markers. Since TSPAN5 is overexpressed in DLC1 deficient HCCs and promotes tumor progression, TSPAN5 is a potentially suitable and novel marker to diagnose HCC disease even at earlier stages. Similar findings are suggested by Lin and colleagues for TSPAN8, as they found a significant overexpression of TSPAN8 in nasopharyngeal carcinoma (NPC) patients. This was confirmed in both poorly differentiated and highly metastatic cells, suggesting the tumor marker TSPAN8 as a diagnostic and prognostic factor (Lin et al. 2019). Also, for the genes VCAN and CDH2, which are also overexpressed by DLC1 loss, their use as predictive markers for early HCC diagnosis or early relapse of HCC has already been suggested (Naboulsi et al. 2016; Seo et al. 2008). Furthermore, our hitherto unknown finding that the overexpression of potential diagnostic markers is due to DLC1 loss opens up new possibilities in tumor characterization and personalized medicine.

7.6.4 Long-term HCC therapy using a combination of senescence induction by TSPAN5 depletion and senolytic therapy.

It is generally known that oncogenic induction triggers a senescence response limiting the proliferation of damaged cells and thus preventing tumor development *in vitro* and *in vivo*

(Collado et al. 2007). Since the tumor-suppressive effect of senescent cells is considered to be very effective, it represents a promising alternative to the use of cytotoxic drugs with a number of severe side effects (Cairney et al. 2012). By treatment with TSPAN5 RNA interference we could confirm an induction of OIS as a cause for proliferation arrest and thus a decrease of tumor growth *in vitro* as well as *in vivo*. Therefore, we hypothesize siTSPAN5 therapy as a novel, innovative and promising strategy for treatment of HCC with TSPAN5 overexpression. An important factor identified only in recent years is that senescent cells inhibit their own proliferation and recruit phagocytotic immune cells that promote clearance and tissue renewal (Muñoz-Espín and Serrano 2014). Often, however, this immune cell-mediated clearance of senescent cells is incomplete, so that a tumor relapse can be triggered by some retained cells in senescence. This process limits the long-term anti-tumorigenic effects of such senescence-inducing agents and implies the consideration of a combination therapy with senescence-inducing compounds and subsequent targeted elimination of senescent cells (Galiana et al. 2020). This is exactly the approach to combine senogenic and targeted senolytic therapy, which Galiana and colleagues tested for antitumor activity in a mouse model with aggressive breast cancer cells. By combining a senescence-inducing drug with subsequent senolysis through treatment with the nano-encapsulated senolytic agent Navitoclax, the authors observed a selective elimination of senescent cells, resulting in inhibited tumor growth and reduced metastasis in breast cancers (Galiana et al. 2020). These findings lead us to the consideration that even in the hypothetical treatment of a DLC1 deficient HCC with TSPAN5 RNA interference, an additional combination with senolytics, which subsequently selectively destroy the senescent cells and thus prevent tumor relapse, would be of advantage. In addition, the combination of TSPAN5 depletion with senolytics in HCC should be investigated for such benefits to optimize the growth inhibitory therapeutic approach of TSPAN5 elimination.

Although liver cancer, most represented by HCC, is among the most common cancers in the human population, there are only a limited number of effective therapeutic approaches to treatment. Thus, despite treatment, there is a high likelihood of tumor relapse, resulting in liver cancer being the third highest fatality rate in men after lung and pancreatic cancer (Sung et al. 2021). In the search for more effective treatment approaches, the molecular

heterogeneity of HCCs must be taken into account. Thus, genomic profiling can be used to detect and investigate changes in gene expression, such as overexpression of TSPAN5 upon loss of the tumor suppressor DLC1, and ultimately to develop novel and improved therapeutic approaches. Hence, genomic profiling of HCC allows the provision of an appropriate therapeutic strategy for personalized treatment with optimal medical outcomes. Our study provides mechanistic insights into the fundamental processes of hepatocarcinogenesis after loss of the tumor suppressor DLC1 and the resulting overexpression of TSPAN5. Furthermore, we evaluated a new promising therapeutic approach for the treatment of HCC with DLC1 loss by silencing TSPAN5 expression. Using TSPAN5 RNA interference, we convincingly demonstrated that tumorigenic properties such as proliferation, migration and invasion are reduced by induction of oncogene-induced senescence *in vitro* and *in vivo*. In order to further optimize the therapy with siTSPAN5 nanoparticles, additional *in vivo* studies are required, for example regarding dosage and possible side effects. A future challenge will be to further enhance senescence-inducing therapies, for example by combining them with senolytics, in order to exclude the possibility of tumor recurrence.

In conclusion, the newly identified DLC1 dependent gene target TSPAN5 represents a very promising target in cancer therapy and especially for the personalized treatment of DLC1 deficient HCC patients in order to reduce tumor development and tumor progression by inducing OIS.

8 Abbreviation index

A	adenine
aa	amino acids
ACS	American Cancer Society
ADAM	a disintegrin and metalloproteinase
AFB	aflatoxin B1
AKT	protein kinase B
ALAS1	aminolevulinic acid synthase 1
APS	ammonium persulfate
ARF	alternative reading frame
ATP	adenosine triphosphate
BO	beads only control
bp	base pairs
BSA	bovine serum albumin
C	cytosine
$CaCl_2$	calcium chloride
CAM	chorio-allantoic-membrane
CAV-1	caveolin 1
CD	cluster of differentiation
CDH2	N-Cadherin
cDNA	complementary DNA

CDK	cyclin-dependent kinase
ChIP	chromatin immunoprecipitation
CLDN1	claudin-1
CLL	chronic lymphocytic leukemia
cm	centimeter
CNN1	calponin 1
CO_2	carbon dioxide
CRISPR	clustered regularly interspaced short palindromic repeats
CSC	cancer stem cell
CTGF	connective tissue growth factor
ctrl	control
CXCL10	C-X-C motif chemokine 10
DAPI	4´6-diamidion-2-phenylindole
DEPC	diethyl dicarbonate
DLC1/2/3	deleted in liver cancer 1/2/3
DMEM	Dulbecco's modified eagle medium
DMF	*N,N*-dimethylformamide
DMSO	dimethyl sulfoxide
DNA	deoxyribonucleic acid
dNTP	deoxynucleoside triphosphate
DTT	dithiothreitol
E2F1	E2F transcription factor 1
E-cadherin	epithelial cadherin

E. coli	Escherichia coli
EBS	Ets binding site
ECL	enhanced chemiluminescence
ECM	extracellular matrix
EDTA	ethylenediaminetetraacetic acid
EF1A1	eukaryotic elongation factor 1A1
EGF	epidermal growth factor
EGFR	epidermal growth factor receptor
EMT	epithelial-mesenchymal transition
ERK1/2	extracellular signal-related kinase 1/2
Ets	erythroblast transformation specific
EV	empty vector
F-actin	filamentous actin
FAT	focal adhesion targeting
FBS	fetal bovine serum
FDA	Food and Drug Administration
FLNA	filamin A
Fw	forward
G	guanine
G1 phase	growth 1 phase
G-actin	globular actin
GAP	GTPase activating protein
GDI	guanine nucleotide dissociation inhibitor

GDP	guanosine diphosphate
GEF	guanine nucleotide exchange factor
GFP	green fluorescent protein
GLIPR1	glioma pathogenesis-related protein 1
GTP	guanosine triphosphate
h	hours
H-Ras	harvey rat sarcoma
H_2O	water
H3K9me3	histone H3 methylated on lysine 9
Hb	hemoglobin
HBS	HEPES buffered saline
HBV	hepatitis B virus
HCC	hepatocellular carcinoma
HCl	hydrochloric acid
HCV	hepatitis C virus
HE	hematoxylin - eosin
HEPES	4-(2-hydroxyethyl)-1-piperazineethanesulfonic acid
HER2	human epidermal growth receptor 2
HIST1H2BK	histon cluster 1 H2B family member K
HLF	human lung fibroblasts
HPV	human papillomavirus
HRP	horseradish peroxidase
HSP90	heat shock protein 90

i.p.	intraperitoneal
IEG	immediate early genes
IgG	Immunoglobulin G
IHC	immunohistochemistry
INK4a	Inhibitor of cyclin-dependent kinase 4a
JAK	janus kinase
KCl	potassium chloride
KD	knockdown
kDa	kilo Dalton
KH_2PO_4	potassium dehydrogen phosphatase
KO	knockout
LatB	latrunculin B
LiCl	lithium chloride
LPA	lysophosphatidic acid
LZ	leucine zipper
M	molar
mA	milliampere
mAbs	monoclonal antibodies
MADS-Box	MCM1, agamous, deficiens, SRF-Box
MALDI-TOF	matrix assisted laser desorption ionization - time of flight
MAP	mitogen-activated protein

MAP1B	microtubule-associated protein 1B
MAPK	mitogen-activated protein kinase
mDia	diaphanous-related formin
MEK	mitogen-activated protein kinase kinase
MEM	minimum essential medium
MEP1A	meprin 1A
MET	mesenchymal-epithelial transition
mg	milligram
Mg^{2+}	magnesium cation
Mig6	mitogen-inducible gene 6
min	minute(s)
MKL1	Megakaryoblastic Leukemia 1
MKL2	Megakaryoblastic Leukemia 2
ml	milliliter
mm	millimeter
mM	millimolar
MMP	matrix metalloproteinase
MRTF-A	myocardin-related transcription factor A
MRTF-B	myocardin-related transcription factor B
mTOR	mechanistic target of rapamycin
Myc	myelocytomatosis oncogene
MYOF	myoferlin
n.s.	not significant
Na_2HPO_4	sodium hydrogen phosphate

NaCl	sodium chloride
$NaHCO_3$	sodium hydrogen carbonate
NaOH	sodium hydroxide
NaN_3	sodium azide
NHL	non-Hodgkin lymphoma
nm	nanometer
nM	nanomolar
NP-40	nonoxinol 40
NT	non-tumorous
OIS	oncogene-induced senescence
PAGE	polyacrylamide gel electrophoresis
PBS	phosphate buffered saline
PCR	polymerase chain reaction
PEI	polyethylenimine
pERK1/2	phosphorylated extracellular signal-related kinase 1/2
PFA	paraformaldehyde
pH	potential of hydrogen
PI	protease inhibitor
PI3K	Phosphoinositide 3-kinase
PIPES	piperazine-N,N'-bis(2-ethanesulfonic acid)
PKC	protein kinase C
PLA	proximity ligation assay
PML	promyelocytic leukemia

PMSF	phenylmethylsulfonyl fluoride
PPARγ	peroxisome proliferator-activated receptor γ
pRb	phosphorylated retinoblastoma protein
PVDF	polyvinylidene fluoride
PVT1	plasma cell tumor heterotopic gene 1
Q	glutamine-rich region
qRT-PCR	quantitative real-time polymerase chain reaction
Raf	rapidly accelerated fibrosarcoma
Ras	rat sarcoma
Rb	retinoblastoma protein
RBM15	RNA binding motif protein 15
RhoGAP	Rho-GTPase-activating protein
RNA	ribonucleic acid
RNAi	RNA interference
Rock	rho-associated coiled-coil containing protein kinase
RPEL	Arg-Pro-X-X-Glu-Leu
rpm	rounds per minute
RPMI	Roswell Park Memorial Institute
rRNA	ribosomal RNA
RT	room temperature
RT-PCR	real-time polymerase chain reaction
rv	reverse

S phase	synthesis phase
S1	security level 1
SA-ß-Gal	senescence-associated β-galactosidase
SAHF	senescence-associated heterochromatin foci
SAM	sterile a motif
SAP	SAF-A/B, Acinus and Pias
SD	standard deviation
SDS	sodium dodecyl sulfate
sec(s)	second(s)
SEM	standard error of the mean
SH2	SRC homology 2
shRNA	shorthairpin ribonucleic acid
siRNA	small interfering ribonucleic acid
SLUG	zinc-finger transcription factor SLUG
SM22	smooth muscle protein 22
SMA	smooth muscle actin
SMC	smooth muscle cell
SMIP	small modular immunopharmaceuticals
SMS	senescence-messaging secretome
SNP	single nucleotide polymorphism
SPE	specific pathogen free
SR-B1	scavanger receptor class B member I
SRE	serum response element
SRF	serum response factor
START	steroidogenic acute regulatory-related lipid transfer

STAT	signal transducer and activator of transcription
T	thymine
T	tumorous
TAD	transcription activation domain
TAGLN	smooth muscle protein 22 (synonym for SM22)
TBS	tris-buffered saline
TBS-T	tris-buffered saline with Tween 20
TCF	ternary complex factor
TCF4	T-cell factor 4
TEM	tetraspanin-enriched microdomains
TEMED	N,N,N',N'-tetramethylethylenediamine
TGFß1	transforming growth factor β1
TM	transmembrane
TM4SF5	transmembrane 4 L6 family member 5
TNSFS10	tumor necrosis factor superfamily member 10
Tris	tris(hydroxymethyl)aminomethane
TRPM7	transient receptor potential cation channel 7
TSPAN	tetraspanin
Tween 20	polysorbate 20
U	uracil
UDCA	ursodeoxycholic acid
UICC	Union for International Cancer Control

V	voltage
v/v	volume to volume
VCAN	versican
WHO	world health organization
WNT	Wingless-type
wt	wild type
X-Gal	5-bromo-4-chloro-3-indolyl-β-D-galactopyranoside
ZO-1	Zonula occludens-1
µg	microgram
µl	microliter
µM	micromolar

9 Index of tables

Table 1: Cell lines and their culture medium 47

Table 2: Cell culture media and their supplements 48

Table 3: Transfection reagents 48

Table 4: Plasmid constructs used for transient plasmid transfection 48

Table 5: Human primers for qRT-PCR and their sequences 49

Table 6: Human primers for ChIP qRT-PCR and their sequences 50

Table 7: Human siRNAs and their sequences 51

Table 8: Primary antibodies and their indicated dilution for immunoblotting 52

Table 9: Secondary antibodies and their indicated dilution for immunoblotting 53

Table 10: Antibodies used for RhoA assay 54

Table 11: Antibodies used for pulldown 54

Table 12: Primary antibodies and their dilution for immunofluorescence or proximity ligation assay 54

Table 13: Secondary antibodies and their dilution for immunofluorescence 55

Table 14: Primary and secondary antibodies and their dilution used for immunohistochemistry 55

Table 15: Antibiotics 56

Table 16: Enzymes 56

Table 17: Stimulants and inhibitors with final working concentration 57

Table 18: DNA and protein ladders 57

Table 19: Kits 58

Table 20: Buffers used for agarose gel electrophoresis 58

Table 21: Quantities of corresponding components for the preparation of LB agar and LB medium 59

Table 22: Reagents used for cDNA synthesis and qRT-PCR 59

Table 23: Buffers and their composition used for ChIP assay 60

Table 24: Solutions and buffers used for Duolink® 61

Table 25: Buffers used for RhoA activation assay 62

Table 26: Buffer used for lysis of cells during actin fractionation 63

Table 27: Buffers used for immunoblotting 63

Table 28: Reagents used for detecting blots 64

Table 29: Fixing solution used for immunofluorescence 64

Table 30: Solutions used for invasion assay 65

Table 31: Solution and buffer used for protein isolation 65

Table 32: Buffers and their composition used for SDS-PAGE 66

Table 33: PBS solutions 66

Table 34: Composition of DEPC H_2O 67

Table 35: Compound of running and stacking gels used for SDS-PAGE 67

Table 36: Tris buffers used for SDS-gels 69

Table 37: Bacterial strains 69

Table 38: Chemicals 69

Table 39: Consumables 72

Table 40: Technical devices 73

Table 41: Mixture with reverse transcriptase for cDNA synthesis 82

Table 42: Primer mix for qRT-PCR 83

Table 43: Temperature program used for qRT-PCR 83

Table 44: Selected top 5 genes that were upregulated in performed microarray experiments after DLC1 loss 95

Table 45: Patient characteristics including age, gender, grading, staging, lymphangiosis and hemangiosis carcinomatosa, R-status and tumor size 137

10 Index of figures

Figure 1: Rho GTPases and their function as complexly regulated molecular switches. 15

Figure 2: Dysregulation of RhoA leads to tumor development and progression. 17

Figure 3: The modular structure of DLC protein family. 19

Figure 4: Model of the two different signaling pathways leading to SRF activation. 26

Figure 5: Model of the TCF-dependent SRF activation. 27

Figure 6: Model of MRTF (MKL) regulation and consequent SRF activation. 28

Figure 7: Structure of myocardin family members. 29

Figure 8: The structure of tetraspanin proteins. 34

Figure 9: The involvement of TSPAN CD81 in hepatitis C virus particle uptake. 38

Figure 10: Various factors leading to senescence. 42

Figure 11: Senescence induction by the ARF/p53 and $p16^{INK4a}$/pRb signaling pathways. 43

Figure 12: DLC1 knockdown efficiency and DLC1 dependent target gene expression in HepG2 cells. 96

Figure 13: Protein overexpression of DLC1 dependent target genes in HepG2 cells. 96

Figure 14: DLC1 knockdown efficiency and target gene upregulation upon DLC1 depletion in Hep3B cells. 97

Figure 15: Protein overexpression of DLC1 dependent target genes in HepG2 cells. 98

Figure 16: MKL1/2 and FLNA dependence of newly identified target genes upon DLC1 loss. 98

Figure 17: MKL1 recruitment to the VCAN, TSPAN5 and CDH2 promoters. 99

Figure 18: MKL1 dependence of novel target genes compared with known MKL1 dependent target gene SM22. 101

Figure 19: SRF dependence of novel target genes. 102

Figure 20: Downregulation of TSPAN5 upon LatB and Y-27632 treatment. 103

Figure 21: Upregulation of TSPAN5 protein level upon LPA treatment. 103

Figure 22: TSPAN5 is required for cell proliferation. 105

Figure 23: TSPAN5 depletion provoked growth arrest in HuH6 cells. 105

Figure 24: TSPAN5 depletion provokes growth arrest. 106

Figure 25: Overexpression of the constitutively active MKL1 variant (MKL1N100) attenuates the proliferation arrest. 107

Figure 26: TSPAN5 knockdown via RNA interference provokes a growth arrest of HepG2 DLC1 KD cells. 108

Figure 27: TSPAN5 depletion leads to proliferation arrest in DLC1 positive and negative HepG2 CRISP Cas9 KO cells. 109

Figure 28: TSPAN5 and CDH2 depletion inhibits cell migration assessed by scratch-wound assay. 110

Figure 29: TSPAN5 depletion provokes migration stop in HuH6 cells. 111

Figure 30: Decreased invasion of HuH7 cells upon TSPAN5 depletion. 112

Figure 31: Inhibited spheroid formation upon TSPAN5 depletion. 113

Figure 32: Induction of cellular senescence upon TSPAN5 depletion. 115

Figure 33: Induction of cellular senescence upon TSPAN5 loss. 115

Figure 34: Accumulation of Histone H3 methylated on Lysine 9 upon TSPAN5 depletion. 116

Figure 35: Activation of ERK1/2 by phosphorylation upon TSPAN5 loss. 117

Figure 36: Accumulation of $p16^{INK4a}$ protein expression upon TSPAN5 depletion. 117

Figure 37: Hypophosphorylation of retinoblastoma protein after TSPAN5 depletion. 118

Figure 38: Accumulation of PML nuclear bodies after TSPAN5 depletion. 119

Figure 39: Induction of CXCL10 and TNFSF10 expression upon TSPAN5 depletion. 120

Figure 40: TSPAN5 loss inhibits EMT. 122

Figure 41: Inactivation of RhoA upon TSPAN5 depletion. 123

Figure 42: Decrease in cellular F-actin upon TSPAN5 depletion. 124

Figure 43: Reduced and reorganized actin skeleton upon TSPAN5 knockdown. 125

Figure 44: Abrogation of MKL1-FLNA interactions upon TSPAN5 knockdown. 126

Figure 45: Downregulation of MKL1/SRF target genes upon TSPAN5 depletion. 127

Figure 46: Downregulation of SM22 upon TSPAN5 knockdown. 128

Figure 47: TSPAN5 reconstitution abolishes downregulation of MKL1 dependent target genes induced by prior TSPAN5 loss. 129

Figure 48: Anti-tumor effects of TSPAN5 knockdown in CAM assay. 131

Figure 49: Decreased Ki67 mRNA level upon TSPAN5 depletion on ovo. 132

Figure 50: Histological changes after TSPAN5 silencing in CAM model. 133

Figure 51: Increased E-Cadherin expression after TSPAN5 loss in HepG2 clone 5 CAM-tumors. 134

Figure 52: Decreased mRNA expression of MKL1 target genes upon TSPAN5 depletion *in vivo*. 135

Figure 53.: Decreased protein level of MKL1 target gene GLIPR1 after TSPAN5 loss *in vivo*. 135

Figure 54: Positive senescence markers after TSPAN5 depletion *in vivo*. 136

Figure 55: TSPAN5 overexpression in human HCC tissue samples. 138

Figure 56: TSPAN5 depletion reduces tumor growth in mice xenograft *in vivo*. 139

Figure 57: TSPAN5 knockdown inhibits proliferate *in vivo*. 140

Figure 58: TSPAN5 depletion reduces MKL1 target genes *in vivo*. 141

Figure 59: Positive senescence markers upon TSPAN5 depletion in HCC xenograft *in vivo*. 142

Figure 60: Model for the tumorigenic effects of TSPAN5 and the anti-tumorigenic effects of TSPAN5 depletion. 168

11 References

ACS (2021): Liver Cancer Survival Rates | Cancer of the Liver Survival Rates. Available online at https://www.cancer.org/cancer/liver-cancer/detection-diagnosis-staging/survival-rates.html, updated on 8/9/2021, checked on 8/9/2021.

Adams, David; Gonzalez-Duarte, Alejandra; O'Riordan, William D.; Yang, Chih-Chao; Ueda, Mitsuharu; Kristen, Arnt V. et al. (2018): Patisiran, an RNAi Therapeutic, for Hereditary Transthyretin Amyloidosis. In *The New England journal of medicine* 379 (1), pp. 11–21. DOI: 10.1056/NEJMoa1716153.

Adams, Peter D. (2007): Remodeling of chromatin structure in senescent cells and its potential impact on tumor suppression and aging. In *Gene* 397 (1-2), pp. 84–93. DOI: 10.1016/j.gene.2007.04.020.

Adamson, P.; Etienne, S.; Couraud, P. O.; Calder, V.; Greenwood, J. (1999): Lymphocyte migration through brain endothelial cell monolayers involves signaling through endothelial ICAM-1 via a rho-dependent pathway. In *Journal of immunology (Baltimore, Md. : 1950)* 162 (5), pp. 2964–2973.

Aigner, Achim (2006): Delivery systems for the direct application of siRNAs to induce RNA interference (RNAi) in vivo. In *Journal of Biomedicine and Biotechnology* 2006 (4), p. 71659. DOI: 10.1155/jbb/2006/71659.

Alberti, Siegfried; Krause, Sven M.; Kretz, Oliver; Philippar, Ulrike; Lemberger, Thomas; Casanova, Emilio et al. (2005): Neuronal migration in the murine rostral migratory stream requires serum response factor. In *Proceedings of the National Academy of Sciences of the United States of America* 102 (17), pp. 6148–6153. DOI: 10.1073/pnas.0501191102.

Alcorta, D. A.; Xiong, Y.; Phelps, D.; Hannon, G.; Beach, D.; Barrett, J. C. (1996): Involvement of the cyclin-dependent kinase inhibitor p16 (INK4a) in replicative senescence of normal human fibroblasts. In *Proceedings of the National Academy of Sciences of the United States of America* 93 (24), pp. 13742–13747. DOI: 10.1073/pnas.93.24.13742.

Alpy, Fabien; Legueux, François; Bianchetti, Laurent; Tomasetto, Catherine (2009): START domain-containing proteins: a review of their role in lipid transport and exchange. In *Medecine sciences : M/S* 25 (2), pp. 181–191. DOI: 10.1051/medsci/2009252181.

Al-Salama, Zaina T.; Syed, Yahiya Y.; Scott, Lesley J. (2019): Lenvatinib: A Review in Hepatocellular Carcinoma. In *Drugs* 79 (6), pp. 665–674. DOI: 10.1007/s40265-019-01116-x.

Anami, Katsuhiro; Oue, Naohide; Noguchi, Tsuyoshi; Sakamoto, Naoya; Sentani, Kazuhiro; Hayashi, Tetsutaro et al. (2016): TSPAN8, identified by Escherichia coli ampicillin secretion trap, is associated with cell growth and invasion in gastric cancer. In *Gastric cancer : official journal of the International Gastric Cancer Association and the Japanese Gastric Cancer Association* 19 (2), pp. 370–380. DOI: 10.1007/s10120-015-0478-z.

Angelini, Pier Davide; Zacarias Fluck, Mariano F.; Pedersen, Kim; Parra-Palau, Josep Lluís; Guiu, Marc; Bernadó Morales, Cristina et al. (2013): Constitutive HER2 signaling promotes breast cancer metastasis through cellular senescence. In *Cancer research* 73 (1), pp. 450–458. DOI: 10.1158/0008-5472.CAN-12-2301.

Angstenberger, Meike; Wegener, Jörg W.; Pichler, Bernd J.; Judenhofer, Martin S.; Feil, Susanne; Alberti, Siegfried et al. (2007): Severe intestinal obstruction on induced smooth muscle-specific ablation of the transcription factor SRF in adult mice. In *Gastroenterology* 133 (6), pp. 1948–1959. DOI: 10.1053/j.gastro.2007.08.078.

Aravind, L.; Koonin, E. V. (2000): SAP - a putative DNA-binding motif involved in chromosomal organization. In *Trends in biochemical sciences* 25 (3), pp. 112–114. DOI: 10.1016/s0968-0004(99)01537-6.

Arsenian, S.; Weinhold, B.; Oelgeschläger, M.; Rüther, U.; Nordheim, A. (1998): Serum response factor is essential for mesoderm formation during mouse embryogenesis. In *The EMBO journal* 17 (21), pp. 6289–6299. DOI: 10.1093/emboj/17.21.6289.

Asati, Vivek; Mahapatra, Debarshi Kar; Bharti, Sanjay Kumar (2016): PI3K/Akt/mTOR and Ras/Raf/MEK/ERK signaling pathways inhibitors as anticancer agents: Structural and pharmacological perspectives. In *European journal of medicinal chemistry* 109, pp. 314–341. DOI: 10.1016/j.ejmech.2016.01.012.

Baarlink, Christian; Wang, Haicui; Grosse, Robert (2013): Nuclear actin network assembly by formins regulates the SRF coactivator MAL. In *Science (New York, N.Y.)* 340 (6134), pp. 864–867. DOI: 10.1126/science.1235038.

Balwani, Manisha; Sardh, Eliane; Ventura, Paolo; Peiró, Paula Aguilera; Rees, David C.; Stölzel, Ulrich et al. (2020): Phase 3 Trial of RNAi Therapeutic Givosiran for Acute Intermittent Porphyria. In *The New England journal of medicine* 382 (24), pp. 2289–2301. DOI: 10.1056/NEJMoa1913147.

Bandyopadhyay, Sucharita; Zhan, Rui; Chaudhuri, Asok; Watabe, Misako; Pai, Sudha K.; Hirota, Shigeru et al. (2006): Interaction of KAI1 on tumor cells with DARC on vascular endothelium leads to metastasis suppression. In *Nature medicine* 12 (8), pp. 933–938. DOI: 10.1038/nm1444.

Barrallo-Gimeno, Alejandro; Nieto, M. Angela (2005): The Snail genes as inducers of cell movement and survival: implications in development and cancer. In *Development (Cambridge, England)* 132 (14), pp. 3151–3161. DOI: 10.1242/dev.01907.

Bennett, Dorothy C. (2003): Human melanocyte senescence and melanoma susceptibility genes. In *Oncogene* 22 (20), pp. 3063–3069. DOI: 10.1038/sj.onc.1206446.

Berditchevski, F. (2001): Complexes of tetraspanins with integrins: more than meets the eye. In *Journal of cell science* 114 (Pt 23), pp. 4143–4151.

Berditchevski, F.; Odintsova, E. (1999): Characterization of integrin-tetraspanin adhesion complexes: role of tetraspanins in integrin signaling. In *The Journal of cell biology* 146 (2), pp. 477–492. DOI: 10.1083/jcb.146.2.477.

Bersini, Simone; Lytle, Nikki K.; Schulte, Roberta; Huang, Ling; Wahl, Geoffrey M.; Hetzer, Martin W. (2020): Nup93 regulates breast tumor growth by modulating cell proliferation and actin cytoskeleton remodeling. In *Life science alliance* 3 (1). DOI: 10.26508/lsa.201900623.

Berthier-Vergnes, O.; Kharbili, M. El; La Fouchardière, A. de; Pointecouteau, T.; Verrando, P.; Wierinckx, A. et al. (2011): Gene expression profiles of human melanoma cells with different invasive potential reveal TSPAN8 as a novel mediator of invasion. In *British journal of cancer* 104 (1), pp. 155–165. DOI: 10.1038/sj.bjc.6605994.

Bian, Hejiao; Lin, Jean Z.; Li, Chendi; Farmer, Stephen R. (2016): Myocardin-related transcription factor A (MRTFA) regulates the fate of bone marrow mesenchymal stem cells and its absence in mice leads to osteopenia. In *Molecular metabolism* 5 (10), pp. 970–979. DOI: 10.1016/j.molmet.2016.08.012.

Bischof, Oliver; Kirsh, Olivier; Pearson, Mark; Itahana, Koji; Pelicci, Pier Giuseppe; Dejean, Anne (2002): Deconstructing PML-induced premature senescence. In *The EMBO journal* 21 (13), pp. 3358–3369. DOI: 10.1093/emboj/cdf341.

Bissell, D. Montgomery; Anderson, Karl E.; Bonkovsky, Herbert L. (2017): Porphyria. In *The New England journal of medicine* 377 (9), pp. 862–872. DOI: 10.1056/NEJMra1608634.

Boismenu, R.; Rhein, M.; Fischer, W. H.; Havran, W. L. (1996): A role for CD81 in early T cell development. In *Science (New York, N.Y.)* 271 (5246), pp. 198–200. DOI: 10.1126/science.271.5246.198.

Borchardt, Hannes; Ewe, Alexander; Morawski, Markus; Weirauch, Ulrike; Aigner, Achim (2021): miR24–3p activity after delivery into pancreatic carcinoma cell lines exerts profound tumor-inhibitory effects through distinct pathways of apoptosis and autophagy induction. In *Cancer letters* 503, pp. 174–184. DOI: 10.1016/j.canlet.2021.01.018.

Borchardt, Hannes; Schulz, Alexander; Datta, Kaustubh; Muders, Michael H.; Aigner, Achim (2019): Silencing of Neuropilins and GIPC1 in pancreatic ductal adenocarcinoma exerts multiple cellular and molecular antitumor effects. In *Sci Rep* 9 (1), p. 15471. DOI: 10.1038/s41598-019-51881-8.

Bos, Johannes L.; Rehmann, Holger; Wittinghofer, Alfred (2007): GEFs and GAPs: critical elements in the control of small G proteins. In *Cell* 129 (5), pp. 865–877. DOI: 10.1016/j.cell.2007.05.018.

Boucheix, C.; Perrot, J. Y.; Mirshahi, M.; Giannoni, F.; Billard, M.; Bernadou, A.; Rosenfeld, C. (1985): A new set of monoclonal antibodies against acute lymphoblastic leukemia. In *Leukemia research* 9 (5), pp. 597–604. DOI: 10.1016/0145-2126(85)90139-0.

Braig, Melanie; Lee, Soyoung; Loddenkemper, Christoph; Rudolph, Cornelia; Peters, Antoine H F M; Schlegelberger, Brigitte et al. (2005): Oncogene-induced senescence as an initial barrier in lymphoma development. In *Nature* 436 (7051), pp. 660–665. DOI: 10.1038/nature03841.

Braumüller, Heidi; Wieder, Thomas; Brenner, Ellen; Aßmann, Sonja; Hahn, Matthias; Alkhaled, Mohammed et al. (2013): T-helper-1-cell cytokines drive cancer into senescence. In *Nature* 494 (7437), pp. 361–365. DOI: 10.1038/nature11824.

Bray, Freddie; Ferlay, Jacques; Soerjomataram, Isabelle; Siegel, Rebecca L.; Torre, Lindsey A.; Jemal, Ahmedin (2018): Global cancer statistics 2018: GLOBOCAN estimates of incidence and mortality worldwide for 36 cancers in 185 countries. In *CA: a cancer journal for clinicians* 68 (6), pp. 394–424. DOI: 10.3322/caac.21492.

Bray, Freddie; Laversanne, Mathieu; Weiderpass, Elisabete; Soerjomataram, Isabelle (2021): The ever-increasing importance of cancer as a leading cause of premature death worldwide. In *Cancer* 127 (16), pp. 3029–3030. DOI: 10.1002/cncr.33587.

Brothman, A. R. (1997): Cytogenetic studies in prostate cancer: are we making progress? In *Cancer genetics and cytogenetics* 95 (1), pp. 116–121. DOI: 10.1016/s0165-4608(96)00302-0.

Brown, J. P.; Wei, W.; Sedivy, J. M. (1997): Bypass of senescence after disruption of p21CIP1/WAF1 gene in normal diploid human fibroblasts. In *Science (New York, N.Y.)* 277 (5327), pp. 831–834. DOI: 10.1126/science.277.5327.831.

Burkhart, Deborah L.; Sage, Julien (2008): Cellular mechanisms of tumour suppression by the retinoblastoma gene. In *Nature reviews. Cancer* 8 (9), pp. 671–682. DOI: 10.1038/nrc2399.

Cairney, Claire J.; Bilsland, Alan E.; Evans, T. R. Jeffry; Roffey, Jon; Bennett, Dorothy C.; Narita, Masashi et al. (2012): Cancer cell senescence: a new frontier in drug development. In *Drug discovery today* 17 (5-6), pp. 269–276. DOI: 10.1016/j.drudis.2012.01.019.

Campisi, Judith (2005): Senescent cells, tumor suppression, and organismal aging: good citizens, bad neighbors. In *Cell* 120 (4), pp. 513–522. DOI: 10.1016/j.cell.2005.02.003.

Campisi, Judith; Di d'Adda Fagagna, Fabrizio (2007): Cellular senescence: when bad things happen to good cells. In *Nature Reviews Molecular Cell Biology* 8 (9), pp. 729–740. DOI: 10.1038/nrm2233.

Cao, Zhan-Qi; Wang, Zhi; Leng, Ping (2019): Aberrant N-cadherin expression in cancer. In *Biomedicine & pharmacotherapy = Biomedecine & pharmacotherapie* 118, p. 109320. DOI: 10.1016/j.biopha.2019.109320.

Castelli, Germana; Pelosi, Elvira; Testa, Ugo (2017): Liver Cancer: Molecular Characterization, Clonal Evolution and Cancer Stem Cells. In *Cancers* 9 (9). DOI: 10.3390/cancers9090127.

Cattaruzza, Sabrina; Schiappacassi, Monica; Ljungberg-Rose, Asa; Spessotto, Paola; Perissinotto, Daniela; Mörgelin, Matthias et al. (2002): Distribution of PG-M/versican variants in human tissues and de novo expression of isoform V3 upon endothelial cell activation, migration, and neoangiogenesis in vitro. In *The Journal of biological chemistry* 277 (49), pp. 47626–47635. DOI: 10.1074/jbc.M206521200.

Cen, Bo; Selvaraj, Ahalya; Burgess, Rebecca C.; Hitzler, Johann K.; Ma, Zhigui; Morris, Stephan W.; Prywes, Ron (2003): Megakaryoblastic leukemia 1, a potent transcriptional coactivator for serum response factor (SRF), is required for serum induction of SRF target genes. In *Molecular and cellular biology* 23 (18), pp. 6597–6608. DOI: 10.1128/mcb.23.18.6597-6608.2003.

Charrin, Stéphanie; Le Naour, François; Silvie, Olivier; Milhiet, Pierre-Emmanuel; Boucheix, Claude; Rubinstein, Eric (2009): Lateral organization of membrane proteins: tetraspanins spin their web. In *The Biochemical journal* 420 (2), pp. 133–154. DOI: 10.1042/BJ20082422.

Chellappan, S. P.; Hiebert, S.; Mudryj, M.; Horowitz, J. M.; Nevins, J. R. (1991): The E2F transcription factor is a cellular target for the RB protein. In *Cell* 65 (6), pp. 1053–1061. DOI: 10.1016/0092-8674(91)90557-f.

Chen, Shuli; Sun, Yingxia; Jin, Zhigao; Jing, Xianghong (2011): Functional and biochemical studies of CD9 in fibrosarcoma cell line. In *Molecular and cellular biochemistry* 350 (1-2), pp. 89–99. DOI: 10.1007/s11010-010-0685-1.

Chen, Zhenbang; Trotman, Lloyd C.; Shaffer, David; Lin, Hui-Kuan; Dotan, Zohar A.; Niki, Masaru et al. (2005): Crucial role of p53-dependent cellular senescence in suppression of Pten-deficient tumorigenesis. In *Nature* 436 (7051), pp. 725–730. DOI: 10.1038/nature03918.

Cheng, Ee-Chun; Luo, Qing; Bruscia, Emanuela M.; Renda, Matthew J.; Troy, James A.; Massaro, Stephanie A. et al. (2009): Role for MKL1 in megakaryocytic maturation. In *Blood* 113 (12), pp. 2826–2834. DOI: 10.1182/blood-2008-09-180596.

Chi, S. W.; Ayed, A.; Arrowsmith, C. H. (1999): Solution structure of a conserved C-terminal domain of p73 with structural homology to the SAM domain. In *The EMBO journal* 18 (16), pp. 4438–4445. DOI: 10.1093/emboj/18.16.4438.

Chiba, Tetsuhiro; Zheng, Yun-Wen; Kita, Kaoru; Yokosuka, Osamu; Saisho, Hiromitsu; Onodera, Masafumi et al. (2007): Enhanced self-renewal capability in hepatic stem/progenitor cells drives cancer initiation. In *Gastroenterology* 133 (3), pp. 937–950. DOI: 10.1053/j.gastro.2007.06.016.

Chicas, Agustin; Wang, Xiaowo; Zhang, Chaolin; McCurrach, Mila; Zhao, Zhen; Mert, Ozlem et al. (2010): Dissecting the unique role of the retinoblastoma tumor suppressor during cellular senescence. In *Cancer cell* 17 (4), pp. 376–387. DOI: 10.1016/j.ccr.2010.01.023.

Ching, Yick-Pang; Wong, Chun-Ming; Chan, Shing-Fai; Leung, Thomas Ho-Yin; Ng, David Chi-Heng; Jin, Dong-Yan; Ng, Irene Oi-lin (2003): Deleted in liver cancer (DLC) 2 encodes a RhoGAP protein with growth suppressor function and is underexpressed in hepatocellular carcinoma. In *The Journal of biological chemistry* 278 (12), pp. 10824–10830. DOI: 10.1074/jbc.M208310200.

Cho, Hee Jun; Kim, Jong-Tae; Baek, Kyoung Eun; Kim, Bo-Yeon; Lee, Hee Gu (2019): Regulation of Rho GTPases by RhoGDIs in Human Cancers. In *Cells* 8 (9). DOI: 10.3390/cells8091037.

Chung, Goh Eun; Yoon, Jung-Hwan; Lee, Jeong-Hoon; Kim, Hwi Young; Myung, Sun Jung; Yu, Su Jong et al. (2011): Ursodeoxycholic acid-induced inhibition of DLC1 protein degradation leads to suppression of hepatocellular carcinoma cell growth. In *Oncology reports* 25 (6), pp. 1739–1746. DOI: 10.3892/or.2011.1239.

Collado, Manuel; Blasco, Maria A.; Serrano, Manuel (2007): Cellular senescence in cancer and aging. In *Cell* 130 (2), pp. 223–233. DOI: 10.1016/j.cell.2007.07.003.

Collado, Manuel; Gil, Jesús; Efeyan, Alejo; Guerra, Carmen; Schuhmacher, Alberto J.; Barradas, Marta et al. (2005): Tumour biology: senescence in premalignant tumours. In *Nature* 436 (7051), p. 642. DOI: 10.1038/436642a.

Collado, Manuel; Serrano, Manuel (2006): The power and the promise of oncogene-induced senescence markers. In *Nature reviews. Cancer* 6 (6), pp. 472–476. DOI: 10.1038/nrc1884.

Copeland, John W.; Treisman, Richard (2002): The diaphanous-related formin mDia1 controls serum response factor activity through its effects on actin polymerization. In *Molecular biology of the cell* 13 (11), pp. 4088–4099. DOI: 10.1091/mbc.02-06-0092.

Coppé, Jean-Philippe; Desprez, Pierre-Yves; Krtolica, Ana; Campisi, Judith (2010): The senescence-associated secretory phenotype: the dark side of tumor suppression. In *Annual review of pathology* 5, pp. 99–118. DOI: 10.1146/annurev-pathol-121808-102144.

Coué, M.; Brenner, S. L.; Spector, I.; Korn, E. D. (1987): Inhibition of actin polymerization by latrunculin A. In *FEBS letters* 213 (2), pp. 316–318. DOI: 10.1016/0014-5793(87)81513-2.

Crews, C. M.; Erikson, R. L. (1993): Extracellular signals and reversible protein phosphorylation: what to Mek of it all. In *Cell* 74 (2), pp. 215–217. DOI: 10.1016/0092-8674(93)90411-i.

Cristofalo, V. J.; Pignolo, R. J. (1996): Molecular markers of senescence in fibroblast-like cultures. In *Experimental gerontology* 31 (1-2), pp. 111–123. DOI: 10.1016/0531-5565(95)02018-7.

Dabrowska, Magdalena; Skoneczny, Marek; Rode, Wojciech (2011): Functional gene expression profile underlying methotrexate-induced senescence in human colon cancer cells. In *Tumour biology : the journal of the International Society for Oncodevelopmental Biology and Medicine* 32 (5), pp. 965–976. DOI: 10.1007/s13277-011-0198-x.

Debacq-Chainiaux, Florence; Erusalimsky, Jorge D.; Campisi, Judith; Toussaint, Olivier (2009): Protocols to detect senescence-associated beta-galactosidase (SA-βgal) activity, a biomarker of senescent cells in culture and in vivo. In *Nature Protocols* 4 (12), pp. 1798–1806. DOI: 10.1038/nprot.2009.191.

Del Gómez Pulgar, Teresa; Benitah, Salvador A.; Valerón, Pilar F.; Espina, Carolina; Lacal, Juan Carlos (2005): Rho GTPase expression in tumourigenesis: evidence for a significant link. In *BioEssays : news and reviews in molecular, cellular and developmental biology* 27 (6), pp. 602–613. DOI: 10.1002/bies.20238.

Derycke, Lara D. M.; Bracke, Marc E. (2004): N-cadherin in the spotlight of cell-cell adhesion, differentiation, embryogenesis, invasion and signalling. In *The International journal of developmental biology* 48 (5-6), pp. 463–476. DOI: 10.1387/ijdb.041793ld.

Descot, Arnaud; Rex-Haffner, Monika; Courtois, Geneviève; Bluteau, Dominique; Menssen, Antje; Mercher, Thomas et al. (2008): OTT-MAL is a deregulated activator of serum response factor-dependent gene expression. In *Molecular and cellular biology* 28 (20), pp. 6171–6181. DOI: 10.1128/MCB.00303-08.

Dhasarathy, Archana; Phadke, Dhiral; Mav, Deepak; Shah, Ruchir R.; Wade, Paul A. (2011): The transcription factors Snail and Slug activate the transforming growth factor-beta signaling pathway in breast cancer. In *PloS one* 6 (10), e26514. DOI: 10.1371/journal.pone.0026514.

Di Micco, Raffaella; Sulli, Gabriele; Dobreva, Miryana; Liontos, Michalis; Botrugno, Oronza A.; Gargiulo, Gaetano et al. (2011): Interplay between oncogene-induced DNA damage response and heterochromatin in senescence and cancer. In *Nat Cell Biol* 13 (3), pp. 292–302. DOI: 10.1038/ncb2170.

Diamond, Michelle E.; Sun, Limin; Ottaviano, Adam J.; Joseph, Mathew J.; Munshi, Hidayatullah G. (2008): Differential growth factor regulation of N-cadherin expression and motility in normal and malignant oral epithelium. In *Journal of cell science* 121 (Pt 13), pp. 2197–2207. DOI: 10.1242/jcs.021782.

Dimri, G. P.; Lee, X.; Basile, G.; Acosta, M.; Scott, G.; Roskelley, C. et al. (1995): A biomarker that identifies senescent human cells in culture and in aging skin in vivo. In *Proceedings of the National Academy of Sciences of the United States of America* 92 (20), pp. 9363–9367. DOI: 10.1073/pnas.92.20.9363.

Dong, Xin; Feng, Mei; Yang, Hui; Liu, Hengkang; Guo, Hua; Gao, Xianshu et al. (2020): Rictor promotes cell migration and actin polymerization through regulating ABLIM1 phosphorylation in Hepatocellular Carcinoma. In *International journal of biological sciences* 16 (15), pp. 2835–2852. DOI: 10.7150/ijbs.46285.

Dransart, Estelle; Olofsson, Birgitta; Cherfils, Jacqueline (2005): RhoGDIs revisited: novel roles in Rho regulation. In *Traffic (Copenhagen, Denmark)* 6 (11), pp. 957–966. DOI: 10.1111/j.1600-0854.2005.00335.x.

Drivalos, Alexandros; Chrisofos, Michael; Efstathiou, Eleni; Kapranou, Amalia; Kollaitis, Gerasimos; Koutlis, Georgios et al. (2016): Expression of α5-integrin, α7-integrin, E-cadherin, and N-cadherin in localized prostate cancer. In *Urologic oncology* 34 (4), 165.e11-8. DOI: 10.1016/j.urolonc.2015.10.016.

drug repurposing hub (2021): REPURPOSING [clue.io]. Available online at https://clue.io/repurposing-app, updated on 8/10/2021, checked on 8/10/2021.

Du, Xiaoli; Qian, Xiaolan; Papageorge, Alex; Schetter, Aaron J.; Vass, William C.; Liu, Xi et al. (2012): Functional interaction of tumor suppressor DLC1 and caveolin-1 in cancer cells. In *Cancer research* 72 (17), pp. 4405–4416. DOI: 10.1158/0008-5472.CAN-12-0777.

Dupuis, Loren E.; Osinska, Hanna; Weinstein, Michael B.; Hinton, Robert B.; Kern, Christine B. (2013): Insufficient versican cleavage and Smad2 phosphorylation results in bicuspid aortic and pulmonary valves. In *Journal of molecular and cellular cardiology* 60, pp. 50–59. DOI: 10.1016/j.yjmcc.2013.03.010.

Durkin, M. E.; Ullmannova, V.; Guan, M.; Popescu, N. C. (2007a): Deleted in liver cancer 3 (DLC-3), a novel Rho GTPase-activating protein, is downregulated in cancer and inhibits tumor cell growth. In *Oncogene* 26 (31), pp. 4580–4589. DOI: 10.1038/sj.onc.1210244.

Durkin, Marian E.; Avner, Miriam R.; Huh, Chang-Goo; Yuan, Bao-Zhu; Thorgeirsson, Snorri S.; Popescu, Nicholas C. (2005): DLC-1, a Rho GTPase-activating protein with tumor suppressor function, is essential for embryonic development. In *FEBS letters* 579 (5), pp. 1191–1196. DOI: 10.1016/j.febslet.2004.12.090.

Durkin, Marian E.; Yuan, Bao-Zhu; Thorgeirsson, Snorri S.; Popescu, Nicholas C. (2002): Gene structure, tissue expression, and linkage mapping of the mouse DLC-1 gene (Arhgap7). In *Gene* 288 (1-2), pp. 119–127. DOI: 10.1016/s0378-1119(02)00462-6.

Durkin, Marian E.; Yuan, Bao-Zhu; Zhou, Xiaoling; Zimonjic, Drazen B.; Lowy, Douglas R.; Thorgeirsson, Snorri S.; Popescu, Nicholas C. (2007b): DLC-1:a Rho GTPase-activating protein and tumour suppressor. In *Journal of cellular and molecular medicine* 11 (5), pp. 1185–1207. DOI: 10.1111/j.1582-4934.2007.00098.x.

Earnest, James T.; Hantak, Michael P.; Park, Jung-Eun; Gallagher, Tom (2015): Coronavirus and influenza virus proteolytic priming takes place in tetraspanin-enriched membrane microdomains. In *Journal of virology* 89 (11), pp. 6093–6104. DOI: 10.1128/JVI.00543-15.

El-Serag, Hashem B. (2007): Epidemiology of hepatocellular carcinoma in USA. In *Hepatology research : the official journal of the Japan Society of Hepatology* 37 Suppl 2, S88-94. DOI: 10.1111/j.1872-034X.2007.00168.x.

EMA (2021): EU/3/20/2300 | European Medicines Agency. Available online at https://www.ema.europa.eu/en/medicines/human/orphan-designations/eu3202300, updated on 8/10/2021, checked on 8/10/2021.

Emadi Baygi, Modjtaba; Soheili, Zahra-Soheila; Essmann, Frank; Deezagi, Abdolkhaleg; Engers, Rainer; Goering, Wolfgang; Schulz, Wolfgang A. (2010): Slug/SNAI2 regulates cell proliferation and invasiveness of metastatic prostate cancer cell lines. In *Tumour biology : the journal of the International Society for Oncodevelopmental Biology and Medicine* 31 (4), pp. 297–307. DOI: 10.1007/s13277-010-0037-5.

Erovic, Boban M.; Pammer, Johannes; Hollemann, David; Woegerbauer, Markus; Geleff, Silvana; Fischer, Michael B. et al. (2003): Motility-related protein-1/CD9 expression in head and neck squamous cell carcinoma. In *Head & neck* 25 (10), pp. 848–857. DOI: 10.1002/hed.10306.

Etienne-Manneville, Sandrine; Hall, Alan (2002): Rho GTPases in cell biology. In *Nature* 420 (6916), pp. 629–635. DOI: 10.1038/nature01148.

Ettrich, Thomas J.; Seufferlein, Thomas (2018): Regorafenib. In *Recent results in cancer research. Fortschritte der Krebsforschung. Progres dans les recherches sur le cancer* 211, pp. 45–56. DOI: 10.1007/978-3-319-91442-8_3.

Ewe, Alexander; Höbel, Sabrina; Heine, Claudia; Merz, Lea; Kallendrusch, Sonja; Bechmann, Ingo et al. (2017): Optimized polyethylenimine (PEI)-based nanoparticles for siRNA delivery, analyzed in vitro and in an ex vivo tumor tissue slice culture model. In *Drug delivery and translational research* 7 (2), pp. 206–216. DOI: 10.1007/s13346-016-0306-y.

Faivre, Sandrine; Rimassa, Lorenza; Finn, Richard S. (2020): Molecular therapies for HCC: Looking outside the box. In *Journal of hepatology* 72 (2), pp. 342–352. DOI: 10.1016/j.jhep.2019.09.010.

Fang, Tingting; Lin, Jiajia; Wang, Yanru; Chen, Guangnan; Huang, Jing; Chen, Jie et al. (2016): Tetraspanin-8 promotes hepatocellular carcinoma metastasis by increasing ADAM12m expression. In *Oncotarget* 7 (26), pp. 40630–40643. DOI: 10.18632/oncotarget.9769.

Farazi, Paraskevi A.; DePinho, Ronald A. (2006): Hepatocellular carcinoma pathogenesis: from genes to environment. In *Nature reviews. Cancer* 6 (9), pp. 674–687. DOI: 10.1038/nrc1934.

Farquhar, Michelle J.; Hu, Ke; Harris, Helen J.; Davis, Christopher; Brimacombe, Claire L.; Fletcher, Sarah J. et al. (2012): Hepatitis C virus induces CD81 and claudin-1 endocytosis. In *Journal of virology* 86 (8), pp. 4305–4316. DOI: 10.1128/JVI.06996-11.

Feldman, John P.; Goldwasser, Ron; Mark, Shlomo; Schwartz, Jeremy; Orion, Itzhak (2009): A mathematical model for tumor volume evaluation using two-dimensions. In *Journal of applied quantitative methods* 4 (4), pp. 455–462.

Feng, Xianguang; Yao, Wenhuan; Zhang, Zengzhen; Yuan, Fangshui; Liang, Li; Zhou, Jingqiang et al. (2018): T-box Transcription Factor Tbx3 Contributes to Human Hepatocellular Carcinoma Cell Migration and Invasion by Repressing E-Cadherin Expression. In *Oncology research* 26 (6), pp. 959–966. DOI: 10.3727/096504017X15145624664031.

Feng, Yangbo; LoGrasso, Philip V.; Defert, Olivier; Li, Rongshi (2016): Rho Kinase (ROCK) Inhibitors and Their Therapeutic Potential. In *Journal of medicinal chemistry* 59 (6), pp. 2269–2300. DOI: 10.1021/acs.jmedchem.5b00683.

Ferbeyre, G.; Stanchina, E. de; Querido, E.; Baptiste, N.; Prives, C.; Lowe, S. W. (2000): PML is induced by oncogenic ras and promotes premature senescence. In *Genes & development* 14 (16), pp. 2015–2027.

Finlay, C. A.; Hinds, P. W.; Levine, A. J. (1989): The p53 proto-oncogene can act as a suppressor of transformation. In *Cell* 57 (7), pp. 1083–1093. DOI: 10.1016/0092-8674(89)90045-7.

Flanagan, L. A.; Chou, J.; Falet, H.; Neujahr, R.; Hartwig, J. H.; Stossel, T. P. (2001): Filamin A, the Arp2/3 complex, and the morphology and function of cortical actin filaments in human melanoma cells. In *The Journal of cell biology* 155 (4), pp. 511–517. DOI: 10.1083/jcb.200105148.

Flores-Téllez, Teresita Nj; Villa-Treviño, Saúl; Piña-Vázquez, Carolina (2017): Road to stemness in hepatocellular carcinoma. In *World journal of gastroenterology* 23 (37), pp. 6750–6776. DOI: 10.3748/wjg.v23.i37.6750.

Friend, S. H.; Horowitz, J. M.; Gerber, M. R.; Wang, X. F.; Bogenmann, E.; Li, F. P.; Weinberg, R. A. (1987): Deletions of a DNA sequence in retinoblastomas and mesenchymal tumors: organization of the sequence and its encoded protein. In *Proceedings of the National Academy of Sciences of the United States of America* 84 (24), pp. 9059–9063. DOI: 10.1073/pnas.84.24.9059.

Furuya, Mitsuko; Kato, Hiroaki; Nishimura, Norihiro; Ishiwata, Isamu; Ikeda, Hitoshi; Ito, Ryoko et al. (2005): Down-regulation of CD9 in human ovarian carcinoma cell might contribute to peritoneal dissemination:

morphologic alteration and reduced expression of beta1 integrin subsets. In *Cancer research* 65 (7), pp. 2617–2625. DOI: 10.1158/0008-5472.CAN-04-3123.

Futreal, P. A.; Barrett, J. C. (1991): Failure of senescent cells to phosphorylate the RB protein. In *Oncogene* 6 (7), pp. 1109–1113.

Fuyuhiro, Yuhiko; Yashiro, Masakazu; Noda, Satoru; Kashiwagi, Shinichiro; Matsuoka, Junko; Doi, Yosuke et al. (2010): Clinical significance of vimentin-positive gastric cancer cells. In *Anticancer research* 30 (12), pp. 5239–5243.

Gale, Nicholas W.; Kaplan, Susan; Lowenstein, Eve J.; Schlessinger, Joseph; Bar-Sagi, Dafna (1993): Grb2 mediates the EGF-dependent activation of guanine nucleotide exchange on Ras. In *Nature* 363 (6424), pp. 88–92. DOI: 10.1038/363088a0.

Galiana, Irene; Lozano-Torres, Beatriz; Sancho, Mónica; Alfonso, María; Bernardos, Andrea; Bisbal, Viviana et al. (2020): Preclinical antitumor efficacy of senescence-inducing chemotherapy combined with a nanoSenolytic. In *Journal of controlled release : official journal of the Controlled Release Society* 323, pp. 624–634. DOI: 10.1016/j.jconrel.2020.04.045.

Gan, Wen-Juan; Wang, Jing-Ru; Zhu, Xiao-Li; He, Xiao-Shun; Guo, Peng-Da; Zhang, Shen et al. (2016): RARγ-induced E-cadherin downregulation promotes hepatocellular carcinoma invasion and metastasis. In *Journal of experimental & clinical cancer research : CR* 35 (1), p. 164. DOI: 10.1186/s13046-016-0441-9.

Gao, Dingcheng; Joshi, Natasha; Choi, Hyejin; Ryu, Seongho; Hahn, Mary; Catena, Raul et al. (2012a): Myeloid progenitor cells in the premetastatic lung promote metastases by inducing mesenchymal to epithelial transition. In *Cancer research* 72 (6), pp. 1384–1394. DOI: 10.1158/0008-5472.CAN-11-2905.

Gao, Dingcheng; Vahdat, Linda T.; Wong, Stephen; Chang, Jenny C.; Mittal, Vivek (2012b): Microenvironmental regulation of epithelial-mesenchymal transitions in cancer. In *Cancer research* 72 (19), pp. 4883–4889. DOI: 10.1158/0008-5472.CAN-12-1223.

Gao, Ran; Liu, Duan; Guo, Wenjun; Ge, Weipeng; Fan, Tianfei; Li, Bolun et al. (2020): Meprin-α (Mep1A) enhances TNF-α secretion by mast cells and aggravates abdominal aortic aneurysms. In *British journal of pharmacology* 177 (12), pp. 2872–2885. DOI: 10.1111/bph.15019.

Garbers, Christoph; Kuck, Fabian; Aparicio-Siegmund, Samadhi; Konzak, Kirstin; Kessenbrock, Mareike; Sommerfeld, Annika et al. (2013): Cellular senescence or EGFR signaling induces Interleukin 6 (IL-6) receptor expression controlled by mammalian target of rapamycin (mTOR). In *Cell cycle (Georgetown, Tex.)* 12 (21), pp. 3421–3432. DOI: 10.4161/cc.26431.

García-Frigola, C.; Burgaya, F.; Calbet, M.; Lecea, L. de; Soriano, E. (2000): Mouse Tspan-5, a member of the tetraspanin superfamily, is highly expressed in brain cortical structures. In *Neuroreport* 11 (14), pp. 3181–3185. DOI: 10.1097/00001756-200009280-00027.

Garrelfs, Sander F.; Frishberg, Yaacov; Hulton, Sally A.; Koren, Michael J.; O'Riordan, William D.; Cochat, Pierre et al. (2021): Lumasiran, an RNAi Therapeutic for Primary Hyperoxaluria Type 1. In *The New England journal of medicine* 384 (13), pp. 1216–1226. DOI: 10.1056/NEJMoa2021712.

Ge, Weipeng; Hou, Cuiliu; Zhang, Wei; Guo, Xiaoxiao; Gao, Pan; Song, Xiaomin et al. (2020): Mep1a contributes to Ang II-induced cardiac remodeling by promoting cardiac hypertrophy, fibrosis and inflammation. In *Journal of molecular and cellular cardiology* 152, pp. 52–68. DOI: 10.1016/j.yjmcc.2020.11.015.

Gedaly, Roberto; Angulo, Paul; Hundley, Jonathan; Daily, Michael F.; Chen, Changguo; Koch, Alvaro; Evers, B. Mark (2010): PI-103 and sorafenib inhibit hepatocellular carcinoma cell proliferation by blocking Ras/Raf/MAPK and PI3K/AKT/mTOR pathways. In *Anticancer research* 30 (12), pp. 4951–4958.

Gheldof, Alexander; Berx, Geert (2013): Cadherins and epithelial-to-mesenchymal transition. In *Progress in molecular biology and translational science* 116, pp. 317–336. DOI: 10.1016/B978-0-12-394311-8.00014-5.

Ghoshal, Kalpana; Datta, Jharna; Majumder, Sarmila; Bai, Shoumei; Kutay, Huban; Motiwala, Tasneem; Jacob, Samson T. (2005): 5-Aza-deoxycytidine induces selective degradation of DNA methyltransferase 1 by a proteasomal pathway that requires the KEN box, bromo-adjacent homology domain, and nuclear localization signal. In *Molecular and cellular biology* 25 (11), pp. 4727–4741. DOI: 10.1128/MCB.25.11.4727-4741.2005.

Giannelli, Gianluigi; Koudelkova, Petra; Dituri, Francesco; Mikulits, Wolfgang (2016): Role of epithelial to mesenchymal transition in hepatocellular carcinoma. In *Journal of hepatology* 65 (4), pp. 798–808. DOI: 10.1016/j.jhep.2016.05.007.

Gilles, Christine; Polette, Myriam; Mestdagt, Mélanie; Nawrocki-Raby, Béatrice; Ruggeri, Philippe; Birembaut, Philippe; Foidart, Jean-Michel (2003): Transactivation of vimentin by beta-catenin in human breast cancer cells. In *Cancer research* 63 (10), pp. 2658–2664.

Goetz, Jacky G.; Lajoie, Patrick; Wiseman, Sam M.; Nabi, Ivan R. (2008): Caveolin-1 in tumor progression: the good, the bad and the ugly. In *Cancer metastasis reviews* 27 (4), pp. 715–735. DOI: 10.1007/s10555-008-9160-9.

Göhring, F.; Schwab, B. L.; Nicotera, P.; Leist, M.; Fackelmayer, F. O. (1997): The novel SAR-binding domain of scaffold attachment factor A (SAF-A) is a target in apoptotic nuclear breakdown. In *The EMBO journal* 16 (24), pp. 7361–7371. DOI: 10.1093/emboj/16.24.7361.

González-Mariscal, L.; Betanzos, A.; Avila-Flores, A. (2000): MAGUK proteins: structure and role in the tight junction. In *Seminars in cell & developmental biology* 11 (4), pp. 315–324. DOI: 10.1006/scdb.2000.0178.

Goodison, Steve; Yuan, Jing; Sloan, Derek; Kim, Ryung; Li, Cheng; Popescu, Nicholas C.; Urquidi, Virginia (2005): The RhoGAP protein DLC-1 functions as a metastasis suppressor in breast cancer cells. In *Cancer research* 65 (14), pp. 6042–6053. DOI: 10.1158/0008-5472.CAN-04-3043.

Gorgoulis, Vassilis G.; Halazonetis, Thanos D. (2010): Oncogene-induced senescence: the bright and dark side of the response. In *Current opinion in cell biology* 22 (6), pp. 816–827. DOI: 10.1016/j.ceb.2010.07.013.

Grant, T. J.; Hua, K.; Singh, A. (2016): Molecular Pathogenesis of Pancreatic Cancer. In *Progress in molecular biology and translational science* 144, pp. 241–275. DOI: 10.1016/bs.pmbts.2016.09.008.

Greco, Céline; Bralet, Marie-Pierre; Ailane, Naouel; Dubart-Kupperschmitt, Anne; Rubinstein, Eric; Le Naour, François; Boucheix, Claude (2010): E-cadherin/p120-catenin and tetraspanin Co-029 cooperate for cell motility control in human colon carcinoma. In *Cancer research* 70 (19), pp. 7674–7683. DOI: 10.1158/0008-5472.CAN-09-4482.

Greider, C. W.; Blackburn, E. H. (1985): Identification of a specific telomere terminal transferase activity in Tetrahymena extracts. In *Cell* 43 (2 Pt 1), pp. 405–413. DOI: 10.1016/0092-8674(85)90170-9.

Greider, C. W.; Blackburn, E. H. (1987): The telomere terminal transferase of Tetrahymena is a ribonucleoprotein enzyme with two kinds of primer specificity. In *Cell* 51 (6), pp. 887–898. DOI: 10.1016/0092-8674(87)90576-9.

Gross, Stephane R.; Kinzy, Terri Goss (2005): Translation elongation factor 1A is essential for regulation of the actin cytoskeleton and cell morphology. In *Nature structural & molecular biology* 12 (9), pp. 772–778. DOI: 10.1038/nsmb979.

Guan, Ming; Zhou, Xiaoling; Soulitzis, Nikolaos; Spandidos, Demetrios A.; Popescu, Nicholas C. (2006): Aberrant methylation and deacetylation of deleted in liver cancer-1 gene in prostate cancer: potential clinical applications. In *Clinical cancer research : an official journal of the American Association for Cancer Research* 12 (5), pp. 1412–1419. DOI: 10.1158/1078-0432.CCR-05-1906.

Guan, X. Y.; Fang, Y.; Sham, J. S.; Kwong, D. L.; Zhang, Y.; Liang, Q. et al. (2000): Recurrent chromosome alterations in hepatocellular carcinoma detected by comparative genomic hybridization. In *Genes, chromosomes & cancer* 29 (2), pp. 110–116.

Guasch, R. M.; Scambler, P.; Jones, G. E.; Ridley, A. J. (1998): RhoE regulates actin cytoskeleton organization and cell migration. In *Molecular and cellular biology* 18 (8), pp. 4761–4771. DOI: 10.1128/mcb.18.8.4761.

Guettler, Sebastian; Vartiainen, Maria K.; Miralles, Francesc; Larijani, Banafshe; Treisman, Richard (2008): RPEL motifs link the serum response factor cofactor MAL but not myocardin to Rho signaling via actin binding. In *Molecular and cellular biology* 28 (2), pp. 732–742. DOI: 10.1128/MCB.01623-07.

Gurrieri, Carmela; Capodieci, Paola; Bernardi, Rosa; Scaglioni, Pier Paolo; Nafa, Khedoudja; Rush, Laura J. et al. (2004): Loss of the tumor suppressor PML in human cancers of multiple histologic origins. In *Journal of the National Cancer Institute* 96 (4), pp. 269–279. DOI: 10.1093/jnci/djh043.

Haeuw, Jean-François; Goetsch, Liliane; Bailly, Christian; Corvaia, Nathalie (2011): Tetraspanin CD151 as a target for antibody-based cancer immunotherapy. In *Biochemical Society transactions* 39 (2), pp. 553–558. DOI: 10.1042/BST0390553.

Haga, Raquel B.; Ridley, Anne J. (2016): Rho GTPases: Regulation and roles in cancer cell biology. In *Small GTPases* 7 (4), pp. 207–221. DOI: 10.1080/21541248.2016.1232583.

Hajra, Karen M.; Chen, David Y-S; Fearon, Eric R. (2002): The SLUG zinc-finger protein represses E-cadherin in breast cancer. In *Cancer research* 62 (6), pp. 1613–1618.

Hamano, Tadanori; Shirafuji, Norimichi; Yen, Shu-Hui; Yoshida, Hirotaka; Kanaan, Nicholas M.; Hayashi, Kouji et al. (2020): Rho-kinase ROCK inhibitors reduce oligomeric tau protein. In *Neurobiology of aging* 89, pp. 41–54. DOI: 10.1016/j.neurobiolaging.2019.12.009.

Hampl, Veronika; Martin, Claudia; Aigner, Achim; Hoebel, Sabrina; Singer, Stephan; Frank, Natalie et al. (2013): Depletion of the transcriptional coactivators megakaryoblastic leukaemia 1 and 2 abolishes hepatocellular carcinoma xenograft growth by inducing oncogene-induced senescence. In *EMBO molecular medicine* 5 (9), pp. 1367–1382. DOI: 10.1002/emmm.201202406.

Han, Jeonghun; Lim, Wanyoung; You, Daeun; Jeong, Yisun; Kim, Sangmin; Lee, Jeong Eon et al. (2019): Chemoresistance in the Human Triple-Negative Breast Cancer Cell Line MDA-MB-231 Induced by Doxorubicin Gradient Is Associated with Epigenetic Alterations in Histone Deacetylase. In *Journal of oncology* 2019, p. 1345026. DOI: 10.1155/2019/1345026.

Hanahan, D.; Weinberg, R. A. (2000): The hallmarks of cancer. In *Cell* 100 (1), pp. 57–70. DOI: 10.1016/s0092-8674(00)81683-9.

Hansen, S. H.; Zegers, M. M.; Woodrow, M.; Rodriguez-Viciana, P.; Chardin, P.; Mostov, K. E.; McMahon, M. (2000): Induced expression of Rnd3 is associated with transformation of polarized epithelial cells by the Raf-MEK-extracellular signal-regulated kinase pathway. In *Molecular and cellular biology* 20 (24), pp. 9364–9375. DOI: 10.1128/mcb.20.24.9364-9375.2000.

Hara, E.; Smith, R.; Parry, D.; Tahara, H.; Stone, S.; Peters, G. (1996): Regulation of p16CDKN2 expression and its implications for cell immortalization and senescence. In *Molecular and cellular biology* 16 (3), pp. 859–867. DOI: 10.1128/mcb.16.3.859.

Harbour, J. W.; Dean, D. C. (2000): The Rb/E2F pathway: expanding roles and emerging paradigms. In *Genes & development* 14 (19), pp. 2393–2409. DOI: 10.1101/gad.813200.

Harley, C. B. (1991): Telomere loss: mitotic clock or genetic time bomb? In *Mutation research* 256 (2-6), pp. 271–282. DOI: 10.1016/0921-8734(91)90018-7.

Harley, C. B.; Futcher, A. B.; Greider, C. W. (1990): Telomeres shorten during ageing of human fibroblasts. In *Nature* 345 (6274), pp. 458–460. DOI: 10.1038/345458a0.

Harris, Helen J.; Davis, Christopher; Mullins, Jonathan G. L.; Hu, Ke; Goodall, Margaret; Farquhar, Michelle J. et al. (2010): Claudin association with CD81 defines hepatitis C virus entry. In *The Journal of biological chemistry* 285 (27), pp. 21092–21102. DOI: 10.1074/jbc.M110.104836.

Hayflick, L.; Moorhead, P. S. (1961): The serial cultivation of human diploid cell strains. In *Experimental cell research* 25 (3), pp. 585–621. DOI: 10.1016/0014-4827(61)90192-6.

Healy, Kevin D.; Hodgson, Louis; Kim, Tai-Young; Shutes, Adam; Maddileti, Savitri; Juliano, Rudolph L. et al. (2008): DLC-1 suppresses non-small cell lung cancer growth and invasion by RhoGAP-dependent and independent mechanisms. In *Molecular carcinogenesis* 47 (5), pp. 326–337. DOI: 10.1002/mc.20389.

Hemler, Martin E. (2005): Tetraspanin functions and associated microdomains. In *Nature Reviews Molecular Cell Biology* 6 (10), pp. 801–811. DOI: 10.1038/nrm1736.

Hemler, Martin E. (2014): Tetraspanin proteins promote multiple cancer stages. In *Nature reviews. Cancer* 14 (1), pp. 49–60. DOI: 10.1038/nrc3640.

Heo, Kyun; Lee, Sukmook (2020): TSPAN8 as a Novel Emerging Therapeutic Target in Cancer for Monoclonal Antibody Therapy. In *Biomolecules* 10 (3). DOI: 10.3390/biom10030388.

Hermanns, C.; Hampl, V.; Holzer, K.; Aigner, A.; Penkava, J.; Frank, N. et al. (2017): The novel MKL target gene myoferlin modulates expansion and senescence of hepatocellular carcinoma. In *Oncogene* 36 (24), pp. 3464–3476. DOI: 10.1038/onc.2016.496.

Herr, Michael J.; Longhurst, Celia M.; Baker, Benjamin; Homayouni, Ramin; Speich, Henry E.; Kotha, Jayaprakash; Jennings, Lisa K. (2014a): Tetraspanin CD9 modulates human lymphoma cellular proliferation via histone deacetylase activity. In *Biochemical and biophysical research communications* 447 (4), pp. 616–620. DOI: 10.1016/j.bbrc.2014.04.046.

Herr, Michael J.; Mabry, Scott E.; Jennings, Lisa K. (2014b): Tetraspanin CD9 regulates cell contraction and actin arrangement via RhoA in human vascular smooth muscle cells. In *PloS one* 9 (9), e106999. DOI: 10.1371/journal.pone.0106999.

Hill, C. S.; Treisman, R. (1995): Differential activation of c-fos promoter elements by serum, lysophosphatidic acid, G proteins and polypeptide growth factors. In *The EMBO journal* 14 (20), pp. 5037–5047.

Hill, C. S.; Wynne, J.; Treisman, R. (1994): Serum-regulated transcription by serum response factor (SRF): a novel role for the DNA binding domain. In *The EMBO journal* 13 (22), pp. 5421–5432.

Hill, C. S.; Wynne, J.; Treisman, R. (1995): The Rho family GTPases RhoA, Rac1, and CDC42Hs regulate transcriptional activation by SRF. In *Cell* 81 (7), pp. 1159–1170. DOI: 10.1016/s0092-8674(05)80020-0.

Höbel, Sabrina; Aigner, Achim (2013): Polyethylenimines for siRNA and miRNA delivery in vivo. In *Wiley interdisciplinary reviews. Nanomedicine and nanobiotechnology* 5 (5), pp. 484–501. DOI: 10.1002/wnan.1228.

Hollstein, M.; Sidransky, D.; Vogelstein, B.; Harris, C. C. (1991): p53 mutations in human cancers. In *Science (New York, N.Y.)* 253 (5015), pp. 49–53. DOI: 10.1126/science.1905840.

Hoy, Sheridan M. (2018): Patisiran: First Global Approval. In *Drugs* 78 (15), pp. 1625–1631. DOI: 10.1007/s40265-018-0983-6.

Hsu, Y-L; Hung, J-Y; Chang, W-A; Lin, Y-S; Pan, Y-C; Tsai, P-H et al. (2017): Hypoxic lung cancer-secreted exosomal miR-23a increased angiogenesis and vascular permeability by targeting prolyl hydroxylase and tight junction protein ZO-1. In *Oncogene* 36 (34), pp. 4929–4942. DOI: 10.1038/onc.2017.105.

Hui, Linping; Zhang, Siyang; Dong, Xinjun; Tian, Dali; Cui, Zeshi; Qiu, Xueshan (2013): Prognostic significance of twist and N-cadherin expression in NSCLC. In *PloS one* 8 (4), e62171. DOI: 10.1371/journal.pone.0062171.

Hulit, James; Suyama, Kimita; Chung, Su; Keren, Rinat; Agiostratidou, Georgia; Shan, Weisong et al. (2007): N-cadherin signaling potentiates mammary tumor metastasis via enhanced extracellular signal-regulated kinase activation. In *Cancer research* 67 (7), pp. 3106–3116. DOI: 10.1158/0008-5472.CAN-06-3401.

Huo, Yi; Zheng, Zhiguo; Chen, Yuling; Wang, Qingtao; Zhang, Zhenyu; Deng, Haiteng (2016): Downregulation of vimentin expression increased drug resistance in ovarian cancer cells. In *Oncotarget* 7 (29), pp. 45876–45888. DOI: 10.18632/oncotarget.9970.

Ibrahim, Ahmed Fawzy; Weirauch, Ulrike; Thomas, Maren; Grünweller, Arnold; Hartmann, Roland K.; Aigner, Achim (2011): MicroRNA Replacement Therapy for miR-145 and miR-33a Is Efficacious in a Model of Colon Carcinoma. In *Cancer research* 71 (15), pp. 5214–5224. DOI: 10.1158/0008-5472.CAN-10-4645.

Ikeyama, S.; Koyama, M.; Yamaoko, M.; Sasada, R.; Miyake, M. (1993): Suppression of cell motility and metastasis by transfection with human motility-related protein (MRP-1/CD9) DNA. In *The Journal of experimental medicine* 177 (5), pp. 1231–1237. DOI: 10.1084/jem.177.5.1231.

Iozzo, R. V. (1998): Matrix proteoglycans: from molecular design to cellular function. In *Annual review of biochemistry* 67, pp. 609–652. DOI: 10.1146/annurev.biochem.67.1.609.

Ishizaki, T.; Maekawa, M.; Fujisawa, K.; Okawa, K.; Iwamatsu, A.; Fujita, A. et al. (1996): The small GTP-binding protein Rho binds to and activates a 160 kDa Ser/Thr protein kinase homologous to myotonic dystrophy kinase. In *The EMBO journal* 15 (8), pp. 1885–1893.

Isola, J. J.; Kallioniemi, O. P.; Chu, L. W.; Fuqua, S. A.; Hilsenbeck, S. G.; Osborne, C. K.; Waldman, F. M. (1995): Genetic aberrations detected by comparative genomic hybridization predict outcome in node-negative breast cancer. In *The American journal of pathology* 147 (4), pp. 905–911.

Itoh, K.; Yoshioka, K.; Akedo, H.; Uehata, M.; Ishizaki, T.; Narumiya, S. (1999): An essential part for Rho-associated kinase in the transcellular invasion of tumor cells. In *Nature medicine* 5 (2), pp. 221–225. DOI: 10.1038/5587.

Iwai, Kaori; Ishii, Masaru; Ohshima, Shiro; Miyatake, Kunio; Saeki, Yukihiko (2007): Expression and function of transmembrane-4 superfamily (tetraspanin) proteins in osteoclasts: reciprocal roles of Tspan-5 and NET-6 during osteoclastogenesis. In *Allergology international : official journal of the Japanese Society of Allergology* 56 (4), pp. 457–463. DOI: 10.2332/allergolint.O-07-488.

Iwasaki, Takeo; Takeda, Yoshito; Maruyama, Kazuichi; Yokosaki, Yasuyuki; Tsujino, Kazuyuki; Tetsumoto, Satoshi et al. (2013): Deletion of tetraspanin CD9 diminishes lymphangiogenesis in vivo and in vitro. In *The Journal of biological chemistry* 288 (4), pp. 2118–2131. DOI: 10.1074/jbc.M112.424291.

Janknecht, R.; Nordheim, A. (1993): Gene regulation by Ets proteins. In *Biochimica et biophysica acta* 1155 (3), pp. 346–356. DOI: 10.1016/0304-419x(93)90014-4.

Jennbacken, Karin; Tesan, Tajana; Wang, Wanzhong; Gustavsson, Heléne; Damber, Jan-Erik; Welén, Karin (2010): N-cadherin increases after androgen deprivation and is associated with metastasis in prostate cancer. In *Endocrine-related cancer* 17 (2), pp. 469–479. DOI: 10.1677/ERC-10-0015.

Jeong, K. J.; Park, S. Y.; Cho, K. H.; Sohn, J. S.; Lee, J.; Kim, Y. K. et al. (2019): Correction: The Rho/ROCK pathway for lysophosphatidic acid-induced proteolytic enzyme expression and ovarian cancer cell invasion. In *Oncogene* 38 (25), pp. 5108–5110. DOI: 10.1038/s41388-019-0769-7.

Johansen, F. E.; Prywes, R. (1995): Serum response factor: transcriptional regulation of genes induced by growth factors and differentiation. In *Biochimica et biophysica acta* 1242 (1), pp. 1–10. DOI: 10.1016/0304-419x(94)00014-s.

Johnson, Jessica L.; Winterwood, Nicole; DeMali, Kris A.; Stipp, Christopher S. (2009): Tetraspanin CD151 regulates RhoA activation and the dynamic stability of carcinoma cell-cell contacts. In *Journal of cell science* 122 (Pt 13), pp. 2263–2273. DOI: 10.1242/jcs.045997.

Juenger, Hendrik; Holst, Martin I.; Duffe, Katja; Jankowski, Jakob; Baader, Stephan L. (2005): Tetraspanin-5 (Tm4sf9) mRNA expression parallels neuronal maturation in the cerebellum of normal and L7En-2 transgenic mice. In *The Journal of comparative neurology* 483 (3), pp. 318–328. DOI: 10.1002/cne.20439.

Kamb, A.; Gruis, N. A.; Weaver-Feldhaus, J.; Liu, Q.; Harshman, K.; Tavtigian, S. V. et al. (1994): A cell cycle regulator potentially involved in genesis of many tumor types. In *Science (New York, N.Y.)* 264 (5157), pp. 436–440. DOI: 10.1126/science.8153634.

Kanai, Y.; Ushijima, S.; Hui, A. M.; Ochiai, A.; Tsuda, H.; Sakamoto, M.; Hirohashi, S. (1997): The E-cadherin gene is silenced by CpG methylation in human hepatocellular carcinomas. In *International journal of cancer* 71 (3), pp. 355–359. DOI: 10.1002/(sici)1097-0215(19970502)71:3<355::aid-ijc8>3.0.co;2-x.

Kanakkanthara, Arun; Rawson, Pisana; Northcote, Peter T.; Miller, John H. (2012): Acquired resistance to peloruside A and laulimalide is associated with downregulation of vimentin in human ovarian carcinoma cells. In *Pharmaceutical research* 29 (11), pp. 3022–3032. DOI: 10.1007/s11095-012-0773-x.

Kanetaka, K.; Sakamoto, M.; Yamamoto, Y.; Yamasaki, S.; Lanza, F.; Kanematsu, T.; Hirohashi, S. (2001): Overexpression of tetraspanin CO-029 in hepatocellular carcinoma. In *Journal of hepatology* 35 (5), pp. 637–642. DOI: 10.1016/s0168-8278(01)00183-0.

Kanetaka, Kengo; Sakamoto, Michiie; Yamamoto, Yoshiya; Takamura, Masaaki; Kanematsu, Takashi; Hirohashi, Setsuo (2003): Possible involvement of tetraspanin CO-029 in hematogenous intrahepatic metastasis of liver

cancer cells. In *Journal of gastroenterology and hepatology* 18 (11), pp. 1309–1314. DOI: 10.1046/j.1440-1746.2003.03182.x.

Kang, Tae-Won; Yevsa, Tetyana; Woller, Norman; Hoenicke, Lisa; Wuestefeld, Torsten; Dauch, Daniel et al. (2011): Senescence surveillance of pre-malignant hepatocytes limits liver cancer development. In *Nature* 479 (7374), pp. 547–551. DOI: 10.1038/nature10599.

Karamatic Crew, Vanja; Burton, Nicholas; Kagan, Alexander; Green, Carole A.; Levene, Cyril; Flinter, Frances et al. (2004): CD151, the first member of the tetraspanin (TM4) superfamily detected on erythrocytes, is essential for the correct assembly of human basement membranes in kidney and skin. In *Blood* 104 (8), pp. 2217–2223. DOI: 10.1182/blood-2004-04-1512.

Kastan, M. B.; Onyekwere, O.; Sidransky, D.; Vogelstein, B.; Craig, R. W. (1991): Participation of p53 protein in the cellular response to DNA damage. In *Cancer research* 51 (23 Pt 1), pp. 6304–6311.

Kaszak, Ilona; Witkowska-Piłaszewicz, Olga; Niewiadomska, Zuzanna; Dworecka-Kaszak, Bożena; Ngosa Toka, Felix; Jurka, Piotr (2020): Role of Cadherins in Cancer-A Review. In *International journal of molecular sciences* 21 (20). DOI: 10.3390/ijms21207624.

Kawai, K.; Yamaga, M.; Iwamae, Y.; Kiyota, M.; Kamata, H.; Hirata, H. et al. (2004): A PLCdelta1-binding protein, p122RhoGAP, is localized in focal adhesions. In *Biochemical Society transactions* 32 (Pt 6), pp. 1107–1109. DOI: 10.1042/BST0321107.

Kawai, Katsuhisa; Kiyota, Minoru; Seike, Junichi; Deki, Yuko; Yagisawa, Hitoshi (2007): START-GAP3/DLC3 is a GAP for RhoA and Cdc42 and is localized in focal adhesions regulating cell morphology. In *Biochemical and biophysical research communications* 364 (4), pp. 783–789. DOI: 10.1016/j.bbrc.2007.10.052.

Kawai, Katsuhisa; Seike, Jun-ichi; Iino, Takuya; Kiyota, Minoru; Iwamae, Yui; Nishitani, Hideo; Yagisawa, Hitoshi (2009): START-GAP2/DLC2 is localized in focal adhesions via its N-terminal region. In *Biochemical and biophysical research communications* 380 (4), pp. 736–741. DOI: 10.1016/j.bbrc.2009.01.095.

Ke, Ai-Wu; Shi, Guo-Ming; Zhou, Jian; Wu, Fei-Zhen; Ding, Zhen-Bin; Hu, Mei-Yu et al. (2009): Role of overexpression of CD151 and/or c-Met in predicting prognosis of hepatocellular carcinoma. In *Hepatology (Baltimore, Md.)* 49 (2), pp. 491–503. DOI: 10.1002/hep.22639.

Kim, T. Y.; Vigil, D.; Der, C. J.; Juliano, R. L. (2009): Role of DLC-1, a tumor suppressor protein with RhoGAP activity, in regulation of the cytoskeleton and cell motility. In *Cancer metastasis reviews* 28 (1-2), pp. 77–83. DOI: 10.1007/s10555-008-9167-2.

Kim, Tai Young; Jong, Hyun-Soon; Song, Sang-Hyun; Dimtchev, Alexandre; Jeong, Sook-Jung; Lee, Jung Weon et al. (2003): Transcriptional silencing of the DLC-1 tumor suppressor gene by epigenetic mechanism in gastric cancer cells. In *Oncogene* 22 (25), pp. 3943–3951. DOI: 10.1038/sj.onc.1206573.

Kim, William Y.; Sharpless, Norman E. (2006): The regulation of INK4/ARF in cancer and aging. In *Cell* 127 (2), pp. 265–275. DOI: 10.1016/j.cell.2006.10.003.

Kircher, Philipp; Hermanns, Constanze; Nossek, Maximilian; Drexler, Maria Katharina; Grosse, Robert; Fischer, Maximilian et al. (2015): Filamin A interacts with the coactivator MKL1 to promote the activity of the transcription factor SRF and cell migration. In *Science signaling* 8 (402), ra112. DOI: 10.1126/scisignal.aad2959.

Kischel, Philippe; Waltregny, David; Dumont, Bruno; Turtoi, Andrei; Greffe, Yannick; Kirsch, Stephanie et al. (2010): Versican overexpression in human breast cancer lesions: known and new isoforms for stromal tumor targeting. In *International journal of cancer* 126 (3), pp. 640–650. DOI: 10.1002/ijc.24812.

Kitadokoro, K.; Bordo, D.; Galli, G.; Petracca, R.; Falugi, F.; Abrignani, S. et al. (2001): CD81 extracellular domain 3D structure: insight into the tetraspanin superfamily structural motifs. In *The EMBO journal* 20 (1-2), pp. 12–18. DOI: 10.1093/emboj/20.1.12.

Knezevic, Nebojsa; Roy, Arun; Timblin, Barbara; Konstantoulaki, Maria; Sharma, Tiffany; Malik, Asrar B.; Mehta, Dolly (2007): GDI-1 phosphorylation switch at serine 96 induces RhoA activation and increased endothelial permeability. In *Molecular and cellular biology* 27 (18), pp. 6323–6333. DOI: 10.1128/MCB.00523-07.

Knobeloch, K. P.; Wright, M. D.; Ochsenbein, A. F.; Liesenfeld, O.; Löhler, J.; Zinkernagel, R. M. et al. (2000): Targeted inactivation of the tetraspanin CD37 impairs T-cell-dependent B-cell response under suboptimal costimulatory conditions. In *Molecular and cellular biology* 20 (15), pp. 5363–5369. DOI: 10.1128/mcb.20.15.5363-5369.2000.

Knoblich, Konstantin; Wang, Hong-Xing; Sharma, Chandan; Fletcher, Anne L.; Turley, Shannon J.; Hemler, Martin E. (2014): Tetraspanin TSPAN12 regulates tumor growth and metastasis and inhibits β-catenin degradation. In *Cellular and molecular life sciences : CMLS* 71 (7), pp. 1305–1314. DOI: 10.1007/s00018-013-1444-8.

Knöll, Bernd; Nordheim, Alfred (2009): Functional versatility of transcription factors in the nervous system: the SRF paradigm. In *Trends in neurosciences* 32 (8), pp. 432–442. DOI: 10.1016/j.tins.2009.05.004.

Knudson, A. G. (1971): Mutation and cancer: statistical study of retinoblastoma. In *Proceedings of the National Academy of Sciences of the United States of America* 68 (4), pp. 820–823. DOI: 10.1073/pnas.68.4.820.

Knudson, A. G. (1973): Mutation and Human Cancer. In George Kleln, Sidney Weinhouse, Alexander Haddow (Eds.), vol. 17: Academic Press (Advances in Cancer Research), pp. 317–352. Available online at https://www.sciencedirect.com/science/article/pii/S0065230X08605345.

Kohl, S.; Giddings, I.; Besch, D.; Apfelstedt-Sylla, E.; Zrenner, E.; Wissinger, B. (1998): The role of the peripherin/RDS gene in retinal dystrophies. In *Acta anatomica* 162 (2-3), pp. 75–84. DOI: 10.1159/000046471.

Koo, Chek Ziu; Harrison, Neale; Noy, Peter J.; Szyroka, Justyna; Matthews, Alexandra L.; Hsia, Hung-En et al. (2020): The tetraspanin Tspan15 is an essential subunit of an ADAM10 scissor complex. In *The Journal of biological chemistry* 295 (36), pp. 12822–12839. DOI: 10.1074/jbc.RA120.012601.

Kovalenko, Oleg V.; Yang, Xiuwei; Kolesnikova, Tatiana V.; Hemler, Martin E. (2004): Evidence for specific tetraspanin homodimers: inhibition of palmitoylation makes cysteine residues available for cross-linking. In *The Biochemical journal* 377 (Pt 2), pp. 407–417. DOI: 10.1042/BJ20031037.

Krause, G.; Patz, M.; Isaeva, P.; Wigger, M.; Baki, I.; Vondey, V. et al. (2012): Action of novel CD37 antibodies on chronic lymphocytic leukemia cells. In *Leukemia* 26 (3), pp. 546–549. DOI: 10.1038/leu.2011.233.

Kugoh, Hiroyuki; Ohira, Takahito; Oshimura, Mitsuo (2015): Studies of Tumor Suppressor Genes via Chromosome Engineering. In *Cancers* 8 (1). DOI: 10.3390/cancers8010004.

Kuilman, Thomas; Peeper, Daniel S. (2009): Senescence-messaging secretome: SMS-ing cellular stress. In *Nature reviews. Cancer* 9 (2), pp. 81–94. DOI: 10.1038/nrc2560.

Kuribayashi, Kageaki; Nakamura, Kiminori; Tanaka, Maki; Sato, Tsutomu; Kato, Junji; Sasaki, Katsunori et al. (2007): Essential role of protein kinase C zeta in transducing a motility signal induced by superoxide and a chemotactic peptide, fMLP. In *The Journal of cell biology* 176 (7), pp. 1049–1060. DOI: 10.1083/jcb.200607019.

Kurrey, N. K.; K, Amit; Bapat, S. A. (2005): Snail and Slug are major determinants of ovarian cancer invasiveness at the transcription level. In *Gynecologic oncology* 97 (1), pp. 155–165. DOI: 10.1016/j.ygyno.2004.12.043.

Kwon, Chang Young; Kim, Kyung Ryoul; Choi, Ha Na; Chung, Myoung Ja; Noh, Sang Jae; Kim, Dae Ghon et al. (2010): The role of serum response factor in hepatocellular carcinoma: implications for disease progression. In *International journal of oncology* 37 (4), pp. 837–844. DOI: 10.3892/ijo_00000734.

Kwon, M. J.; Park, S.; Choi, J. Y.; Oh, E.; Kim, Y. J.; Park, Y-H et al. (2012): Clinical significance of CD151 overexpression in subtypes of invasive breast cancer. In *British journal of cancer* 106 (5), pp. 923–930. DOI: 10.1038/bjc.2012.11.

Lahoute, Charlotte; Sotiropoulos, Athanassia; Favier, Marilyne; Guillet-Deniau, Isabelle; Charvet, Claude; Ferry, Arnaud et al. (2008): Premature aging in skeletal muscle lacking serum response factor. In *PloS one* 3 (12), e3910. DOI: 10.1371/journal.pone.0003910.

Lane, D. P.; Crawford, L. V. (1979): T antigen is bound to a host protein in SV40-transformed cells. In *Nature* 278 (5701), pp. 261–263. DOI: 10.1038/278261a0.

Lang, Shona H.; Hyde, Catherine; Reid, Ian N.; Hitchcock, Ian S.; Hart, Claire A.; Bryden, A. A. Gordon et al. (2002): Enhanced expression of vimentin in motile prostate cell lines and in poorly differentiated and metastatic prostate carcinoma. In *The Prostate* 52 (4), pp. 253–263. DOI: 10.1002/pros.10088.

LaPak, Kyle M.; Burd, Christin E. (2014): The molecular balancing act of p16(INK4a) in cancer and aging. In *Molecular cancer research : MCR* 12 (2), pp. 167–183. DOI: 10.1158/1541-7786.MCR-13-0350.

Laurent-Puig, P.; Legoix, P.; Bluteau, O.; Belghiti, J.; Franco, D.; Binot, F. et al. (2001): Genetic alterations associated with hepatocellular carcinomas define distinct pathways of hepatocarcinogenesis. In *Gastroenterology* 120 (7), pp. 1763–1773. DOI: 10.1053/gast.2001.24798.

Lazareth, Hélène; Henique, Carole; Lenoir, Olivia; Puelles, Victor G.; Flamant, Martin; Bollée, Guillaume et al. (2019): The tetraspanin CD9 controls migration and proliferation of parietal epithelial cells and glomerular disease progression. In *Nature communications* 10 (1), p. 3303. DOI: 10.1038/s41467-019-11013-2.

Lazzerini Denchi, Eros; Attwooll, Claire; Pasini, Diego; Helin, Kristian (2005): Deregulated E2F activity induces hyperplasia and senescence-like features in the mouse pituitary gland. In *Molecular and cellular biology* 25 (7), pp. 2660–2672. DOI: 10.1128/MCB.25.7.2660-2672.2005.

Le Naour, F.; Rubinstein, E.; Jasmin, C.; Prenant, M.; Boucheix, C. (2000): Severely reduced female fertility in CD9-deficient mice. In *Science (New York, N.Y.)* 287 (5451), pp. 319–321. DOI: 10.1126/science.287.5451.319.

Lee, Bo Yun; Han, Jung A.; Im, Jun Sub; Morrone, Amelia; Johung, Kimberly; Goodwin, Edward C. et al. (2006): Senescence-associated beta-galactosidase is lysosomal beta-galactosidase. In *Aging cell* 5 (2), pp. 187–195. DOI: 10.1111/j.1474-9726.2006.00199.x.

Lee, Jeong-Heon; Skalnik, David G. (2012): Rbm15-Mkl1 interacts with the Setd1b histone H3-Lys4 methyltransferase via a SPOC domain that is required for cytokine-independent proliferation. In *PloS one* 7 (8), e42965. DOI: 10.1371/journal.pone.0042965.

Lee, Mee-Hyun; Kundu, Joydeb Kumar; Chae, Jung-Il; Shim, Jung-Hyun (2019): Targeting ROCK/LIMK/cofilin signaling pathway in cancer. In *Archives of pharmacal research* 42 (6), pp. 481–491. DOI: 10.1007/s12272-019-01153-w.

Lee, Sae Hwan; Song, Il Han; Noh, Ran; Kang, Ha Yan; Kim, Suk Bae; Ko, Soon Young et al. (2015): Clinical outcomes of patients with advanced hepatocellular carcinoma treated with sorafenib: a retrospective study of routine clinical practice in multi-institutions. In *BMC cancer* 15, p. 236. DOI: 10.1186/s12885-015-1273-2.

Lee, Sin-Ae; Lee, Sung-Yul; Cho, Ik-Hyun; Oh, Min-A; Kang, Eun-Sil; Kim, Yong-Bae et al. (2008): Tetraspanin TM4SF5 mediates loss of contact inhibition through epithelial-mesenchymal transition in human hepatocarcinoma. In *The Journal of clinical investigation* 118 (4), pp. 1354–1366. DOI: 10.1172/JCI33768.

Leitner, Laura; Shaposhnikov, Dmitry; Mengel, Alexander; Descot, Arnaud; Julien, Sylvia; Hoffmann, Reinhard; Posern, Guido (2011): MAL/MRTF-A controls migration of non-invasive cells by upregulation of cytoskeleton-associated proteins. In *Journal of cell science* 124 (Pt 24), pp. 4318–4331. DOI: 10.1242/jcs.092791.

Leung, T.; Manser, E.; Tan, L.; Lim, L. (1995): A novel serine/threonine kinase binding the Ras-related RhoA GTPase which translocates the kinase to peripheral membranes. In *The Journal of biological chemistry* 270 (49), pp. 29051–29054. DOI: 10.1074/jbc.270.49.29051.

Li, G.; Herlyn, M. (2000): Dynamics of intercellular communication during melanoma development. In *Molecular medicine today* 6 (4), pp. 163–169. DOI: 10.1016/s1357-4310(00)01692-0.

Li, Hongyan; Fung, King-Leung; Jin, Dong-Yan; Chung, Stephen S. M.; Ching, Yick-Pang; Ng, Irene Oi-lin et al. (2007): Solution structures, dynamics, and lipid-binding of the sterile alpha-motif domain of the deleted in liver cancer 2. In *Proteins* 67 (4), pp. 1154–1166. DOI: 10.1002/prot.21361.

Li, Na; Zhan, Xianquan (2019): Signaling pathway network alterations in human ovarian cancers identified with quantitative mitochondrial proteomics. In *The EPMA journal* 10 (2), pp. 153–172. DOI: 10.1007/s13167-019-00170-5.

Li, Shijie; Chang, Shurong; Qi, Xiaoxia; Richardson, James A.; Olson, Eric N. (2006): Requirement of a myocardin-related transcription factor for development of mammary myoepithelial cells. In *Molecular and cellular biology* 26 (15), pp. 5797–5808. DOI: 10.1128/MCB.00211-06.

Li, Shijie; Czubryt, Michael P.; McAnally, John; Bassel-Duby, Rhonda; Richardson, James A.; Wiebel, Franziska F. et al. (2005): Requirement for serum response factor for skeletal muscle growth and maturation revealed by tissue-specific gene deletion in mice. In *Proceedings of the National Academy of Sciences of the United States of America* 102 (4), pp. 1082–1087. DOI: 10.1073/pnas.0409103102.

Liao, Yi-Chun; Lo, Su Hao (2008): Deleted in liver cancer-1 (DLC-1): a tumor suppressor not just for liver. In *The international journal of biochemistry & cell biology* 40 (5), pp. 843–847. DOI: 10.1016/j.biocel.2007.04.008.

Liao, Yi-Chun; Shih, Yi-Ping; Lo, Su Hao (2008): Mutations in the focal adhesion targeting region of deleted in liver cancer-1 attenuate their expression and function. In *Cancer research* 68 (19), pp. 7718–7722. DOI: 10.1158/0008-5472.CAN-08-2042.

Liao, Yi-Chun; Si, Lizhen; deVere White, Ralph W.; Lo, Su Hao (2007): The phosphotyrosine-independent interaction of DLC-1 and the SH2 domain of cten regulates focal adhesion localization and growth suppression activity of DLC-1. In *The Journal of cell biology* 176 (1), pp. 43–49. DOI: 10.1083/jcb.200608015.

Liggett, W. H., JR; Sidransky, D. (1998): Role of the p16 tumor suppressor gene in cancer. In *Journal of clinical oncology : official journal of the American Society of Clinical Oncology* 16 (3), pp. 1197–1206. DOI: 10.1200/JCO.1998.16.3.1197.

Lin, A. W.; Barradas, M.; Stone, J. C.; van Aelst, L.; Serrano, M.; Lowe, S. W. (1998): Premature senescence involving p53 and p16 is activated in response to constitutive MEK/MAPK mitogenic signaling. In *Genes & development* 12 (19), pp. 3008–3019. DOI: 10.1101/gad.12.19.3008.

Lin, Mu-En; Herr, Deron R.; Chun, Jerold (2010): Lysophosphatidic acid (LPA) receptors: signaling properties and disease relevance. In *Prostaglandins & other lipid mediators* 91 (3-4), pp. 130–138. DOI: 10.1016/j.prostaglandins.2009.02.002.

Lin, Xiao; Bi, Zhuofei; Hu, Qian; Li, Qingjian; Liu, Jieqiong; Luo, Man-Li et al. (2019): TSPAN8 serves as a prognostic marker involving Akt/MAPK pathway in nasopharyngeal carcinoma. In *Annals of translational medicine* 7 (18), p. 470. DOI: 10.21037/atm.2019.08.02.

Linzer, D. I.; Levine, A. J. (1979): Characterization of a 54K dalton cellular SV40 tumor antigen present in SV40-transformed cells and uninfected embryonal carcinoma cells. In *Cell* 17 (1), pp. 43–52. DOI: 10.1016/0092-8674(79)90293-9.

Liu, Gang; Grant, Wayne M.; Persky, Daniel; Latham Jr, Vaughan M.; Singer, Robert H.; Condeelis, John (2002): Interactions of elongation factor 1α with F-actin and β-actin mRNA: implications for anchoring mRNA in cell protrusions. In *Molecular biology of the cell* 13 (2), pp. 579–592.

Liu, Hua; Yin, Yan; Liu, Ting; Gao, Yanying; Ye, Qing; Yan, Junqing; Ha, Fushuang (2021): Long non-coding RNA PVT1 regulates the migration of hepatocellular carcinoma HepG2 cells via miR-3619-5p/MKL1 axis. In *Bosnian journal of basic medical sciences* 21 (2), pp. 187–197. DOI: 10.17305/bjbms.2020.4641.

Liu, Li; Cao, Yichen; Chen, Charles; Zhang, Xiaomei; McNabola, Angela; Wilkie, Dean et al. (2006): Sorafenib blocks the RAF/MEK/ERK pathway, inhibits tumor angiogenesis, and induces tumor cell apoptosis in hepatocellular carcinoma model PLC/PRF/5. In *Cancer research* 66 (24), pp. 11851–11858. DOI: 10.1158/0008-5472.CAN-06-1377.

Liu, Sijin; Goldstein, Robert H.; Scepansky, Ellen M.; Rosenblatt, Michael (2009): Inhibition of rho-associated kinase signaling prevents breast cancer metastasis to human bone. In *Cancer research* 69 (22), pp. 8742–8751. DOI: 10.1158/0008-5472.CAN-09-1541.

Liu, Weidong; Xu, Zhentao; Zhou, Jie; Xing, Shuang; Li, Zhiqiang; Gao, Xu et al. (2020): High Levels of HIST1H2BK in Low-Grade Glioma Predicts Poor Prognosis: A Study Using CGGA and TCGA Data. In *Frontiers in oncology* 10, p. 627. DOI: 10.3389/fonc.2020.00627.

Llovet, Josep M.; Ricci, Sergio; Mazzaferro, Vincenzo; Hilgard, Philip; Gane, Edward; Blanc, Jean-Frédéric et al. (2008): Sorafenib in advanced hepatocellular carcinoma. In *The New England journal of medicine* 359 (4), pp. 378–390. DOI: 10.1056/NEJMoa0708857.

Lukasik, D.; Wilczek, E.; Wasiutynski, A.; Gornicka, B. (2011): Deleted in liver cancer protein family in human malignancies (Review). In *Oncology letters* 2 (5), pp. 763–768. DOI: 10.3892/ol.2011.345.

Ma, Li; Chua, Mei-Sze; Andrisani, Ourania; So, Samuel (2014): Epigenetics in hepatocellular carcinoma: an update and future therapy perspectives. In *World journal of gastroenterology* 20 (2), pp. 333–345. DOI: 10.3748/wjg.v20.i2.333.

Ma, Stephanie; Chan, Kwok-Wah; Hu, Liang; Lee, Terence Kin-Wah; Wo, Jana Yim-Hung; Ng, Irene Oi-lin et al. (2007a): Identification and characterization of tumorigenic liver cancer stem/progenitor cells. In *Gastroenterology* 132 (7), pp. 2542–2556. DOI: 10.1053/j.gastro.2007.04.025.

Ma, Xianyong; Renda, Matthew J.; Wang, Lin; Cheng, Ee-Chun; Niu, Chao; Morris, Stephan W. et al. (2007b): Rbm15 modulates Notch-induced transcriptional activation and affects myeloid differentiation. In *Molecular and cellular biology* 27 (8), pp. 3056–3064. DOI: 10.1128/MCB.01339-06.

Mack, C. P.; Somlyo, A. V.; Hautmann, M.; Somlyo, A. P.; Owens, G. K. (2001): Smooth muscle differentiation marker gene expression is regulated by RhoA-mediated actin polymerization. In *The Journal of biological chemistry* 276 (1), pp. 341–347. DOI: 10.1074/jbc.M005505200.

Marchio, A.; Meddeb, M.; Pineau, P.; Danglot, G.; Tiollais, P.; Bernheim, A.; Dejean, A. (1997): Recurrent chromosomal abnormalities in hepatocellular carcinoma detected by comparative genomic hybridization. In *Genes, chromosomes & cancer* 18 (1), pp. 59–65.

Mareel, Marc; Leroy, Ancy (2003): Clinical, cellular, and molecular aspects of cancer invasion. In *Physiological reviews* 83 (2), pp. 337–376. DOI: 10.1152/physrev.00024.2002.

Martincorena, Iñigo; Campbell, Peter J. (2015): Somatic mutation in cancer and normal cells. In *Science (New York, N.Y.)* 349 (6255), pp. 1483–1489. DOI: 10.1126/science.aab4082.

Matsui, T.; Amano, M.; Yamamoto, T.; Chihara, K.; Nakafuku, M.; Ito, M. et al. (1996): Rho-associated kinase, a novel serine/threonine kinase, as a putative target for small GTP binding protein Rho. In *The EMBO journal* 15 (9), pp. 2208–2216.

Matsumoto, Y.; Tanaka, K.; Harimaya, K.; Nakatani, F.; Matsuda, S.; Iwamoto, Y. (2001): Small GTP-binding protein, Rho, both increased and decreased cellular motility, activation of matrix metalloproteinase 2 and invasion of human osteosarcoma cells. In *Japanese journal of cancer research : Gann* 92 (4), pp. 429–438. DOI: 10.1111/j.1349-7006.2001.tb01113.x.

Matters, G. L.; Bond, J. S. (1999): Expression and regulation of the meprin beta gene in human cancer cells. In *Molecular carcinogenesis* 25 (3), pp. 169–178.

Matters, Gail L.; Manni, Andrea; Bond, Judith S. (2005): Inhibitors of polyamine biosynthesis decrease the expression of the metalloproteases meprin alpha and MMP-7 in hormone-independent human breast cancer cells. In *Clinical & experimental metastasis* 22 (4), pp. 331–339. DOI: 10.1007/s10585-005-0660-5.

McDonald, Meghan E.; Li, Chendi; Bian, Hejiao; Smith, Barbara D.; Layne, Matthew D.; Farmer, Stephen R. (2015): Myocardin-related transcription factor A regulates conversion of progenitors to beige adipocytes. In *Cell* 160 (1-2), pp. 105–118. DOI: 10.1016/j.cell.2014.12.005.

Mechanobiology Institute (2021): How is SRF signaling activated? | MBInfo. Edited by University of Singapore. Available online at https://www.mechanobio.info/what-is-mechanosignaling/signaling-pathways/what-is-serum-response-factor/how-is-srf-signaling-activated/, updated on 8/9/2021, checked on 8/9/2021.

Medjkane, Souhila; Perez-Sanchez, Cristina; Gaggioli, Cedric; Sahai, Erik; Treisman, Richard (2009): Myocardin-related transcription factors and SRF are required for cytoskeletal dynamics and experimental metastasis. In *Nat Cell Biol* 11 (3), pp. 257–268. DOI: 10.1038/ncb1833.

Mendez, Melissa G.; Kojima, Shin-Ichiro; Goldman, Robert D. (2010): Vimentin induces changes in cell shape, motility, and adhesion during the epithelial to mesenchymal transition. In *FASEB journal : official publication of the Federation of American Societies for Experimental Biology* 24 (6), pp. 1838–1851. DOI: 10.1096/fj.09-151639.

Meng, Jing; Ai, Xiaoyu; Lei, Yueyang; Zhong, Weilong; Qian, Baoxin; Qiao, Kailiang et al. (2019): USP5 promotes epithelial-mesenchymal transition by stabilizing SLUG in hepatocellular carcinoma. In *Theranostics* 9 (2), pp. 573–587. DOI: 10.7150/thno.27654.

Meng, Jing; Chen, Shuang; Han, Jing-Xia; Qian, Baoxin; Wang, Xiao-Rui; Zhong, Wei-Long et al. (2018): Twist1 Regulates Vimentin through Cul2 Circular RNA to Promote EMT in Hepatocellular Carcinoma. In *Cancer research* 78 (15), pp. 4150–4162. DOI: 10.1158/0008-5472.CAN-17-3009.

Mercher, Thomas; Raffel, Glen D.; Moore, Sandra A.; Cornejo, Melanie G.; Baudry-Bluteau, Dominique; Cagnard, Nicolas et al. (2009): The OTT-MAL fusion oncogene activates RBPJ-mediated transcription and induces acute megakaryoblastic leukemia in a knockin mouse model. In *The Journal of clinical investigation* 119 (4), pp. 852–864. DOI: 10.1172/JCI35901.

Miano, Joseph M.; Long, Xiaochun; Fujiwara, Keigi (2007): Serum response factor: master regulator of the actin cytoskeleton and contractile apparatus. In *American journal of physiology. Cell physiology* 292 (1), C70-81. DOI: 10.1152/ajpcell.00386.2006.

Michaloglou, Chrysiis; Vredeveld, Liesbeth C. W.; Soengas, Maria S.; Denoyelle, Christophe; Kuilman, Thomas; van der Horst, Chantal M A M et al. (2005): BRAFE600-associated senescence-like cell cycle arrest of human naevi. In *Nature* 436 (7051), pp. 720–724. DOI: 10.1038/nature03890.

Mikuličić, Snježana; Fritzen, Anna; Scheffer, Konstanze; Strunk, Johannes; Cabañas, Carlos; Sperrhacke, Maria et al. (2020): Tetraspanin CD9 affects HPV16 infection by modulating ADAM17 activity and the ERK signalling pathway. In *Medical microbiology and immunology* 209 (4), pp. 461–471. DOI: 10.1007/s00430-020-00671-5.

Mikuriya, Yoshihiro; Tashiro, Hirotaka; Kuroda, Shintaro; Nambu, Junko; Kobayashi, Tsuyoshi; Amano, Hironobu et al. (2015): Fatty liver creates a pro-metastatic microenvironment for hepatocellular carcinoma through activation of hepatic stellate cells. In *International journal of cancer* 136 (4), E3-13. DOI: 10.1002/ijc.29096.

Ming, Lihua; Thorgeirsson, Snorri S.; Gail, Mitchell H.; Lu, Peixin; Harris, Curtis C.; Wang, Nengjin et al. (2002): Dominant role of hepatitis B virus and cofactor role of aflatoxin in hepatocarcinogenesis in Qidong, China. In *Hepatology (Baltimore, Md.)* 36 (5), pp. 1214–1220. DOI: 10.1053/jhep.2002.36366.

Minty, Adrian; Kedes, Larry (1986): Upstream regions of the human cardiac actin gene that modulate its transcription in muscle cells: presence of an evolutionarily conserved repeated motif. In *Molecular and cellular biology* 6 (6), pp. 2125–2136.

Miralles, Francesc; Posern, Guido; Zaromytidou, Alexia-Ileana; Treisman, Richard (2003): Actin dynamics control SRF activity by regulation of its coactivator MAL. In *Cell* 113 (3), pp. 329–342. DOI: 10.1016/s0092-8674(03)00278-2.

Mishima, K.; Handa, J. T.; Aotaki-Keen, A.; Lutty, G. A.; Morse, L. S.; Hjelmeland, L. M. (1999): Senescence-associated beta-galactosidase histochemistry for the primate eye. In *Investigative ophthalmology & visual science* 40 (7), pp. 1590–1593.

Mizoshiri, Naoki; Shirai, Toshiharu; Terauchi, Ryu; Tsuchida, Shinji; Mori, Yuki; Hayashi, Daichi et al. (2019): The tetraspanin CD81 mediates the growth and metastases of human osteosarcoma. In *Cellular oncology (Dordrecht)* 42 (6), pp. 861–871. DOI: 10.1007/s13402-019-00472-w.

Mjaatvedt, C. H.; Yamamura, H.; Capehart, A. A.; Turner, D.; Markwald, R. R. (1998): The Cspg2 gene, disrupted in the hdf mutant, is required for right cardiac chamber and endocardial cushion formation. In *Developmental biology* 202 (1), pp. 56–66. DOI: 10.1006/dbio.1998.9001.

Moradpour, Darius; Penin, François; Rice, Charles M. (2007): Replication of hepatitis C virus. In *Nature Reviews Microbiology* 5 (6), pp. 453–463. DOI: 10.1038/nrmicro1645.

Morreau, H.; Galjart, N. J.; Gillemans, N.; Willemsen, R.; van der Horst, G T; d'Azzo, A. (1989): Alternative splicing of beta-galactosidase mRNA generates the classic lysosomal enzyme and a beta-galactosidase-related protein. In *The Journal of biological chemistry* 264 (34), pp. 20655–20663.

Muehlich, S.; Hampl, V.; Khalid, S.; Singer, S.; Frank, N.; Breuhahn, K. et al. (2012): The transcriptional coactivators megakaryoblastic leukemia 1/2 mediate the effects of loss of the tumor suppressor deleted in liver cancer 1. In *Oncogene* 31 (35), pp. 3913–3923. DOI: 10.1038/onc.2011.560.

Muehlich, Susanne; Cicha, Iwona; Garlichs, Christoph D.; Krueger, Bettina; Posern, Guido; Goppelt-Struebe, Margarete (2007): Actin-dependent regulation of connective tissue growth factor. In *American journal of physiology. Cell physiology* 292 (5), C1732-8. DOI: 10.1152/ajpcell.00552.2006.

Muehlich, Susanne; Schneider, Nadine; Hinkmann, Fabian; Garlichs, Christoph D.; Goppelt-Struebe, Margarete (2004): Induction of connective tissue growth factor (CTGF) in human endothelial cells by lysophosphatidic acid, sphingosine-1-phosphate, and platelets. In *Atherosclerosis* 175 (2), pp. 261–268. DOI: 10.1016/j.atherosclerosis.2004.04.011.

Muehlich, Susanne; Wang, Ruigong; Lee, Seung-Min; Lewis, Thera C.; Dai, Chao; Prywes, Ron (2008): Serum-induced phosphorylation of the serum response factor coactivator MKL1 by the extracellular signal-regulated kinase 1/2 pathway inhibits its nuclear localization. In *Molecular and cellular biology* 28 (20), pp. 6302–6313. DOI: 10.1128/MCB.00427-08.

Muenzner, Julienne K.; Kunze, Philipp; Lindner, Pablo; Polaschek, Sandra; Menke, Kira; Eckstein, Markus et al. (2018): Generation and characterization of hepatocellular carcinoma cell lines with enhanced cancer stem cell potential. In *Journal of cellular and molecular medicine* 22 (12), pp. 6238–6248. DOI: 10.1111/jcmm.13911.

Muñoz-Espín, Daniel; Serrano, Manuel (2014): Cellular senescence: from physiology to pathology. In *Nature reviews. Molecular cell biology* 15 (7), pp. 482–496. DOI: 10.1038/nrm3823.

Murray, John W.; Edmonds, Brian T.; Liu, Gang; Condeelis, John (1996): Bundling of actin filaments by elongation factor 1 alpha inhibits polymerization at filament ends. In *The Journal of cell biology* 135 (5), pp. 1309–1321.

Naboulsi, Wael; Megger, Dominik A.; Bracht, Thilo; Kohl, Michael; Turewicz, Michael; Eisenacher, Martin et al. (2016): Quantitative Tissue Proteomics Analysis Reveals Versican as Potential Biomarker for Early-Stage Hepatocellular Carcinoma. In *Journal of proteome research* 15 (1), pp. 38–47. DOI: 10.1021/acs.jproteome.5b00420.

Nagai, Tomoyuki; Arao, Tokuzo; Nishio, Kazuto; Matsumoto, Kazuko; Hagiwara, Satoru; Sakurai, Toshiharu et al. (2016): Impact of Tight Junction Protein ZO-1 and TWIST Expression on Postoperative Survival of Patients with Hepatocellular Carcinoma. In *Digestive diseases (Basel, Switzerland)* 34 (6), pp. 702–707. DOI: 10.1159/000448860.

Nakamoto, Taisei; Murayama, Yoko; Oritani, Kenji; Boucheix, Claude; Rubinstein, Eric; Nishida, Makoto et al. (2009): A novel therapeutic strategy with anti-CD9 antibody in gastric cancers. In *Journal of gastroenterology* 44 (9), pp. 889–896. DOI: 10.1007/s00535-009-0081-3.

Nara, Y.; Kato, Y.; Torii, Y.; Tsuji, Y.; Nakagaki, S.; Goto, S. et al. (1997): Immunohistochemical localization of extracellular matrix components in human breast tumours with special reference to PG-M/versican. In *The Histochemical journal* 29 (1), pp. 21–30. DOI: 10.1023/a:1026460700592.

Narita, Masashi; Nũnez, Sabrina; Heard, Edith; Narita, Masako; Lin, Athena W.; Hearn, Stephen A. et al. (2003): Rb-mediated heterochromatin formation and silencing of E2F target genes during cellular senescence. In *Cell* 113 (6), pp. 703–716. DOI: 10.1016/s0092-8674(03)00401-x.

Nevins, J. R. (2001): The Rb/E2F pathway and cancer. In *Human molecular genetics* 10 (7), pp. 699–703. DOI: 10.1093/hmg/10.7.699.

Ng, David Chi-Heng; Chan, Shing-Fai; Kok, Kin Hang; Yam, Judy Wai Ping; Ching, Yick-Pang; Ng, Irene Oi-lin; Jin, Dong-Yan (2006): Mitochondrial targeting of growth suppressor protein DLC2 through the START domain. In *FEBS letters* 580 (1), pp. 191–198. DOI: 10.1016/j.febslet.2005.11.073.

Nikitovic, D.; Zafiropoulos, A.; Katonis, P.; Tsatsakis, A.; Theocharis, A. D.; Karamanos, N. K.; Tzanakakis, G. N. (2006): Transforming growth factor-beta as a key molecule triggering the expression of versican isoforms v0 and v1, hyaluronan synthase-2 and synthesis of hyaluronan in malignant osteosarcoma cells. In *IUBMB life* 58 (1), pp. 47–53. DOI: 10.1080/15216540500531713.

Nishida-Aoki, Nao; Tominaga, Naoomi; Takeshita, Fumitaka; Sonoda, Hikaru; Yoshioka, Yusuke; Ochiya, Takahiro (2017): Disruption of Circulating Extracellular Vesicles as a Novel Therapeutic Strategy against Cancer Metastasis. In *Molecular therapy : the journal of the American Society of Gene Therapy* 25 (1), pp. 181–191. DOI: 10.1016/j.ymthe.2016.10.009.

Nizamudeen, Zubair Ahmed; Chakrabarti, Lisa; Sottile, Virginie (2018): Exposure to the ROCK inhibitor fasudil promotes gliogenesis of neural stem cells in vitro. In *Stem cell research* 28, pp. 75–86. DOI: 10.1016/j.scr.2018.02.001.

Nobes, C. D.; Lauritzen, I.; Mattei, M. G.; Paris, S.; Hall, A.; Chardin, P. (1998): A new member of the Rho family, Rnd1, promotes disassembly of actin filament structures and loss of cell adhesion. In *The Journal of cell biology* 141 (1), pp. 187–197. DOI: 10.1083/jcb.141.1.187.

Nobusue, Hiroyuki; Onishi, Nobuyuki; Shimizu, Takatsune; Sugihara, Eiji; Oki, Yoshinao; Sumikawa, Yuko et al. (2014): Regulation of MKL1 via actin cytoskeleton dynamics drives adipocyte differentiation. In *Nature communications* 5, p. 3368. DOI: 10.1038/ncomms4368.

Nowak-Sliwinska, Patrycja; Segura, Tatiana; Iruela-Arispe, M. Luisa (2014): The chicken chorioallantoic membrane model in biology, medicine and bioengineering. In *Angiogenesis* 17 (4), pp. 779–804. DOI: 10.1007/s10456-014-9440-7.

Nuessle, Johannes M.; Giehl, Klaudia; Herzog, Rosa; Stracke, Sylvia; Menke, Andre (2011): TGFβ1 suppresses vascular smooth muscle cell motility by expression of N-cadherin. In *Biological chemistry* 392 (5), pp. 461–474. DOI: 10.1515/BC.2011.053.

Nurrish, S. J.; Treisman, R. (1995): DNA binding specificity determinants in MADS-box transcription factors. In *Molecular and cellular biology* 15 (8), pp. 4076–4085. DOI: 10.1128/mcb.15.8.4076.

O'Brien, L. E.; Jou, T. S.; Pollack, A. L.; Zhang, Q.; Hansen, S. H.; Yurchenco, P.; Mostov, K. E. (2001): Rac1 orientates epithelial apical polarity through effects on basolateral laminin assembly. In *Nat Cell Biol* 3 (9), pp. 831–838. DOI: 10.1038/ncb0901-831.

Ogata, Seiji; Morishige, Ken-Ichirou; Sawada, Kenjiro; Hashimoto, Kae; Mabuchi, Seiji; Kawase, Chiaki et al. (2009): Fasudil inhibits lysophosphatidic acid-induced invasiveness of human ovarian cancer cells. In *International journal of gynecological cancer : official journal of the International Gynecological Cancer Society* 19 (9), pp. 1473–1480. DOI: 10.1111/IGC.0b013e3181c03909.

Oh, Jiyeon; Richardson, James A.; Olson, Eric N. (2005): Requirement of myocardin-related transcription factor-B for remodeling of branchial arch arteries and smooth muscle differentiation. In *Proceedings of the National Academy of Sciences of the United States of America* 102 (42), pp. 15122–15127. DOI: 10.1073/pnas.0507346102.

Okuda, K. (2000): Hepatocellular carcinoma. In *Journal of hepatology* 32 (1 Suppl), pp. 225–237. DOI: 10.1016/s0168-8278(00)80428-6.

Olovnikov, A. M. (1971): Principle of marginotomy in template synthesis of polynucleotides. In *Doklady Akademii nauk SSSR* 201 (6), pp. 1496–1499.

Olson, Eric N.; Nordheim, Alfred (2010): Linking actin dynamics and gene transcription to drive cellular motile functions. In *Nature reviews. Molecular cell biology* 11 (5), pp. 353–365. DOI: 10.1038/nrm2890.

Osmanagic-Myers, Selma; Kiss, Attila; Manakanatas, Christina; Hamza, Ouafa; Sedlmayer, Franziska; Szabo, Petra L. et al. (2019): Endothelial progerin expression causes cardiovascular pathology through an impaired mechanoresponse. In *The Journal of clinical investigation* 129 (2), pp. 531–545. DOI: 10.1172/JCI121297.

Otsubo, Chihiro; Otomo, Ryo; Miyazaki, Makoto; Matsushima-Hibiya, Yuko; Kohno, Takashi; Iwakawa, Reika et al. (2014): TSPAN2 is involved in cell invasion and motility during lung cancer progression. In *Cell reports* 7 (2), pp. 527–538. DOI: 10.1016/j.celrep.2014.03.027.

OuYang, Han-Yue; Xu, Jing; Luo, Jun; Zou, Ru-Hai; Chen, Keng; Le, Yong et al. (2016): MEP1A contributes to tumor progression and predicts poor clinical outcome in human hepatocellular carcinoma. In *Hepatology (Baltimore, Md.)* 63 (4), pp. 1227–1239. DOI: 10.1002/hep.28397.

Ovalle, Susana; Gutiérrez-López, María Dolores; Olmo, Nieves; Turnay, Javier; Lizarbe, María Antonia; Majano, Pedro et al. (2007): The tetraspanin CD9 inhibits the proliferation and tumorigenicity of human colon carcinoma cells. In *International journal of cancer* 121 (10), pp. 2140–2152. DOI: 10.1002/ijc.22902.

Paradis, V.; Youssef, N.; Dargère, D.; Bâ, N.; Bonvoust, F.; Deschatrette, J.; Bedossa, P. (2001): Replicative senescence in normal liver, chronic hepatitis C, and hepatocellular carcinomas. In *Human pathology* 32 (3), pp. 327–332. DOI: 10.1053/hupa.2001.22747.

Park, C. S.; Kim, T-K; Kim, H. G.; Kim, Y-J; Jeoung, M. H.; Lee, W. R. et al. (2016): Therapeutic targeting of tetraspanin8 in epithelial ovarian cancer invasion and metastasis. In *Oncogene* 35 (34), pp. 4540–4548. DOI: 10.1038/onc.2015.520.

Park, K. R.; Inoue, T.; Ueda, M.; Hirano, T.; Higuchi, T.; Konishi, I. et al. (2000): Anti-CD9 monoclonal antibody-stimulated invasion of endometrial cancer cell lines in vitro: possible inhibitory effect of CD9 in endometrial cancer invasion. In *Molecular human reproduction* 6 (8), pp. 719–725. DOI: 10.1093/molehr/6.8.719.

Parlakian, Ara; Tuil, David; Hamard, Ghislaine; Tavernier, Geneviève; Hentzen, Daniele; Concordet, Jean-Paul et al. (2004): Targeted inactivation of serum response factor in the developing heart results in myocardial defects and embryonic lethality. In *Molecular and cellular biology* 24 (12), pp. 5281–5289. DOI: 10.1128/MCB.24.12.5281-5289.2004.

Paulus, W.; Baur, I.; Dours-Zimmermann, M. T.; Zimmermann, D. R. (1996): Differential expression of versican isoforms in brain tumors. In *Journal of neuropathology and experimental neurology* 55 (5), pp. 528–533. DOI: 10.1097/00005072-199605000-00005.

Pearson, M.; Carbone, R.; Sebastiani, C.; Cioce, M.; Fagioli, M.; Saito, S. et al. (2000): PML regulates p53 acetylation and premature senescence induced by oncogenic Ras. In *Nature* 406 (6792), pp. 207–210. DOI: 10.1038/35018127.

Peeper, D. S.; van der Eb, A J; Zantema, A. (1994): The G1/S cell-cycle checkpoint in eukaryotic cells. In *Biochimica et biophysica acta* 1198 (2-3), pp. 215–230. DOI: 10.1016/0304-419x(94)90015-9.

Pellegrini, L.; Tan, S.; Richmond, T. J. (1995): Structure of serum response factor core bound to DNA. In *Nature* 376 (6540), pp. 490–498. DOI: 10.1038/376490a0.

Peñas, P. F.; García-Díez, A.; Sánchez-Madrid, F.; Yáñez-Mó, M. (2000): Tetraspanins are localized at motility-related structures and involved in normal human keratinocyte wound healing migration. In *The Journal of investigative dermatology* 114 (6), pp. 1126–1135. DOI: 10.1046/j.1523-1747.2000.00998.x.

Peng, Jei-Ming; Bera, Rabindranath; Chiou, Chih-Yung; Yu, Ming-Chin; Chen, Tse-Chin; Chen, Chia-Wei et al. (2018): Actin cytoskeleton remodeling drives epithelial-mesenchymal transition for hepatoma invasion and metastasis in mice. In *Hepatology (Baltimore, Md.)* 67 (6), pp. 2226–2243. DOI: 10.1002/hep.29678.

Peng, Jin; Zhang, Gong; Wang, Quansheng; Huang, Jianguo; Ma, Huan; Zhong, Yahua et al. (2012): ROCK cooperated with ET-1 to induce epithelial to mesenchymal transition through SLUG in human ovarian cancer cells. In *Bioscience, biotechnology, and biochemistry* 76 (1), pp. 42–47. DOI: 10.1271/bbb.110411.

Personeni, Nicola; Rimassa, Lorenza; Pressiani, Tiziana; Smiroldo, Valeria; Santoro, Armando (2019): Cabozantinib for the treatment of hepatocellular carcinoma. In *Expert review of anticancer therapy* 19 (10), pp. 847–855. DOI: 10.1080/14737140.2019.1674141.

Perz, Joseph F.; Armstrong, Gregory L.; Farrington, Leigh A.; Hutin, Yvan J. F.; Bell, Beth P. (2006): The contributions of hepatitis B virus and hepatitis C virus infections to cirrhosis and primary liver cancer worldwide. In *Journal of hepatology* 45 (4), pp. 529–538. DOI: 10.1016/j.jhep.2006.05.013.

Petersen, I.; Bujard, M.; Petersen, S.; Wolf, G.; Goeze, A.; Schwendel, A. et al. (1997): Patterns of chromosomal imbalances in adenocarcinoma and squamous cell carcinoma of the lung. In *Cancer research* 57 (12), pp. 2331–2335.

Petit, V.; Thiery, J. P. (2000): Focal adhesions: structure and dynamics. In *Biology of the cell* 92 (7), pp. 477–494. DOI: 10.1016/s0248-4900(00)01101-1.

Petrova, Yuliya I.; Schecterson, Leslayann; Gumbiner, Barry M. (2016): Roles for E-cadherin cell surface regulation in cancer. In *Molecular biology of the cell* 27 (21), pp. 3233–3244. DOI: 10.1091/mbc.E16-01-0058.

Pipes, G. C. Teg; Creemers, Esther E.; Olson, Eric N. (2006): The myocardin family of transcriptional coactivators: versatile regulators of cell growth, migration, and myogenesis. In *Genes & development* 20 (12), pp. 1545–1556. DOI: 10.1101/gad.1428006.

Porter, Andrew P.; Papaioannou, Alexandra; Malliri, Angeliki (2016): Deregulation of Rho GTPases in cancer. In *Small GTPases* 7 (3), pp. 123–138. DOI: 10.1080/21541248.2016.1173767.

Posern, Guido; Miralles, Francesc; Guettler, Sebastian; Treisman, Richard (2004): Mutant actins that stabilise F-actin use distinct mechanisms to activate the SRF coactivator MAL. In *The EMBO journal* 23 (20), pp. 3973–3983. DOI: 10.1038/sj.emboj.7600404.

Qi, Yaoyue; Li, Hui; Lv, Jing; Qi, Weiwei; Shen, Liwei; Liu, Shihai et al. (2020): Expression and function of transmembrane 4 superfamily proteins in digestive system cancers. In *Cancer Cell International* 20 (1), p. 314. DOI: 10.1186/s12935-020-01353-1.

Qian, Xiaolan; Li, Guorong; Asmussen, Holly K.; Asnaghi, Laura; Vass, William C.; Braverman, Richard et al. (2007): Oncogenic inhibition by a deleted in liver cancer gene requires cooperation between tensin binding and Rho-specific GTPase-activating protein activities. In *Proceedings of the National Academy of Sciences of the United States of America* 104 (21), pp. 9012–9017. DOI: 10.1073/pnas.0703033104.

Qiao, Feng; Bowie, James U. (2005): The many faces of SAM. In *Science's STKE : signal transduction knowledge environment* 2005 (286), re7. DOI: 10.1126/stke.2862005re7.

Quelle, D. E.; Zindy, F.; Ashmun, R. A.; Sherr, C. J. (1995): Alternative reading frames of the INK4a tumor suppressor gene encode two unrelated proteins capable of inducing cell cycle arrest. In *Cell* 83 (6), pp. 993–1000. DOI: 10.1016/0092-8674(95)90214-7.

Raal, Frederick J.; Kallend, David; Ray, Kausik K.; Turner, Traci; Koenig, Wolfgang; Wright, R. Scott et al. (2020): Inclisiran for the Treatment of Heterozygous Familial Hypercholesterolemia. In *The New England journal of medicine* 382 (16), pp. 1520–1530. DOI: 10.1056/NEJMoa1913805.

Rahman, Nur-Taz; Schulz, Vincent P.; Wang, Lin; Gallagher, Patrick G.; Denisenko, Oleg; Gualdrini, Francesco et al. (2018): MRTFA augments megakaryocyte maturation by enhancing the SRF regulatory axis. In *Blood advances* 2 (20), pp. 2691–2703. DOI: 10.1182/bloodadvances.2018019448.

Rajesh, Sundaresan; Sridhar, Pooja; Tews, Birke Andrea; Fénéant, Lucie; Cocquerel, Laurence; Ward, Douglas G. et al. (2012): Structural basis of ligand interactions of the large extracellular domain of tetraspanin CD81. In *Journal of virology* 86 (18), pp. 9606–9616. DOI: 10.1128/JVI.00559-12.

Rasmussen, Carol A.; Kaufman, Paul L.; Ritch, Robert; Haque, Reza; Brazzell, R. Kim; Vittitow, Jason L. (2014): Latrunculin B Reduces Intraocular Pressure in Human Ocular Hypertension and Primary Open-Angle Glaucoma. In *Translational vision science & technology* 3 (5), p. 1. DOI: 10.1167/tvst.3.5.1.

Ray, Kausik K.; Wright, R. Scott; Kallend, David; Koenig, Wolfgang; Leiter, Lawrence A.; Raal, Frederick J. et al. (2020): Two Phase 3 Trials of Inclisiran in Patients with Elevated LDL Cholesterol. In *The New England journal of medicine* 382 (16), pp. 1507–1519. DOI: 10.1056/NEJMoa1912387.

Reeves, Helen L.; Zaki, Marco Y. W.; Day, Christopher P. (2016): Hepatocellular Carcinoma in Obesity, Type 2 Diabetes, and NAFLD. In *Digestive diseases and sciences* 61 (5), pp. 1234–1245. DOI: 10.1007/s10620-016-4085-6.

Ribatti, Domenico (2014): The chick embryo chorioallantoic membrane as a model for tumor biology. In *Experimental cell research* 328 (2), pp. 314–324. DOI: 10.1016/j.yexcr.2014.06.010.

Ribatti, Domenico (2017): The chick embryo chorioallantoic membrane (CAM) assay. In *Reproductive toxicology (Elmsford, N.Y.)* 70, pp. 97–101. DOI: 10.1016/j.reprotox.2016.11.004.

Ricciardelli, Carmela; Brooks, John H.; Suwiwat, Supaporn; Sakko, Andrew J.; Mayne, Keiko; Raymond, Wendy A. et al. (2002): Regulation of stromal versican expression by breast cancer cells and importance to relapse-free

survival in patients with node-negative primary breast cancer. In *Clinical cancer research : an official journal of the American Association for Cancer Research* 8 (4), pp. 1054–1060.

Ricciardelli, Carmela; Sakko, Andrew J.; Ween, Miranda P.; Russell, Darryl L.; Horsfall, David J. (2009): The biological role and regulation of versican levels in cancer. In *Cancer metastasis reviews* 28 (1-2), pp. 233–245. DOI: 10.1007/s10555-009-9182-y.

Rich, Jeremy N. (2016): Cancer stem cells: understanding tumor hierarchy and heterogeneity. In *Medicine* 95 (1 Suppl 1), S2-S7. DOI: 10.1097/MD.0000000000004764.

Riley, D. J.; Lee, E. Y.; Lee, W. H. (1994): The retinoblastoma protein: more than a tumor suppressor. In *Annual review of cell biology* 10, pp. 1–29. DOI: 10.1146/annurev.cb.10.110194.000245.

Roberts, P. J.; Der, C. J. (2007): Targeting the Raf-MEK-ERK mitogen-activated protein kinase cascade for the treatment of cancer. In *Oncogene* 26 (22), pp. 3291–3310. DOI: 10.1038/sj.onc.1210422.

Rossman, Kent L.; Der, Channing J.; Sondek, John (2005): GEF means go: turning on RHO GTPases with guanine nucleotide-exchange factors. In *Nature reviews. Molecular cell biology* 6 (2), pp. 167–180. DOI: 10.1038/nrm1587.

Saadatmand, S.; Kruijf, E. M. de; Sajet, A.; Dekker-Ensink, N. G.; van Nes, J G H; Putter, H. et al. (2013): Expression of cell adhesion molecules and prognosis in breast cancer. In *The British journal of surgery* 100 (2), pp. 252–260. DOI: 10.1002/bjs.8980.

Sabbatini, Maria Eugenia; Williams, John A. (2013): Cholecystokinin-mediated RhoGDI phosphorylation via PKCα promotes both RhoA and Rac1 signaling. In *PloS one* 8 (6), e66029. DOI: 10.1371/journal.pone.0066029.

Sahai, Erik; Marshall, Christopher J. (2002): RHO-GTPases and cancer. In *Nature reviews. Cancer* 2 (2), pp. 133–142. DOI: 10.1038/nrc725.

Saint-Pol, Julien; Billard, Martine; Dornier, Emmanuel; Eschenbrenner, Etienne; Danglot, Lydia; Boucheix, Claude et al. (2017): New insights into the tetraspanin Tspan5 using novel monoclonal antibodies. In *The Journal of biological chemistry* 292 (23), pp. 9551–9566. DOI: 10.1074/jbc.M116.765669.

Sasaki, A.; Masuda, Y.; Ohta, Y.; Ikeda, K.; Watanabe, K. (2001): Filamin associates with Smads and regulates transforming growth factor-beta signaling. In *The Journal of biological chemistry* 276 (21), pp. 17871–17877. DOI: 10.1074/jbc.M008422200.

Satelli, Arun; Li, Shulin (2011): Vimentin in cancer and its potential as a molecular target for cancer therapy. In *Cellular and molecular life sciences : CMLS* 68 (18), pp. 3033–3046. DOI: 10.1007/s00018-011-0735-1.

Schäfer, Jens; Höbel, Sabrina; Bakowsky, Udo; Aigner, Achim (2010): Liposome-polyethylenimine complexes for enhanced DNA and siRNA delivery. In *Biomaterials* 31 (26), pp. 6892–6900. DOI: 10.1016/j.biomaterials.2010.05.043.

Schiffelers, Raymond M.; Ansari, Aslam; Xu, Jun; Zhou, Qin; Tang, Qingquan; Storm, Gert et al. (2004): Cancer siRNA therapy by tumor selective delivery with ligand-targeted sterically stabilized nanoparticle. In *Nucleic acids research* 32 (19), e149. DOI: 10.1093/nar/gnh140.

Scholzen, T.; Gerdes, J. (2000): The Ki-67 protein: from the known and the unknown. In *Journal of cellular physiology* 182 (3), pp. 311–322. DOI: 10.1002/(SICI)1097-4652(200003)182:3<311::AID-JCP1>3.0.CO;2-9.

Schratt, Gerhard; Philippar, Ulrike; Berger, Jürgen; Schwarz, Heinz; Heidenreich, Olaf; Nordheim, Alfred (2002): Serum response factor is crucial for actin cytoskeletal organization and focal adhesion assembly in embryonic stem cells. In *The Journal of cell biology* 156 (4), pp. 737–750. DOI: 10.1083/jcb.200106008.

Schwarz-Sommer, Zsuzsanna; Huijser, Peter; Nacken, Wolfgang; Saedler, Heinz; Sommer, Hans (1990): Genetic control of flower development by homeotic genes in Antirrhinum majus. In *Science (New York, N.Y.)* 250 (4983), pp. 931–936.

Scott, Lesley J. (2020): Givosiran: First Approval. In *Drugs* 80 (3), pp. 335–339. DOI: 10.1007/s40265-020-01269-0.

Scott, Lesley J.; Keam, Susan J. (2021): Lumasiran: First Approval. In *Drugs* 81 (2), pp. 277–282. DOI: 10.1007/s40265-020-01463-0.

Seigneuret, Michel (2006): Complete predicted three-dimensional structure of the facilitator transmembrane protein and hepatitis C virus receptor CD81: conserved and variable structural domains in the tetraspanin superfamily. In *Biophysical journal* 90 (1), pp. 212–227. DOI: 10.1529/biophysj.105.069666.

Sekimata, M.; Kabuyama, Y.; Emori, Y.; Homma, Y. (1999): Morphological changes and detachment of adherent cells induced by p122, a GTPase-activating protein for Rho. In *The Journal of biological chemistry* 274 (25), pp. 17757–17762. DOI: 10.1074/jbc.274.25.17757.

Selvaraj, Ahalya; Prywes, Ron (2003): Megakaryoblastic leukemia-1/2, a transcriptional co-activator of serum response factor, is required for skeletal myogenic differentiation. In *The Journal of biological chemistry* 278 (43), pp. 41977–41987. DOI: 10.1074/jbc.M305679200.

Seng, T. J.; Low, J. S. W.; Li, H.; Cui, Y.; Goh, H. K.; Wong, M. L. Y. et al. (2007): The major 8p22 tumor suppressor DLC1 is frequently silenced by methylation in both endemic and sporadic nasopharyngeal, esophageal, and cervical carcinomas, and inhibits tumor cell colony formation. In *Oncogene* 26 (6), pp. 934–944. DOI: 10.1038/sj.onc.1209839.

Seo, Dong Dae; Lee, Han Chu; Kim, Ha Jung; Min, Hyun Ju; Kim, Kang Mo; Lim, Young Suk et al. (2008): Neural cadherin overexpression is a predictive marker for early postoperative recurrence in hepatocellular carcinoma patients. In *Journal of gastroenterology and hepatology* 23 (7 Pt 1), pp. 1112–1118. DOI: 10.1111/j.1440-1746.2007.05182.x.

Serrano, M.; Lin, A. W.; McCurrach, M. E.; Beach, D.; Lowe, S. W. (1997): Oncogenic ras provokes premature cell senescence associated with accumulation of p53 and p16INK4a. In *Cell* 88 (5), pp. 593–602. DOI: 10.1016/s0092-8674(00)81902-9.

Serrano, Manual; Hannon, Gregory J.; Beach, David (1993): A new regulatory motif in cell-cycle control causing specific inhibition of cyclin D/CDK4. In *Nature* 366 (6456), pp. 704–707. DOI: 10.1038/366704a0.

Sharpless, N. E.; DePinho, R. A. (1999): The INK4A/ARF locus and its two gene products. In *Current opinion in genetics & development* 9 (1), pp. 22–30. DOI: 10.1016/s0959-437x(99)80004-5.

Sharpless, Norman E.; DePinho, Ronald A. (2006): The mighty mouse: genetically engineered mouse models in cancer drug development. In *Nature reviews. Drug discovery* 5 (9), pp. 741–754. DOI: 10.1038/nrd2110.

Sharrocks, Andrew D. (2001): The ETS-domain transcription factor family. In *Nature Reviews Molecular Cell Biology* 2 (11), pp. 827–837. DOI: 10.1038/35099076.

Shaw, P. E.; Schröter, H.; Nordheim, A. (1989): The ability of a ternary complex to form over the serum response element correlates with serum inducibility of the human c-fos promoter. In *Cell* 56 (4), pp. 563–572. DOI: 10.1016/0092-8674(89)90579-5.

Shay, J. W.; Bacchetti, S. (1997): A survey of telomerase activity in human cancer. In *European journal of cancer (Oxford, England : 1990)* 33 (5), pp. 787–791. DOI: 10.1016/S0959-8049(97)00062-2.

Sheng, Wang; Wang, Guizhi; La Pierre, David P.; Wen, Jianping; Deng, Zhaoqun; Wong, Chung-Kwun Amy et al. (2006): Versican mediates mesenchymal-epithelial transition. In *Molecular biology of the cell* 17 (4), pp. 2009–2020. DOI: 10.1091/mbc.e05-10-0951.

Sherr, C. J. (2001): The INK4a/ARF network in tumour suppression. In *Nature reviews. Molecular cell biology* 2 (10), pp. 731–737. DOI: 10.1038/35096061.

Sherr, C. J.; Roberts, J. M. (1999): CDK inhibitors: positive and negative regulators of G1-phase progression. In *Genes & development* 13 (12), pp. 1501–1512. DOI: 10.1101/gad.13.12.1501.

Sherr, Charles J. (2004): Principles of tumor suppression. In *Cell* 116 (2), pp. 235–246. DOI: 10.1016/s0092-8674(03)01075-4.

Sherwood, S. W.; Rush, D.; Ellsworth, J. L.; Schimke, R. T. (1988): Defining cellular senescence in IMR-90 cells: a flow cytometric analysis. In *Proceedings of the National Academy of Sciences of the United States of America* 85 (23), pp. 9086–9090. DOI: 10.1073/pnas.85.23.9086.

Shibue, Tsukasa; Weinberg, Robert A. (2017): EMT, CSCs, and drug resistance: the mechanistic link and clinical implications. In *Nature Reviews Clinical Oncology* 14 (10), pp. 611–629. DOI: 10.1038/nrclinonc.2017.44.

Shore, P.; Sharrocks, A. D. (1995): The MADS-box family of transcription factors. In *European journal of biochemistry* 229 (1), pp. 1–13. DOI: 10.1111/j.1432-1033.1995.tb20430.x.

Sikora, Ewa; Mosieniak, Grazyna; Sliwinska, Malgorzata Alicja (2016): Morphological and Functional Characteristic of Senescent Cancer Cells. In *Current drug targets* 17 (4), pp. 377–387. DOI: 10.2174/1389450116666151019094724.

Sleeman, Katherine E.; Brito, Maja de; Etkind, Simon; Nkhoma, Kennedy; Guo, Ping; Higginson, Irene J. et al. (2019): The escalating global burden of serious health-related suffering: projections to 2060 by world regions, age groups, and health conditions. In *The Lancet Global Health* 7 (7), e883-e892. DOI: 10.1016/S2214-109X(19)30172-X.

Slupsky, JR; Seehafer, J. G.; Tang, Shou-Ching; Masellis-Smith, A.; Shaw, A. R.E. (1989): Evidence that monoclonal antibodies against CD9 antigen induce specific association between CD9 and the platelet glycoprotein IIb-IIIa complex. In *Journal of Biological Chemistry* 264 (21), pp. 12289–12293.

Smith, Elenoe C.; Thon, Jonathan N.; Devine, Matthew T.; Lin, Sharon; Schulz, Vincent P.; Guo, Yanwen et al. (2012): MKL1 and MKL2 play redundant and crucial roles in megakaryocyte maturation and platelet formation. In *Blood* 120 (11), pp. 2317–2329. DOI: 10.1182/blood-2012-04-420828.

Song, Y-F; Xu, R.; Zhang, X-H; Chen, B-B; Chen, Q.; Chen, Y-M; Xie, Y. (2006): High-frequency promoter hypermethylation of the deleted in liver cancer-1 gene in multiple myeloma. In *Journal of clinical pathology* 59 (9), pp. 947–951. DOI: 10.1136/jcp.2005.031377.

Sotiropoulos, A.; Gineitis, D.; Copeland, J.; Treisman, R. (1999): Signal-regulated activation of serum response factor is mediated by changes in actin dynamics. In *Cell* 98 (2), pp. 159–169. DOI: 10.1016/s0092-8674(00)81011-9.

Staib, Frank; Hussain, S. Perwez; Hofseth, Lorne J.; Wang, Xin W.; Harris, Curtis C. (2003): TP53 and liver carcinogenesis. In *Human mutation* 21 (3), pp. 201–216. DOI: 10.1002/humu.10176.

Stapleton, D.; Balan, I.; Pawson, T.; Sicheri, F. (1999): The crystal structure of an Eph receptor SAM domain reveals a mechanism for modular dimerization. In *Nature structural biology* 6 (1), pp. 44–49. DOI: 10.1038/4917.

Staus, Dean P.; Blaker, Alicia L.; Taylor, Joan M.; Mack, Christopher P. (2007): Diaphanous 1 and 2 regulate smooth muscle cell differentiation by activating the myocardin-related transcription factors. In *Arteriosclerosis, thrombosis, and vascular biology* 27 (3), pp. 478–486. DOI: 10.1161/01.ATV.0000255559.77687.c1.

Staus, Dean P.; Weise-Cross, Laura; Mangum, Kevin D.; Medlin, Matt D.; Mangiante, Lee; Taylor, Joan M.; Mack, Christopher P. (2014): Nuclear RhoA signaling regulates MRTF-dependent SMC-specific transcription. In *American journal of physiology. Heart and circulatory physiology* 307 (3), H379-90. DOI: 10.1152/ajpheart.01002.2013.

Stehelin, D.; Varmus, H. E.; Bishop, J. M.; Vogt, P. K. (1976): DNA related to the transforming gene(s) of avian sarcoma viruses is present in normal avian DNA. In *Nature* 260 (5547), pp. 170–173. DOI: 10.1038/260170a0.

Stipp, Christopher S.; Kolesnikova, Tatiana V.; Hemler, Martin E. (2003): Functional domains in tetraspanin proteins. In *Trends in biochemical sciences* 28 (2), pp. 106–112. DOI: 10.1016/S0968-0004(02)00014-2.

Stossel, T. P.; Condeelis, J.; Cooley, L.; Hartwig, J. H.; Noegel, A.; Schleicher, M.; Shapiro, S. S. (2001): Filamins as integrators of cell mechanics and signalling. In *Nature reviews. Molecular cell biology* 2 (2), pp. 138–145. DOI: 10.1038/35052082.

Sullivan, Amy L.; Benner, Christopher; Heinz, Sven; Huang, Wendy; Xie, Lan; Miano, Joseph M.; Glass, Christopher K. (2011): Serum response factor utilizes distinct promoter- and enhancer-based mechanisms to regulate cytoskeletal gene expression in macrophages. In *Molecular and cellular biology* 31 (4), pp. 861–875. DOI: 10.1128/MCB.00836-10.

Sun, Jing-Hui; Luo, Qing; Liu, Ling-Ling; Song, Guan-Bin (2016): Liver cancer stem cell markers: Progression and therapeutic implications. In *World journal of gastroenterology* 22 (13), pp. 3547–3557. DOI: 10.3748/wjg.v22.i13.3547.

Sun, Kai; Battle, Michele A.; Misra, Ravi P.; Duncan, Stephen A. (2009): Hepatocyte expression of serum response factor is essential for liver function, hepatocyte proliferation and survival, and postnatal body growth in mice. In *Hepatology (Baltimore, Md.)* 49 (5), pp. 1645–1654. DOI: 10.1002/hep.22834.

Sun, Yi; Boyd, Kelli; Xu, Wu; Ma, Jing; Jackson, Carl W.; Fu, Amina et al. (2006): Acute myeloid leukemia-associated Mkl1 (Mrtf-a) is a key regulator of mammary gland function. In *Molecular and cellular biology* 26 (15), pp. 5809–5826. DOI: 10.1128/MCB.00024-06.

Sung, Hyuna; Ferlay, Jacques; Siegel, Rebecca L.; Laversanne, Mathieu; Soerjomataram, Isabelle; Jemal, Ahmedin; Bray, Freddie (2021): Global Cancer Statistics 2020: GLOBOCAN Estimates of Incidence and Mortality Worldwide for 36 Cancers in 185 Countries. In *CA: a cancer journal for clinicians* 71 (3), pp. 209–249. DOI: 10.3322/caac.21660.

Svitkina, Tatyana (2018): The Actin Cytoskeleton and Actin-Based Motility. In *Cold Spring Harbor perspectives in biology* 10 (1). DOI: 10.1101/cshperspect.a018267.

Syed, Viqar; Mukherjee, Kasturi; Lyons-Weiler, James; Lau, Kin-Mang; Mashima, Tetsuo; Tsuruo, Takashi; Ho, Shuk-mei (2005): Identification of ATF-3, caveolin-1, DLC-1, and NM23-H2 as putative antitumorigenic, progesterone-regulated genes for ovarian cancer cells by gene profiling. In *Oncogene* 24 (10), pp. 1774–1787. DOI: 10.1038/sj.onc.1207991.

Tahara, H.; Sato, E.; Noda, A.; Ide, T. (1995): Increase in expression level of p21sdi1/cip1/waf1 with increasing division age in both normal and SV40-transformed human fibroblasts. In *Oncogene* 10 (5), pp. 835–840.

Takeda, Yoshito; Kazarov, Alexander R.; Butterfield, Catherine E.; Hopkins, Benjamin D.; Benjamin, Laura E.; Kaipainen, Arja; Hemler, Martin E. (2007): Deletion of tetraspanin Cd151 results in decreased pathologic angiogenesis in vivo and in vitro. In *Blood* 109 (4), pp. 1524–1532. DOI: 10.1182/blood-2006-08-041970.

Takemura, K.; Hirayama, R.; Hirokawa, K.; Inagaki, M.; Tsujimura, K.; Esaki, Y.; Mishima, Y. (1994): Expression of vimentin in gastric cancer: a possible indicator for prognosis. In *Pathobiology : journal of immunopathology, molecular and cellular biology* 62 (3), pp. 149–154. DOI: 10.1159/000163895.

Tamanoi, Fuyuhiko (2019): Recent excitements in the study of the CAM assay. In *The Enzymes* 46, pp. 1–9. DOI: 10.1016/bs.enz.2019.10.002.

Tanaka, Y.; Tateishi, K.; Nakatsuka, T.; Kudo, Y.; Takahashi, R.; Miyabayashi, K. et al. (2016): Sharpin promotes hepatocellular carcinoma progression via transactivation of Versican expression. In *Oncogenesis* 5 (12), e277. DOI: 10.1038/oncsis.2016.76.

Tcherkezian, Joseph; Lamarche-Vane, Nathalie (2007): Current knowledge of the large RhoGAP family of proteins. In *Biology of the cell* 99 (2), pp. 67–86. DOI: 10.1042/BC20060086.

Tellapuri, Sreeshma; Sutphin, Patrick D.; Beg, Muhammad S.; Singal, Amit G.; Kalva, Sanjeeva P. (2018): Staging systems of hepatocellular carcinoma: A review. In *Indian journal of gastroenterology : official journal of the Indian Society of Gastroenterology* 37 (6), pp. 481–491. DOI: 10.1007/s12664-018-0915-0.

Thornton, Sarah; Anand, Nisha; Purcell, Dan; Lee, Jonathan (2003): Not just for housekeeping: protein initiation and elongation factors in cell growth and tumorigenesis. In *Journal of molecular medicine (Berlin, Germany)* 81 (9), pp. 536–548. DOI: 10.1007/s00109-003-0461-8.

Toledo, Marion de; Anguille, Christelle; Roger, Laureline; Roux, Pierre; Gadea, Gilles (2012): Cooperative anti-invasive effect of Cdc42/Rac1 activation and ROCK inhibition in SW620 colorectal cancer cells with elevated blebbing activity. In *PloS one* 7 (11), e48344. DOI: 10.1371/journal.pone.0048344.

Tomita, K.; van Bokhoven, A.; van Leenders, G. J.; Ruijter, E. T.; Jansen, C. F.; Bussemakers, M. J.; Schalken, J. A. (2000): Cadherin switching in human prostate cancer progression. In *Cancer research* 60 (13), pp. 3650–3654.

Tonoli, Hélène; Barrett, J. Carl (2005): CD82 metastasis suppressor gene: a potential target for new therapeutics? In *Trends in molecular medicine* 11 (12), pp. 563–570. DOI: 10.1016/j.molmed.2005.10.002.

Treisman, R. (1986): Identification of a protein-binding site that mediates transcriptional response of the c-fos gene to serum factors. In *Cell* 46 (4), pp. 567–574. DOI: 10.1016/0092-8674(86)90882-2.

Treisman, R. (1994): Ternary complex factors: growth factor regulated transcriptional activators. In *Current opinion in genetics & development* 4 (1), pp. 96–101. DOI: 10.1016/0959-437x(94)90097-3.

Treisman, R. (1995): Journey to the surface of the cell: Fos regulation and the SRE. In *The EMBO journal* 14 (20), pp. 4905–4913.

Treisman, R.; Ammerer, G. (1992): The SRF and MCM1 transcription factors. In *Current opinion in genetics & development* 2 (2), pp. 221–226. DOI: 10.1016/s0959-437x(05)80277-1.

Treisman, Richard (1992): The serum response element. In *Trends in biochemical sciences* 17 (10), pp. 423–426.

Tripathi, V.; Popescu, N. C.; Zimonjic, D. B. (2014): DLC1 induces expression of E-cadherin in prostate cancer cells through Rho pathway and suppresses invasion. In *Oncogene* 33 (6), pp. 724–733. DOI: 10.1038/onc.2013.7.

Turner, Frances E.; Broad, Simon; Khanim, Farhat L.; Jeanes, Alexa; Talma, Sonia; Hughes, Sharon et al. (2006): Slug regulates integrin expression and cell proliferation in human epidermal keratinocytes. In *The Journal of biological chemistry* 281 (30), pp. 21321–21331. DOI: 10.1074/jbc.M509731200.

Uehata, M.; Ishizaki, T.; Satoh, H.; Ono, T.; Kawahara, T.; Morishita, T. et al. (1997): Calcium sensitization of smooth muscle mediated by a Rho-associated protein kinase in hypertension. In *Nature* 389 (6654), pp. 990–994. DOI: 10.1038/40187.

Uygur, Berna; Wu, Wen-Shu (2011): SLUG promotes prostate cancer cell migration and invasion via CXCR4/CXCL12 axis. In *Molecular cancer* 10, p. 139. DOI: 10.1186/1476-4598-10-139.

van der Flier, A.; Sonnenberg, A. (2001): Structural and functional aspects of filamins. In *Biochimica et biophysica acta* 1538 (2-3), pp. 99–117. DOI: 10.1016/s0167-4889(01)00072-6.

van Golen, Kenneth L.; Wu, Zhi-Fen; Qiao, XiaoTan; Bao, LiWei; Merajver, Sofia D. (2000): RhoC GTPase overexpression modulates induction of angiogenic factors in breast cells. In *Neoplasia* 2 (5), pp. 418–425.

Vartiainen, Maria K.; Guettler, Sebastian; Larijani, Banafshe; Treisman, Richard (2007): Nuclear actin regulates dynamic subcellular localization and activity of the SRF cofactor MAL. In *Science (New York, N.Y.)* 316 (5832), pp. 1749–1752. DOI: 10.1126/science.1141084.

Vega, Francisco M.; Ridley, Anne J. (2008): Rho GTPases in cancer cell biology. In *FEBS letters* 582 (14), pp. 2093–2101. DOI: 10.1016/j.febslet.2008.04.039.

Vennin, Claire; Rath, Nicola; Pajic, Marina; Olson, Michael F.; Timpson, Paul (2020): Targeting ROCK activity to disrupt and prime pancreatic cancer for chemotherapy. In *Small GTPases* 11 (1), pp. 45–52. DOI: 10.1080/21541248.2017.1345712.

Verdoni, Angela M.; Ikeda, Sakae; Ikeda, Akihiro (2010): Serum response factor is essential for the proper development of skin epithelium. In *Mammalian genome : official journal of the International Mammalian Genome Society* 21 (1-2), pp. 64–76. DOI: 10.1007/s00335-009-9245-y.

Visvikis, Orane; Maddugoda, Madhavi P.; Lemichez, Emmanuel (2010): Direct modifications of Rho proteins: deconstructing GTPase regulation. In *Biology of the cell* 102 (7), pp. 377–389. DOI: 10.1042/BC20090151.

Voringer, Sandra; Schreyer, Laura; Nadolni, Wiebke; Meier, Melanie A.; Woerther, Katharina; Mittermeier, Constanze et al. (2020): Inhibition of TRPM7 blocks MRTF/SRF-dependent transcriptional and tumorigenic activity. In *Oncogene* 39 (11), pp. 2328–2344. DOI: 10.1038/s41388-019-1140-8.

Voutilainen, Kirsi; Anttila, Maarit; Sillanpää, Sari; Tammi, Raija; Tammi, Markku; Saarikoski, Seppo; Kosma, Veli-Matti (2003): Versican in epithelial ovarian cancer: relation to hyaluronan, clinicopathologic factors and prognosis. In *International journal of cancer* 107 (3), pp. 359–364. DOI: 10.1002/ijc.11423.

Wang, D.; Chang, P. S.; Wang, Z.; Sutherland, L.; Richardson, J. A.; Small, E. et al. (2001): Activation of cardiac gene expression by myocardin, a transcriptional cofactor for serum response factor. In *Cell* 105 (7), pp. 851–862. DOI: 10.1016/s0092-8674(01)00404-4.

Wang, Da-Zhi; Li, Shijie; Hockemeyer, Dirk; Sutherland, Lillian; Wang, Zhigao; Schratt, Gerhard et al. (2002): Potentiation of serum response factor activity by a family of myocardin-related transcription factors. In *Proceedings of the National Academy of Sciences of the United States of America* 99 (23), pp. 14855–14860. DOI: 10.1073/pnas.222561499.

Wang, Dunrui; Qian, Xiaolan; Rajaram, Megha; Durkin, Marian E.; Lowy, Douglas R. (2016a): DLC1 is the principal biologically-relevant down-regulated DLC family member in several cancers. In *Oncotarget* 7 (29), pp. 45144–45157. DOI: 10.18632/oncotarget.9266.

Wang, Dunrui; Qian, Xiaolan; Sanchez-Solana, Beatriz; Tripathi, Brajendra K.; Durkin, Marian E.; Lowy, Douglas R. (2020): Cancer-Associated Point Mutations in the DLC1 Tumor Suppressor and Other Rho-GAPs Occur Frequently and Are Associated with Decreased Function. In *Cancer research* 80 (17), pp. 3568–3579. DOI: 10.1158/0008-5472.CAN-19-3984.

Wang, Min; Ren, Dong; Guo, Wei; Huang, Shuai; Wang, Zeyu; Li, Qiji et al. (2016b): N-cadherin promotes epithelial-mesenchymal transition and cancer stem cell-like traits via ErbB signaling in prostate cancer cells. In *International journal of oncology* 48 (2), pp. 595–606. DOI: 10.3892/ijo.2015.3270.

Wang, X.; Zhang, W.; Tang, J.; Huang, R.; Li, J.; Xu, D. et al. (2016c): LINC01225 promotes occurrence and metastasis of hepatocellular carcinoma in an epidermal growth factor receptor-dependent pathway. In *Cell death & disease* 7 (3), e2130. DOI: 10.1038/cddis.2016.26.

Wang, Xiao; Chen, Jian; Wang, Jingtao; Yu, Fudong; Zhao, Senlin; Zhang, Yu et al. (2016d): Metalloproteases meprin-α (MEP1A) is a prognostic biomarker and promotes proliferation and invasion of colorectal cancer. In *BMC cancer* 16, p. 383. DOI: 10.1186/s12885-016-2460-5.

Wang, Yu; Nie, Hao; Zhao, Xin; Qin, Yong; Gong, Xingguo (2016e): Bicyclol induces cell cycle arrest and autophagy in HepG2 human hepatocellular carcinoma cells through the PI3K/AKT and Ras/Raf/MEK/ERK pathways. In *BMC cancer* 16 (1), p. 742. DOI: 10.1186/s12885-016-2767-2.

Watanabe, N.; Kato, T.; Fujita, A.; Ishizaki, T.; Narumiya, S. (1999): Cooperation between mDia1 and ROCK in Rho-induced actin reorganization. In *Nat Cell Biol* 1 (3), pp. 136–143. DOI: 10.1038/11056.

Waterhouse, Roseann; Ha, Cam; Dveksler, Gabriela S. (2002): Murine CD9 is the receptor for pregnancy-specific glycoprotein 17. In *The Journal of experimental medicine* 195 (2), pp. 277–282. DOI: 10.1084/jem.20011741.

Weeks, Hoi Ping; Sanders, Andrew J.; Kynaston, Howard G.; Jiang, Wen G. (2016): The Association Between WAVE1 and -3 and the ARP2/3 Complex in PC 3 Cells. In *Anticancer research* 36 (3), pp. 1135–1142.

Weinberg, R. A. (1995): The retinoblastoma protein and cell cycle control. In *Cell* 81 (3), pp. 323–330. DOI: 10.1016/0092-8674(95)90385-2.

Whitmarsh, A. J.; Yang, S. H.; Su, M. S.; Sharrocks, A. D.; Davis, R. J. (1997): Role of p38 and JNK mitogen-activated protein kinases in the activation of ternary complex factors. In *Molecular and cellular biology* 17 (5), pp. 2360–2371. DOI: 10.1128/mcb.17.5.2360.

WHO (2021): International Agency for Research on Cancer Global cancer observatory - cancer fact sheets. Available online at https://gco.iarc.fr/today/fact-sheets-cancers, updated on 8/9/2021, checked on 8/9/2021.

Wiederkehr, A.; Staple, J.; Caroni, P. (1997): The motility-associated proteins GAP-43, MARCKS, and CAP-23 share unique targeting and surface activity-inducing properties. In *Experimental cell research* 236 (1), pp. 103–116. DOI: 10.1006/excr.1997.3709.

Wight, Thomas N. (2002): Versican: a versatile extracellular matrix proteoglycan in cell biology. In *Current opinion in cell biology* 14 (5), pp. 617–623. DOI: 10.1016/s0955-0674(02)00375-7.

Wight, Thomas N. (2017): Provisional matrix: A role for versican and hyaluronan. In *Matrix biology : journal of the International Society for Matrix Biology* 60-61, pp. 38–56. DOI: 10.1016/j.matbio.2016.12.001.

Winkles, J. A. (1998): Serum- and polypeptide growth factor-inducible gene expression in mouse fibroblasts. In *Progress in nucleic acid research and molecular biology* 58, pp. 41–78. DOI: 10.1016/s0079-6603(08)60033-1.

Wong, Chun-Ming; Lee, Joyce Man-Fong; Ching, Yick-Pang; Jin, Dong-Yan; Ng, Irene Oi-lin (2003): Genetic and Epigenetic Alterations of DLC-1 Gene in Hepatocellular Carcinoma. In *Cancer research* 63 (22), pp. 7646–7651. Available online at https://cancerres.aacrjournals.org/content/63/22/7646.

Wong, Chun-Ming; Yam, Judy Wai-Ping; Ching, Yick-Pang; Yau, Tai-On; Leung, Thomas Ho-Yin; Jin, Dong-Yan; Ng, Irene Oi-lin (2005): Rho GTPase-activating protein deleted in liver cancer suppresses cell proliferation and invasion in hepatocellular carcinoma. In *Cancer research* 65 (19), pp. 8861–8868. DOI: 10.1158/0008-5472.CAN-05-1318.

Worthylake, R. A.; Lemoine, S.; Watson, J. M.; Burridge, K. (2001): RhoA is required for monocyte tail retraction during transendothelial migration. In *The Journal of cell biology* 154 (1), pp. 147–160. DOI: 10.1083/jcb.200103048.

Wright, W. E.; Piatyszek, M. A.; Rainey, W. E.; Byrd, W.; Shay, J. W. (1996): Telomerase activity in human germline and embryonic tissues and cells. In *Developmental genetics* 18 (2), pp. 173–179. DOI: 10.1002/(SICI)1520-6408(1996)18:2<173::AID-DVG10>3.0.CO;2-3.

Wu, Hao; Liu, Tiantian; Qi, Jianni; Qin, Chengyong; Zhu, Qiang (2020): Four Autophagy-Related lncRNAs Predict the Prognosis of HCC through Coexpression and ceRNA Mechanism. In *BioMed research international* 2020, p. 3801748. DOI: 10.1155/2020/3801748.

Wu, Hui-Ta; Xie, Cheng-Rong; Lv, Jie; Qi, He-Qiang; Wang, Fei; Zhang, Sheng et al. (2018): The tumor suppressor DLC1 inhibits cancer progression and oncogenic autophagy in hepatocellular carcinoma. In *Laboratory investigation; a journal of technical methods and pathology* 98 (8), pp. 1014–1024. DOI: 10.1038/s41374-018-0062-3.

Wu, P. P.; Zhu, H. Y.; Sun, X. F.; Chen, L. X.; Zhou, Q.; Chen, J. (2015): MicroRNA-141 regulates the tumour suppressor DLC1 in colorectal cancer. In *Neoplasma* 62 (5), pp. 705–712. DOI: 10.4149/neo_2015_084.

Wu, Ping-ping; Jin, Yue-ling; Shang, Yan-fang; Jin, Zhi; Wu, Peng; Huang, Pei-lin (2009): Restoration of DLC1 gene inhibits proliferation and migration of human colon cancer HT29 cells. In *Annals of clinical and laboratory science* 39 (3), pp. 263–269.

Wyllie, A. H.; Kerr, J. F.; Currie, A. R. (1980): Cell death: the significance of apoptosis. In *International review of cytology* 68, pp. 251–306. DOI: 10.1016/s0074-7696(08)62312-8.

Wynford-Thomas, D. (1999): Cellular senescence and cancer. In *The Journal of pathology* 187 (1), pp. 100–111. DOI: 10.1002/(SICI)1096-9896(199901)187:1<100::AID-PATH236>3.0.CO;2-T.

Xie, Cheng-Rong; Sun, Hong-Guang; Sun, Yu; Zhao, Wen-Xiu; Zhang, Sheng; Wang, Xiao-Min; Yin, Zhen-Yu (2015): Significance of genetic variants in DLC1 and their association with hepatocellular carcinoma. In *Molecular medicine reports* 12 (3), pp. 4203–4209. DOI: 10.3892/mmr.2015.3970.

Xu, Wenping; Zhao, Quanyi; Wu, Min; Fang, Mingming; Xu, Yong (2019): MKL1 mediates TNF-α induced pro-inflammatory transcription by bridging the crosstalk between BRG1 and WDR5. In *Journal of biomedical research* 33 (3), pp. 164–172. DOI: 10.7555/JBR.32.20170025.

Xue, Wen; Krasnitz, Alexander; Lucito, Robert; Sordella, Raffaella; Vanaelst, Linda; Cordon-Cardo, Carlos et al. (2008): DLC1 is a chromosome 8p tumor suppressor whose loss promotes hepatocellular carcinoma. In *Genes & development* 22 (11), pp. 1439–1444. DOI: 10.1101/gad.1672608.

Yáñez-Mó, María; Barreiro, Olga; Gordon-Alonso, Mónica; Sala-Valdés, Mónica; Sánchez-Madrid, Francisco (2009): Tetraspanin-enriched microdomains: a functional unit in cell plasma membranes. In *Trends in cell biology* 19 (9), pp. 434–446. DOI: 10.1016/j.tcb.2009.06.004.

Yang, Haiping; Wang, Longqiang; Zhao, Jun; Chen, Yongbing; Lei, Zhe; Liu, Xia et al. (2015): TGF-β-activated SMAD3/4 complex transcriptionally upregulates N-cadherin expression in non-small cell lung cancer. In *Lung cancer (Amsterdam, Netherlands)* 87 (3), pp. 249–257. DOI: 10.1016/j.lungcan.2014.12.015.

Yang, Xuyu; Zhou, Xiaoling; Tone, Paul; Durkin, Marian E.; Popescu, Nicholas C. (2016): Cooperative antiproliferative effect of coordinated ectopic expression of DLC1 tumor suppressor protein and silencing of MYC oncogene expression in liver cancer cells: Therapeutic implications. In *Oncology letters* 12 (2), pp. 1591–1596. DOI: 10.3892/ol.2016.4781.

Yarmola, E. G.; Somasundaram, T.; Boring, T. A.; Spector, I.; Bubb, M. R. (2000): Actin-latrunculin A structure and function. Differential modulation of actin-binding protein function by latrunculin A. In *The Journal of biological chemistry* 275 (36), pp. 28120–28127. DOI: 10.1074/jbc.M004253200.

Yaseen, Ibrahim H.; Monk, Peter N.; Partridge, Lynda J. (2017): Tspan2: a tetraspanin protein involved in oligodendrogenesis and cancer metastasis. In *Biochemical Society transactions* 45 (2), pp. 465–475. DOI: 10.1042/BST20160022.

Yauch, Robert L.; Berditchevski, Fedor; Harler, Mary Beth; Reichner, Jonathan; Hemler, Martin E. (1998): Highly stoichiometric, stable, and specific association of integrin α3β1 with CD151 provides a major link to phosphatidylinositol 4-kinase, and may regulate cell migration. In *Molecular biology of the cell* 9 (10), pp. 2751–2765.

Yoo, Christine B.; Jones, Peter A. (2006): Epigenetic therapy of cancer: past, present and future. In *Nature reviews. Drug discovery* 5 (1), pp. 37–50. DOI: 10.1038/nrd1930.

Yuan, B. Z.; Miller, M. J.; Keck, C. L.; Zimonjic, D. B.; Thorgeirsson, S. S.; Popescu, N. C. (1998): Cloning, characterization, and chromosomal localization of a gene frequently deleted in human liver cancer (DLC-1) homologous to rat RhoGAP. In *Cancer research* 58 (10), pp. 2196–2199.

Yuan, Bao-Zhu; Durkin, Marian E.; Popescu, Nicholas C. (2003a): Promoter hypermethylation of DLC-1, a candidate tumor suppressor gene, in several common human cancers. In *Cancer genetics and cytogenetics* 140 (2), pp. 113–117. DOI: 10.1016/s0165-4608(02)00674-x.

Yuan, Bao-Zhu; Jefferson, Amy M.; Baldwin, Kimberly T.; Thorgeirsson, Snorri S.; Popescu, Nicholas C.; Reynolds, Steven H. (2004): DLC-1 operates as a tumor suppressor gene in human non-small cell lung carcinomas. In *Oncogene* 23 (7), pp. 1405–1411. DOI: 10.1038/sj.onc.1207291.

Yuan, Bao-Zhu; Zhou, Xiaoling; Durkin, Marian E.; Zimonjic, Drazen B.; Gumundsdottir, Katrin; Eyfjord, Jorunn E. et al. (2003b): DLC-1 gene inhibits human breast cancer cell growth and in vivo tumorigenicity. In *Oncogene* 22 (3), pp. 445–450. DOI: 10.1038/sj.onc.1206064.

Zahra, Fatema Tuz; Choleva, Efrossini; Sajib, Md Sanaullah; Papadimitriou, Evangelia; Mikelis, Constantinos M. (2019): In Vitro Spheroid Sprouting Assay of Angiogenesis. In *Methods in molecular biology (Clifton, N.J.)* 1952, pp. 211–218. DOI: 10.1007/978-1-4939-9133-4_17.

Zender, L.; Xue, W.; Cordón-Cardo, C.; Hannon, G. J.; Lucito, R.; Powers, S. et al. (2005): Generation and analysis of genetically defined liver carcinomas derived from bipotential liver progenitors. In *Cold Spring Harbor symposia on quantitative biology* 70, pp. 251–261. DOI: 10.1101/sqb.2005.70.059.

Zender, Lars; Spector, Mona S.; Xue, Wen; Flemming, Peer; Cordon-Cardo, Carlos; Silke, John et al. (2006): Identification and validation of oncogenes in liver cancer using an integrative oncogenomic approach. In *Cell* 125 (7), pp. 1253–1267. DOI: 10.1016/j.cell.2006.05.030.

Zeng, Zhuoying; Lu, Jingjing; Wu, Desheng; Zuo, Ran; Li, Yuxi; Huang, Haiyan et al. (2021): Poly(ADP-ribose) glycohydrolase silencing-mediated H2B expression inhibits benzo(a)pyrene-induced carcinogenesis. In *Environmental toxicology* 36 (3), pp. 291–297. DOI: 10.1002/tox.23034.

Zhang, Wenfeng; Di Mu; Feng, Kai (2017): Hierarchical potential differentiation of liver cancer stem cells. In *Advances in clinical and experimental medicine : official organ Wroclaw Medical University* 26 (7), pp. 1137–1141. DOI: 10.17219/acem/66343.

Zhang, X. A.; Bontrager, A. L.; Hemler, M. E. (2001): Transmembrane-4 superfamily proteins associate with activated protein kinase C (PKC) and link PKC to specific beta(1) integrins. In *The Journal of biological chemistry* 276 (27), pp. 25005–25013. DOI: 10.1074/jbc.M102156200.

Zhang, Xueli; Wang, Liang; Zhang, Haitao; Tu, Fang; Qiang, Yong; Nie, Cuifang (2019): Decreased expression of ZO-1 is associated with tumor metastases in liver cancer. In *Oncology letters* 17 (2), pp. 1859–1864. DOI: 10.3892/ol.2018.9765.

Zhang, Zhenwei; Miao, Lei; Wang, Lianghua (2012): Inflammation amplification by Versican: the first mediator. In *International journal of molecular sciences* 13 (6), pp. 6873–6882. DOI: 10.3390/ijms13066873.

Zhangyuan, Guangyan; Wang, Fei; Zhang, Haitian; Jiang, Runqiu; Tao, Xuewen; Yu, Decai et al. (2020): VersicanV1 promotes proliferation and metastasis of hepatocellular carcinoma through the activation of EGFR-PI3K-AKT pathway. In *Oncogene* 39 (6), pp. 1213–1230. DOI: 10.1038/s41388-019-1052-7.

Zhao, Xiaobin; Lapalombella, Rosa; Joshi, Trupti; Cheney, Carolyn; Gowda, Aruna; Hayden-Ledbetter, Martha S. et al. (2007): Targeting CD37-positive lymphoid malignancies with a novel engineered small modular immunopharmaceutical. In *Blood* 110 (7), pp. 2569–2577. DOI: 10.1182/blood-2006-12-062927.

Zhao, Yan; Yan, Quanmei; Long, Xing; Chen, Xinmin; Wang, Yining (2008): Vimentin affects the mobility and invasiveness of prostate cancer cells. In *Cell biochemistry and function* 26 (5), pp. 571–577. DOI: 10.1002/cbf.1478.

Zhong, Dandan; Zhang, Jingfeng; Yang, Shuai; Soh, Unice J. K.; Buschdorf, Jan Paul; Zhou, Yi Ting et al. (2009): The SAM domain of the RhoGAP DLC1 binds EF1A1 to regulate cell migration. In *Journal of cell science* 122 (Pt 3), pp. 414–424. DOI: 10.1242/jcs.027482.

Zhong, S.; Salomoni, P.; Pandolfi, P. P. (2000): The transcriptional role of PML and the nuclear body. In *Nat Cell Biol* 2 (5), E85-90. DOI: 10.1038/35010583.

Zhou, Jian; Fujiwara, Toshifumi; Ye, Shiqiao; Li, Xiaolin; Zhao, Haibo (2014): Downregulation of Notch modulators, tetraspanin 5 and 10, inhibits osteoclastogenesis in vitro. In *Calcified tissue international* 95 (3), pp. 209–217. DOI: 10.1007/s00223-014-9883-2.

Zhou, Xiaoling; Thorgeirsson, Snorri S.; Popescu, Nicholas C. (2004): Restoration of DLC-1 gene expression induces apoptosis and inhibits both cell growth and tumorigenicity in human hepatocellular carcinoma cells. In *Oncogene* 23 (6), pp. 1308–1313. DOI: 10.1038/sj.onc.1207246.

Zhu, Cheng-Pei; Wang, An-Qiang; Zhang, Hao-Hai; Wan, Xue-Shuai; Yang, Xiao-Bo; Chen, Shu-Guang; Zhao, Hai-Tao (2015): Research progress and prospects of markers for liver cancer stem cells. In *World journal of gastroenterology* 21 (42), pp. 12190–12196. DOI: 10.3748/wjg.v21.i42.12190.

Zhu, Fang; Zhang, Zhe; Wu, Gang; Li, Zhenyu; Zhang, Ruiguang; Ren, Jinghua; Nong, Li (2011): Rho kinase inhibitor fasudil suppresses migration and invasion though down-regulating the expression of VEGF in lung

cancer cell line A549. In *Medical oncology (Northwood, London, England)* 28 (2), pp. 565–571. DOI: 10.1007/s12032-010-9468-5.

Zhu, J.; Woods, D.; McMahon, M.; Bishop, J. M. (1998): Senescence of human fibroblasts induced by oncogenic Raf. In *Genes & development* 12 (19), pp. 2997–3007. DOI: 10.1101/gad.12.19.2997.

Zhu, Rongxuan; Gires, Olivier; Zhu, Liqun; Liu, Jun; Li, Junjian; Yang, Hao et al. (2019): TSPAN8 promotes cancer cell stemness via activation of sonic Hedgehog signaling. In *Nature communications* 10 (1), p. 2863. DOI: 10.1038/s41467-019-10739-3.

Zhu, Yan-Jing; Zheng, Bo; Wang, Hong-Yang; Chen, Lei (2017): New knowledge of the mechanisms of sorafenib resistance in liver cancer. In *Acta pharmacologica Sinica* 38 (5), pp. 614–622. DOI: 10.1038/aps.2017.5.

Zhuge, Y.; Xu, J. (2001): Rac1 mediates type I collagen-dependent MMP-2 activation. role in cell invasion across collagen barrier. In *The Journal of biological chemistry* 276 (19), pp. 16248–16256. DOI: 10.1074/jbc.m010190200.

Zijlstra, Andries; Lewis, John; Degryse, Bernard; Stuhlmann, Heidi; Quigley, James P. (2008): The inhibition of tumor cell intravasation and subsequent metastasis via regulation of in vivo tumor cell motility by the tetraspanin CD151. In *Cancer cell* 13 (3), pp. 221–234. DOI: 10.1016/j.ccr.2008.01.031.

Zitvogel, Laurence; Pitt, Jonathan M.; Daillère, Romain; Smyth, Mark J.; Kroemer, Guido (2016): Mouse models in oncoimmunology. In *Nature Reviews Cancer* 16 (12), pp. 759–773. DOI: 10.1038/nrc.2016.91.

Zöller, Margot (2009): Tetraspanins: push and pull in suppressing and promoting metastasis. In *Nature reviews. Cancer* 9 (1), pp. 40–55. DOI: 10.1038/nrc2543.

Zuo, Qiang; Huang, Hui; Shi, Min; Zhang, Futing; Sun, Jiping; Bin, Jianping et al. (2012): Multivariate analysis of several molecular markers and clinicopathological features in postoperative prognosis of hepatocellular carcinoma. In *Anatomical record (Hoboken, N.J. : 2007)* 295 (3), pp. 423–431. DOI: 10.1002/ar.21531.

12 Publications

Parts of the results of this thesis have been published in peer-reviewed journals:

- **Schreyer L**, Mittermeier C, Franz MJ, Meier MA, Martin DE, Maier K, Hübner K, Schneider-Stock R, Singer S, Holzer K, Ribback S, Liebl B, Gudermann T, Aigner A, Muehlich S.

  Tetraspanin 5 (TSPAN5), a novel gatekeeper of the tumor suppressor DLC1 and Myocardin-related transcription factors (MRTFs), controls HCC growth and senescence

  Cancers, 2021 Oct 26; 13(21): 5373. doi: 10.3390/cancers13215373

- Voringer S, **Schreyer L**, Nadolni W, Meier MA, Woerther K, Mittermeier C, Ferioli S, Singer S, Holzer K, Zierler S, Chubanov V, Liebl B, Gudermann T, Muehlich S

  Inhibition of TRPM7 blocks MRTF/SRF-dependent transcriptional and tumorigenic activity

  Oncogene, 2019 Dec 16; (39): 2328-44. doi: org/10.1038/s41388-019-1140-8

Talks and Posters

Parts of the results were presented at poster sessions or in short talks at the following congresses:

- **Schreyer L**, Mittermeier C, Martin DE, Maier K, Singer S, Holzer K, Ribback S, Liebl B, Gudermann T, Aigner A, Muehlich S.

  Tetraspanin 5 (TSPAN5) as a novel regulator of hepatocellular carcinoma (HCC) growth upon loss of the tumor suppressor Deleted in Liver Cancer 1 (DLC1)

  6th German Pharm-Tox Summit / 87. Annual Meeting of the German Society of Pharmacology and Toxicology, Jena 2021

- **Schreyer L,** Meier MA, Muehlich S

  Targeting the transmembrane protein Tetraspanin 5 (TSPAN5) in DLC1 deficient cancers as a novel therapeutical approach

  FAU Symposium: Learning by Nature – from biology to innovation

13 Acknowledgements

First of all, I would like to thank Prof. Dr. Susanne Mühlich for the opportunity to perform my PhD thesis in her research group and for entrusting me with my very interesting and exciting research topic. Many thanks also for the excellent supervision, always encouraging manner, energetic support in all questions, the thematic discussions, methodical advice and support in all matters concerning this project!

I would especially like to thank PD Dr. Martin for being my doctor father and for his great interest in my project and all the helpful advises.

Further, I would like to thank Prof. Dr. Liebl for the financial support, that he trusted in me and my work and for being my external representative of this thesis.

I am very thankful to Prof. Dr. Gudermann for giving me the opportunity to perform my PhD thesis in the laboratories of the Walther Straub Institute.

Furthermore, I would like to thank Prof. Dr. Stingele, Prof. Dr. Koch, Prof. Dr. Biel and Prof. Dr. Frieß for their willingness to be a member of my examination board.

Additionally, I would like to thank all the previous and present members of the Mühlich lab, Melanie Meier, Andreas Konopa, Miriam Franz, Vanessa Wolf, Constanze Mittermeier, Sandra Voringer, Katharina Wörther, Cem Asci and Max Lewandowski for their nice, helpful and always energetic support over the last years, the friendly talks and the pleasant atmosphere in the Munich as well as in the Erlangen lab. Especially thanks to Clara-Mae Beer for her technical support and all her help and assistance.

My special gratitude goes to my parents, who have accompanied and encouraged me throughout the time of my PhD and the whole time of my life and without whose support I would not have been able to do this work! Thank you for always being there for me!

Last but not least, I'm extremely grateful to Patrick for always being there for me, for his tireless and lovely support and always cheering me up. I am grateful for having you in my life!